

KAUNAS UNIVERSITY OF TECHNOLOGY

SAULIUS NIAURONIS

INVESTIGATION OF HUMAN OCULO-  
MANUAL COORDINATION CONTROL  
SYSTEM

Doctoral dissertation  
Technological sciences, Electrical and electronic engineering (01T)

2015, Kaunas

Dissertation was carried out in 2010-2014 at Kaunas University of Technology, Biomedical Engineering Institute. Experimental research was performed at Siauliai University, Biomedical Engineering Center. Research was funded by Lithuanian State Studies Foundation and Research Council of Lithuania.

**Scientific Supervisor:**

Prof. Dr. Habil. Arūnas LUKOŠEVIČIUS (Kaunas University of Technology, Technological Sciences, Electrical and Electronic Engineering – 01T).

**Scientific Advisor:**

Prof. Dr. Habil. Vincas LAURUTIS (Šiauliai University, Technological Sciences, Electrical and Electronic Engineering – 01T).

## LIST OF ABBREVIATIONS

ADHD – Attention Deficit Hyperactivity Disorder;  
Arcmin – unit of angular measurement equal to 1/60 of one degree;  
Arcsec – unit of angular measurement equal to 1/60 of one arcmin;  
CBM – cerebellum;  
CBT - corticobulbar tract;  
CCS – Coordination Control System;  
CNS – Central Nervous System;  
DLPN – Dorso-Lateral Pontine Nuclei;  
DOF – Degree Of Freedom;  
EBN – Excitatory Burst Neuron;  
FASD – Fetal Alcohol Spectrum Disorder;  
FEF – Frontal Eye Fields;  
FPA – Frontal Pursuit Area;  
GJ – Gaze Jumps (coordination strategy);  
GMS – Gaze Moves Smoothly (coordination strategy or a movement manner);  
HCI – human-computer interaction;  
IBN – Inhibitory Burst Neuron;  
ID – Index of Difficulty (by Fitts' or its derivative Steering laws);  
LIP – Lateral Intra-Parietal area;  
LLBN – Long-Lead Burst Neuron;  
LSF – Least Squares Fitted;  
MST – Middle Superior Temporal area;  
MT – Middle Temporal area;  
MVN/rLVN – Medial and Rostro-Lateral Vestibular Nuclei;  
NPH - nucleus prepositus hypoglossi;  
NRTP – Nucleus Reticularis Tegmenti Pontis;  
Oculo-manual – eye and hand movement related;  
Oculo-manual guiding – the case, when hand is moving a cursor and eyes are supervising its trajectory. Both eye and hand systems work in a coordinated way;  
Oculo-motor – eye movement related;  
OGS – Object Guiding Subsystem;  
OPN – Omni-Pauser Neurons;  
PD – Parkinson's disease;  
PPRF – a Peri-Pontine Reticular Formation;  
SC – Superior Colliculus;  
SD or  $\sigma$  – Standard Deviation;  
SD-AM – Standard Deviation from mean for points Above Mean;  
SD-UM – Standard Deviation from mean for points Under Mean;  
TAID – Trial-Assumed Index of Difficulty;  
TN – Tonic Neurons;  
VI and V2 - occipital visual areas;  
Visuo-manual – visual to manual;  
Visuo-motor – visual to oculo-motor;  
VN - vestibular nuclei;  
VR – Visual Reconstructor;

## TABLE OF CONTENTS

INTRODUCTION.....	6
The subject of research.....	6
Relevance of research.....	6
Scientific problem.....	7
Working hypothesis.....	7
The aim of the dissertation.....	7
Tasks of the work.....	7
Scientific novelty.....	8
Practical value of the work.....	8
Statements presented for defense.....	8
Approval of the results.....	9
Structure and contents of the dissertation.....	9
1. REVIEW ON EYE AND HAND MOVEMENT RESEARCH.....	10
1.1. Eye movements.....	10
1.1.1. Fixational eye movements.....	11
1.1.2. Saccadic eye movements.....	13
1.1.3. Smooth pursuit eye movements.....	22
1.2. Models of the eye movement system.....	29
1.2.1. A Model of the Saccade Generator.....	29
1.2.2. Models of a smooth pursuit system.....	32
1.2.3. Neural model for visual tracking of unpredictably moving target....	34
1.3. Hand movements.....	39
1.4. Hand movement models.....	44
1.5. Eye-hand coordination.....	47
1.5.1. Eye-hand coordination in object guiding.....	49
1.5.2. Eye-hand coordination models.....	50
1.6. Summary and conclusions.....	54
1.7. Tasks towards the aim of the work.....	55
2. PRELIMINARY MODEL AND EMPIRICAL RESEARCH PLANNING ....	56
2.1. Preliminary model for simulating human oculo-manual coordination.....	56
2.2. Experimental research required for understanding and modeling human oculo-manual coordination.....	57
2.3. Common methodology of planned experimental research.....	59
2.4. New mathematical expression for pursuit gain calculation.....	60
2.5. Trajectory shifting in time as a means to evaluate a lag or prediction of the tracking.....	62
2.6. Usage of Fitts' Law derivatives for visual trajectory evaluation.....	63
2.7. Standard deviation from a mean for above-mean and under-mean values	64
2.8. Summary and conclusions.....	65
3. EXPERIMENTAL INVESTIGATION OF SMOOTH PURSUIT EYE MOVEMENTS AND COORDINATED EYE-HAND MOVEMENTS.....	66
3.1. Influence of catch-up saccades on a quality of smooth pursuit.....	66
3.2. Eye-hand coordination while controlling hand-moved object.....	71

3.2.1.	Abrupt hand movements and saccadic eye movements.....	71
3.2.2.	Oculo-manual tracking of a moving object .....	72
3.2.3.	Oculo-motor tracking of a self-moved target .....	75
3.2.4.	The control of a hand-moved object in visual environment .....	76
3.3.	Eye movements when guiding a hand-moved object in visual environment and their comparison to smooth pursuit eye movements.....	77
3.3.1.	The oculo-motor strategies for an object guiding.....	77
3.3.2.	Oculo-manual guiding eye movements and their dependence on characteristics of hand movements.....	83
3.3.3.	Differences of guiding and smooth pursuit eye movements.....	91
3.4.	Summary and conclusions .....	92
4.	MODELING OF OCULO-MANUAL COORDINATION SYSTEM.....	94
4.1.	Modeling the human behavior .....	94
4.2.	Neurophysiological modeling.....	97
4.3.	Model for simulating oculo-manual guiding .....	99
4.4.	Model adequacy.....	104
4.5.	Summary and conclusions .....	110
5.	APPLICATIONS OF EYE AND COORDINATED EYE-HAND MOVEMENTS FOR DESIGNING ELECTRONIC SYSTEMS.....	111
5.1.	Eye movement application in human-computer interaction .....	111
5.2.	Eye movement application in diagnostics .....	115
5.3.	Possible applications of the eye-hand coordination model.....	118
5.4.	Summary and conclusions .....	120
	CONCLUSIONS .....	121
	LIST OF REFERENCES.....	122
	LIST OF PUBLICATIONS ON THE THEME OF DISSERTATION .....	133
	APPENDICES .....	135

## **INTRODUCTION**

### **The subject of research**

Human oculo-manual coordination control system.

### **Relevance of research**

Development of computer technology modifies all the tools humans use in work environment and in everyday life. Because of new computer-based devices, different human-computer interaction types are required to control effectively and comfortably them and therefore various possibilities are being explored. Bounding to human limb based control is not an option anymore since it has some limitations: it is slow, requires an effort, usually consume more energy that is actually needed to implement a control command. Especially when computational technology has reached the level, when even precise internal human signals can be processed in real-time. One of possible and well-investigated areas is eye movements. Knowledge and increasing capabilities in technology influenced decrease in price, increase in accuracy and precision and lower sizes of eye movement tracking devices, thus allowing eye-movement signals to be used in mass-production tools such as tablet and mobile computers. Anyway, human-computer interaction at the beginning of development of this technology was expected to be different than it is now. It was supposed to be able to replace traditional input devices such as the computer mouse. During recent years, scientists and engineers realized that eye movements, because of their sensory-related nature could not be used alone for versatile control of a computer. Midas touch, fixation eye movements and similar problems can be avoided only by losing some key features such as promptness, precision or comfort level.

Since eye movements alone can be used for human-computer interaction only for the basic level of control, complex methods combining eye movements and limb movements could be used to achieve an increase of effectiveness and comfort level of control. The problem is that scientific community is divided into specialized groups and there is a lack of research on eye-hand coordination. The relatively young society of eye movement researchers mostly treats hand movement control system as an independent source of control signal. It is known for years that eye movements influence the hand movement characteristics and vice versa, but the models of interaction between the two systems are very basic. At the point when it is essential to complement a utilization of eye movements and hand movements one other, the knowledge on human limb movements and on human eye movements separately, is no longer sufficient. Emerging need for understanding the control system responsible for eye-hand coordination leads to this investigation. Knowing coordination principles and parameters of oculo-motor and manual movement control, faster and more convenient interaction methods and devices will be possible to design.

In recent years, scientific community has made a big step forward in exploration of human brain. Understanding how human oculo-manual coordination works is

beneficial not only for a purpose to control computer-based systems. It leads to a better understanding of neural pathways in a human brain. Since areas in the brain, and at the same time the transfer of information between them, are affected by diseases and living style, introduction of a new set of the parameters based on oculo-manual coordination, promises some new ways of evaluating subject's neural health, peculiarities based on previous experience or expertise in a specific field.

### **Scientific problem**

In book „Cybernetics“, which was published in 1948, Norbert Wiener used mathematical methods of technology sciences, to describe processes of biological systems and also to describe known pathologies of such systems. This novel point of view has led to entire scientific movement, assessing biological systems from physical, technological and mathematical perspectives. Such knowledge is useful as for knowing as for diagnosing and treating living systems. Also for creating novel interaction interfaces for human to control machines. However, some human systems, such as the one used to control the coordination of human eye and arm movements, is not researched comprehensively. It is obvious, that knowledge on unexplored processes cannot be used.

Visually empty environment or reach-and-grasp-related tasks are examined in most of known research and models of eye's and arm's voluntary (non-tracking) movement coordination. There is a lack of research, where eye and arm coordination in visual environments during smooth voluntary hand movement, is investigated.

### **Working hypothesis**

As eye movements, observed during guiding a hand-manipulated object through visible path, contains some features, which are specific to smooth pursuit eye movements, it is reasonable to expect, that a common neurophysiological control system is being used. More to that – models of smooth pursuit eye movement control can be extended to explain and simulate hand-guiding eye movements.

**The aim of the dissertation** is to investigate the characteristics of the coordinated eye and hand movement control system that are relevant for developing human-computer interfaces and methods for diagnosing neurophysiological disorders.

### **Tasks of the work**

1. To review the previous study and existing knowledge on eye movements, hand movements and the control system of their coordination.
2. To evaluate the nature and the purpose of catch-up saccades and their influence on the quality of the pursuit.

3. To analyze the characteristics of the coordinated oculo-manual guiding movements and to compare them with the characteristics of the oculo-manual pursuit.
4. To determine the structure of the control system for coordinated oculo-manual guiding movements and to propose its neurophysiology-consistent mathematical model.
5. To assess the potential oculo-motor and coordinated oculo-manual movement applications in human-computer interaction and in diagnostic systems.

### **Scientific novelty**

Eye-hand coordination related functions of eye and hand movement parameters were identified experimentally. These interrelations were used for identifying neural-level processes and for developing a new mathematical model of oculo-manual coordination control system. This model explains how hand movement signals influence eye movement signals in tasks, where both types of movement are needed. Also, a mathematic model for simulating human eye-hand coordination control during the task of object guiding was developed and its output's adequacy to real human behavior was investigated.

Potential new applications for eye alone or simultaneous eye and hand movement tracking and analyzing were assessed and two of them were developed.

### **Practical value of the work**

Fundamental knowledge on oculo-manual coordination can be used to predict the behavior of an average subject in specific tasks. More to that, this behavior can be forecasted using developed models. These forecasts are valuable while assessing new human-computer interaction methods and interfaces.

Since the hand movement or eye movement analysis are known to provide some neurology-based diagnostic information, it is considered, that the knowledge on average human oculo-manual coordination parameters and their comparison to the parameters of a test subject, can be used in diagnosing the same (with a higher reliability) or other neurological disorders. It also can be used in assessment of personal characteristics, which is needed while recruiting employees for highly responsible jobs in areas such as military or aerospace.

### **Statements presented for defense**

1. Human system of smooth pursuit with catch-up saccades is also being used for a non-pursuit related purpose, i. e. while guiding a hand-moved object through a visible path.
2. Neural circuits responsible for eye-hand coordination during hand-moved object manipulation in visual environment were identified, and a human

- neurophysiology-consistent mathematical model, was designed. This model is capable of simulating human oculo-manual eye-hand coordination while guiding a hand-moved object along a visible path.
3. Models and knowledge on eye-hand coordination allow diagnosis of neural and ocular disorders in their early stages or in an effortless ways. There also are possible applications of such models in HCI and personal characteristic assessment.

### **Approval of the results**

Results of this dissertation are published in total in 16 publications and in 6 published abstracts. 3 publications are in journals, referred in the Journals of the master list of Thomson Reuters Web of Knowledge (with impact factor). One publication is published in a journal, referred in other international databases. Also, 10 publications are published in international peer reviewed scientific conference proceedings and 2 publications in Lithuanian peer reviewed scientific conference proceedings. Results were presented in 13 conferences that took part in Lithuania, France, Cyprus and Sweden. Paper presented in the conference “Biomedical Engineering 2013” has won a first place award. In 2011-2014 a doctoral fellowship, granted by Lithuanian State Science and Studies Foundation and Research Council of Lithuania, was received.

### **Structure and contents of the dissertation**

In chapter 1, the previous research on eye-hand coordination related eye movements, their models and control system, hand movements and their control system and also the eye-hand coordination and its control system, is reviewed and the most important information, used in later chapters of this dissertation is provided.

Chapter 2 introduces to common methodology and necessity for experimental research executed in this work.

The results of experimental investigation on smooth pursuit eye movements and eye-hand coordination are presented in chapter 3. This experimentally obtained data is very important in neurophysiologic and mathematical modeling, which is explained in details in chapter 4.

Possible areas of application of the new knowledge and the model acquired by this work are discussed in chapter 5. Also, some possible applications were tested and assessed in practice.

Conclusions of the dissertation are presented after each chapter and the main conclusions of the dissertation are presented after chapter 5.

The total volume of the thesis is 133 pages, 122 figures, 16 tables, 187 references and 4 appendices.

# 1. REVIEW ON EYE AND HAND MOVEMENT RESEARCH

## 1.1. Eye movements

The apparently simple task of scanning various objects of interest necessitates remarkable coordination of two independent oculo-motor systems (fig. 1.1). The versional system controls conjugate movement of the eyes, that is, movement of the eyes in the same direction to see objects positioned in various directions from us. The vergence system controls disjunctive movement of the eyes, that is, movement of the eyes in opposing directions to see objects singly at different distances from us. These two systems can shift the eyes horizontally, vertically, and in a cyclorotary manner in all directions of gaze and distances. Tables 1.1 and 1.2 provide overviews of the versional and vergence eye movement systems, respectively. You visually track the target moving in a jumping manner by a series of foveating saccades with intervening periods of fixation. If the target starts moving smoothly, you rapidly rotate your head and body (in conjunction with your tracking eye movements) to follow its path. These retinal, ocular, and combined head and body movements primarily stimulate: the saccadic system to attempt to acquire foveation; the pursuit system to match eye velocity to the velocity of the smoothly moving target; the vestibular system to stabilize gaze during the initial (approximately 30 s) transient phase of head and body rotation, and the optokinetic system to stabilize gaze during the later, sustained phase of head and body rotation. If the target is moving directly toward you, it stimulates the three active vergence subsystems – the disparity, accommodative, and proximal branches – because target disparity, blur, and proximity are dynamically changing during the approach of the target.

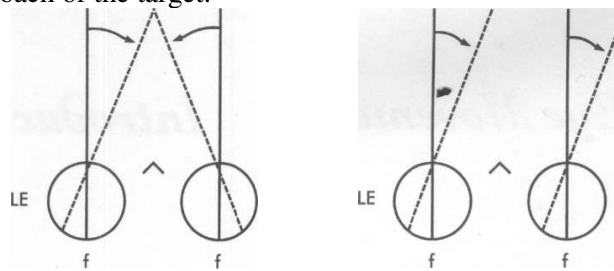


**Fig. 1.1** Schematic drawing of version (**left**) and vergence (**right**) eye movements. *LE* - Left eye; *RE* - right eye; *f* - fovea.

**Table 1.1** Versional eye movements.

Subsystem*	Stimulus	Function
Fixational	Stationary target	To stabilize a target onto the fovea
Saccadic	Step of target displacement	To acquire an eccentric target onto the fovea
Pursuit	Target velocity	To match eye and target velocities to stabilize the retinal image
Optokinetic	Target or field velocity	To maintain a stable image during sustained head movement
Vestibular	Head acceleration	To maintain a stable image with the target on the fovea during transient head movement

*\*All the subsystems listed here allow one to track a target moving in lateral extent.*

**Table 1.2** Vergence eye movements.

Subsystem*	Stimulus
Disparity (or fusional)	Target disparity
Accommodative	Target blur
Proximal	Apparent nearness or perceived distance of target
Tonic	Baseline neural innervation (midbrain)

\*All the subsystems listed here (except for tonic vergence) allow one to track a target moving in depth

When a person executes tasks of oculo-manual pointing, tracking or guiding in a 2D space, there is no need for vergence eye movements. Also some of the versional eye movements (optokinetic and vestibular) are not involved in oculo-manual coordination. It mainly utilizes fixational, saccadic and pursuit versional eye movements. Also, the properties of such eye movements are influenced by the oculo-manual coordination system. In further chapters types of eye movements involved in oculo-manual coordination in a 2D plane will be analyzed.

### 1.1.1. Fixational eye movements

During attempted steady fixation on a stationary object of regard, the eye does not remain perfectly motionless even when head is restrained. Both slow and rapid small-amplitude eye movements occur. However, the image of the object is still retained within an acceptable foveal retinal locus (approximately 0.5 deg [161]).

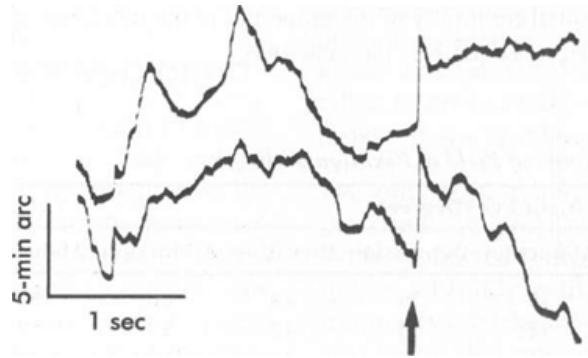
Fixational area increases with increased fixation duration. Also, the two-dimensional spatial plot is not a circular pattern but rather a pattern exhibiting a distinct directional bias. Clearly, as one might expect, fixation is central and in close proximity ( $\pm 5$  arcmin) to the target most of the time. [139].

The first fixational eye movement component is tremor: a high-frequency movement typically ranging from 30 to 100 Hz, although lower and higher frequencies may be found. The average amplitude either horizontally or vertically is approximately 20 arcsec (approximately the size of one cone diameter) and ranges from 5 to 30 arcsec. There is an inverse relationship between tremor frequency and amplitude. Tremor velocity may be as high as 30 arcmin/s. Tremor is not correlated between the two eyes. Thus, it has been thought to represent noise in the oculo-motor system that originated from irregular firing of brainstem motor neurons, that is, incomplete smooth tetanus, and resulted in independent random fluctuations in extraocular muscle fiber discharges [153]. The tremor is superimposed on the two movements described next.

The second component is drift (Fig. 1.2). Drift is a low-velocity movement, typically 1 to 8 arcmin/s with a mean of 5 arcmin/s (crossing 15 cones per second) and a maximum of 30 arcmin/s [110]. It should be emphasized that during natural activities such as ambulation, retinal-image velocity from head perturbations may be as high as 3 degrees per second [162]. This maximum motion is just at the threshold for degradation of visual acuity and stereoacuity [179]. The movement is irregular and of a variable low frequency ( $<0.5$  Hz). Its amplitude is typically 1-5 arcmin. Drift

amplitude increases slightly when retinal errors are generated only from the near and far retinal periphery [146]. Drift makes up more than 95% of one's total fixation time. Like tremor, it is not correlated between the two eyes. Drift is also traditionally believed to represent noise in the oculo-motor system and therefore to be error producing; however, there is evidence that it may be error correcting at times [111].

**Fig. 1.2** Simultaneous records of the miniature movements of the two eyes. The small-amplitude, high-frequency component is the tremor; the large, relatively slow excursions are drift; and at the arrow both eyes execute a microsaccade. It is evident that drift movements are essentially dissociated in the two eyes, whereas the microsaccade is virtually conjugate. From [181].



The third component of fixation is the microsaccade (Fig. 1.2). Microsaccades have a frequency of occurrence of 1 to 2 per second. They have a mean amplitude of 5 arcmin, are rarely larger than 10 arcmin, and may range from 1 to 25 arcmin. Microsaccades have a duration ranging from 10-25 ms and an amplitude dependent peak velocity ranging from 1 to 20 deg/s [129]. They typically have a large dynamic overshoot component. Unlike tremor and drift, microsaccades are always binocular and have a high amplitude correlation (0.6 to 0.9) between the eyes, [122] what suggests that they are under central neurologic control. They are traditionally believed to be error correcting, although prominent exceptions may occur both in persons with normal vision and in patients with abnormal vision.

The neurophysiology of fixation. There are midbrain oculo-motor neurons whose firing rate (within their active range) is linearly related and therefore proportional to gaze angle [143]. To shift the eyes to different gaze angles, a saccade is used. A saccade's neural signal consists of a pulse of increased innervation to move the eye rapidly by some specific magnitude and a step of innervation (integrated pulse) to hold the eye in this new position. Therefore, one can think of the steady-state gaze-related neural signal simply as a step. If this step of innervation is properly maintained without any decay (assuming a perfect integrator), it prevents the eye from shifting back to the midline due to the elastic restoring forces of the extraocular muscles and surrounding orbital contents; thus accurate fixation is sustained. Small fluctuations in this signal, however, give rise to tremor and drift. The neurologic substrate involved in neural integration and related gaze-holding functions consists of the nucleus prepositus hypoglossi and medial vestibular nucleus for horizontal conjugate movements and, probably, the interstitial nucleus of Cajal for vertical conjugate movements [102].

The fixational eye movement system exhibits no significant age-related changes in overall stability [110].

### 1.1.2. Saccadic eye movements

Saccades are accurate, high-velocity, ballistic eye movements used to foveate objects of interest. Most naturally occurring saccades (85%) are less than 15 deg in amplitude [9]. During a saccade a neural signal related directly to eye movement (or its intended or attempted movement) called efference copy is generated. This motor-based information, in the form of a corollary discharge signal, is sent to higher-level brain centers and informs the brain that the world has not shifted but rather that the eye (and retinal image) indeed has, thus leading to perceptual stability [102].

Saccades are neurally generated by the combination of a high-frequency pulse and a much lower-frequency step. The pulse is necessary for overcoming the viscous resistance of the globe and orbital contents and is responsible for moving the eye rapidly to the new position. The step is necessary for overcoming the elastic restoring forces of the eye and orbital contents and is responsible for maintaining the eye in this new position. This pulse-step controller signal produces excitation to the agonist muscle, which is mirrored by a similar inhibitory signal to the antagonist muscle. These signals, however, are effectively smoothed because of the relatively slow development of muscle tensions and resultant forces necessary to move the globe to produce this rapid movement [4] (Fig. 1.3).

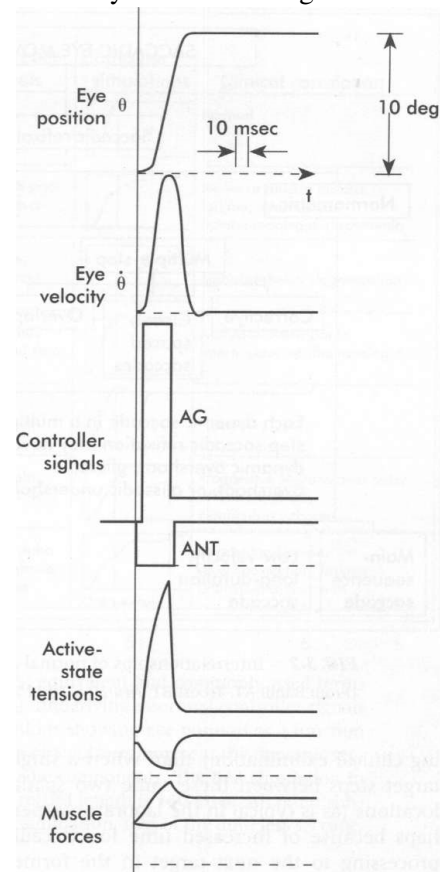


**Fig. 1.3** Signals involved in the transformation of input commands into eye movements. The pulse-step controller signal has abrupt transitions that are filtered out by the activation and deactivation time constants to produce the active-state tensions. These in turn are filtered by the series elasticity and the nonlinear force-velocity relationship to produce the forces that are applied to the globe. *AG* – agonist; *ANT* – antagonist. From [4].

Saccadic eye movements may be categorized [9] as shown in Fig. 1.4. In this chapter, the larger refixation saccades are discussed. Essentially a saccade is either normometric or dysmetric. A normometric (also called orthometric) saccade consists of a single, accurate movement having appropriate gain and dynamics. The underlying neural controller signal consists of a single, precisely matched pulse-step combination. In contrast, in a dysmetric saccade some of the conditions just stipulated for a normometric saccade are not met. Dysmetric saccades can be either single-step or multiple-step movements and can be either too small (hypometric) or too large (hypermetric) with respect to the intended target position.

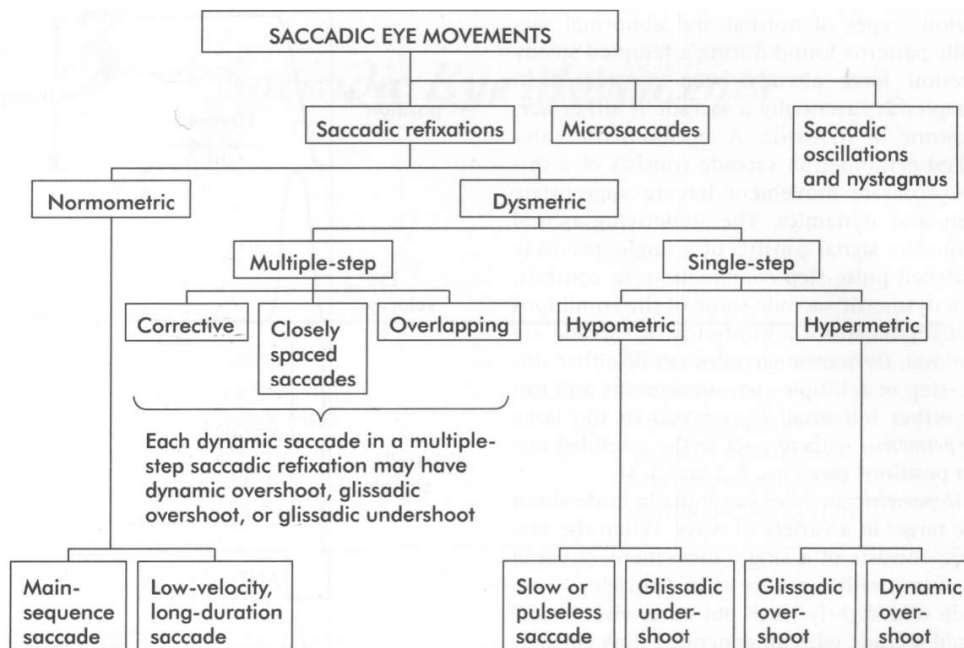


**Fig. 1.4** Normal and abnormal saccadic eye movement subtypes. From [9].

Hypometric saccades can initially undershoot the target in a variety of ways. When the saccade consists of a single movement, it could represent either a very slow pulseless saccade or a slightly small but otherwise normal rapid saccade with an appended slow glissadic component (for example, the pulse is too small for the appropriate step). If of the multiple-step variety, the saccade could represent a low-gain saccade, which necessitates one or more subsequent smaller corrective movements to attain precise foveation. A primary saccade that has nearly normal gain (that is, amplitude of the initial eye movement divided by amplitude of the target movement: normal values are  $0.92 \pm 0.03$ ) [25] and is only slightly reduced may represent a normal strategy adopted by the saccadic system so that any subsequent corrective saccade ( $\sim 150$  ms later) requires less computation (for example, only amplitude, not direction) [10]. That type of saccade could also be due to prediction, in which the eye moves in advance of the step target change, but in such cases the gain of the primary saccade is lower and more variable ( $0.8 \pm 0.10$ ) [25]. Closely spaced or overlapping saccades are generally due to fatigue or disease.

Hypermetric saccades can initially overshoot the target in a variety of ways. Such saccades that consist of a single movement could represent either a slightly larger but otherwise normal saccade with an appended slow glissadic component (for example, the pulse is too large for the appropriate step) or a dynamic overshoot (for example, the pulse quickly switches direction to produce a small ( $0.25$  deg), rapid ( $15$  ms), nonvisually-guided reversal in the direction of saccadic eye movement). This latter movement may represent a time optimal behavior that places the target within the general foveal region as rapidly as possible. The multiple-step variety, in which

the first saccade overshoots the target and a subsequent, visually guided corrective saccade occurs (150 ms later) to attain foveation, represents a high-gain saccade (that is, static overshoot), which is typically seen in cerebellar disease [151] and is infrequently seen in persons with normal vision [23].

Saccade dynamics in other than horizontal directions are quite similar to those found for horizontal saccades. For example, the relationship between saccade amplitude and its correlated peak velocity is the same [12]. However, the trajectory for oblique saccades is more curved than that found in either their vertical or horizontal counterparts [14].

Saccadic latency, or reaction time, typically refers to the time from onset of the non-predictable step of target movement to onset of the saccadic eye movement initiated to foveate the displaced target. Saccadic latency is approximately 180-200 ms, with a SD of 30 ms [10]. Saccadic latency can be affected by a variety of factors. Under typical clinical test conditions, however, the physical characteristics of the target itself (luminance, size, and so forth) have little impact (<30 ms) on saccadic initiation and its potential diagnostic importance [12]. Factors such as target predictability, as well as patient motivation and attention, play a much larger role in the elicitation of a saccade.

This saccadic delay includes both noncognitive and cognitive factors: [13]

- Afferent or visual neurosensory delay of approximately 50 ms, which includes neural transmission time from the retina to visual cortex to high-level centers involved in the saccadic decision making process.
- Efferent or neuromotor delay of approximately 30 ms, which includes neural transmission time within higher-level centers involved in the saccadic decision making process, as well as lower-level signal processing within the midbrain.
- Computational delay of approximately 50 ms, which, along with the first two factors listed, may be regarded as noncognitive.
- Decision-making processing delay of at least 50 ms. The brain is deciding whether and where to change gaze in the field, thus involving higher-level cognitive processing.

There is a systematic increase in latency (horizontal and vertical) with age in adults (1 to 2 ms per year) as is expected and is found in all types of reaction time measures in elderly persons [124, 126, 177]. This result suggests increased higher-level processing time or reduction in neural transmissibility [126]. Peak saccadic velocity (horizontal and vertical) has also been shown to decrease with increased age in adults (1 deg/s per year) in most studies, [124, 126, 177] possibly because firing asynchrony in the neural elements would produce a slightly less peaked brief pulse component. Saccadic gain, accuracy, and anticipation effects do not appear to change considerably with age in most studies [177]. The magnitude of all the effects just mentioned, however, is generally not large enough to be detected on routine clinical examination.

Short-term saccadic adaptation (also called parametric adaptation) [91] refers to the normal, self-correcting, rapid (within a few minutes) dynamic changes in effective calibration of the saccadic eye movement system (by the cerebellum [151]) that reduce the probability of occurrence of an inaccurate saccade. Such changes under normal

conditions could arise as a result of fluctuations or small errors in the neural and biomechanical properties of the saccadic eye movement system. To maintain accurate saccades in the presence of such potential internal system variations, it is necessary to monitor the initial system error and dynamically compensate as necessary to keep this error within system tolerance and normal limits (for example, hypometria with <10% of the initial error) [10].

Short-term saccadic adaptation has the following properties [152, 62]:

- Adaptation may occur after as few as 70 saccades.
- Because the time course of adaptation is exponential, it can be defined in terms of the time constant (that is, the number of conditioning saccades needed to attain 63% of the final adaptation amount).
- The system response decrease is faster, easier, and more complete than the system response increase. A decrease probably represents a general overall reduction in gain, whereas an increase may represent a specific endpoint adjustment.
- Adaptation is directionally selective; therefore, response changes are unidirectional.
- Response reduction is adapted for a range of saccade amplitudes; therefore, the effect exhibits transfer beyond the specific step amplitude used to obtain the initial adaptation.
- The system exhibits the same time course of adaptation whether the error step amplitude is progressively increased or just remains fixed at the final level.
- The individual is not consciously aware of the ongoing adaptive process.

One way to assess the overall neurologic integrity of the saccadic eye movement system noninvasively in the clinic or clinic laboratory (other than using various brain imaging techniques) is to record them objectively and then quantify the relationship between saccades of various amplitudes and their respective peak velocities. This relationship has been called the main sequence [6]. The main sequence can also be extended to include saccade duration and saccade peak acceleration and deceleration. One such combined plot [5] for normal individuals is presented in Fig. 1.5. Clearly, as saccade amplitude increases, the correlated saccade duration ( $2.2 \times \text{amplitude} + 21$  ms), peak velocity, and peak acceleration systematically increase over the range for which they are typically tested (Table 1.3). Saccades evoked by most normal means and conditions faithfully follow this relationship. However, important exceptions are: drugs that reduce alertness, diseases (systemic: Grave's disease; neurologic: Alzheimer's disease, acquired immunodeficiency syndrome), peripheral nerve palsy, darkness (10% slower), infancy, age, reduced attention, fatigue, orbital direction (centripetal slightly faster than centrifugal), gaze angle (extreme gaze resulting from biomechanic and neurologic limitations), hemifield (upper hemifield is slightly slower than lower).

**Table 1.3** Saccadic magnitude, peak velocity, and duration for representative saccades in normal young adults. From [5].

Magnitude (deg)	Peak velocity and SD (deg/s)	Duration and SD (ms)
5	261 ±42	42 ± 8
10	410 ±67	51 ± 8
15	499 ± 43	54 ±7
20	657 ± 78	64 ±6

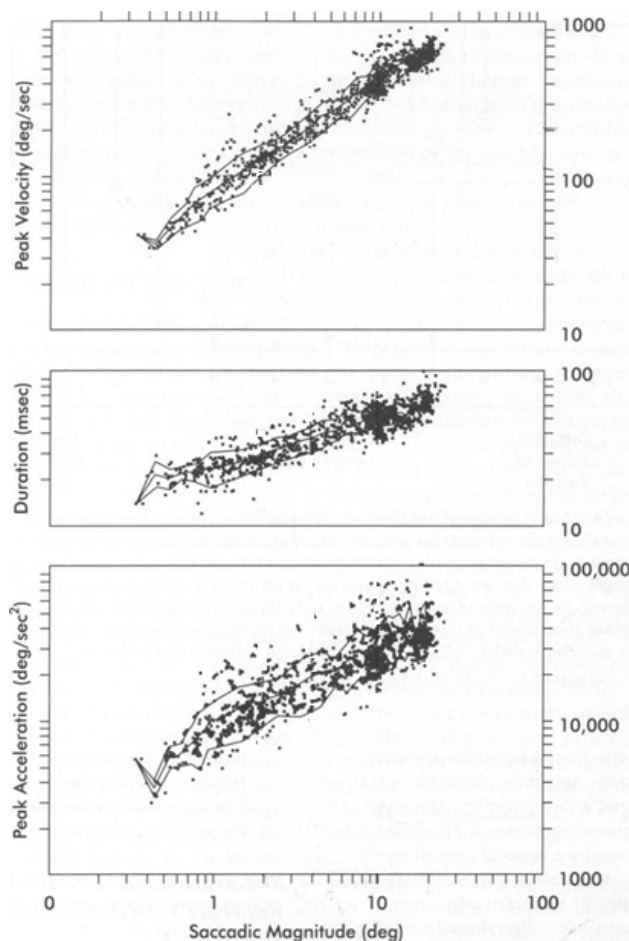


**Fig. 1.5** Main-sequence diagrams showing peak velocity, duration, and the peak acceleration as functions of saccadic magnitude for the saccadic eye movements of 13 individuals with normal vision. From [5].

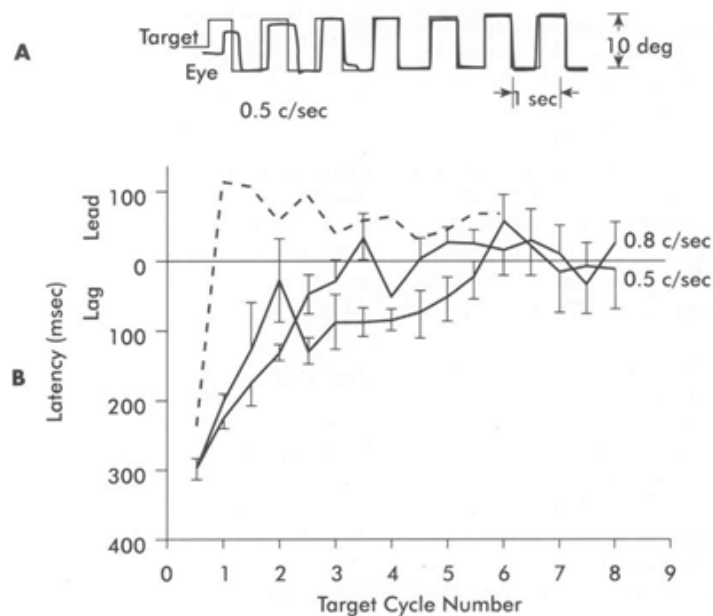
The main sequence relationship reflects the pulse component of the pulse-step neurologic controller signal for saccades: under normal test conditions for saccades (horizontal, vertical, and oblique) [12] generated over the central field ( $\pm 20$  deg), each point fits within the normal dispersion of peak velocity values for that amplitude, thus suggesting normal integrity of the central and peripheral neurologic pathways (when

system biomechanics are normal). There are no objectively documented, irrefutable cases of supernormal saccades truly falling above the normal range. However, saccades with clearly reduced peak velocities may occur as a result of various drugs and diseases, and these may effectively reduce, degrade, or distort the pulse component of the pulse-step neurocontroller signal.

Saccades are generally considered to exhibit prediction when their reaction times range from approximately 200 ms before to 150 ms after target movement (Figs. 1.6 A, B, and 1.7 A, B, C, D). Predicted saccades are generally hypometric [25].

Individuals of all ages and backgrounds demonstrate prediction, frequently within 5 cycles or so of repetitive target motion [52, 145]. Presence of this is evident in experimental findings in both adults and young children. In the classic study by Stark and colleagues [160, 161]. Trained adults horizontally tracked either unpredictable steps (with respect to direction, amplitude, and duration) or predictable steps (10 deg amplitude and 0.05-2 Hz frequencies) over the central field. Prediction was greatest at the intermediate frequencies (0.4-1.0 Hz) with a peak at 0.8 Hz. However, prediction was still present to some degree with frequencies as low as 0.2 Hz and as high as 1.5 Hz. Similar results in adults were later found by Dallos and Jones [35]. Young children demonstrate the same predictive capacity [145].

**Fig. 1.6** **A:** Saccadic tracking. Typical eye response to a 0.8 cycles/s horizontal target. **B:** Time course of adaptation of the saccadic latency to periodic square-waves averaged for two naive human subjects. Each point represents the mean of seven runs; the vertical bars represent standard errors of the mean. The dashed line is the average of three runs on one naive subject at 0.5 cycles/sec under experimental conditions. From [52].



The major neuroanatomic structures involved in the generation of saccadic eye movements. The neural control aspect may be divided into two main categories [102]. The first, considered to reflect higher-level control processes, includes the primary structures involved in target selection, localization, and initial calculation of the desired change in eye position, as well as external shaping of the final neural signal. The second, considered to reflect lower-level control processes, includes primary structures involved in the actual generation of the pulse-step controller signal to the oculo-motor neurons.

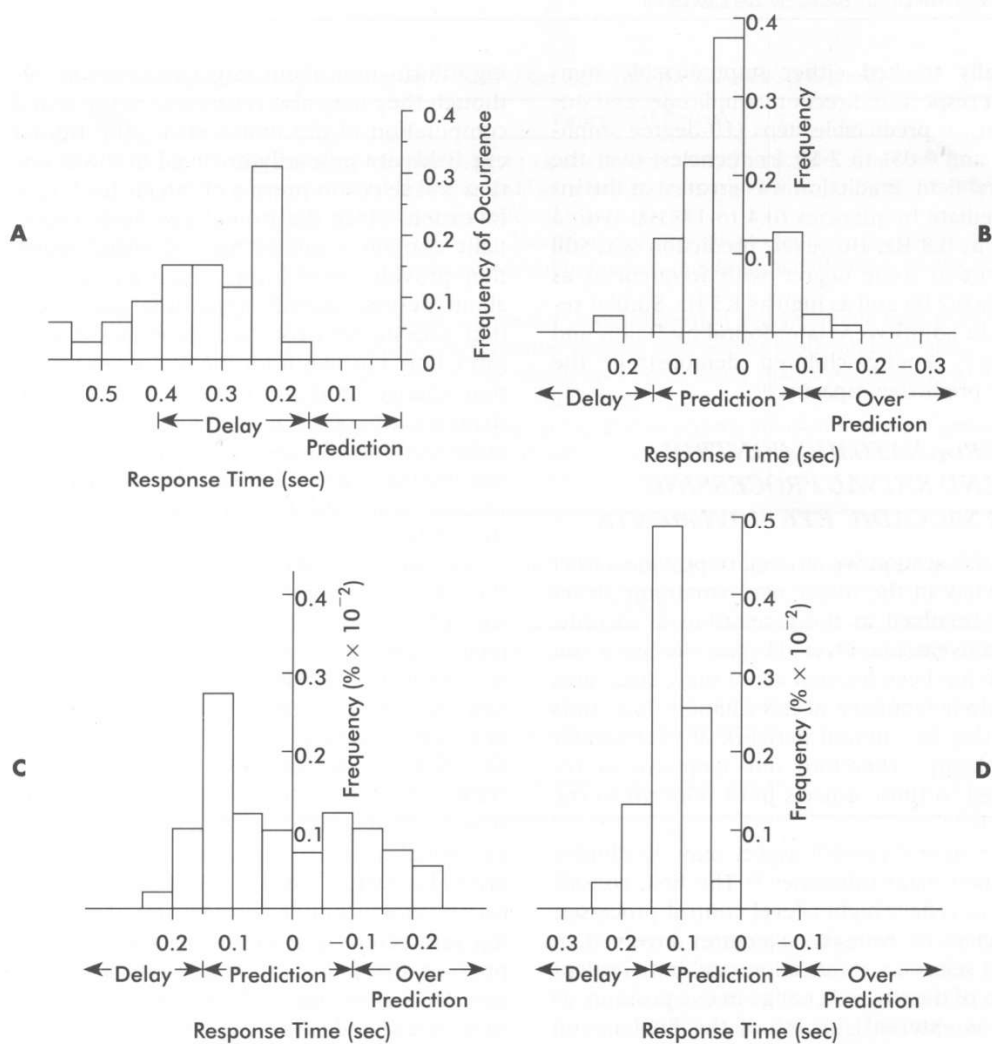


**Fig. 1.7** Histograms of the frequency of occurrence of eye movement response times for target motions of irregular steps and regular square-waves of different frequencies. Irregular steps (A). Square-waves, 0.4 cycles/s (B). Square-waves, 1.0 cycles/s (C). Square-wave, 1.5 cycles/s (D). From [160].

The primary higher-level control structures [44, 58, 118] include the frontal eye fields, parietal lobes, superior colliculus, and cerebellum (Tables 1.4 and 1.5). The frontal eye fields and parietal lobes are cortical structures that transmit information to the superior colliculus. The parietal lobes are primarily involved in providing information about target localization, although they may also contribute to the initial computation of the motor error. The frontal eye fields are primarily involved in the attention and selection process of targets for future foveation. Since the frontal eye fields essentially contain a neural map of visual space, they provide the requisite initial information about desired saccade amplitude and direction. The superior colliculus

processes this information, encodes it for the desired eye position change, and transmits it to brainstem structures involved in generating the coded pulse-step signal. The cerebellum acts as a calibration site [151] attempting to maintain saccadic gain within normal tolerances and thus influencing the final pulse outcome.

**Table 1.4** Higher-level neuroanatomic sites that influence saccadic pulse generation.

Site	Functional Role(s)
Frontal eye fields	Regions mapped with respect to size and direction of a saccade; send such information related to future saccade generation to superior colliculus; inhibit fixation "reflex" to permit occurrence of future saccade.
Parietal lobe	Sends information related to localizing and attending to future targets in the fields and sends computations related to saccade amplitude and direction to superior colliculus.
Superior colliculus	Receives input related to intended saccade direction and amplitude from frontal eye fields and parietal lobes; regions mapped with respect to size and direction of future intended saccade; encodes desired eye position change with respect to fovea and relays this information to brainstem.
Cerebellum	Receives input from brainstem and related structures involved in saccade generation; outputs to brainstem and other saccade-related sites to maintain or adapt saccadic gain, or both, and therefore controls saccadic accuracy.

**Table 1.5** Effects of lesions in some higher-level sites on saccadic eye movements.

Site	Effect
Frontal eye fields	May produce increased saccadic latencies, slowed saccades, and impaired predictive tracking.
Parietal lobe	May produce increased saccadic latencies, hypometria, slowed saccades, impaired predictive tracking, and moderate ocular motor apraxia.
Superior colliculus	Isolated lesions not reported.
Cerebellum	May produce saccadic dysmetria (especially hypermetria).

The second, lower-level process involves the actual generation of the pulse-step neural controller signal [79]. This signal-processing phase demands precise synchronization of two basic neural elements – burst and pause neurons [102] (Fig. 1.8). The burst neurons for horizontal saccades are located within the paramedian pontine reticular formation (PPRF) or pons; those for vertical and torsional saccades are situated within the rostral interstitial nucleus of the medial longitudinal fasciculus (MLF). The short-lead excitatory burst neurons (EBN) only begin high-frequency firing just before and during a saccade. They produce the pulse of neural activity that is correlated with the peak velocity and amplitude of a saccade. The long-lead excitatory burst neurons (LLBN) exhibit firing rates that are of low frequency and irregular, and their activity may occur several hundred milliseconds before a saccade. Long-lead excitatory burst neurons are probably involved in synchronization of overall premotor saccadic pulse generation. In contrast, the pause neurons, which are located in the nucleus raphe inter-positus of the midbrain, fire continuously except just before and during a saccade. They act to inhibit the EBN during saccadic-free periods.

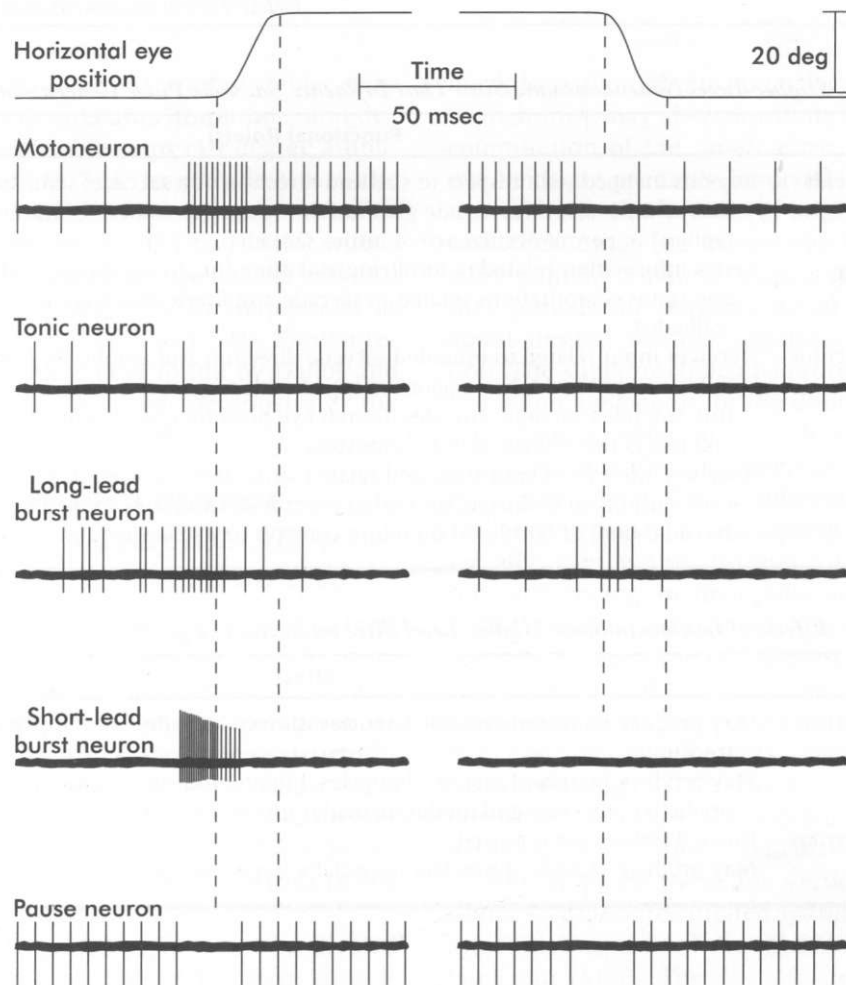


**Fig. 1.8** Typical neural discharge patterns of brainstem cells during saccadic eye movements. The vertical dashed lines mark the onset and offset of a saccade in the ipsilateral (**left**) and contralateral (**right**) directions. All the cell types shown except the motor neuron are found in the paramedian pontine reticular formation. Tonic neurons are better named eye position-related and are most frequently found in the vestibular nucleus and the nucleus prepositus. From [79].

Thus the basic sequence of events is as follows (Fig. 1.9):

1. The pause cells receive information from higher-level centers, such as the superior colliculus and frontal eye fields and perhaps the LLBN, that a saccade is being planned. These signals act to inhibit the pause cells.
2. The inhibited pause cells thereby release their inhibitory influence on the EBN, thus allowing the EBN to fire precisely when the pause cells are quiescent. This EBN signal is the pulse component of the pulse-step saccadic neural signal.
3. The pulse signal bifurcates; it goes to the oculo-motor neurons as well as to the neural integrator. The neural integrator for horizontal saccades is located in the

nucleus prepositus hypoglossi and in the medial vestibular nucleus, whereas for vertical saccades it is located in the interstitial nucleus of Cajal (and related midbrain structures).

4. The neural integrator converts this eye velocity-coded information into eye position-coded information; therefore, the pulse becomes a step.
5. The individual pulse and step components combine at the oculo-motor neurons to become the pulse-step controller signal that is transmitted to the appropriate oculo-motor nerve(s) and then to the extraocular muscle(s) to produce a saccadic eye movement.

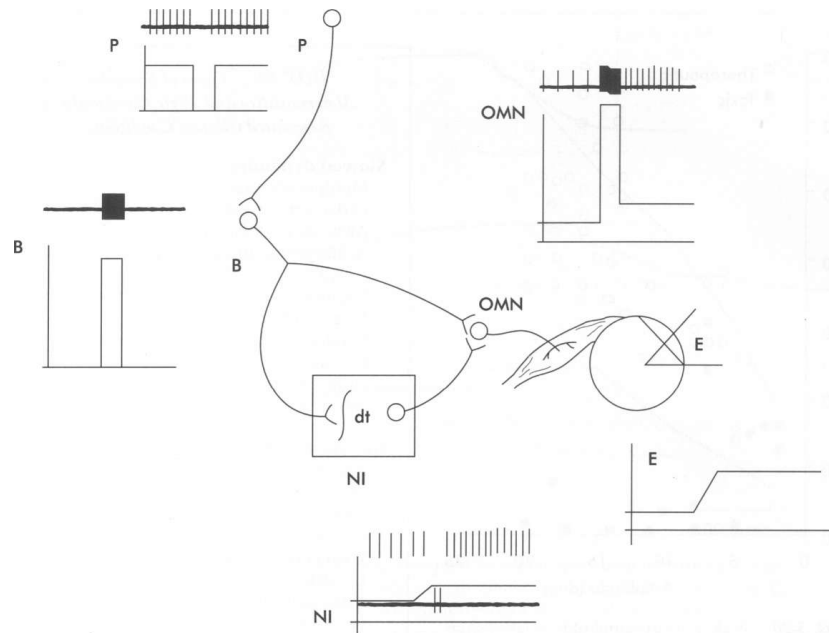
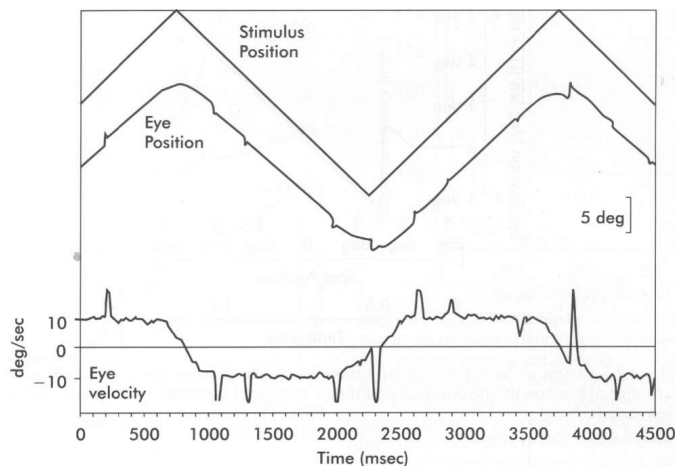


**Fig. 1.9** The relationship between pause cells (*P*), burst cells (*B*), and the cells of the neural integrator (*NI*) in the generation of the saccadic pulse and step. Pause cells cease discharging just before each saccade, allowing the burst cells to generate the pulse. The pulse is integrated (*dt*) by the neural integrator to produce the step. The pulse and step combine to produce the innervational change on the ocular motoneurons (*OMN*) that produces the saccadic eye movements (*E*). Vertical lines represent individual discharges of neurons. Underneath the schematized neural (spike) discharge is a plot of discharge rate versus time. All presented as a function of time. From [102].

### 1.1.3. Smooth pursuit eye movements

The pursuit system is used for the smooth tracking of discrete objects of interest moving in a field of vision. At the most basic level the pursuit system's goal is to match eye velocity to target velocity as closely as possible [160, 182]. Any positional error in smooth tracking resulting in either a lead or a lag of the eye with respect to the target is typically corrected by an independently generated saccade [24, 134] (Fig. 1.10). Thus, sustained periods of foveal pursuit allow maximal resolution, information gathering, and processing of fine details of a moving object.

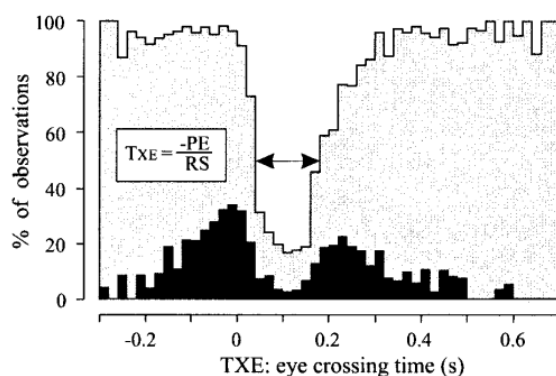
**Fig. 1.10** Individual eye movements in response to triangle-wave constant velocity stimuli moving at 0.33 Hz. Upward deflections of the curves indicate rightward movements. Slow eye velocity changed before each change in target motion. From [21].



It is known that the occurrence of catch-up saccades during smooth pursuit eye movements depends on two

parameters: a retinal slip (difference between the velocities of the target and the eye) and a position error (distance between the positions of the target and the gaze) [97, 93]. The triggering of catch-up saccades is dependent on another tracking parameter (which depends on both position error and retinal slip by an equation provided in Fig. 1.11): the eye crossing time. It is the prediction of oculo-motor system of the time at which the eye trajectory will cross the target. On average, for the eye crossing time between 40 and 180 ms, no saccade is triggered and target tracking remains purely smooth. Conversely, when the eye crossing time become smaller than 40 ms or larger than 180 ms, a saccade is triggered after a short latency (around 125 ms). [26]

**Fig. 1.11** Quantitative analysis of the limits between smooth and saccadic zones. The relative number of saccade trials (gray histogram, n=2733) is illustrated as a function of the eye crossing time  $T_{XE} = -PE/RS$ . The black histogram shows the proportion of late saccade trials (n=542). Bins of 20 ms are represented. The double arrow shows the limits of the smooth zone ( $40 \text{ ms} < T_{XE} < 180 \text{ ms}$ ). From [26].



Important facts about the pursuit system are briefly listed as follows:

- The pursuit system is traditionally viewed as a continuous control system [141, 160, 182], thus it samples the stimulus continuously and responds to any change within one latency period or reaction time. In contrast, the saccadic system has been conceptualized as a sampled-data or discrete system with a (relative) refractory period.
- The initial 100 ms presaccadic pursuit movement, however, is effectively open-loop (i. e. not yet altered by visual feedback information); the initial 20 to 40 ms portion is independent of target stimulus characteristics and simply functions to

initiate an eye movement in the correct direction. Only the latter 60 ms period is loosely related to target velocity and eccentricity [105, 170] (Fig. 1.19). Subsequent pursuit related to either real or perceived target velocity is under visual feedback control (closed-loop).

- The pursuit system has a latency of 100 ms with little variability ( $\pm 5$  ms); latency is slightly longer (by as much as 25 ms) for slow target velocities ( $< 5$  deg/s) [30] (Fig. 1.13).

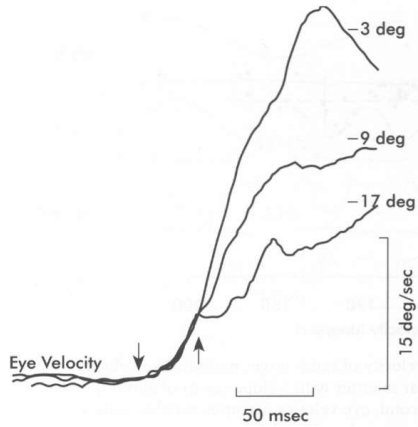


**Fig. 1.12** Eye velocity during the onset of pursuit to 15 deg/s ramp target motion; the ramp of motion had different eccentricities. The velocity of the early component (arrows) was the same for all starting positions, but the velocity of the late component varied. From [105].

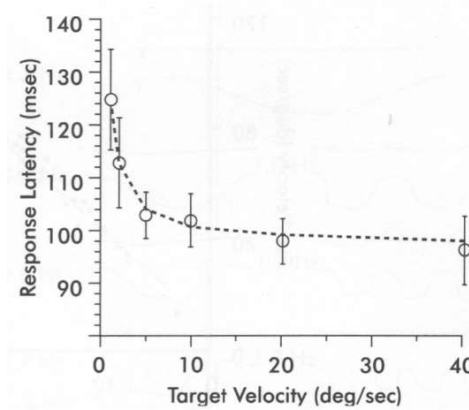
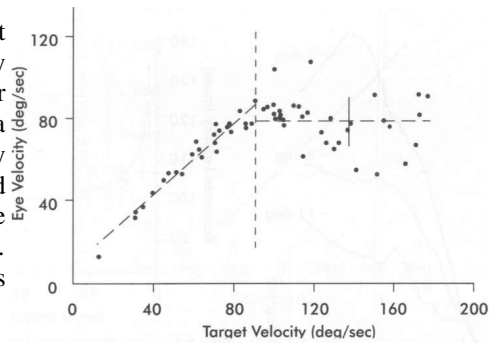


**Fig. 1.13** The relationship between target velocity and mean response latency for seven subjects. The vertical bars represent SD (inter-subject variability). The dashed line connects latencies predicted by a model in which latency is  $98 \text{ ms} + (0.028 \text{ degrees per target velocity})$ . From [30].

- Closed-loop pursuit gain (ratio of eye velocity to target velocity, determined at the midpoint or maximal-velocity portion of the response) is generally 0.9 to 0.95 [49] (low normal is 0.747), indicating a high degree of accuracy for target velocities up to 30 to 40 deg/s. Beyond this, in some subjects under optimal conditions, relatively high-gain pursuit up to 100 to 150 deg/s is possible [115] (Fig. 1.14); otherwise, a velocity saturation is evident and thereafter gain is generally markedly reduced and more variable.
- The value for open-loop gain is generally 20, [142] although a value as low as 4 may still be regarded as normal [8].
- Vertical pursuit has a lower gain, greater phase lag, and more frequent, larger error-correcting saccades than horizontal pursuit [144].
- Only with a (sustained) retinal velocity error of  $> 3$  deg/s would the increased retinal-image motion (not including spatial degradation that is due to retinal eccentricity) reduce effective resolution of the target [104].
- Steady-state gain is little affected by moderate target eccentricity [34].

- Gain may be reduced (by 10% to 20% or more) with addition of either a stationary or a moving background, [127] especially if positioned at or near the target plane [67].

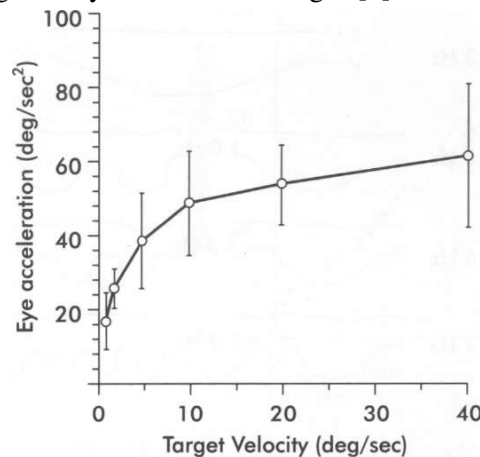
**Fig. 1.14** Eye velocity plotted against target velocity of ramp target motion. Eye velocity increases with target velocity in a roughly linear manner with a slope (gain) of about 0.9. At a target velocity of about 100 deg/s, eye velocity becomes variable, fails to increase further, and in fact seems to decrease. Variability at large velocities is indicated as SD by the solid line. Vertical dashed line represents the 90 deg/s break point. From [115].



- Gain reduces with increased target amplitude over the range of 5 to 20 deg (for a fixed frequency), presumably because of acceleration saturation limits [102].
- Pursuit ability is enhanced by the addition of either auditory or proprioceptive and tactile information, or both, related to target position, as occurs in many real-life tracking tasks [70].
- The pursuit system receives numerous inputs from the visual motion pathways, including information about direction and movement [104].
- The primary input to pursuit has been regarded to be target velocity, [134] although target acceleration appears to play an important role, [102, 142] and target position may even assist to drive the system under certain conditions [132].
- Pursuit gain is related to maximal target acceleration rather than to its velocity; in addition, maximal eye acceleration rather than velocity is related to retinal-error velocity [102]. These two pieces of information provide strong support for the notion that the various visual inputs function as commands for eye acceleration. This way sensed and processed velocity tracking errors would result in related changes in eye velocity [102, 104].
- Pre-saccadic pursuit acceleration is generally less than 50 deg/s<sup>2</sup> [8] and is dependent on target velocity [30] (Fig. 1.15).

Most oculo-motor subsystems exhibit some degree of reduced performance with advancing age: reduced (dual-mode) closed-loop gain [123, 130, 73, 124]; increased overall saccade frequency [32,

**Fig. 1.15** The dependence of pre-saccadic acceleration on target velocity for the same subjects as presented in Fig. 1.20. There is an increase of only 10 deg/s<sup>2</sup> in acceleration for a fourfold increase in target velocity above 10 deg/s. From [30].



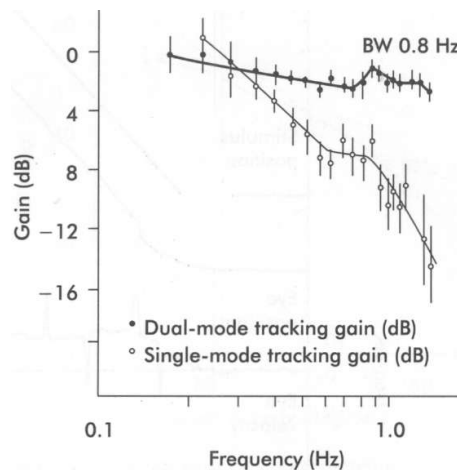
123, 124]; reduced initial acceleration [123, 124]; increased velocity latency [123, 124]; increased distractibility (an increased number of anticipatory saccades during pursuit in the presence of a competing visual stimulus) [77]; increased square-wave jerk frequency [77].

Prediction denotes a pattern of target motion that is constrained so that one obtains considerable information from past target movement that permits highly likely guesses about its future behavior [160, 161]. When an experienced or even a naive subject is provided with a predictable stimulus, he or she rapidly learns to predict and track the target accurately [161]. In fact, it is difficult for one not to predict or anticipate target motion, even when it is presented in a non-predictable manner [59]. Individuals may even track smoothly moving predictable targets that disappear for up to a few seconds, although their nonvisual feedback-related predictive gain during this period is noticeably reduced [109, 128, 33].

From experimental trials, using both predictable stimuli (simple sinusoids of constant amplitude frequencies) and non-predictable stimuli (sum of four to seven simple sinusoids) it is known that, with a predictable input the eye reasonably faithfully tracks the target to approximately 1 Hz before the gain reduces, and the lag increases. In contrast, with the non-predictable input, response attenuation with considerable lag present is the rule, since such a target is quite difficult to follow because of its lack of predictability [35, 161]. It is evident from the eye movement records associated with the non-predictable input that, in addition to overall reduction in pursuit component, there is a concurrent increase in saccadic component (i. e. catch-up saccades) to correct the resultant dynamically accumulating position error. Thus with the higher-frequency sinusoidal inputs increasingly greater amounts and sizes of saccades are being used to assist and improve overall tracking performance and are used in keeping the target on the fovea for maximal visual acuity benefit. In the computation of dual-mode pursuit gain, saccades actually contaminate the results and give the impression of better smooth pursuit tracking performance than is really the case. Therefore, Bahill, Iandolo, and Troost [7] performed a Bode gain analysis both with and without inclusion of these saccades. The results are presented in Fig. 1.16. As expected, the single-mode tracking (pursuit without saccades) was considerably poorer at the intermediate and high frequencies when compared with the more typical dual-mode tracking (pursuit with saccades) results.

The mentioned studies suggest the

**Fig. 1.16** Single-mode pursuit Bode gain plot. Computed from 35 minutes of artifact-free data gathered on five separate days on one individual (*BW*). The vertical bars represent the 95% confidence intervals. From [7].

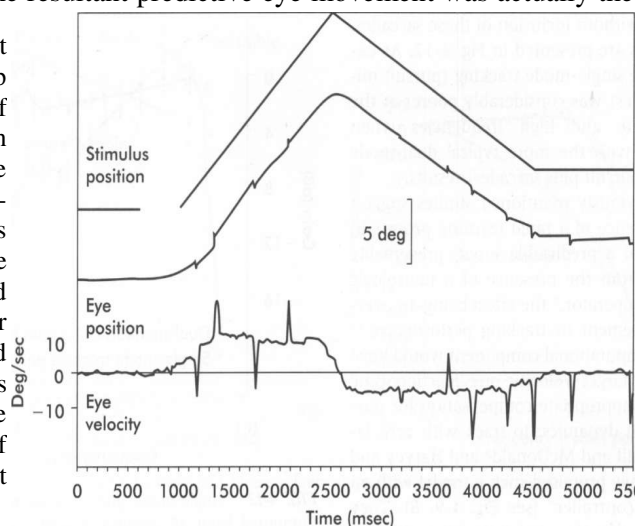


occurrence of a rapid learning process in response to a predictable input, presumably

resulting from the presence of a neurologic predictor operator, the effect being an overall improvement in tracking performance [35]. Such a computational component would have to predict target velocity one reaction time later, with appropriate compensation for pursuit system dynamics, to track with zero latency. Bahill and McDonald [8], also Harvey and Bahill [61] have proposed such a model with an adaptive controller. They speculated that the model would use menu selection to predict target velocity. The pursuit system would have a menu or listing of target waveforms that it has learned to track. Once the system identifies a waveform (target movement pattern), it would use that equation to compute the requisite neural adaptive signal. If a novel stimulus is then presented, it would attempt to track the target, probably using a least means square estimation process (e. g. tracking until the resultant error is minimal), until a new equation accurately describing the target waveform is established and added to its menu.

Some investigations [20, 24] have attempted to link so-called anticipatory smooth eye movements [75, 178] to predictive eye movements. Anticipatory eye movements are low-velocity smooth movements (generally  $<1$  deg/s and rarely  $>4$  deg/s) that occur either before expected target motion or before its cessation [20, 24]. Furthermore, their initiation and velocity characteristics are stimulus dependent [24]. Boman and Hotson [24] observed that similar predictive eye movements occurred before and during the change in direction of motion of their double-ramp stimulus. Using quantitative modeling to compare anticipatory with predictive movements at these two points, the authors demonstrated that the predictive movements were really the summation of anticipatory movements. That is, at the double-ramp directional turnaround point (Fig. 1.17), the resultant predictive eye movement was actually the

**Fig. 1.17** Individual eye movement to a predictable double-ramp stimulus with an occlusion of stimulus and 180 deg direction change. Upward deflections of the curves indicate rightward movements. In this trial the target was extinguished at time 0.6 s. The target reappeared 0.4 s later and moved rightward at 10 deg/s for 1.5 s, reversed direction and moved leftward at 6 deg/s for 2 s and then stopped. Slow eye velocities changed before each of these three changes in target motion. From [20].



summation of an anticipatory deceleration to the soon to be terminated 10 deg/s ramp portion and an anticipatory acceleration to the soon to begin 6 deg/s ramp position. The authors also speculated that anticipatory slow eye movements may serve an important function by aiding resynchronization of eye movements in expectation of abrupt directional changes of the target, as well as disengaging the eye from active

fixation to prepare for the subsequent active pursuit, once the formerly fixated target actually begins to move smoothly [20, 24].

The details on the primary neuroanatomic structures involved in the generation of pursuit eye movements are less well defined than for the saccadic system. Much has been learned from lesion studies in monkeys and case reports in humans. The following is a simplified representation of the pursuit neural pathway [79, 102, 104, 132] (Fig. 1.18 A): The primary striate visual cortex (VI) contains cells responding to stimulus motion, which project heavily to the middle temporal (MT) area of the extrastriate visual cortex. The MT area encodes and processes the direction and velocity of stimulus motion, and then it projects to the adjacent medial superiorotemporal (MST) visual area. The MST area encodes both visual signals related to pursuit and the efference copy of the eye movement command. Both the MT and MST areas project to the posteroparietal cortex (PPC), which plays a role in attentional aspects of target motion. The MT and MST areas and the PPC project to the frontal eye fields (FEFs, area 8), which contain neurons that fire during pursuit, especially during predictive movements. The MT and MST areas and FEFs project to the dorsolateral pontine nucleus (DLPN), which contains cells exhibiting direction selectivity, and they discharge in response to pursuit movements. The DLPN also receives the efference copy signal from the MST area. The DLPN projects to the cerebellum (flocculus, paraflocculus, and vermis). The flocculus and paraflocculus contain Purkinje cells that discharge with respect to gaze velocity during pursuit; the vermal neurons encode target velocity in space (eye velocity plus retinal slip velocity). The cerebellum projects to the brainstem, especially to the medial vestibular nucleus (MVN), which discharges according to gaze velocity, and the nucleus prepositus hypoglossi (NPH). Both brainstem structures are probably involved in neural integration, which converts the eye velocity signals to eye position signals, which in turn project to the oculo-motor neurons to move the eye smoothly (Fig. 1.18 B). Insult or disease anywhere along these pathways may cause a pursuit defect. These are listed in Table 1.6.

**Table 1.6** Effects of lesions on horizontal pursuit eye movements.

Site	Effect
Primary visual cortex	Unilateral lesion produces a contralateral defect.
Middle temporal area	Lesion produces a scotoma specific only for visual motion.
Middle superiorotemporal area	Unilateral lesion produces an ipsilateral defect.
Posteroparietal cortex	Lesion produces an ipsilateral defect.
Frontal eye fields	Bilateral lesion produces a bilateral defect, and a unilateral lesion produces an ipsilateral defect.
Dorsolateral pontine nucleus	Lesion produces an ipsilateral defect.
Cerebellum	Lesion of either the flocculus or paraflocculus produces a severe defect of pursuit gain, whereas a lesion of the vermis produces a modest defect of pursuit gain; a total cerebellectomy abolishes all pursuit.

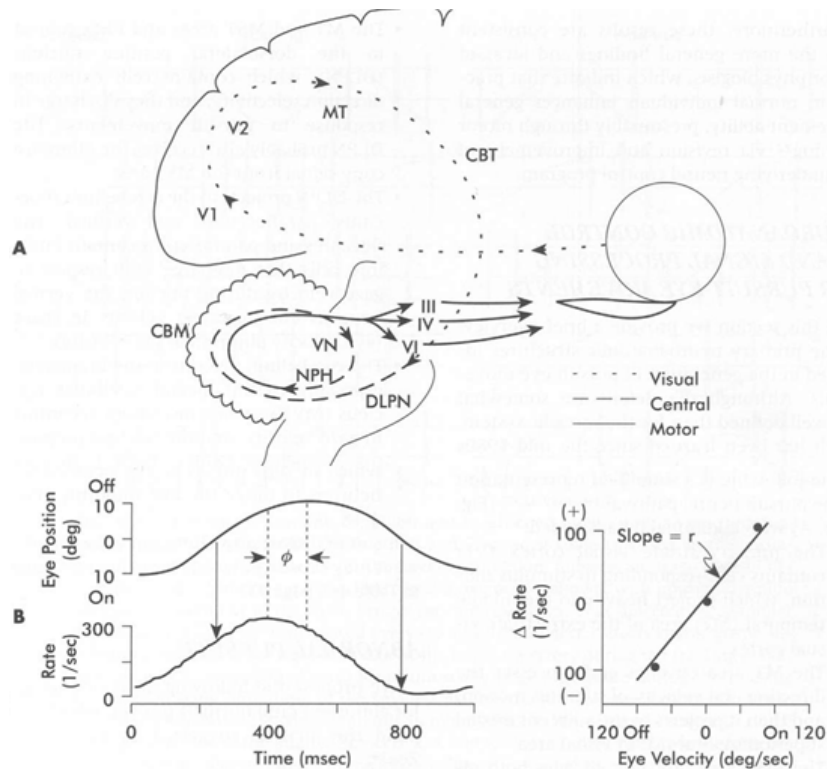


**Fig. 1.18 A:** Schematic representation of aspects of information flow in the smooth pursuit system. *CBT* - corticobulbar tract; *NPH* - nucleus prepositus hypoglossi; *VI* and *V2* - occipital visual areas; *VN* - vestibular nuclei; *III*, *IV*, and *VI* – oculo-motor, trochlear and abducens nuclei. **B:** Firing rate of an oculo-motor neuron during a sinusoidal tracking eye movement. Vertical arrows show the increment and decrement in rate from that found during fixation for eye movements through the same position with velocity in the on or off direction. ( $\phi$  is the phase lead of discharge rate with respect to eye position. Right graph shows the change in rate-to-velocity relationship of this neuron. From [79].

## 1.2. Models of the eye movement system

### 1.2.1. A Model of the Saccade Generator

When we look about, the nervous system must perceive a visual object with the peripheral retina, select it from all other objects and construct a command for the lower brain-stem circuits that will move the eye where we want it. Target selection is a complex task. In terms of brain-stem circuits, however, one can speculate on the more specific question of how the burst neurons are governed so that the intensity (in spikes/s) and duration of the burst is just correct to move the eyes by an amount appropriate to the retinal error of the selected target. A classic theory for this task uses a local feedback scheme [183, 184, 173].

It is assumed that saccades are generated in a retinotopic coordinate system. That is, if a target appears 10 deg to the right of the fovea, the activity evoked at the retinal location is to be translated into the pulse carried by burst cells in such a manner that the burst has the correct intensity and duration to create a 10 deg saccade to the right. Such system would operate in a manner that is independent of initial eye position, being concerned only with changes in position. Yet it would appear that other motor systems probably use internal copies of eye position in the head and head position on the body, to create an internal representation of the location of a seen target in space to which, say, the hand is directed by a command in a body-oriented coordinate system. Most body movements must be directed by signals in such a reference frame. It may therefore be the case that the input to the saccade-generating circuit is, similarly, a signal proportional to desired eye position in the head:  $E_d$  in Fig. 1.19 [112]. The virtue of the idea is that it then becomes quite simple to construct a scheme for timing the saccadic pulse automatically by feedback. At the right in Fig. 1.19 the neural integrator ( $NI$ ), parallel feed-forward path, and plant are shown; for saccades, it is best to use the plant transfer function of equation:

$$\frac{E(s)}{\Delta R_m(s)} = \frac{e^{-s\tau}}{(sT_{e1} + 1)(sT_{e2} + 1)} ; \quad (1.1)$$

where time constant  $T_{e1}$  is a parameter describing how rapidly the eye will respond to changes (240 ms);  $T_{e2}$  is a second, smaller time constant with a value of about 16 ms. The term containing  $T_{e2}$  causes the eye to respond even more poorly to input signals that contain frequency components above 10 Hz. The term in the numerator is the Laplace representation of the latency or pure delay,  $\tau$ , (about 8 ms) between changes in neuronal activity and changes in eye position.

The output of the neural integrator is an internal signal,  $E'$  proportional to instantaneous eye position. If, this signal were compared to desired eye position,  $E_d$  and their difference, motor error,  $e_m$  were allowed to drive the burst cells, the eye would always be driven until  $E'$  matched  $E_d$  and  $e_m$  became zero, at which point the burst would end and the eyes would stop on target. In this way the burst amplitude and duration would automatically be always just appropriate to the desired saccade size. All that is required is an inhibitory, tonic-cell interneuron ( $T_i$  Fig. 1.28) to close the feedback loop.

Fig 1.19 shows left and right burst cells,  $B_L$  and  $B_R$ , driving the neural integrator in push-pull and being driven by separate feedback loops. The relationship between the instantaneous discharge rates  $B_L$  and  $B_R$  and motor error,  $e_m$ , is shown in the boxes in Fig. 1.19. In the monkey, this relation rises steeply as  $e_m$ , increased from zero and, for most cells, saturates around 1000 spikes/s when  $e_m$  reaches 10 to 20 deg. It is the shape of this curve that allows the model to simulate saccades of all sizes with the correct waveform and peak velocities and durations that match experimental data. If one analyzes this feedback scheme, however, one discovers that the system is unstable. This odd situation comes about because saccades, to be useful, must be both fast and brief. The first feature requires a high gain so that even a small motor error of, say, 5 deg can cause a typical burst neuron to discharge at 700 spikes/s and move the eye at a peak velocity of about 300 deg/s. The second feature requires a wide

bandwidth. The result is that the gain around the loop is greater than 1.0 at frequencies where the phase shift exceeds 180 deg, which, according to feedback theory, insures instability and oscillations. The neural integrator creates a constant 90 deg phase lag at all frequencies. Any delays in the loop, which are all lumped into  $\tau_l$ , will create another 90 deg lag at the frequency  $1/(4\tau_l)$ . It would be reasonable to suppose that synaptic and recruitment delays around the loop could easily amount to 10 ms. This value for  $\tau_l$  causes a total phase shift around the loop of 180 deg at the frequency 25 Hz. According to theory, the system should oscillate near this frequency. The system oscillates because  $e_m$  does not become zero until 10 ms after the eye has reached the target. Since the burst cells do not stop in time, the eye goes past the target before it stops. This creates an error,  $e_m$ , in the opposite direction so the contralateral burst cells are activated to bring the eye back on target. But they make the same overshoot mistake and the process continues, resulting in oscillations. The fact that the model predicts saccadic oscillations is interesting because there are several situations, normal and pathological, in which oscillations, discussed below, do occur.

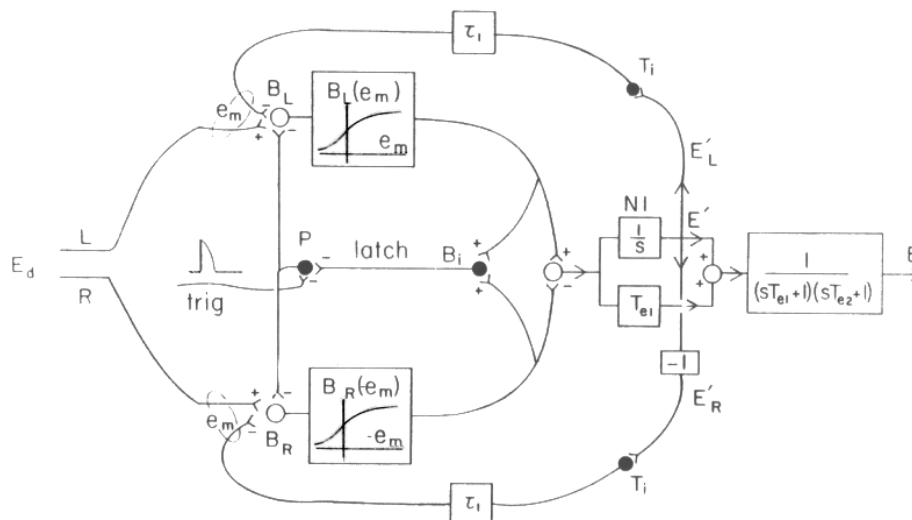


**Fig. 1.19** A model for generating saccades. An internal copy of eye position ( $E'$ ) from the neural integrator ( $NI$ ) is hypothesized to feed back through inhibitory tonic cells ( $T_i$ ) to be compared with a signal from higher centers proportional to desired eye position ( $E_d$ ). The difference is motor error ( $e_m$ ) which drives left and right burst cells ( $B_L, B_R$ ). Pause cells ( $P$ ) inhibit burst neurons. A trigger signal ( $trig$ ) inhibits the pause cells to initiate a saccade. Inhibitory burst interneurons ( $B_i$ ) keep pause cells off (*latch*) until  $e_m$  is zero, the burst is over, and the eye is on target. This model provides a hypothetical explanation for a large number of normal and abnormal saccadic behaviors.

Nevertheless, it seems that nature had deliberately designed a control system to be unstable. A simple solution, however, which allows the high gain-wide bandwidth features to be retained, is to turn the circuit off when it is not in use. The pause cells seem to represent just such a mechanism. It is generally believed (and indirectly supported by anatomical studies) that pause cells inhibit burst cells so that saccades

cannot occur so long as the former are active. Consequently, one might propose that saccades are initiated by turning off the pause cells. It is proposed that a trigger signal (*trig*, Fig. 1.19) momentarily silences the pause cells and releases the burst cells to initiate a saccade to the position  $E_d$ . If, however, the trigger pulse disappears before the saccade is over, the pause cell would be allowed to reinhibit the burst cells and stop the saccade. To prevent this, it is proposed that an inhibitory burst interneuron exists ( $B_i$ , Fig. 1.19) that can prevent the pause cell from firing so long as either the left or right burst cells are active. This pathway (*latch*, Fig. 1.19) allows an on-going saccade to run to completion before the pause cells are released to disable the pulse generator once again.

This model has the following features:

1. It is compatible with the results of stimulating the pause cells during a saccade, which can stop the saccade momentarily in midflight [79].
2. By decreasing the slope and amplitude of the burst-rate function ( $B(e_m)$  in Fig. 1.19), one can describe slow saccades seen in certain neurological disorders thought to affect the pontine reticular formation [183].
3. If the primary saccade is over before the trigger signal is over, another small saccade in the opposite direction will occur as the system, without inhibition from the pause cells, starts to oscillate. Such movements do occur and are called dynamic overshoot. In the case of microsaccades, which have a short duration, inhibition of pause cells by the trigger signal may permit several, back-to-back, microsaccades to occur. Such microsaccadic oscillations are commonly observed in studies of human microsaccades. The model in Fig. 1.19 mimics all these naturally occurring examples of saccadic oscillations [173]. If the pause cells can be kept off for many seconds, continuous saccadic oscillations occur similar to voluntary nystagmus.
4. There are patients whose abnormal eye movements can be described as an exaggeration of all the movements just mentioned in 5: very large dynamic overshoot and episodes of spontaneous oscillations called ocular flutter. Increasing the delay  $\tau_l$  and putting a lag in the latch circuit in the scheme in Fig. 1.19 can simulate these abnormal movements [184].

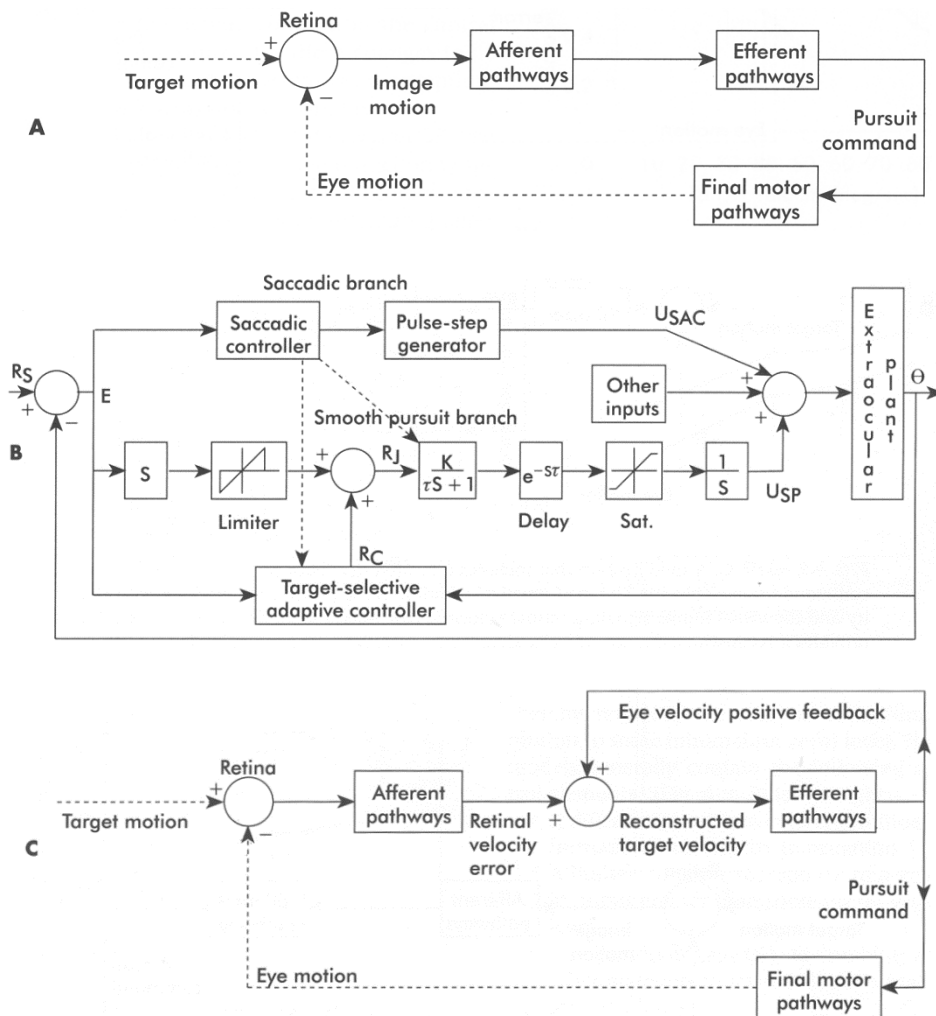
It has been demonstrated in monkeys that there is a very close relationship between instantaneous motor error  $e_m(t)$  and instantaneous burst rate  $B(t)$ , which supports the idea that burst cells are driven by motor error  $e_m$  as indicated in Fig. 1.19 by the relationship  $B(e_m)$  [173].

Some physiology nonrelated models for a saccade amplitude prediction on-line just from the first data collected exist. The ones using Kalman filter based models are producing the best results. Such prediction models are mainly used in fast response applications of eye movement tracking and analysis [84].

### 1.2.2. Models of a smooth pursuit system

Early models of the pursuit system considered it to function as a basic velocity servomechanism [160, 182] (Fig. 1.20 A). Its role was simply to match eye velocity to target velocity, thereby reducing the residual retinal-image motion to some minimal

(or zero) level. The general structure of such model is presented in Fig. 1.20 B [8]. However, as pointed out by Lisberger, Morris, and Tychsen, [104] there are two major problems with the basic model configuration. First, periods of perfect velocity tracking would result in zero system error; thus, there would be no error signal to drive the system. The pursuit system would effectively be open-loop. Second, there would be system instability because of the delay of approximately 100 ms in combination with the system's relatively high gain. Young, Forster, and van Houtte [21] and Robinson [140] proposed solutions to the preceding dilemma. They suggested that target velocity relative to the external environment constituted the brain neural signal that drives the pursuit system in an accurate and stable manner; it was proposed that a reconstructed target velocity signal (eye velocity plus retinal target velocity) served to drive the pursuit system (Fig. 1.20 C). Furthermore, in the current models of pursuit, weighted information about retinal velocity, as well as retinal position and acceleration, is also included as input signals (Fig. 1.20 D).



The figure is continued in a next page

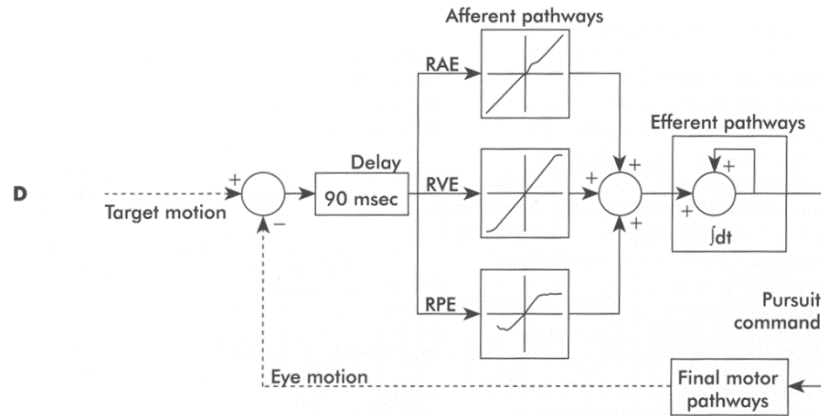


**Fig. 1.20** Models of the pursuit system. **A:** A simple negative-feedback control system in which image motion provides the central command to the efferent pathways. **B:** Target-selective adaptive control model. **C:** A modification that includes a positive-feedback pathway for the pursuit command for eye velocity. The mathematical addition of the positive feedback of eye velocity and the visual inputs signaling retinal velocity error (target velocity minus eye velocity) provides a reconstructed target velocity signal, which serves as the central command to the efferent pathways. The solid lines indicate the flow of neural signals; the dashed lines represent physical events. The block labeled *retina* compares target motion and eye motion, and its output is image motion, or target motion with respect to the eye. **D:** A computer model that simulates pursuit on a millisecond time scale and its relation to the pathways subserving pursuit. Retinal inputs are processed through a 90 ms delay, and retinal acceleration (*RAE*), velocity (*RVE*), and position errors (*RPE*) are transformed according to the relationships obtained in psychophysical experiments. The efferent pathways contain eye-velocity positive feedback and perform a mathematical integration. From [61, 104].

### 1.2.3. Neural model for visual tracking of unpredictably moving target

In 2007 Grossberg et. al. described a neural model of interaction between smooth pursuit and saccadic controllers during a variety of oculo-motor tasks (Fig. 1.21) [57]. This model unifies many recent single neuron recordings and key behavioral trends observed under various experimental conditions [36, 37, 35, 87, 88, 119, 120, 164]. Also, it answers mathematically to several fundamental questions. It provides an assumption, that when a saccade is elicited during smooth pursuit, the two systems operate in parallel until the saccade lands. This assumption is supported by data of Lisberger [103]. Such operation is feasible because the representation of target velocity computed by the model is robust in the face of the loss or degradation of target-related visual inputs, such as occurs during a catch-up saccade, but as also occurs during brief occlusions of a tracked target, and also as a normal consequence of successful smooth pursuit eye movement, which zeros target motion, but not background motion, in the retinal frame. The assumption of parallel operation, combined with the shared omni-pauser stage, enables the model to explain post-saccadic enhancement of smooth pursuit. The model offers a two-part answer to the question of how saccades to moving targets are accurate. Parallel operation means that

the saccade is not pre-compensating for target motion to the extent that it would if the smooth pursuit system were quiescent during the saccade.

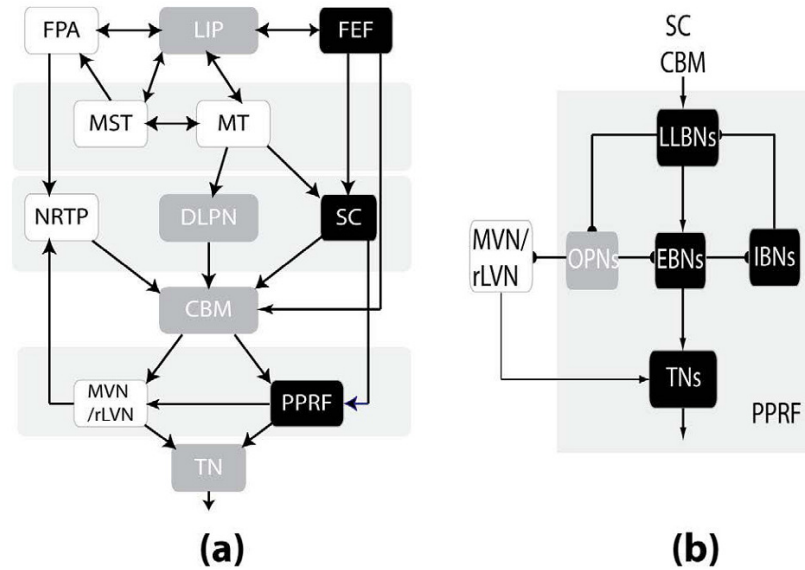


**Fig. 1.21** Modeled interactions among brain regions implicated in oculo-motor control. Black boxes denote areas belonging to the saccadic eye movement system, white boxes - the smooth pursuit eye-movement system, and grey boxes - both systems. (b): Constituents of the saccade generator in the *PPRF*, and projection of omnipause neurons to the pursuit neurons of the *MVN/rLVN*. Arrows indicate excitatory connections, and semi-circles indicate inhibitory connections. From [57].

However, despite parallel operation of smooth pursuit system, occasions of inaccurate catch-up saccade regularly arise, because of velocity saturation in the smooth pursuit system or because of underestimates of target velocity in the brief pre-saccadic interval. The resulting post-saccadic foveation errors cause the cerebellum to learn to use target velocity information to improve the metrics of catch-up saccades. This allows the model to treat evidence for motion-based adjustments of saccade metrics as indicative of a secondary input, (not only the positional gaze error), for catch-up saccades that are accurate despite target motion during the saccade.

Saccades do degrade vision, so it is also important to understand what mechanisms prevent excessive corrective saccades to appear during near-accurate tracking. Small foveation errors activate a pathway, which includes MT, rostral SC and the OPNs, whose excitation inhibits saccades. After an overshooting saccade, another pathway, from MT to the DLPN, enables a transient reduction of smooth pursuit eye movement gain. Slowed down smooth pursuit allows the target to catch up with the gaze without any backwards-oriented saccades.

There also is an oculomotor control system model by Lee et. al. [100], which treats symmetric control of two cameras for a robotic vision, and addresses how to track a moving target. This model exhibits saccade size adaptation for moving targets. It uses retinal slip information to correct the amplitude of saccades made to moving

targets. The model estimates the corrective displacement by multiplying the target's pre-saccadic retinal slip by a constant proportional to saccadic duration and adds it to the retinal-position error to program a compensatory saccade. These corrections are quite large, because this model's saccadic system shuts off the smooth pursuit system during a saccadic suppression. Without parallel operation of saccadic and smooth pursuit systems, an increase in gaze position and velocity errors after saccades is observed. Also the model by Lee et. al. is unable to explain post-saccadic enhancement of eye velocity.

The model by Grossberg et. al. (Fig 1.21) consists of two parallel interacting processing streams of saccadic and smooth pursuit movements. Components of these streams and pathways between these components are explained in equations, which use the symbols listed in table 1.7.

**Table 1.7** Symbols of the commonly used cells and connection weights in the equations.

SMOOTH PURSUIT SYSTEM		SACCADIC SYSTEM		Symbol	Represents
Symbol	Stands For	Symbol	Stands For		
$v(i,j)$	Retinal velocity input at position (i,j)	$r_{ij}$	Retinal input at position (i,j)	$\theta$	Directions along which the muscle can move the eye
$m_{jvd}^-$	MT <sup>-</sup> cells	$a_{ij}$	LIP cells	$d$	Directions along which the target can move
$m_{jvd}^+$	MT <sup>+</sup> cells	$b_{ij}$	SC burst layer cell	$t_\theta$	Tonic neuron activity along $\theta$
$s_d^V$	MST <sub>V</sub> cells	$u_{ij}$	SC buildup layer cell	$o$	Omnipauser neuron activity
$s_d^D$	MST <sub>D</sub> cells	$u_{ff}$	SC fixation cell	$\Psi$	Eye Position
$f_d^I$	FPA input cells	$f_{ij}^I$	FEF Planning layer cells		
$f_d^S$	FPA summation cells	$f_{ij}^O$	FEF output layer cells		
$f_d^O$	FPA output cell	$f_{ff}^I$	FEF fixation layer cell		
$g^P$	Signal reflecting target choice for SPEM by a cortico-BG-thalamo-cortical loop	$g^P$	Signal reflecting target choice for SAC by a cortico-BG-thalamo-cortical loop		
$p_{vd}^D$	DLPN cells	$n_{ij}$	Nigral cell		
$p_{ad}^N$	NRTP acceleration cells	$c_{ij}^F$	Cerebellar controlled FEF input		
$p_{vd}^N$	NRTP velocity cells	$c_{ij}^S$	Cerebellar controlled SC input		
$W_{vd}^D$	Adaptive weights between DLPN and saccadic part of Cerebellum	$W_{ij}^S, W_{ij}^F$	Adaptive weights for both horizontal and vertical saccades from cerebellum for SC and FEF signal		
$I_\theta^P$	Pursuit drive along $\theta$	$I_\theta^S$	Saccade drive along $\theta$		
$c_d^P$	Cerebellar pursuit cells	$l_\theta$	Long lead Burst cells along $\theta$		
$h_\theta$	Pursuit neurons along $\theta$	$e_\theta$	Excitatory Burst cells along $\theta$		

The smooth pursuit stream contains visual area MT cells, which are of two types: MT<sup>-</sup> (respond vigorously to small stimuli moving in their receptive field at a particular speed and in a particular direction) and MT<sup>+</sup> (respond to large stimulus sizes), are selective to the direction and speed of visual stimuli and provide inputs to the model's MST cells, which pool MT inputs to become direction-selective and speed-sensitive, but not speed-selective:

$$\frac{dm_{ijvd}^-}{dt} = -m_{ijvd}^- + (1 - m_{ijvd}^-)(\beta_{ij}^-(v_{ij}, d_{ij})(1 + [s_d^-]^+) + \sum_{ab} a_{ab} W_{abij}) - (1 + m_{ijvd}^-) \sum_{e \neq d} s_e^-, \quad (1.2)$$

$$\frac{dm_{ijvd}^+}{dt} = -m_{ijvd}^+ + (1 - m_{ijvd}^+)(\beta_{ij}^+(v_{ij}, d_{ij})(1 + [s_d^+]^+) + \sum_{ab} a_{ab} W_{abij}) - (1 + m_{ijvd}^+) \sum_{e \neq d} s_e^+; \quad (1.3)$$

where  $W_{abij} = \begin{cases} 1 & \text{if } a - \delta/2 < i < a + \delta/2 \text{ and } b - \delta/2 < i < b + \delta/2; \\ 0 & \text{otherwise} \end{cases}$ ;  $\delta$  is a diameter of LIP neurons response field;  $\beta_{ij}(v_{ij}, d_{ij})$  is the directional tuned input;  $\sum_{e \neq d} s_e$  is the inhibition from MT recipient MST cells coding for nonmatching directions.

Because MST cells also receive corollary discharge inputs corresponding to current eye velocity from MVN cells (Fig. 1.21 a), they can compute an internal estimate of target velocity that remains accurate even as eye velocity grows to match target velocity, and thus gradually cancels the target-related retinal image motion that drives MT cells:

$$\frac{ds_d^-}{dt} = -s_d^- + (1 - s_d^-)[2.5 \sum_{ij} [m_{ijvd}^-]^+ v_{ij} + 5.5[s_D^-]^+ + 2(k_d - k_D)]^+ - 75 \sum_{e \neq d} s_e^-, \quad (1.4)$$

$$\frac{ds_d^+}{dt} = -s_d^+ + (1 - s_d^+)[0.1 \sum_{ij} [m_{ijvd}^+]^+ + 5.5[s_D^+]^+ + 2(k_D - k_d)]^+ - 15 \sum_{e \neq d} s_e^+; \quad (1.5)$$

where  $(k_d - k_D)$  is the corollary discharge;

The robust estimate of target velocity computed by model MST cells provides a key basis for the model's frontal cortical representation of desired pursuit velocity. In particular, the FPA, at the rostral bank of the arcuate sulcus, receives strong inputs from MST. Model and real FPA cells have high direction-selectivity and speed-sensitivity, but almost no speed-selectivity.

The model FPA cells project to the model NRTP (nucleus reticularis tegmenti pontis) which includes two types of cells: acceleration and velocity cells:

$$\frac{df_d^I}{dt} = -2f_d^I + (1 - f_d^I)(50[s_d^-]^+ + 10f_d^R) - 10 \sum_{e \neq d} f_e^I, \quad (1.6)$$

$$\frac{df_d^R}{dt} = -f_d^R + (1 - f_d^R)[f_d^I]^+, \quad (1.7)$$

$$\frac{df_d^S}{dt} = -f_d^S + (1 - f_d^S)15[s_d^+]^+ - (1 + f_d^S) \sum_{e \neq d} f_e^S, \quad (1.8)$$

$$\frac{df_d^O}{dt} = -10f_d^O + (1 - f_d^O)(15[s_d^I]^+ + [f_d^S]^+ + 15\mu^d + 1.5[g^p - 0.5]^+) - 25(1 + f_d^O) \sum_{e \neq d} f_e^O. \quad (1.9)$$

Model NRTP velocity cells (equation (1.10)) integrate the output of NRTP acceleration cells:

$$\frac{dp_{vd}^D}{dt} = -p_{vd}^D + 0.1(1 - p_{vd}^D) \sum_{ij} [m_{ijvd}^-]^+ - 100(1 - p_{vd}^D) \sum_{\substack{e \neq d \\ f \neq v}} p_{fe}^D, \quad (1.10)$$

$$\frac{dp_{ad}^N}{dt} = -p_{ad}^N + 45(1 - p_{ad}^N)[f_d^O - k^d]^+ - 50 \sum_{e \neq d} p_{ae}^N. \quad (1.11)$$

NRTP acceleration cells compute the difference between an excitatory target-velocity command from FPA and an inhibitory eye-velocity signal from MVNs. This inhibitory process is predicted but has no direct data support at present. The computed difference estimates the eye acceleration needed to match target velocity. These two classes of cells allow the NRTP to play a key role in smooth pursuit initiation. Parallel to the FPA-NRTP pathway, a second pathway exists for the transmission of smooth pursuit-related information from the cortex to the cerebellum via the pons: Model MT cells project to DLPN (dorsal lateral pontine nucleus) cells of the brain stem. The DLPN cells have been implicated in maintenance of smooth pursuit. In the model, the DLPN cells have similar speed and directional selectivities as MT cells, but they lack their retinotopic specificity

$$\frac{dp_{vd}^N}{dt} = -0.4p_{vd}^N + 40(1 - p_{vd}^N)[p_{ad}^N]^+. \quad (1.12)$$

In the model saccadic system, retinotopically organized visual signals are processed to produce saccadic target choices in the model SC (equations (1.13)-(1.15)), LIP (equation (1.16)), and FEF (equations (1.17)-(1.21)):

$$\frac{db_{ij}}{dt} = -20b_{ij} + (1.2 - b_{ij})B_{ij}^E - (1 + b_{ij})B_{ij}^I; \quad (1.13)$$

where  $B_{ij}^E$  is the excitatory input signal,

$$\frac{du_{ij}}{dt} = -0.1u_{ij} + (1 - u_{ij})U_{ij}^E - u_{ij}U_{ij}^I; \quad (1.14)$$

where  $U_{ij}^E$  is the excitatory SC buildup input;  $U_{ij}^I$  is the inhibitory SC buildup input,

$$\frac{du_{ff}}{dt} = -0.1u_{ff} + (0.1 - u_{ff})(10\zeta + r_{00} + K^E) - u_{ff} \left( 10 \sum_{\substack{k=1 \\ k \neq f}}^N \sum_{\substack{j=1 \\ j \neq f}}^N u_{kj} M_j M_k + 10 \sum_{\substack{k=1 \\ k \neq f}}^N \sum_{\substack{j=1 \\ j \neq f}}^N b_{kj} \right); \quad (1.15)$$

where  $K_e = \sum_{i,j \in F_\delta} m_{ijvd}$ , where  $F_\delta = \left\{ (i, j) \text{ such that } f - \delta \leq i \leq f + \delta \text{ and } f - \delta \leq j \leq f + \delta \right\}$ ;  $\delta$  is

the radius of response field of the MT cell at position  $(i, j)$  and  $f$  is the position of the fovea,

$$\frac{da_{ij}}{dt} = (1 - ma_{ij}) \left[ I_{ij} + [f_{ij}^I]^+ + f(f_{ij}^O) + f(a_{ij}) \right] - a_{ij} \left[ 20 \sum_{\substack{x \neq i \\ y \neq j}} [a_{xy}]^+ + a_{ij}^R \right], \quad (1.16)$$

$$\frac{df_{ij}^I}{dt} = (1 - f_{ij}^I) F_{ij}^{PE} - (f_{ij}^I + 0.4) F_{ij}^{PI}; \quad (1.17)$$

where:

$$F_{ij}^{PE} = 10[a_{ij}]^+ + 15I_{ij} + 1.5[g^S - 0.5]^+ + 2f(f_{ij}^I), \quad (1.18)$$

$$F_{ij}^{Pl} = 0.8 + 10 \left( [f_{ff}^l]^+ e^{-(i-f)^2 + (j-f)^2} \right) + 20 \sum_{\substack{r \neq i \\ s \neq j}} f_{rs}^l + 10 S_{on}, \quad (1.19)$$

$$\frac{df_{ff}^l}{dt} = -0.1 f_{ff}^l + \left( 1 - f_{ff}^l \right) (10\zeta + r_{00}) - \left( 1 + f_{ff}^l \right) F_{ff}^l, \quad (1.20)$$

$$\frac{df_{ij}^o}{dt} = \left( 1 - f_{ij}^o \right) F_{ij}^{oE} - \left( f_{ij}^o + 0.8 \right) F_{ij}^{oI}. \quad (1.21)$$

FEF outputs serve as inputs to corresponding retinotopic loci in two layers of the motor error map of the model's SC. There is also communication between the two SC layers. In particular, activated loci in the burst cell layer excite corresponding cells in the buildup cell layer of the SC. Outputs from the SC reach the cerebellum and the saccade generator circuit in the PPRF, which contains populations of saccadic and smooth pursuit-related cells, some of which provide direct input to the oculo-motor neurons that innervate eye muscles. Model saccadic control signals from cerebellar and SC stages converge at model LLBN, which activity encodes the gaze-position error and these cells excite corresponding EBNs:

$$\frac{dl_{\theta}}{dt} = -1.3 l_{\theta} + I_{\theta}^S - 2I_{\theta}^S - 2b_{\theta}. \quad (1.22)$$

The model EBNs project to the TNs, which integrate inputs from EBNs and excite the model oculo-motor neurons:

$$\frac{de_{\theta}}{dt} = -3.5e_{\theta} + (2 - e_{\theta})(5l_{\theta} + 1) - (1 + e_{\theta})(2l_{\theta} + 20v(o)). \quad (1.23)$$

The EBNs also excite IBNs, which in turn inhibit the LLBNs, thereby completing an internal negative feedback loop that controls ballistic saccades:

$$\frac{db_{\theta}}{dt} = -15b_{\theta} + 50e_{\theta}. \quad (1.24)$$

Except during saccades, the EBNs receive strong inhibition from model OPNs, so-called because they pause deeply to disinhibit saccades of all directions. In the brain, OPNs are located in the nucleus raphe interpositus. The pursuit neurons (PNs) found in the MVN/rLVN are modeled as receiving input from the cerebellum and projecting directly to the TNs, which are thus shared by saccadic and smooth pursuit systems. The PNs are weakly inhibited by, and themselves inhibit, the OPNs, also shared by both systems. About 50% of the OPNs show 34% reduced activity during smooth pursuit, whereas most OPNs pause more deeply during saccades. Thus, the spontaneously active and inhibitory OPNs normally oppose both saccades and smooth pursuit eye movements. Shallow pausing by OPNs can release smooth pursuit eye movements but not saccades, whose releases require deeper pauses.

### 1.3. Hand movements

There are infinitely many ways of how to achieve a specific movement skill. For example, when reaching for an object, many different hand paths can be taken

between start and endpoint, also the path can be traversed at arbitrary speed profiles. Moreover, due to the large number of DOFs in the primate movement systems, there is additionally an infinite number of ways of how a chosen hand path can be realized by postural arm configurations. On the biomechanical level, there is an even larger level of redundancy as there are many more muscles than DOFs in the human body, and this level of redundancy becomes even worse on the neuronal level. Thinking this way, it is extremely unlikely that two different individuals would use similar movement strategies to accomplish the same movement goal. However, behavioral research shows that there is many regularities, not just across individuals, but also even across different species. Such regularities have led the way towards the understanding of perceptuomotor control, as they seem to indicate some fundamental organizational principles in the central nervous system.

In point to point reaching arm movements, the hand path is approximately straight and the tangential velocity trajectory along the path is close to bell-shaped. But the velocity profiles in joint space and muscle space are much more complex. Therefore, natural hypothesis that point-to-point reaching movements are planned in external coordinates and not in internal ones, arises. After more-detailed examination of reaching movements, it is clear, that, reaching movements are only approximately straight and shows a characteristic amount of curvature as a function of where in the workspace the start and endpoint of the movement are [22]. Also, the symmetry of the bell-shaped velocity profile is varying systematically as a function of movement speed [28]. These behavioral specifics had led to variety of models for explanation. Initial computational models of arm control focused on accounting for the bell-shaped velocity profile of hand movement, using principles of optimal control based on a kinematic optimization criterion for movement planning that favors smooth acceleration of the hand. Such models would create perfectly straight-line movements and perfectly symmetric bell-shaped velocity profiles. As the observed behavior is different, it was assumed that movement plans were executed imperfectly by an equilibrium point controller [92]. An alternative viewpoint was suggested by Kawato and colleagues. Their research emphasizes that the CNS takes the dynamical properties of the musculo-skeletal system into account and plans trajectories minimizing the “wear and tear” in the actuators, expressed as a minimum torque-change or minimum motor-command-change optimization criterion. This way, behavioral features of arm and hand control are an intentional outcome of an underlying computational principle, which employs models of the entire movement system and its environment. [171].

One more viewpoint exists, which suggests that the features of arm and hand movement could also be influenced by the noise characteristics of neural firing, i.e. the decreasing signal to noise ratio of motor neurons when their firing frequency increases. Thus, the neuronal level together with the behavioral goal of accurate reaching is responsible for behavioral characteristics observed. [59].

Perceptual distortion could also potentially contribute to the curvature features in reaching movements. While dynamical properties of feedback loops in motor planning could generate asymmetries of bell-shaped velocity profiles [28]. Motor

learning imperfection and delays in the control system could also influence the behavior.

For motor learning to be efficient, it is mandatory that a higher level of abstraction would be used for motor planning than individual motor commands. Otherwise, the search space for exploration during learning will become too large for finding appropriate actions for a new movement task. Units of action, also called basis behaviors or gestures, could offer such an abstraction. Pattern generators and the few different behavioral modes of oculo-motor control can be thought as examples of such movement primitives. For arm and hand control, it is still a topic of ongoing research whether some form of units of actions exist [163]. Finding behavioral evidence for segmentation of movement could provide some first insights into the existence of movement primitives [64].

Kinematic hand trajectory features have been used as one major indicator to investigate movement segmentation for several decades. Using the number of modes of the tangential hand velocity profile in linear and curvilinear drawing movements, it was concluded that arm movements might generally consist discrete strokes between start points, via points, and end points. More to that, these strokes are piecewise planar in three-dimensional movement [163]. These and later studies influenced, that stroke-based movement generation and piecewise planarity of the hand movement became one of the main hypotheses for movement segmentation [48].

Sternad and Schaal however, reinterpreted these indicators of segmentation partially as an artifact, in particular for rhythmic movement, which is also assumed to be segmented into planar strokes [163]. Features of apparent movement segmentation could also arise from principles of trajectory formation that use oscillatory movement primitives in joint space [65]. When such oscillations are transformed by the nonlinear kinematics of an arm into hand movement, complex kinematic features of hand trajectories can arise that, nevertheless, are not due to movement segmentation. Sternad and Schaal [163] suggested that movement primitives should be sought in terms of dynamic systems theory, looking for dynamic regimes like point and limit cycle attractors, and using perturbation experiments to find principles of segmenting movements into these basic regimes.

The  $2/3$  power law is another related behavioral feature of primate hand movements trajectories [48]. In rhythmic drawing movements, Lacquaniti et al. noted a power law relationship with proportionality constant  $k$  between the curvature of the trajectory path  $c(t)$  and the angular velocity  $a(t)$  of the hand:

$$a(t) = kc(t)^{2/3}. \quad (1.25)$$

There is no known physical necessity for movement systems to satisfy this relation between kinematic (i.e., velocity) and geometric (i.e., curvature) properties of hand movements. The power law is observed in numerous behavioral experiments [48] and even population code activity in motor cortices [48], thus it may reflect an important principle of movement generation in the CNS. The origins of this law are controversial. Schaal and Sternad [148] reported strong violations of the power law in large scale drawing patterns and interpreted it as an epiphenomenon of smooth movement generation [48]. Nevertheless, the power law remains at an interesting

descriptive feature of regularities of human motor control and has proven to be useful even in modeling the perception of movement [46].

Fitts' Law describes the speed to accuracy tradeoff for hand movements [45]. In rapid reaching for a target, the movement time  $MT$  was empirically found to depend on the distance of movement  $A$  and the target width  $W$  (which is an equivalent to the required accuracy) in a logarithmic relationship:

$$MT = a + b \log_2 \left( 2 \frac{A}{W} \right); \quad (1.26)$$

where  $a$  and  $b$  are proportionality constants (depending on motor system properties).

And Index of task Difficulty ( $ID$ ) can be evaluated by:

$$ID = \log_2 \left( 2 \frac{A}{W} \right). \quad (1.27)$$

Since Fitts' Law is a robust phenomenon of human arm and hand movement, many computational models are using it as a way to verify the validity. Unfortunately, Fitts' Law could be modeled in many different ways so far, including models from dynamics system theory, noise properties of neuronal firing, and computational constraints in movement planning [125, 28]. Thus, it seems that the constraints provided by this law are very unspecific and does not reveal the organization of the nervous system. Nevertheless, the Fitts' Law remains a behavioral landmark. Thus, there are many models of its extension [108, 107].

Trajectory-based interactions, such as drawing curves, navigating through nested-menus, and moving in 3D worlds, has become common tasks in computer interfaces. Fitts' law is dedicated to pointing tasks, which, in computer interfaces, are also often used, but performances in more complex trajectory-based tasks like drawing or steering, cannot be successfully modeled with it. Therefore, exploring the possible existence of robust regularities in trajectory-based tasks and using "steering through tunnels" as experimental paradigm to represent such tasks, a steering law was stated [1]. It treats such "tunnel" as an infinite number of subsequent pointing targets:

$$ID_\infty = \lim_{N \rightarrow \infty} ID_N = \frac{A}{W \ln 2}. \quad (1.28)$$

And the time required for such motor task can be defined:

$$MT = a + b \frac{A}{W}. \quad (1.29)$$

$ID$  for a narrowing tunnel ( $ID_{NT}$ ) of starting width  $W_1$  and end width  $W_2$ :

$$ID_\infty = \int_0^A \frac{dx}{W(x)} = \int_0^A \frac{dx}{W_1 + \frac{x}{A}(W_2 - W_1)}, \quad (1.30)$$

$$ID_{NT} = \frac{A}{W_2 - W_1} \ln \frac{W_2}{W_1}. \quad (1.31)$$

And for curved path  $C$  (Fig. 1.22), index of difficulty ( $ID_C$ ) is evaluated as:

$$ID_C = \int_C \frac{ds}{W(s)}. \quad (1.32)$$

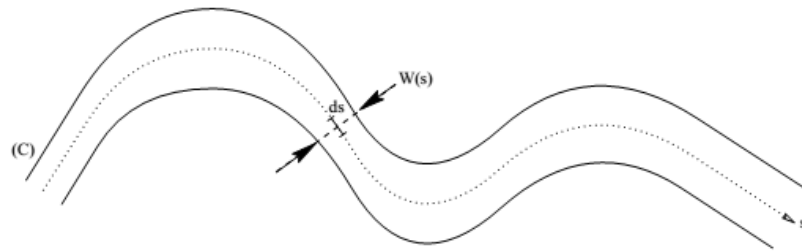


**Fig. 1.22** Integrating along a curve. From [1].

The steering Law model was verified using experimental data: result correlation is 0.968 and more depending on the type of path geometry [1].

As already discussed, when reaching for a target, the high number of degrees of freedom in the human body's structure usually allows close to infinite number of postures for each hand position attained during the reaching trajectory. An active area of research in motor control is thus concerned with how redundancy is resolved, whether there is within and/or across subject consistency of the resolution of redundancy, and whether it is possible to deduce constraints on motor planning and execution from the resolution of redundancy [150].

The redundancy resolution is well described by a multi-term optimization criterion that primarily tries to keep joint angular position as far as possible away from the extreme positions of each joint and also minimizes some physiological cost [29]. When starting a reaching movement, the movement slowly converges to the optimal posture on the way to the goal rather than trying to achieve optimality immediately. Such strategy resembles the method of resolved motion rate control in control theory, suggested as a neural network model of human motor planning by Bullock et. al. [29]. Grea, Desmurget, and Prablanc [55] reported similar behavior in reach and grasp movements. The final posture at a grasp target was highly repeatable even if the target changed its position and orientation during the reaching movement. Thus, it was concluded that the CNS for reach and grasp plans not only the final hand position, but also the final joint space position. However, the optimization methods by Bullock et al. [29] could result in similar behavior, without explicitly planning the final joint space posture. An elegant alternative view to optimization methods is a view, where motor control and planning is based on force fields. Thus, some more work is still needed before a final conclusion is settled on the issue of redundancy resolution.

Body size and biomechanical properties throughout development continuously changes, so the ability to learn motor control is of fundamental importance in biological movement systems. Moreover, primates show an unusual flexibility of how to devise new hand and arm movement related motor skills to solve novel tasks. Thus learning has an important role in computational models of motor control.

Decade ago there was a controversy whether motor learning should be accounted by equilibrium point control or internal model control. Evidence that various, in particular fast, movement behaviors cannot be accounted for by equilibrium point control has led to increasing consensus that internal model control is a viable concept for biological motor learning, and that the equilibrium point control strategy in its original and appealing simplicity is not tenable. Behavioral learning

experiments that were created in the wake of the equilibrium point control discussion sparked a new branch of research on motor learning. Adaptation to virtual force fields, to altered perceptual environments, or to virtual objects are among the main behavioral paradigms to investigate motor learning with the goal to better understand the time course, representations, control circuits, retention, and functional anatomy of motor learning [159].

#### **1.4. Hand movement models**

A huge amount of internal model concepts is widespread in neuroscience. Most of these concepts are supported by neurophysiological, behavioral and imaging data. Also, a specific theory on inverse dynamics model learning is directly supported by unit recordings from cerebellar Purkinje cells. M. Kawato [180] proposed multiple paired forward inverse model approach describing how diverse objects and environments can be controlled and learned separately. The minimum variance model is another major advance in the computational theory of motor control. There also are models, integrating two different approaches on trajectory planning, strongly suggesting that both kinematic and dynamic internal models are utilized in movement planning and control [78].

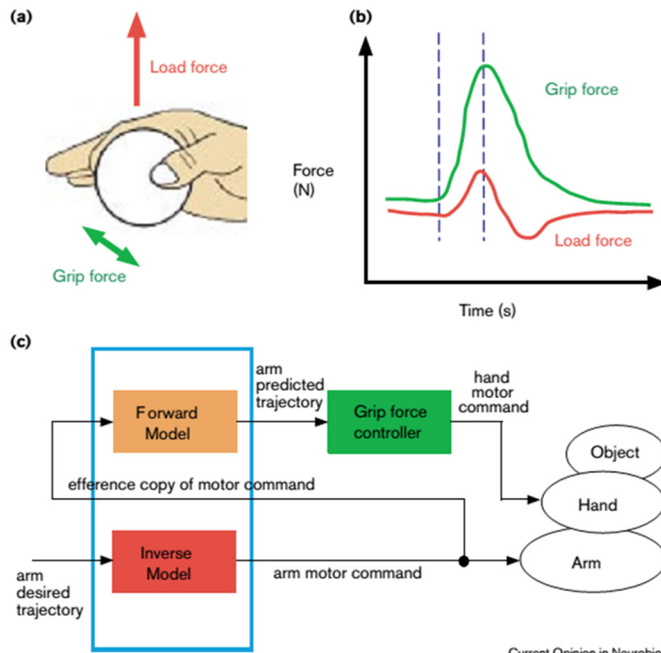
Internal models are neural formations used for simulating input/output characteristics, or their inverses, of the motor apparatus. Forward internal models do predict sensory consequences using efference copies of issued motor commands as an input. Inverse internal models, on the other hand, are used to calculate and plan necessary feed-forward motor commands having a desired trajectory information as an input. Fast and coordinated arm movements cannot be executed solely under feedback control, since biological feedback loops have small gains and are slow. The internal model hypothesis proposes that the brain through motor learning needs to acquire an inverse dynamics model of the object to be controlled. After that, motor control can be executed in a pure feed-forward manner. In theory, an inverse model can be approximated by a forward model of the motor apparatus embedded in an internal feedback loop.

Use of internal models is supported evaluating the data collected in behavioral experiments when point-to-point reaching arm movements are distorted by an applied static force field. This force field leads to arm movement trajectory distortion, which is reduced gradually during repeated trials. Thus, the inverse dynamics model changes to the inverse of the combined arm dynamics and the applied force field. This adaptation is assumed to involve plastic changes of the synaptic efficacy of neurons constituting the inverse dynamics model. If a force field is removed, the inverse dynamics model continues to generate the motor commands compensating for the arm dynamics, as well as the non-existing force field. This leads to observed opposite direction distortions.

Studies on coordination between reaching and grasping is the most convincing proof for existence of forward models. The grip force used for maintaining a ball in a hand with two fingers is always just slightly greater than the minimum force needed to prevent slip as in natural conditions as in those, when arm's dynamics is altered

using external means [47]. Figure 1.23 illustrates grip force – load force control, but the scheme can be generalized to coordination of any two combined motor commands.

**Fig. 1.23** Grip force created by a hand and load force created by an arm (a). The grip force is controlled precisely: it is always just slightly greater than the minimum grip force needed to prevent slip (b). This grip-force–load-force coupling is explained by a framework that contains both the inverse and forward models of the arm (c). From [78].



There are plenty of cerebellar learning theories that allocate supervised learning, reinforcement learning, and unsupervised learning to the cerebellum, the basal ganglia and the cerebral cortex, respectively. Since the learning acquisition of internal models is best performed by supervised learning, the cerebellar cortex seems the most appropriate location as the storage site of internal models. In addition, imaging, physiological and lesion studies have demonstrated that the cerebellum is at least one of the possible sites for internal models for arm movements [149].

Since the experimental data reports an intermediate level of a generalization (ability for a control system to cope with different than trained trajectories and movements), there is a need for modular structures in the control system [78]. This is because a single internal model with an imperfect generalization capability is unable to learn or deal with a whole range of different behavioral situations. Different modules exhibit some amount of generalization, but in order to remove possible interference between them, some regulatory mechanism controlling their learning and involvement in a specific situation, must exist [60]. The model for the manipulation of many different objects with a finite number of internal model modules, while at the same time efficiently utilizing contextual information such as the vision of objects, verbal instructions, or the sequence of object presentation, is illustrated in Fig. 1.24. Each of many modules comprises such elements: a forward model, an inverse model and a responsibility predictor. Learning, switching and blending of these multiple modules is controlled depending on how good the predictions made by the selected model or their group are. Also, a predictive switching between modules is done based on contextual information by responsibility predictors. Contextual information for the

responsibility predictor can be different: vision, audition, tactile information, reasoning, verbal instruction, sequence of movement elements, outputs from other responsibility predictors, descending signals from higher brain regions, etc. A soft maximum function, gathering all products of the prior probability and the likelihood, finally computes the responsibility signal, which specifies the control contribution of the inverse model, as well as the learning responsibility of inverse and forward models within each module. E. g. suppose that a human needs to manipulate one of several objects (upper part of Fig. 1.24). According to visual information, an appropriate module e. g. the one for a ball, will be selected. On actual manipulation of the object, the forward model for the ball module predicts sensory consequence from the efference copy of issued motor commands. If its prediction is adequate, that module will continue to be used. However, if the primary information was erroneous and the object actually grasped is a bowling ball, the prediction of the selected module is bad and the prediction of the module for a dumbbell is better. This way the ball module will be turned off and the dumbbell module will be turned on after actual movement execution.

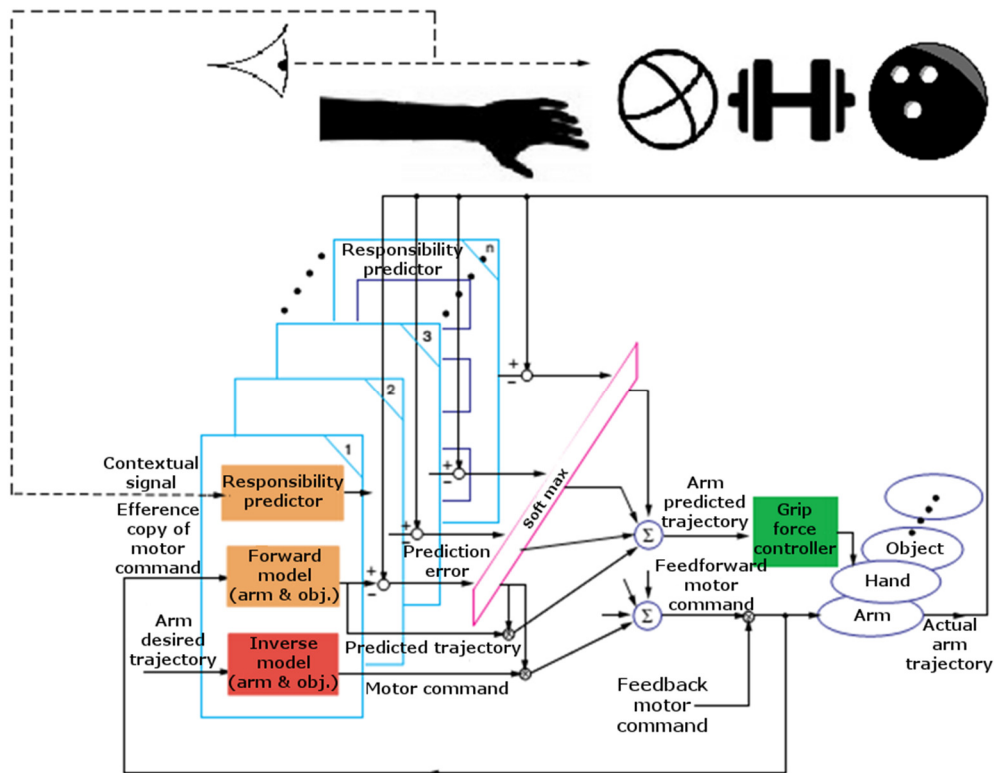


**Fig. 1.24** Multiple paired forward and inverse models in the context of grip-load forces coupling for multiple manipulated objects. From [60].

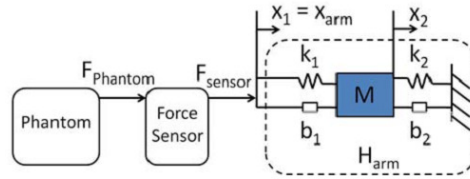
Even if physiology of the arm movement dynamics is revealed, arm and hand movements is still very complex and variable object for modeling. Arm movement

restraints depend highly on the application and tools being used. This is why only partial (for one or some of joints moving in restricted number of degrees of freedom, e. g. wrist [89]) or task-specific models of arm dynamics exist. Most models created with a purpose to simulate full arm dynamics are accounted for movements in three-dimensional space. Parameters for such models are obtained from experimental trials using some arm movement tracking devices such as haptic devices [51]. This way, the system being identified is illustrated in Fig. 1.25 and expressed by a transfer function:

$$H_{arm}(s) = \frac{X_{arm}(s)}{F_{sensor}(s)} = \frac{Ms^2 + (b_1 + b_2)s + k_1 + k_2}{b_1Ms^3 + (b_1b_2 + k_1M)s^2 + (b_2k_1 + b_1k_2)s + k_1k_2}. \quad (1.33)$$

Grip force sensor was also used in this experimental research in order to investigate if parameters of arm dynamics are grip force-dependent. No statistically significant dependency of arm movement dynamics and grip force was observed [51].

**Fig. 1.25** This block diagram represents the identified system. The left most block represents the haptic device that exerts a force on the human arm. A force sensor was placed between the haptic device and the subject's arm. The dashed box on the right contains the mass-springs-dampers model for the human arm. Mass  $M$  represents the arm's inertia. The spring  $k_1$  and the damper  $b_1$  represent the hand grasp stiffness while the spring  $k_2$  and the damper  $b_2$  represent the arm stiffness.  $F_{phantom}$  is the measured force applied at the end effector of the haptic interface and  $x_{arm}$  is the measured position of the stylus center that is attached to the force sensor. From [51].



The fitting results for each axis are provided in table 1.8. This research also included a study on variability of the parameters of the arm's model.

**Table 1.8** Nominal arm model parameters. From [51].

Axis	M(kg)	k <sub>1</sub> (N/m)	k <sub>2</sub> (N/m)	b <sub>1</sub> (Ns/m)	b <sub>2</sub> (Ns/m)
X-axis	0.2179	379.5	78.75	1.839	4.645
Y-axis	0.2692	552.4	105.3	3.609	6.430
Z-axis	0.2041	769.9	271.7	0.7764	18.06

## 1.5. Eye-hand coordination

From the research of arm and hand movements and their control it is clear that most of the human limb movements are more or less dependent on visual information. Since any incoming visual information is closely related to oculo-motor system, some eye-hand movement coordination is needed. Also the behavioral studies where subjects had to reach and grasp one of two equivalent objects shows that “we look to where we have already selected to grasp”, suggesting that oculo-motor system is dependent on arm movement control system too [66]. It is also known that for different purpose arm/hand movements, the coordination patterns are also different

and these patterns also depend on manipulators or objects being used and individual characteristics of a subject [157].

Even if an arm and an eyeball has different dynamic parameters, their coordinated movements has some similarities because the need for coordination is the factor inducing the use of shared neural circuitry e. g. the unexpected change in the direction of the target being tracked by eye and hand is tackled in the same manner with very similar parameters [43]. However differences of oculomotor and limb motor systems certainly requires some different result-oriented uses. Peripheral and central vision both plays an important role in eye-hand coordination while drawing or guiding an object, but the timing of when the visual information is present is critical in choosing weather this information will be used for instant correction of hand's movement direction or for subsequent movement planning [82]. An impact on eye-hand coordination depending on motivation and arousal is observed too [39]. On the other hand, there appears no significant changes in eye-hand coordination depending on age or Parkinson's disease. Only the eye and hand movement speed is affected [19]

Experimental research where the accuracy of eye movements is compared for situations when a target is not only a location indicated by visual, but also by a proprioceptive signal suggests that coordinate systems for eye and limb systems are different, but the efference copy of the position of the hand is provided to oculo-motor system which has a poorly calibrated internal model for coordinate translation [138]. This is supported by other studies concluding that all motor tasks are planned in their own-centered spatial coordinates, while all coordination types require the translation between different coordinate systems [18].

Observing that performance in oculo-manual tracking of a moving target is the best when hand movements lag 75 to 100 ms after the eye, Mial and Reckess concluded [116], that not only arm movement efferent copy is used for planning eye movements, but also eye movement signal can be used by an arm motion control system. Knowing the results of other functional neural imaging and lesion studies they adapted Smith Predictor model (Fig. 1.26) and suggested, that some of the forward models in cerebellum are also time specific sensory predictors. Also, they suggested that these predictive signals are used for eye-hand coordination [116]. They also used functional imaging study to confirm their hypothesis. The results observed were coherent having in mind earlier in this thesis explained multiple paired forward and inverse model. Cerebellum appears to be differently active during situations when eye-hand coordination proceeds normally (model selection phase) and when there is no learned model to select (active learning phase) [117].

During search and selection tasks, humans use some eye-hand coordination strategies. If the approximate location of the target is known, participants perform hand-moved pointer movements that are initiated without eye guidance in parallel to an eye movement to the target item. If visual search for a target is required prior to selection, users parallelize search and pointer movements. While looking for the target, hand moves a pointer roughly following the scanpath of an eye to keep the pointer close to the searched area. Thus, they minimize the amplitude of the required hand movement, once the target is found. Also, human might employ the hand-moved

pointer as an active reference tool for marking potential targets or as a reference for keeping track of the search area [17].

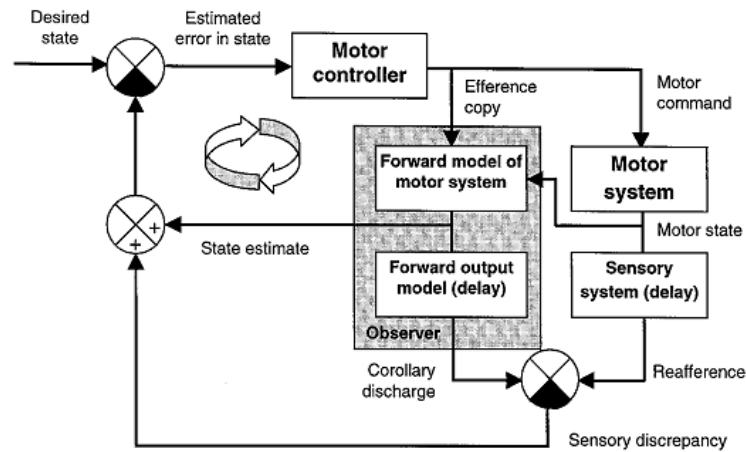


**Fig. 1.26** The Smith Predictor model. From [116].

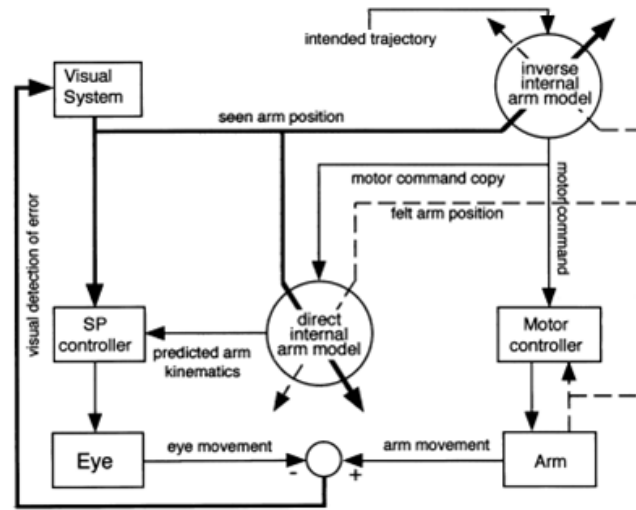
### 1.5.1. Eye-hand coordination in object guiding

When subjects visually pursue a moving target, performance significantly improves if the target is under manual control by the subject or correlates with a simultaneous manual task. An investigation reported that subjects initiated the pursuit of an externally controlled visual target with an average 150 ms latency. If a target movement correlated with passive movement of the hand, this latency reduced to 130 ms. And if the target was self-moved, eye movement had an average 5ms lead [174] and maximum smooth pursuit velocity was higher than double [53].

There is also an evidence of the anticipatory use of gaze in acquiring information about objects for future manipulation [168]. During performance of natural tasks where the plot contains many objects and points of interest, subjects sometimes fixate objects that are manipulated by hand several seconds later. Such eye movements are called “look-ahead fixations”. Experimental research has shown that hand movements following such fixations (even if there was some intervening fixations) were more accurate [114]. It is also known that during object manipulation there are some areas in the plot, where a fixation is critical. E. g. the grasp bar of a tool or the target for a use of the tool. Also, there are some optional such landmarks: obstacles in a tool movement path or a tip of the tool. It is suggested that such landmarks are a sign of oculo-motor system aided motor command planning [71]. For tasks of drawing, it is known that a gaze-point leads the hand-moved pointer and most of the time. Fixation lasts approximately 200 ms after hand-moved pointer overtakes the gaze-point. Also, the saccades in drawing tasks are usually planned to local curvature complexity maximums in each local segment of hand movement trajectory [137, 165].

If a spatial or temporal relation between hand movement and hand-manipulated object's visual position is synthetically modified, smooth pursuit gain significantly decreases. This can be taken as one more proof that an internal model (Fig. 1.27) of the arm dynamics is used not only in planning arm motor commands, but also in planning eye movements. Changes in smooth pursuit gain are not observed in deafferented subjects, what tells that arm proprioception signal contributes to this internal model as well [147].

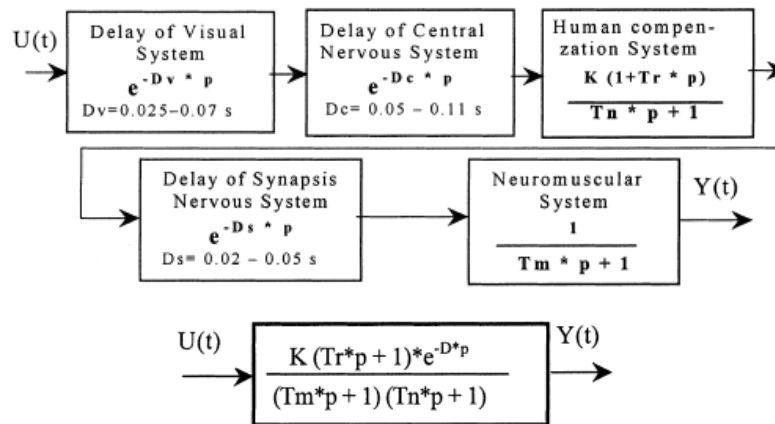
**Fig. 1.27** The simplified model on involvement of the internal model of arm dynamics as a supplementary source of hand motion information. Bold lines represent the visual signal. Thin lines show the outflow and efferent copy signals. Dashed lines indicate the proprioceptive signal. Diagonal arrows indicate that the signal is used to update/adapt the system. From [147].



### 1.5.2. Eye-hand coordination models

Human eye-hand coordination models are required in situations when human operator behavior must be evaluated (e. g. design of a human-operated control system). Alexik has shown that linear model output (Fig. 1.28) is too far from reality and suggested a non-linear model of oculo-manual tracking (Fig. 1.29). This model was fitted with different parameter sets, having in mind different personal-characteristics (“slow”, “skilled”, “cautious”) of the operator [2].

**Fig. 1.28** Linear model of the operator: block scheme and the transfer function. From [2].





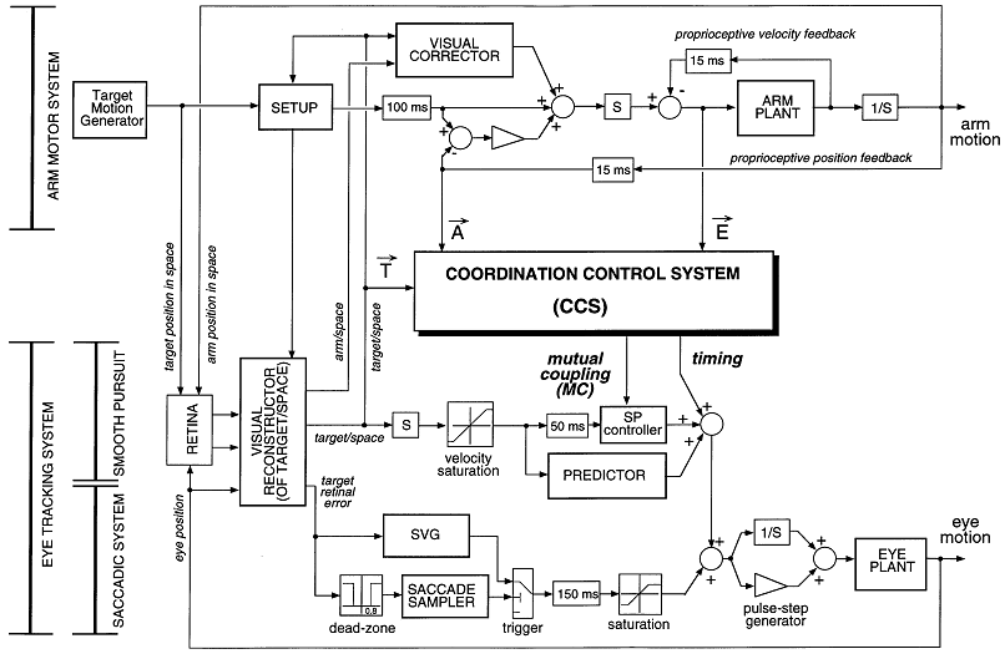


Fig. 1.30 Block diagram of the model. From [99].

Target velocity for smooth pursuit simulation is saturated to 100 deg/s. Predictor compensates for the delay due to visual (50 ms) and the smooth pursuit (40 ms) systems. The predictor forecasts the velocity of the target for next 400 ms, on the basis of a cubic spline interpolation of the actual target velocity during last 150 ms. Smooth pursuit controller, with a transfer function:

$$SP_c(s) = \frac{0.93}{0.13s + 1}, \quad (1.35)$$

has a higher relative contribution to overall smooth pursuit branch output than the predictor.

Arm branch is also a simplified model. Intended arm movement is delayed by 100 ms processing delay, differentiated and sent to arm motor plant. Inputs are the target position provided by visual reconstructor and the positional error compensating signal from visual corrector which compares the positions of the target and the arm pointer. Visual corrector uses PID controller to realize intermittency of arm movement. Proprioceptive velocity and position feedback loops has 15 ms delay each.

The coordination control system (Fig. 1.31) has two purposes: 1) to change the dynamics of smooth pursuit system when the arm and eye movements are correlated. If eye and arm movements (including delay) is strongly correlated, the transfer function of smooth pursuit controller is being changed to:

$$SP_c(s) = \frac{0.93}{0.021(1 + 5.5mc)s + 1}; \quad (1.36)$$

2) to simulate situations when because of intention to move arm and eye together, efferent arm motor command copy is available for smooth pursuit system. This allows the movements of both systems to start at almost the same time. In order for this to take a part only at the beginning of the movement, a smoothing function  $G(t)$  is used:

$$Timing = x \cdot G(x); \quad (1.37)$$

$$\text{where } G(x) = \frac{2-x}{0.2x^7+400}.$$

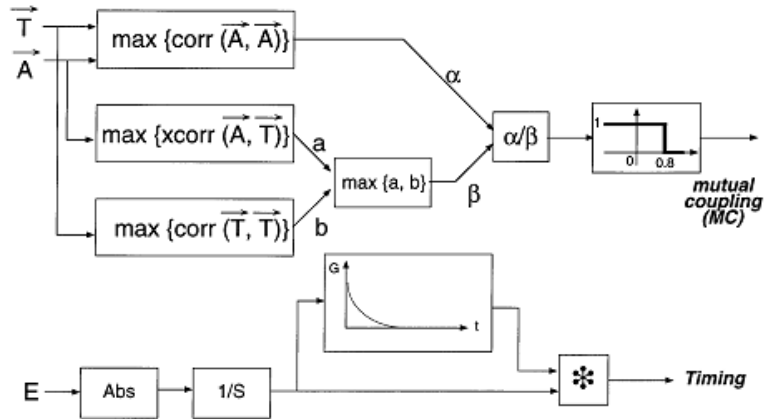


**Fig. 1.31** Block diagram of the coordination control system model. From [99].

Most of the parameters of coordination for this model were determined empirically. According to a publication on verification of this model, simulation outputs of this model were examined and compared to experimental data (Fig. 1.32-1.34). It was also tested by introducing artificial delays in and reversal of the relation between arm movement and arm-moved pointer movement [176].

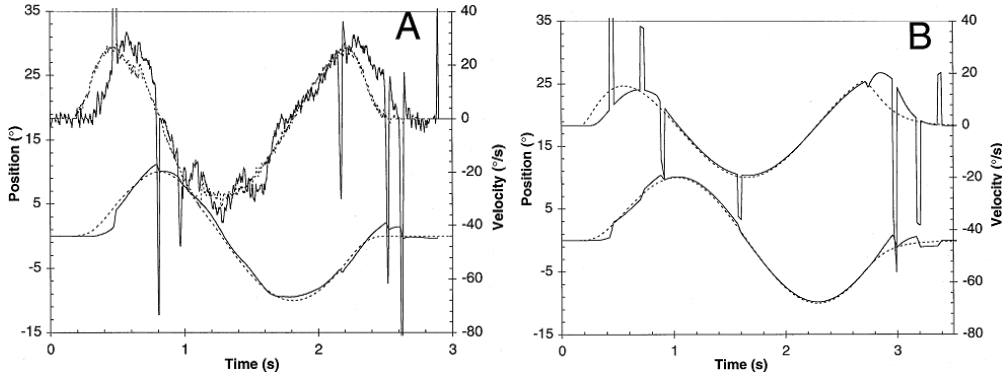


**Fig. 1.32** Performance of a human subject during oculo-motor tracking of a moving visual target (A). Output of the eye-tracking model following a characteristic equal target (B). The thin lines represent eye position (bottom trace) and velocity (top trace) and the dotted lines represent target position and velocity. From [176].

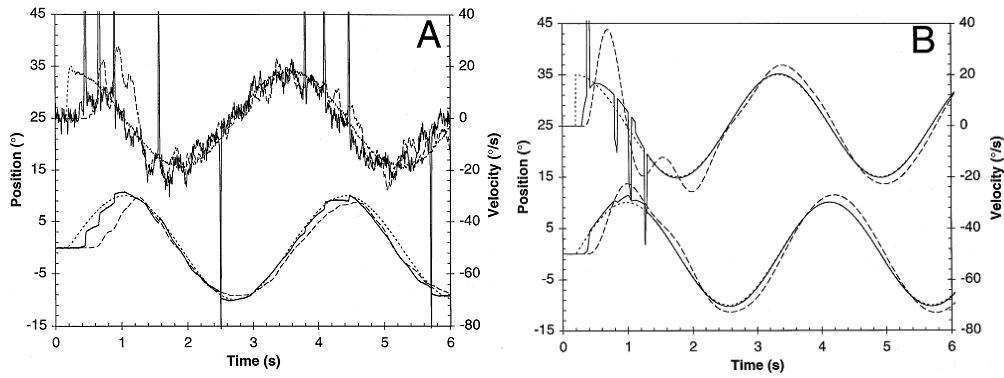


**Fig. 1.33** Performance of a human subject during oculo-manual tracking of a moving visual target (A). Output of the eye-tracking model following a characteristic equal target (B). The thin lines represent eye position (bottom trace) and velocity (top trace) and the dotted lines represent target position and velocity. From [176].

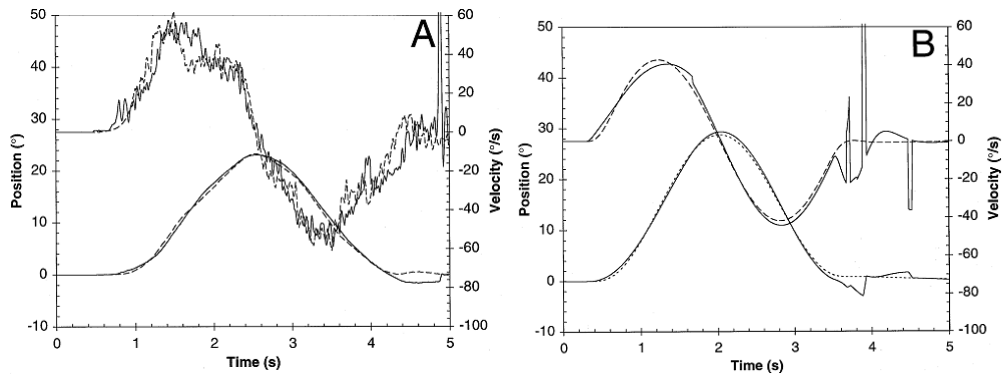


**Fig. 1.34** Performance of a human subject during oculo-motor tracking of a self-moved visual target (A). Output of the eye-tracking model following a characteristic equal target (B). The thin lines represent eye position (bottom trace) and velocity (top trace) and the dotted lines represent target position and velocity. From [176].

## 1.6. Summary and conclusions

1. Explicit mathematical and neurophysiological models of eye-movement control system do exist.
2. Arm movement research and modeling is complicated because of multiple-joint freedom and complexity of arm movements. Some controversy in fundamental principles of arm-movement control system structure was reduced only recently, therefore there is a lack of more explicit investigation. The present models for motor command planning and execution remain in an abstract phase. In order to quantitatively model arm movements during oculo-manual guiding, simplified models reproducing experimentally observed output by using automatic control

theory principles only, must be fitted for this specific arm/hand movement simulation.

3. Eye-hand coordination for ocular, oculo-manual and self-moved target tracking is researched to the level when neurophysiology-based models do exist. Since eye-hand coordination in everyday environment is involved not only in tracking of a visual stimuli, but also in hand guiding tasks: much of recent year research is focused on this. Most of the investigations focus on eye-hand coordination during reach and grasp or similar (reposition of objects, tool usage on a specific object, etc.) arm movements.
4. Eye-hand coordination while guiding a hand in visible environments is investigated insufficiently to understand and identify processes taking part. Only some presumptions of processes involved in such real-life tasks can be done by using knowledge on reach and grasp eye-hand coordination. There are no models for explaining or simulating eye-hand coordination during oculo-manual guiding.
5. It is likely that in oculo-manual guiding, control systems of arm movement and smooth pursuit eye movement are interacting or even are partially shared. Since such interaction is implemented in existing models for oculo-manual tracking of a moving stimulus, it can be hypothesized that such models can be extended for simulation of the oculo-manual guiding eye and arm/hand movements.

### **1.7. Tasks towards the aim of the work**

Review of existing knowledge lead to settlement of further task of the work:

1. Since smooth pursuit eye movement control system appears to be very closely involved, it is a good starting point. Especially knowing that smooth pursuit or similar movements are to be expected in a guiding of hand-moved target. Smooth pursuit eye movements consists of two very different subtypes: smooth pursuit and catch-up saccades. Knowledge on catch-up saccades, their role and the influence on the quality of the pursuit is insufficient to compare such saccades to other eye movements, which are used during object-guiding.
2. Oculo-manual guiding movements must be compared to the oculo-manual pursuit by characteristics. This will provide a basis for identifying differences in two control systems.
3. The differences identified in previously settled task can be integrated with the existing neurophysiological models of eye movement, arm movement and eye-arm coordinated movement control. The result is one, neurophysiology-consistent mathematical model of control system for coordinating oculo-manual guiding movements. Such model will not only explain, but also will simulate the eye-hand coordinated movements of a human executing object-guiding task.
4. New models and knowledge collected while fulfilling earlier described tasks might be used in engineering novel methods, technologies and systems. It is necessary to assess possible areas and benefits of application.

## 2. PRELIMINARY MODEL AND EMPIRICAL RESEARCH PLANNING

### 2.1. Preliminary model for simulating human oculo-manual coordination

There was found no models for oculo-manual guiding in visual paths. The closest model for target tracking tasks including tracking a hand-moved target, is the one by Lazzari S. et. al. (presented in chapter 1.5.2). This verified quantitative model is implemented in “Matlab Simulink” environment and its structure is consistent with the physiology of the human. This existing model is a good start for designing a model, simulating human performance in manual object guiding through a visual path, because it has a simplified arm model, a simple two-part eye model (smooth pursuit and saccadic subsystems) and a Coordination Control System (CCS), capable of simulating ocular pursuit of the self-moved target. Main part of the model is CCS, which has inputs of visual target position, arm afferent signal and efferent copy of arm position. CCS controls the timing of the smooth pursuit and the bandwidth of eye movements. This model can be augmented or partially modified to design the system, capable of simulating human performance during the object-guiding task. In fig. 2.1, required or possibly required modifications of model structure are marked.

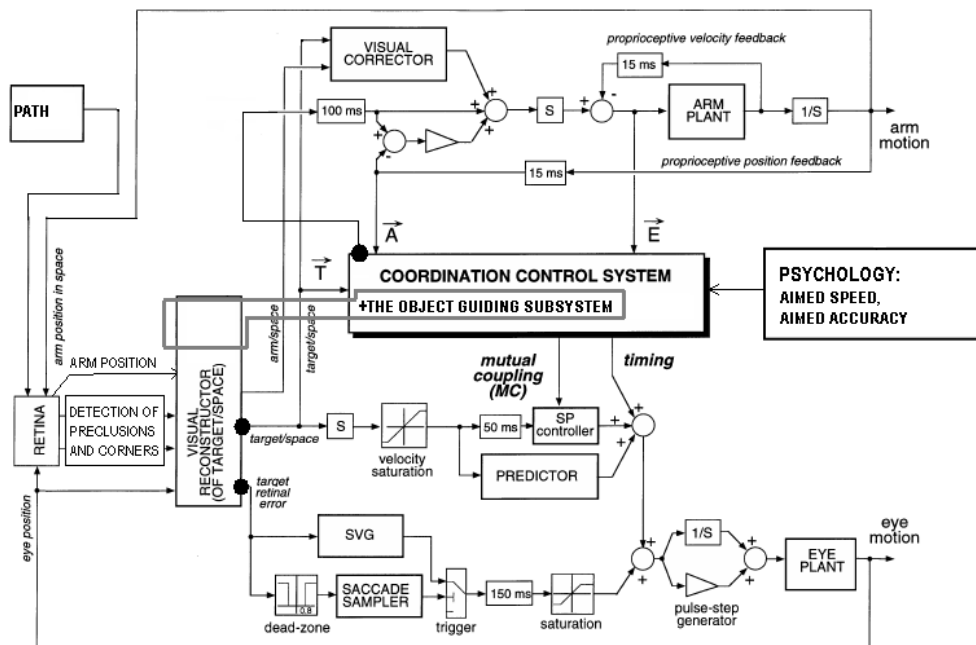


**Fig. 2.1** Preliminary model for oculo-manual guiding task simulation. Black dots mark signals, which are different than in an existing model for oculo-manual target tracking.

It is clear that input for such model is no longer only an arm-moved stimulus movement, but also the view of a scene (using both peripheral and foveal vision). Also, some mechanism in higher-than-motor level of the brain responsible for arm and eye movement pathway decision exists. It can be speculated that its main input

parameters are the conspicuous areas in a scene observed. This perceived pathway replaces the signal of target position and movement (i. e. some of its points become target locations for the movement of the eye and the arm). Coordination of following through this pathway depending on psychology-related decisions is a function of some Object Guiding Subsystem (OGS), which is a part of CCS. This OGS, which was found to be researched very poorly, can also be simply a consequent mechanism of other functions of CCS.

As there is very limited knowledge on eye-hand coordination during oculo-manual guiding, before mentioned extensions of the model can be done quantitatively, it is important to understand and identify coordination processes during oculo-manual guiding tasks. Experimental research plan and methodology is detailed in next section.

Some computational tools needed for easier experimental data processing and modeling were formulated:

1. Smooth eye movement gain is one of the main factors in target pursuit and oculo-manual guiding. An expression, reducing the need of unnecessary computations while processing experimental data, for average gain calculation is desirable.
2. As oculo-manual guiding at a first glance is different from smooth pursuit mainly in gain and timing (lag or prediction), a tool for assessing the timing (in experimental data) is needed.
3. Human before and during the oculo-manual guiding is undoubtedly performing an assumption of visual environment's difficulty. In order for the model to simulate human-like performance, a mathematic tool for assessment of a difficulty of a path is essential.
4. Model will be fitted by using trend-lines of experimentally obtained dependencies of main parameters. These dependencies are expected to vary around the trend-line in a probability distribution with some skewness. It would be uninformative to analyze those variations by only providing SD. A computational tool allowing indicating both skewness and SD is also proposed.

## **2.2. Experimental research required for understanding and modeling human oculo-manual coordination**

### **1. Experimental research on eye movements:**

1.1. Since smooth pursuit eye movement control system appears to be very closely involved, it is a good starting point. Especially knowing that smooth pursuit or similar movements are to be expected in a guiding of hand-moved target. Smooth pursuit eye movements consists of two very different subtypes: smooth pursuit and catch-up saccades. Arm movements, on the other hand, comparing the dynamic parameters are more similar to smooth eye movements: mass (and inertia) of the arm parts is too high to be moved in a fast and precise manner. As the most obvious difference is the absence of catch-up saccades in arm movements, it is important to understand what influence those catch-up saccades has for visual tracking quality. It is generally thought of catch-up saccades as of any other saccadic eye movements, what is not absolutely right. The purpose of catch-up saccades is different: they are

not used voluntarily for reposition of a gaze (as a pointer of attention). They are used by the lower neural layers to correct for an increasing deterioration of incoming visual information (what is not absolutely true, because of different purposes of foveal and peripheral vision). This hypothesis of specific purpose for catch-up saccades can also be supported by a question: if the eye movement control system and the eyes themselves are capable of moving in velocities of up to 1000 deg/s (during a saccade), why then the eye control system is moving the eyes in maximum velocity of 80 deg/s even if the target being tracked moves faster? An answer could be the physiology of a retina. Central (or foveal) region of a retina contains high amount of cones and peripheral areas contains no cones, but rods. Since a better perception of motion is using the peripheral areas of the retina, it is beneficial to maintain the object of interest in periphery. On the other hand, there is also an interest on the object itself, so central vision is also important. As human brain is capable to reconstruct visual space from snapshots (as all the scenes are acquainted using fastest possible method: saccadic scanning), it is not a problem if the target being tracked is in central vision area only for partial time. Another benefit from such excessive eye movement strategy is that central vision can be used to acquire more visual information about the adjacency of a tracking object. Such strategy appears to be valid and even more significant for guiding eye movements: it is important not only to see the object being manipulated, but also to estimate its movement and a space nearby. This is why catch-up saccades or at least similar eye movements are to be expected in oculo-manual guiding. This is why smooth pursuit eye movements (including properties of catch-up saccades) and their control system is so important in analyzing oculo-manual guiding.

1.2. During oculo-motor tracking or oculo-manual guiding, not only the visual space is reconstructed from snapshots, but also visual occlusions do occur. They have a weak impact on a visual space perception, but eye movement control at such situations is complicated – smooth eye movements for tracking an invisible object are considered to be normally non-useable. Eye movement during such occlusions analysis can lead to a deeper understanding of eye movement control system. Also, this is the way to answer a question if the strategy of simultaneous viewing the object in both central and peripheral areas of the retina is a result of an on-line or off-line planning. Experimental research on this topic is provided in appendix B.

1.3. Another in natural conditions often observed phenomenon is visual illusions. Our environment often has some objects, which because of their interposition introduce some level of one or several types of visual illusion. In order to understand how such natural conditions can possibly affect eye-hand coordination it is important to understand their nature and effect on eye movements (appendix C).

2. Experimental research on eye-hand coordination while controlling hand-moved object:

2.1.1 Eye-hand coordination in natural environments also manifest by rapid eye and hand movements of reaching, pointing, etc. Even while guiding a hand-moved object, such movements are necessary just before the guiding or in cases of complex situations. Pointing movement properties also could be compared to catch-up saccades. Such oculo-manual coordination is primitive and easy to understand. Therefore, a small experimental trial of reaching (pointing) will be performed to

compare dynamic characteristics of arm/hand while performing the same task using different hand position registration devices. Also, the characteristics of such eye-hand coordination are important in evaluation of possible eye movement applications.

2.1.2 It is known that hand movements influence eye movements and eye movements influence hand movements in form of accuracy and timing (function of CCS in fig. 2.1). In order to collect quantitative data, experimental research is needed. The same trajectory can be traced by hand while tracking by gaze, tracked by gaze as unpredictable trajectory, tracked by gaze and by hand as unpredictable trajectory. Results can reveal differences in timing and accuracy of tracking. For different modes of coordination, the timing and the accuracy will be different and will provide an information on mutual coupling between arm movement and eye movement systems.

2.2. The most valuable information for a model can be obtained by investigating the eye-hand coordination while guiding a hand-moved object in a visible environment. Experimental trials should reveal the interaction of the hand movement and the movements of the eye. The results could be comparable to trajectory tracing by hand, but should reveal the supervisory purpose of eye movements. Guiding in different paths must be examined: wide and narrow, straight or with a corner, with visual obstacles or changes in path's width. The obtained results must also be evaluated by analyzing inter-subject and extra-subject variability and their dependency on subject's personal skills (appendix D). Since such hand-moved object guiding in visually restricted space is a natural task and has not been investigated, it can provide some significant information about human neurophysiology. After identification of processes taking action during oculo-manual guiding, measures that will be used in the model, must be defined and quantitatively measured using experimental data.

### **2.3. Common methodology of planned experimental research**

During all experiments, movements of both eyes were recorded with video-oculography based eye tracker EyeGaze System (LC Technologies Ltd). This system captures and analyses images of each eye at 60 Hz rate simultaneously, thus the result is a 120 Hz eye tracking data. All the visual stimuli and hand-moved objects were presented on 15 inch fast response monitor by a specialized stimuli generation and experiment control software. Data recording and experiment control was processed by the same software in order to maintain timing as accurate as possible. Gaze tracking instrumentation was setup so, that 1-degree eye angle corresponded to 46 pixels on computer screen. Stimulus to be tracked or manipulated was a disc-shaped object of high contrast color (in black background) with a diameter of (0.25 deg). Absolute hand position (if needed), reported by tablet WACOM Intuos 2 (in some experiments additional hand position input devices were used), was also registered and retained for further processing. The spatial relationship between amplitude on computer screen and amplitude on pen tablet was equal to one.

Healthy subjects, 18-45 years old, were recruited after informed consent. Subject quantity varied from 8 to 22, data of experienced users (subjects involved in experiment coordination) was used only if consistent with common trend. None of the

subjects has showed any visual, oculo-motor or oculo-manual pathology. Subjects had normal or corrected to normal visual acuity.

The missing eye tracking data during eye blinks was filled using automated script, which uses simple interpolation. All the data processing was performed offline using specialized MATLAB scripts, which were prepared for this purpose.

In order to evaluate possible discrepancies of the timing, additional experiment was executed. Computer graphic system lags (time from stimuli change in software to actual stimuli appearance on the screen) were measured using photo-diode and digital oscilloscope. Also, the timing of EyeGaze System was refined. Analysis of collected data has revealed timing parameters for the off-line processing of collected experimental data. Computer graphic system functions distorting the timing, such as V-sync were disabled.

#### 2.4. New mathematical expression for pursuit gain calculation

Traditionally pursuit gain  $G$  is specified as the ratio of slow phase of eye movement velocity  $V_{ES}$  and target velocity  $V_T$  [15]:

$$G = \frac{V_T}{V_{ES}}. \quad (2.1)$$

Due to difference between the target and eye movement velocities, catch-up saccades with suitable amplitude are needed. As seen in Fig. 2.2, eye velocity during catch-up saccade is the sum of a slow and a quick ( $V_{EQ}$ ) phases of eye velocities:

$$V_E(t) = V_{ES}(t) + V_{EQ}(t). \quad (2.2)$$

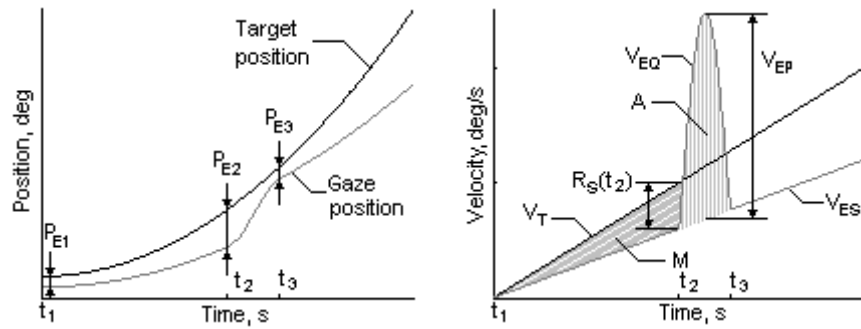


**Fig. 2.2** Illustration of the trajectories and parameters of the target and gaze positions (**left** sketch) and velocities (**right** sketch) for a single catch-up saccade.

The distances in which the eye is moved during slow and quick phases, and position errors, which are left at the end for one single saccade (time interval from  $t_1$  to  $t_3$ ) could be defined by equation:

$$P_{E1} + \underbrace{\int_{t_1}^{t_2} [V_T(t) - V_{ES}(t)] dt}_M = \underbrace{\int_{t_2}^{t_3} [V_{EQ}(t) - V_{ES}(t)] dt}_A + P_{E3}; \quad (2.3)$$

where  $P_{E1}$  and  $P_{E3}$  are the position errors at times  $t_1$  and  $t_3$  respectively; integral  $M$  represents area  $M$  and integral  $A$  – area  $A$ , which correspond to the amplitude of catch-up saccade.

Assuming that during time interval between two catch-up saccades and during a catch-up saccade, the target and eye velocities increase linearly, for the left part of the equation (2.3) we can define the area  $M$ :

$$M = [V_T(t_3) - V_{ES}(t_3)]T_{ID} = [V_T(t_2)(1-G)T_{ID}]; \quad (2.4)$$

where  $G$  is pursuit gain and  $T_{ID}$  is the time interval between  $t_1$  and  $t_3$ .

Integral in the right side of the equation (2.3) can be replaced by [49]:

$$A = qV_{EP}T_D; \quad (2.5)$$

where  $q = 0.61$  is a coefficient evaluating bell shape of a catch-up saccade;  $T_D$  is the time interval between  $t_2$  and  $t_3$ .

Now the pursuit gain  $G$  can be expressed from this modified equation (2.3):

$$P_{E3} + qV_{EP}T_D = V_T(1-G)T_{ID} + P_{E1}, \quad (2.6)$$

$$G = 1 - \frac{P_{E1} - P_{E3} + A}{V_T T_{ID}}. \quad (2.7)$$

Every single catch-up saccade is performed to reduce and minimize position error, but during long tracking, only sequence of them is able to perform a precise pursuit.

For the sequence of  $n$  catch-up saccades, equation (2.6) can be rewritten:

$$P_{E(n+1)} - P_{E1} = \sum_{i=1}^n [qV_{EP_i}T_{D_i} - V_{T_i}(1-G_i)T_{ID_i}]; \quad (2.8)$$

where expression  $qV_{EP_i}T_{D_i} = A_i$  represents distance  $D_{EQ_i}$  of eye movement by  $i$ -th catch-up saccade with a peak velocity  $V_{EP_i}$  and duration  $T_{D_i}$ ; expression  $V_{T_i}(1-G_i)T_{ID_i}$  represents distance  $D_{ES_i}$  of eye movement during  $i$ -th slow phase, when target velocity was  $V_{T_i}$ , pursuit gain -  $G_i$  and time interval  $T_{ID_i}$ ; expression  $P_{E(n+1)} - P_{E1}$  represents position error at the end of the sequence of catch-up saccades, which during long tracking ( $n > 10$ ) can be neglected.

Equation (2.8) fits physiological mechanism of the triggering of catch-up saccades. There is only one external input parameter – transient target velocity  $V_T$ , one parameter of the oculo-motor system - pursuit gain  $G$  and one output parameter - peak velocity of catch-up saccade  $V_{EP}$ .

Using the positions and the distances of the target and eye movement trajectories, we can assume that the distance of target trajectory  $D_T$  is tracked in  $n$

segments of the slow and fast eye movement trajectories:  $D_{ESi}$ ,  $D_{EQi}$ , respectively. Such way the expression (2.8) can be expressed this way:

$$\sum_{i=1}^n A_i = \sum_{i=1}^n D_{Ti} (1 - G_i) . \quad (2.9)$$

This equation presents pursuit gain not in the velocity form (usual form), but express the relation between the distances of the target and catch-up saccades in the sequence of them. The average of the pursuit gain  $G_A$  during the sequence of catch-up saccades could be calculated using the expression (2.10):

$$G_A = \frac{1}{D_T} \sum_{i=1}^n D_{ESi} = 1 - \frac{1}{D_T} \sum_{i=1}^n A_i . \quad (2.10)$$

If to be assumed that during inter-saccadic interval  $T_I$  target velocity  $V_T$  and slow phase eye velocity  $V_{ES}$  do not change significantly, average pursuit gain  $G_A$  could be defined by the average of  $G_i$ :

$$G_A = \frac{1}{n} \sum_{i=1}^n G_i ; \quad (2.11)$$

where

$$G_i = \frac{V_{ESi} T_I}{V_{Ti} T_I} = \frac{D_{ESi}}{D_{Ti}} . \quad (2.12)$$

This expression of average pursuit gain was tested for adequacy by an experimental trial, which results are presented in appendix A.

## 2.5. Trajectory shifting in time as a means to evaluate a lag or prediction of the tracking

When a gaze or a hand-moved cursor is tracking a moving target, some level of lag or some level of anticipation is involved. Since the trajectories of hand and gaze movements cannot be easily and accurately determined in mathematical equations, some more practical method is required.

For this purpose, in experimental research discussed in later chapters, a trajectory shifting in time method, based on sliding inner-product was used. If a cross-correlation is:

$$XC \stackrel{\text{def}}{=} \int_{-\infty}^{\infty} T(t)^* F(t) dt ; \quad (2.13)$$

where  $XC$  is the cross-correlation;  $T(t)^*$  is a complex conjugate of the trajectory of the target;  $F(t)$  is the trajectory of the follower (hand-moved cursor or gaze).

Then the trajectory  $F(t)$  can be shifted in  $t$  axis by a time  $t_s$ :

$$XC(t_s) \stackrel{\text{def}}{=} \int_{-\infty}^{\infty} T(t)^* F(t + t_s) dt . \quad (2.14)$$

As signals of digital eye and hand movement tracking equipment are discrete and experiment duration is finite ( $M$  collected data readings), equation (2.14) can be expressed in:

$$XC[n] = \sum_{m=1}^M T[m] * F[m + n]; \quad (2.15)$$

where  $n$  is the collected data reading sequence number corresponding to time;  $M$  is the count of collected data readings.

In order to obtain for a dataset of a function  $XC(t_s)$ , it is needed to calculate  $XC$  with various  $t_s$  values. These values can be in a limited range, because the latency or anticipation of a tracking is expected to be within a range of -500 ms to 500 ms. As the experimental results are sampled at 8.33 ms:

$$XC[n] = \sum_{m=0}^M T[m] * F[m + n], \quad -60 < n < 60. \quad (2.16)$$

Equations (2.14 and 2.16) provides functions, which has its peak values at a time  $t_s$  (or at a data sample  $n$ ) where both  $F(t + t_s)$  (or  $F[m+n]$ ) and  $T(t)$  (or  $T[m]$ ) correlate the best. Thus:

$$t_{latency} = \arg \max_{t_s} (XC(t_s)) \quad (2.17)$$

OR

$$t_{latency} = \arg \max_n (XC[n]) \cdot 0.00833; \quad (2.18)$$

where  $t_{latency}$  is the latency or anticipation time (if negative) of the follower's movement in the respect with the target's movement.

It is also easy to compare the overall tracking accuracy of several followers as:

$$XCmax = \max_{t_s} (XC(t_s)). \quad (2.19)$$

The same can be done using SD of tracking error ( $SDE$ ) instead of cross-correlation. In such case, the equations (2.15), (2.18) and (2.19) respectively are changed by:

$$SDE[n] = \sqrt{\frac{1}{M-1} \sum_{m=1}^M ((T[m] - F[m+n]) - \overline{(T[m] - F[m+n])})^2}, \quad (2.20)$$

$$t_{latency} = \arg \min_n (SDE[n]) \cdot 0.00833, \quad (2.21)$$

$$XCmax = \min_n (SDE[n]). \quad (2.22)$$

## 2.6. Usage of Fitts' Law derivatives for visual trajectory evaluation

In order to evaluate indexes of difficulty of the visual paths, used in experimental trials in chapter 3.3, Fitts' law derivatives can be used. Steering law is

the most suitable for this purpose. Based on equations (1.26) to (1.29) it can be stated that index of difficulty (ID) for oculo-manual guiding of a hand-moved object along straight visible paths can be evaluated using this equation:

$$ID = \frac{A}{W}; \quad (2.23)$$

where  $A$  is the distance of a straight path;  $W$  is the width of the path.

Equation (2.23) is true if the object being guided is relatively small (or has a sharp tip as a mouse cursor do). If the cursor is larger, then the difficulty increases as the allowed hand movement fluctuation across the path reduces. If the width of the object in the perpendicular to hand movement direction is  $w$ , then equation (2.23) can be expressed:

$$ID = \frac{A}{W - w}. \quad (2.24)$$

According to equation (1.32), equations (2.23) and (2.24) is also valid for curved paths as long as the width of the path (and the size of the cursor) are constant.

## 2.7. Standard deviation from a mean for above-mean and under-mean values

Some of experimentally obtained results are scattered around their mean value in a probability distribution with some positive or negative skewness. In order to represent variability of such data in charts, skewness could be used together with SD since simple SD is not suitable. But such a way would be too unapparent. However, it is possible to use SD to correctly represent variability of such data: data samples above mean should be grouped and be used to calculate the variability above mean, and data samples below the mean can be used to calculate the variability in another direction from the mean value.

Regular corrected sample standard deviation formula is:

$$\sigma = \sqrt{\frac{1}{n-1} \sum_{i=1}^n (x_i - \bar{x})^2}; \quad (2.25)$$

where,  $\sigma$  is the SD;  $n$  is the total number of samples;  $\bar{x}$  is the mean of all samples.

SD from the mean  $\bar{x}$  for only the above-mean samples ( $\sigma_{AM}$ ) can be expressed:

$$\sigma_{AM} = \sqrt{\frac{1}{n_{AM}-1} \sum_{i=1}^{n_{AM}} (x_{AMi} - \bar{x})^2}; \quad (2.26)$$

where,  $\sigma_{AM}$  is the SD for points above the mean value ( $SD-AM$ );  $n_{AM}$  is the number of data samples above the mean  $\bar{x}$ ;  $x_{AMi}$  is the  $i$ -th sample from a set of samples-above-the-mean;  $\bar{x}$  - the mean of all samples.

The same can be done with data samples below the mean  $\bar{x}$ :

$$\sigma_{UM} = \sqrt{\frac{1}{n_{UM} - 1} \sum_{i=1}^{n_{UM}} (x_{UMi} - \bar{x})^2} ; \quad (2.27)$$

where,  $\sigma_{UM}$  is the SD for points under the mean value (*SD-UM*);  $n_{UM}$  is the the number of data samples above the mean  $\bar{x}$ ;  $x_{UMi}$  is the  $i$ -th sample from a set of samples-below-the-mean;  $\bar{x}$  - the mean of all samples.

## 2.8. Summary and conclusions

1. Oculo-manual guiding is expected to be similar to smooth pursuit eye movements in an eye movement-purpose way. However, this working hypothesis must be tested. Since known research does not deal with such question, the only way to prove or deny this working hypothesis is a comparison of experimentally obtained data.
2. To explain eye-hand coordination during oculo-manual guiding, a model of oculo-manual self-moved target tracking is about to be extended to simulate eye and hand movements during oculo-manual path following. Preliminary extended model is proposed.
3. Oculo-manual guiding model structure can be decided and model can be fitted only after a set of experimental trials. It appeared, that quantity of experimental research required to come up with a working model is more than it was expected. Points that are unexplored or explored insufficiently were revealed and used for experimental research planning. The plan and common methodology of empirical research and data processing was settled.
4. Computational tools for experimental data processing and modeling were proposed: the expression for faster average gain calculation in experimental data processing; a sliding inner-product (or shifted time cross-correlation) method, adapted for current equipment and planed experimental trials; the use of Steering law (Fitts' law derivative) for mathematical evaluation of indexes of difficulty of visual paths, which were used in experimental trials; the definition of SD, which is more suitable for datasets with non-zero skewness distributions.

### 3. EXPERIMENTAL INVESTIGATION OF SMOOTH PURSUIT EYE MOVEMENTS AND COORDINATED EYE-HAND MOVEMENTS

#### 3.1. Influence of catch-up saccades on a quality of smooth pursuit

In order to evaluate an influence of catch-up saccades to an overall accuracy of smooth pursuit, nine subjects were asked to visually track a moving target. The target was moving in 3 two-dimensional 20x20 deg sized different trajectories: non-predictable (NPR) (Fig. 3.1), which was generated by summing 13 different sinusoids and predictable circular and square shaped trajectories. The set of experiments was repeated with three different average speeds of target's movement: L – 5 deg/s (peak velocity - 12.5 deg/s) duration 60 s.; M – 10 deg/s (peak velocity - 25 deg/s) duration 30 s.; H – 20 deg/s (peak velocity - 50 deg/s) duration 15 s. Due to long tracking (more than 10s), the sequences of successive catch-up saccades were obtained (Fig. 3.1) and their parameters were evaluated.

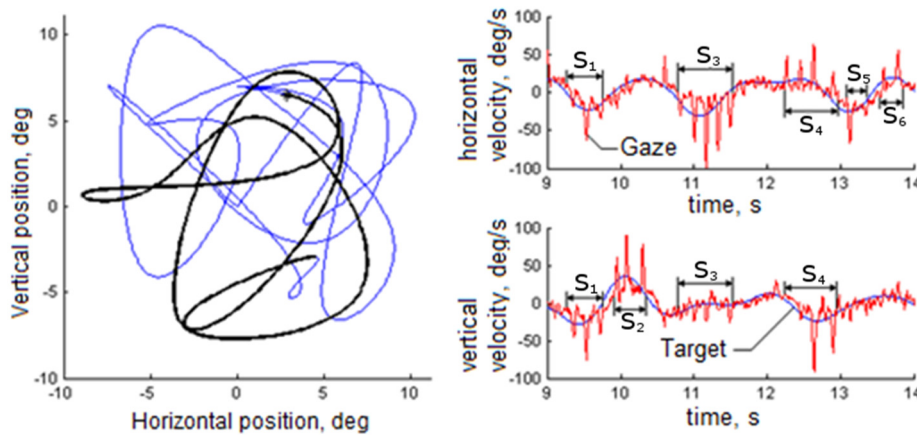


**Fig. 3.1** Non-predictable trajectory of target's movement (**right**); velocities of target and eye movement in horizontal and vertical axes for a part of the trajectory marked by a bold line in the right graph (**left**). S<sub>1</sub> to S<sub>6</sub> are the sequences of catch-up saccades.

Relationships between the parameters of the sequences of catch-up saccades (amplitude, peak velocity, inter-saccadic interval), driving parameters of catch-up saccades (position error, retinal slip) and parameter of oculo-motor system (pursuit gain) were analyzed and are provided in Fig. 3.2.

Scatter of peak velocities in Fig. 3.2 C is observed because different amplitude catch-up saccades are executed at the beginning and the end of the sequences of catch-up saccades. For larger instantaneous target velocities, larger position errors and retinal slips (Fig. 3.2 A, B) were allowed before the catch-up. Therefore, to prevent from further increase of errors, catch-up saccades are used more frequently (Fig. 3.2 E) and they have higher amplitudes (Fig. 3.2 D).

Most regular inter-saccadic time intervals in the range of 100 ms – 150 ms are associated with higher average target speeds and instantaneous target velocities (Fig.

3.3 C). If the velocity of the target is high, pursuit system is forced to perform catch-up saccades as quickly as possible. Otherwise, oculo-motor system has enough time to prepare and elicit a catch-up saccade, so durations of inter-saccadic intervals are not only larger, but also more scattered.

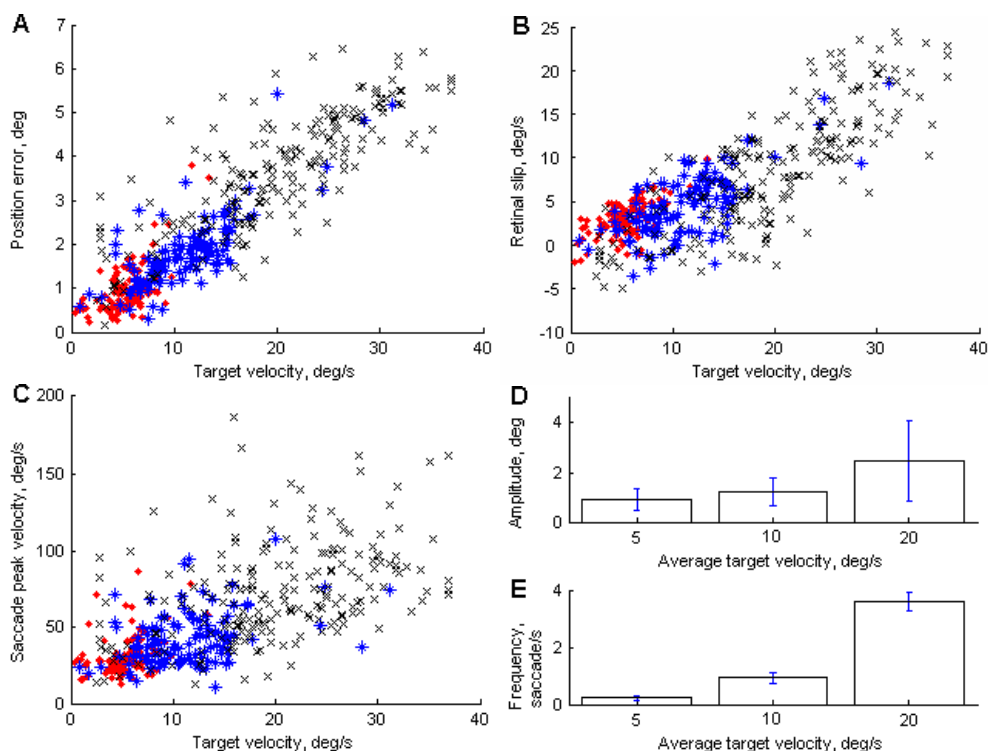


**Fig. 3.2** Sequence mean values of the position error  $P_E$  (A), retinal slip  $R_S$  (B) and peak velocity (C) of catch-up saccades as the functions of the instantaneous target velocity for 3 average target speeds: L (diamonds), M (stars) and H (crosses). Amplitudes (D) of catch-up saccades and frequencies (E) shown as functions of average target speeds.

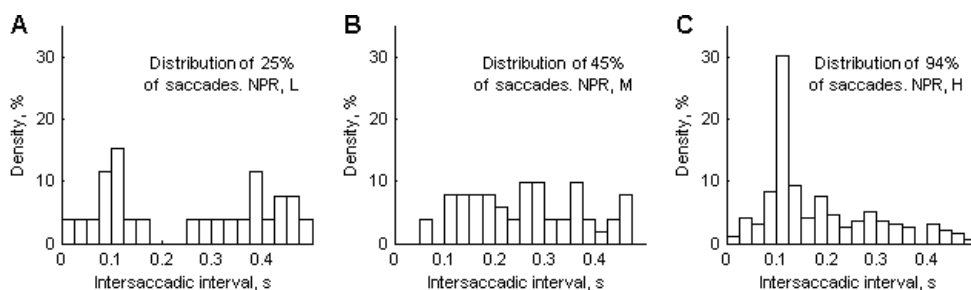


**Fig. 3.3** Distributions of the inter-saccadic time intervals  $T_1$  in the sequence for 3 integral target velocities: L (A), M (B) and H (C).  $n_L = 265$ ,  $n_M = 429$ ,  $n_H = 322$ ;  $T_{bin} = 25$  ms.

As seen from a Fig. 3.4, catch-up saccades reduce tracking errors approximately in the range of 20% to 64%. Reduction of the position error is more effective when

the target movement trajectory is predictable (especially square-shaped) and the target movement velocity is higher.

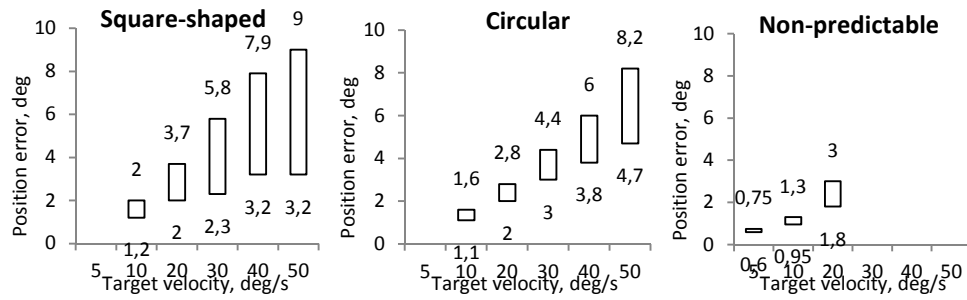


**Fig. 3.4** Position error before (tops of bars) and after (bottoms of bars) a catch-up saccade.

Relationship between the amplitudes of catch-up saccades and position errors together with retinal slips at which they were elicited is calculated to correspond to this equation [37]:

$$A = 0.1 + 0.85P_E + 0.09R_S \quad (3.1)$$

Large discrepancies (Fig. 3.5) of the experimental data support understanding that successive catch-up saccades are programmed and executed using not only the values of position error and retinal slip as the driving parameters.

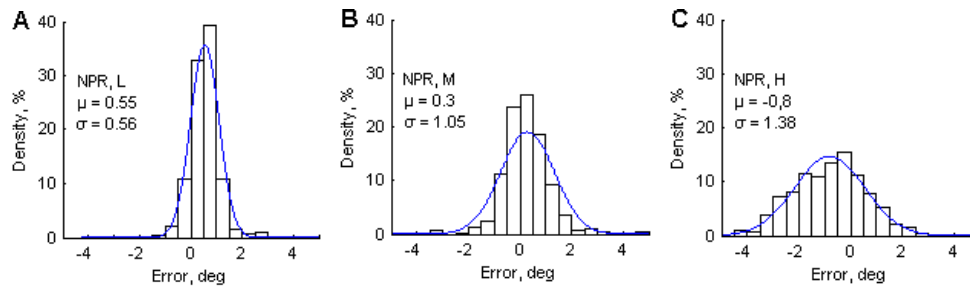


**Fig. 3.5** Distribution of discrepancies (errors) between the amplitudes of catch-up saccades obtained during experiments with three average target speeds L (A), M (B), H (C) and calculated results, obtained by equation proposed by de Brouwer, Missal and Lefevre (2001).  $n_L = 265$ ,  $n_M = 429$ ,  $n_H = 322$ ;  $A_{bin} = 0.5$  deg.

Obtained data proves high precision of the direction of catch-up saccades to the target position, which is acquired before catch-up saccade onset. Also the sequence effect is observed – sequence of catch-up saccades maintains the same direction, therefore the direction of first saccade is always correct, but further catch-up saccades, maintaining the same direction, can have wrong direction (Fig. 3.6).

Obtained data proves high precision of the direction of catch-up saccades to the target position, which is acquired before catch-up saccade onset (Fig. 3.7 A, B). However, changes of the direction of tracking eye movements are possible only during slow component (Fig. 3.6). Directions of catch-up saccades are programmed during slow phase eye movement. Also, the match between slow phases of eye movement

and catch-up saccades directions before the onset of catch-up saccade is better than after catch-up saccade (Fig.3.7 C, D, E, F).

**Fig. 3.6** Sequence effect. The direction of first saccade was correct and subsequent catch-up saccade, maintaining the same direction, has wrong direction. Catch-up saccades  $e_1$  to  $e_{13}$  corresponds to episodes  $tr_1$  to  $tr_{13}$  in a time-manner.

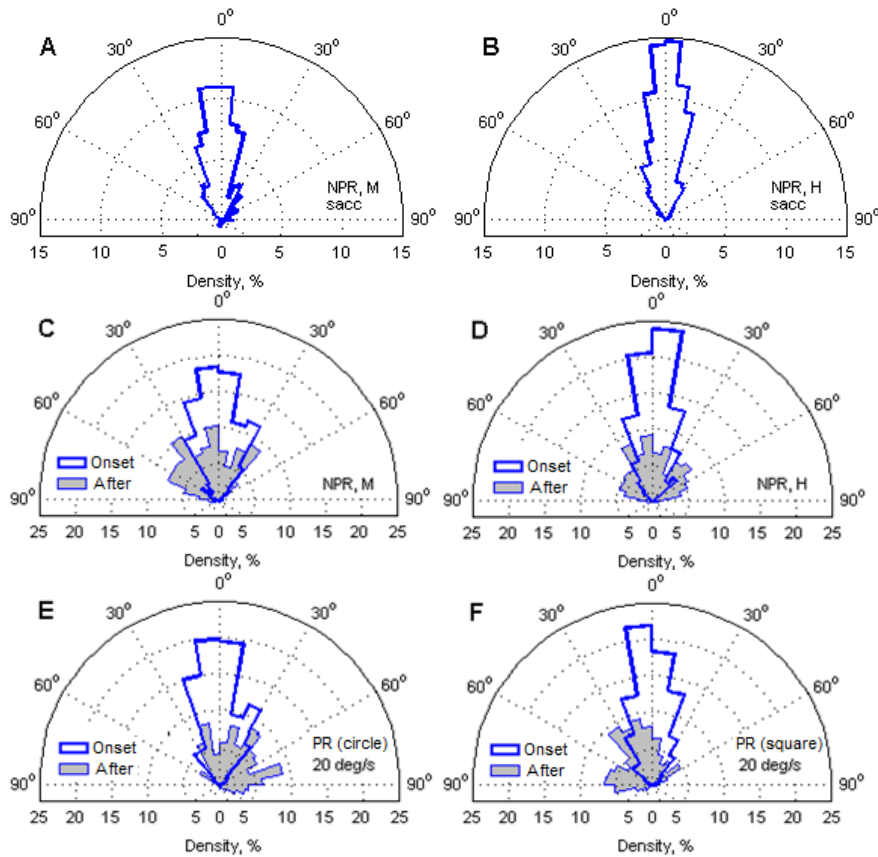
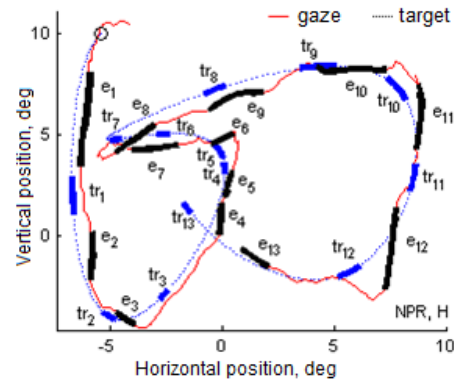


**Fig. 3.7** Scatter of the misalignment between directions of catch-up saccades and target position at the catch-up saccade onset for middle (M) and high (H) target velocities (**A**, **B**). Scatter of misalignment between directions of slow phases of eye movements and catch-up saccades before catch-up saccades onset (solid line) and after catch-up saccade (gray color filled shape) for high (H) and medium (M) target speeds for NPR trajectories (**C**, **D**) and for circular and square-shaped trajectories (**E**, **F**).  $n_M = 429$ ,  $n_H = 322$ ;  $n_{circle} = 251$ ,  $n_{square} = 304$ ;  $bin_{Msacc}, Hsacc = 5$  deg,  $bin_{NPR, PR} = 10$  deg.

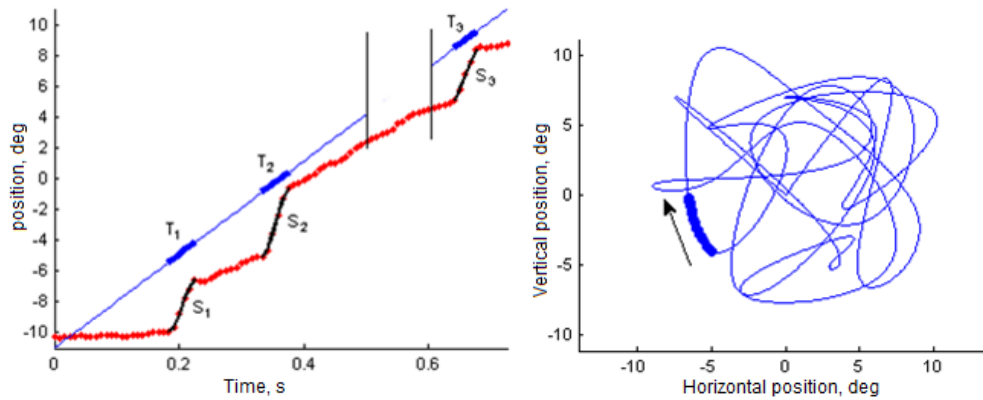


**Fig. 3.8** Visibility occlusions (**left**) and moving segment of the trajectory instead of the disc-shaped target (**right**).

Also it was investigated how an oculomotor system controls smooth pursuit eye movements without input signals. Another experimental trial was executed, this time, at some parts of the trajectory, target disappeared for 100 ms. No changes in eye movement parameters was observed, indicating, that oculomotor system is driven by an internally generated error signal calculated from an extrapolated target trajectory, thus visual feedback is used only in long term.

One more experimental trial was executed. This time, to the contrary, the target motion included additional information: the target was replaced by a moving segment of the trajectory (which indicates additional information about the motion of the target). Also no significant difference was observed in smooth pursuit characteristics. It can be concluded, that oculo-motor system already has properties of the past target trajectory in the short-term memory.

Experimental results indicated that an oculo-motor system was able to react to the instantaneous target velocity and did not use the information about an average target speed. Due to large variety of target velocities and shapes of non-predictable and predictable trajectory segments, the parameters of successive catch-up saccades were more scattered comparing with the results from previous studies, indicating flexibility of the coordination of a quick and slow eye movements. Catch-up saccades reduced position errors from 20% to 64% (reduction of tracking error reduced better for higher target velocities and predictable trajectories). The directions of catch-up saccades are oriented towards the target position at the onset of catch-up saccade with the scatter of misalignment inside the 15 deg range. During long tracking, one single catch-up saccade is not able to decrease tracking errors and time delays, therefore, the sequences of successive catch-up saccades are elicited. The more the segment of target motion or all trajectory of target movement is predictable (or even repeatable), the larger the amplitudes of catch-up saccades are elicited and the bigger the reduction of position errors is obtained. Providing oculo-motor system with additional information about past target motion, does not improve tracking. Due to suppression of vision during saccades, the inter-saccadic interval between two catch-up saccades must be at least 100 ms.

Investigation on oculo-motor response to visual occlusions in a trajectory of a target and smooth pursuit system's reaction to visual illusions is provided in appendices B and C.

### 3.2. Eye-hand coordination while controlling hand-moved object

#### 3.2.1. Abrupt hand movements and saccadic eye movements

In order to evaluate the timing and the principles of oculo-motor and oculo-manual control of a virtual object in a computer environment, a small investigation was implemented. Five subjects had to move a computer cursor to a target, which changed its coordinates each 2 s. Target moved so, that all required repositioning movement amplitudes were in a range from 8 to 15 deg. The movement of the pointer was executed using traditional computer mouse or a touchpad. Recorded data was used to calculate amplitudes, peak velocity and acceleration, duration of the abrupt eye and hand movements.

Experimental results proves that gaze is being repositioned using double step saccade (Fig. 3.9, 3.10). It is also clear, that gaze is positioned at the target earlier than hand-moved computer cursor (either moved using touchpad or mouse). In addition, the trajectory of a saccade is straighter than the trajectory of the hand-moved cursor (especially when the touchpad was used). It should be noticed, that there are no fixation-similar movements for the hand. Not only oculo-motor system uses double-step abrupt movements. Hand-moved pointer is also usually repositioned in two or more steps. This clearly can be seen from Fig. 3.11.

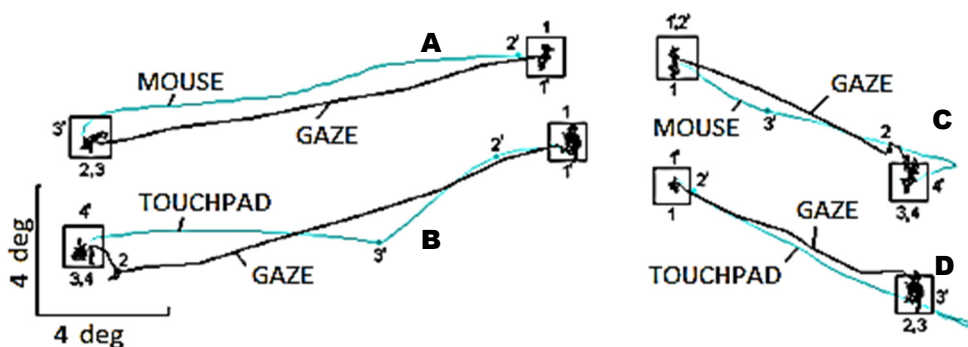


**Fig. 3.9** Trajectories of abrupt repositioning movements for the gaze and the hand-moved cursor. Numbers 1 to 4 indicates successive time-points corresponding to time-points 1' to 4'. 15 deg (A, B) and 8 deg (C, D) amplitude movements of the gaze, mouse (A, C) and touchpad (B, D) moved cursors are illustrated.

With a purpose to compare the velocities of saccadic eye movements and abrupt hand movements, velocities of a saccade and a corresponding hand movement are plotted in Fig. 3.11. It is easy to see, that gaze movements are 2-3 times faster than hand movements using either interface. The total average repositioning time for the gaze is 0.45 s ( $\sigma = 0.1$  s), for the mouse-moved cursor: 1.15 s ( $\sigma = 0.23$  s), and for the

touchpad-moved cursor: 1.3 s ( $\sigma = 0.3$  s). As the peak velocity of both eye and hand movements increased together with repositioning amplitude, only a small influence of repositioning distance on total repositioning time was observed: less than 0.1 s change corresponding to difference of 15-8=7 deg. This change was similar for both eye and hand movements.

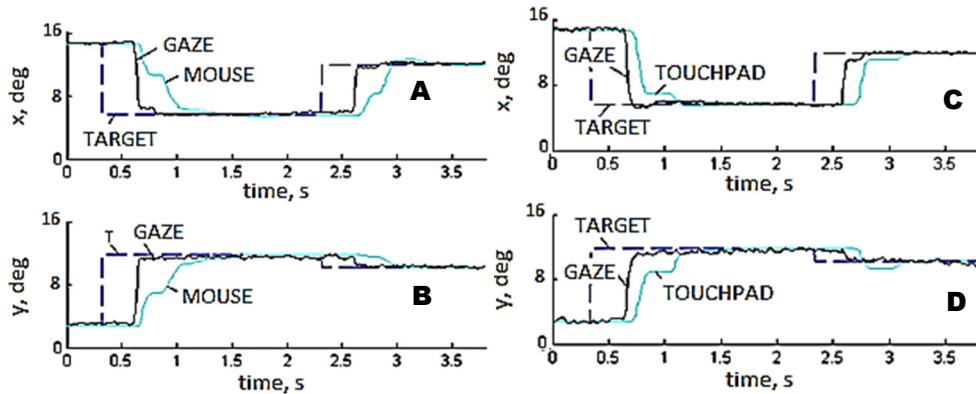


**Fig. 3.10** The position of the target, gaze and computer cursor controlled by a mouse (**A, B**) and by a touchpad (**C, D**) as a function of time in horizontal ( $x$ ) and vertical ( $y$ ) axis.

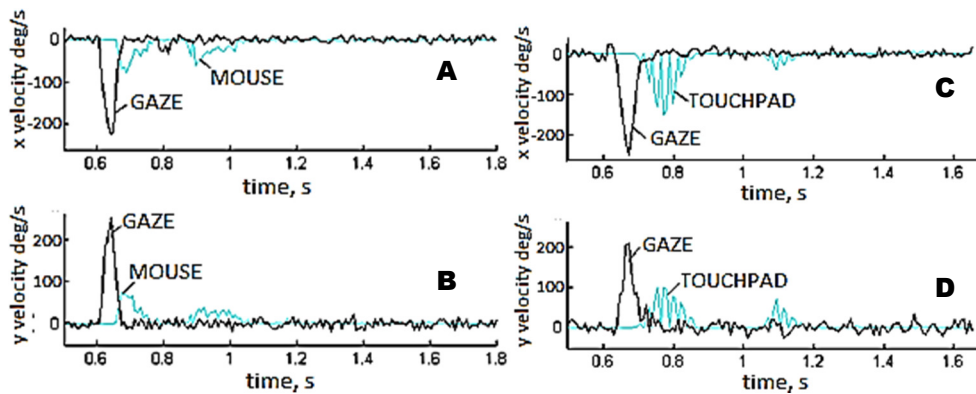


**Fig. 3.11** Velocities of the gaze and computer cursor controlled by a mouse (**A, B**) and by a touchpad (**C, D**) as a function of time in the horizontal ( $x$ ) and vertical ( $y$ ) axis.

It can be stated, that eye is being moved faster, its trajectory is straighter and the lag of the hand movement (higher than the one of oculo-motor movement) allows visual signal to be used as a feedback for hand control. Temporary stops of the hand movement during cursor repositioning support this hypothesis.

### 3.2.2. Oculo-manual tracking of a moving object

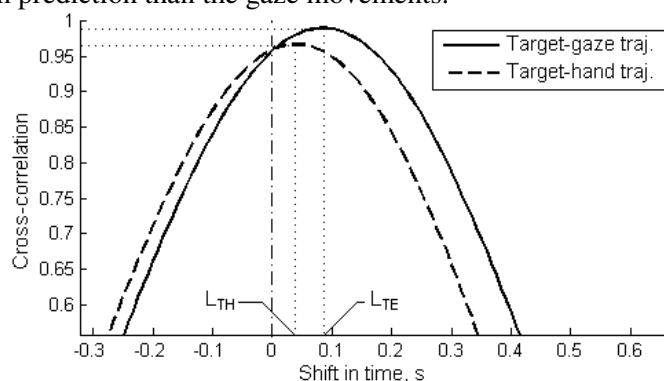
The coordination of hand and eye movements [147] has been widely investigated during reaching arm movements, but oculo-motor tracking of a visual target with a hand-moved cursor is more complicated and less investigated. The major observations is that there is some level of prediction of the target movement and that

two systems (eye and arm movement control) are separate, but influencing each other's signals strongly. In this research, the prediction phenomena in coordinated gaze and hand movements during oculo-manual tracking was investigated. In order to evaluate the levels of prediction, timing of movements was analyzed using the artificial shifting in time (section 2.5) of the trajectories of the gaze and the hand with regard to the target trajectory and calculation of the largest cross-correlation between them. The obtained shift in time, at which correlation has its maximum (or SD of the tracking error has its minimum), corresponds to the lag/prediction of the movement. This variable is used as an objective indicator of prediction between the gaze and the target and between the hand and the target movement.

The tracking experiments had two modes. In the first mode, subjects tracked the target only by gaze. In the second mode, oculo-manual tracking was performed using gaze and traditional computer mouse with default Windows XP operating system's sensitivity settings. The experiments were repeated using different average target movement velocities: 5, 10 and 20 deg/s. Six subjects participated in this trial.

In Fig. 3.12 target-gaze and target-hand cross-correlation functions are plotted. Both functions indicate high correlation between target and gaze and between target and hand. Main their difference is the shift in time (latency), at which cross-correlations have their maximum values. Taking in account the large latencies in neurological pathways (more than 100 ms), target-hand latency  $L_{TH} = 41$  ms and target-gaze latency  $L_{TE} = 85$  ms are small. The smaller the latency means the bigger the prediction. Therefore, it is obvious that tracking movements of the hand demonstrates a longer-term prediction than the gaze movements.

**Fig. 3.12** Cross-correlation between target and gaze (solid line) and between target and hand (dotted line) as a dependency of artificial gaze/hand movement trajectory shift in time.



In Fig. 3.13, the SD of the tracking error as a function of the latency is shown. Graphs indicate that in the real time (zero shift in time), tracking errors have closely the same values, but if the trajectories were shifted by the critical shifts in time  $L_{TH}$  and  $L_{TE}$ , the standard deviation of the errors will get their minimum values  $E_{TH} = 1.3$  deg. and  $E_{TE} = 0.7$  deg. In Fig. 3.14 the experimental results of the relationships between SD of the target-gaze and target-hand tracking errors and corresponding critical shifts in time for each subject are plotted for three target velocities.

In Fig. 3.14 the tracking by hand data is situated leftwards indicating smaller target's tracking by hand latency and better (i. e. longer) prediction for hand movements. In a few experimental trials when target was moving in the moderate

velocity (10 deg/s), hand movements are not lagging but even leading the target and demonstrate anticipation of the target's trajectory.

**Fig. 3.13** SD of the tracking error between target and gaze (solid line) and between target and hand (dotted line) as a dependency of artificial gaze/hand movement trajectory shift in time.

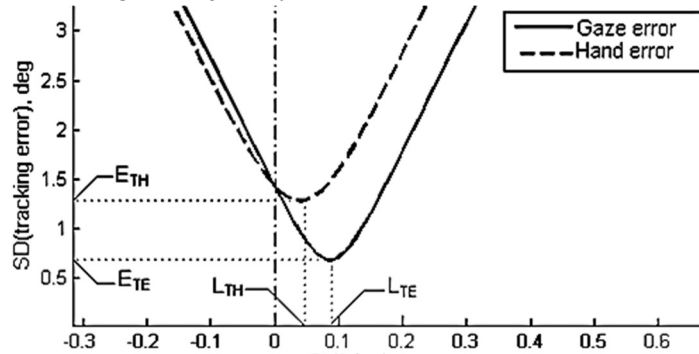
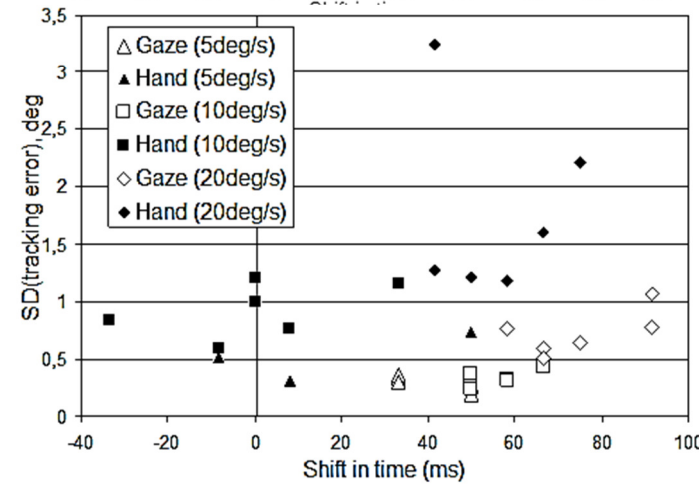


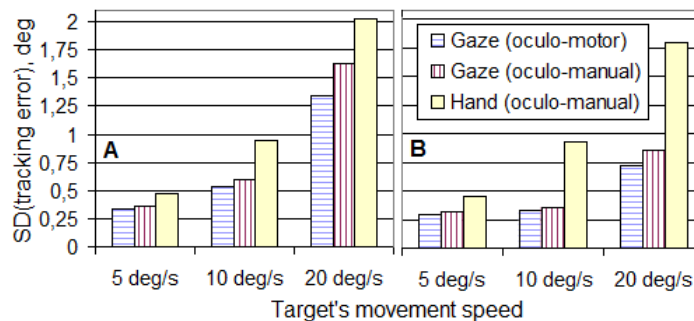
**Fig. 3.14** Relationship between SD of the target-gaze and the target-hand tracking error and the shift in time for three target velocities.



Data plotted in figures 3.14, 3.15 and 3.16 illustrate the averaged experimental results obtained during the two modes: the oculo-manual target tracking and target tracking only by the gaze (oculo-motor) tracking. Results in Fig. 4.15 A show that oculo-motor tracking is the most precise for all target velocities. This means that an oculo-manual tracking activity intervene the tracking precision of the gaze. The six subject averaged data of the tracking errors with the tracking lag removed (minimal tracking error i. e. at the critical shift in time) is plotted in Fig. 4.15 B. As it is seen, tracking errors of the gaze for higher velocities are significantly lower than tracking errors with the lag involved. Tracking errors of the hand are almost the same and do not depend on the lag. In Fig. 4.16 the averaged data of critical shifts in time as a function of the target velocity is presented. For moderate target's movement speeds, the average critical shift in time is close to a zero. Also, if the target is moving faster, the latency of the tracking is higher, what means that the control system is forced to use longer-term prediction.

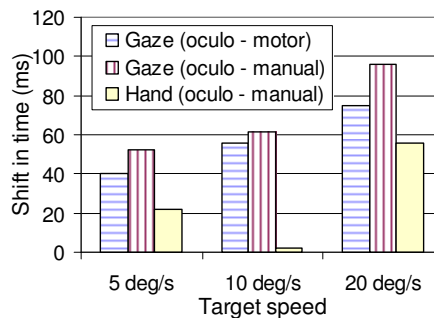
During oculo-manual tracking, hand tracking movements demonstrate a significantly longer-term prediction with a real-time-optimized tracking error. Such

**Fig. 3.15** Averaged data of the SD of tracking errors. With zero shift in time (A), with critical shift in time (B).



prediction allows tracking the moving target in the same performance as the gaze even if hand movement is more complex (more muscles to operate, higher inertia, longer motor-command path, etc.). If the lag (average of 85 ms) of the gaze were eliminated, the target-

**Fig. 3.16** Averages of the critical shifts in time for the three target's movement speeds.



gaze tracking errors would become significantly lower. On the other hand – the elimination of the hand lag (average of 41 ms) almost does not decrease the tracking error. Therefore, it is clear, that prediction system of the hand is more sophisticated than the one of the eye movements. Also, the target-gaze tracking precision during oculo-motor tracking is better than during oculo-manual tracking, what means that eye movements are affected by the presence of manual tracking task.

### 3.2.3. Oculo-motor tracking of a self-moved target

One experimental trial was designed with a purpose to investigate how human arm efference copy signal affects the oculo-motor tracking. Two-phase trial was used. In a first phase, subjects had to move an object with their hand and watch it by gaze. They first were shown a target, moving in a non-predictable trajectory and in an average speed of 10 deg/s (the same trajectory as for the trial introduced in the section 3.2.2) and asked to move the hand-moved object in a similar trajectory. The recorded hand movement trajectory was presented in a second phase – for repeated oculo-motor tracking. Eight subjects participated in this experimental trial. This way, subjects have tracked a visual target, which moved in the same trajectory both times, but in the phase one, oculo-motor tracking was enhanced by additional information from arm movement subsystem. Those two conditions were compared in order to evaluate the use and the benefits of this additional information for oculo-motor system.

For time difference evaluation, the artificial trajectory shifting in time (section 2.5) was used. Also, the cross-correlations of trajectories of the target/object and the eye movement were calculated and compared. Also, these cross-correlations were

compared with the latency-removed eye movement signal (the trajectory of the eye movement was shifted in time equal to tracking latency).

The experimental results are provided in table 3.1. It is seen, that oculo-motor tracking precision is better when hand movements are not used (the same was concluded from earlier experiments in the section 3.2.2). Either (real-time and shifted in time to remove latency) eye movement trajectory cross-correlate to visible target's/object's trajectory better (0.9 to 0.92 and 0.91 to 0.96). But the latency is vice-versa: the use of an efference copy from the arm movement control subsystem is reducing the eye movement latency from 131 ms ( $\sigma = 45$  ms) to 40 ms ( $\sigma = 86$  ms). Almost two-time increase in SD allows hypothesizing that not all subjects use this additional signal equally.

**Table 3.1** Comparison of oculo-motor tracking average characteristics when tracking a self-moved object and a target moving in a non-predictable trajectory

Phase 1			Phase 2		
Cross-correlation		Oculo-motor latency (ms)	Cross-correlation		Oculo-motor latency (ms)
gaze to hand	gaze (shifted) to hand		gaze to hand	gaze (shifted) to hand	
0.895	0.912	40	0.917	0.964	131
SD: 0.13	SD: 0.12	SD: 86	SD: 0.1	SD: 0.05	SD: 45

#### 3.2.4. The control of a hand-moved object in visual environment

Human behavior in a manual control coordinated by vision incorporates perfect synchronization between the gaze and position of an object, which is controlled by the hand [43]. Investigation of eye-hand coordination is useful for developing an alternative ways to control of computer cursor [17, 186] and for an assessment of a sensorimotor system of patients [131, 176, 159]. It is known that hand movements are affected by and affects movements of eyes [137]. The character of the influence depends on the executed action. Participation of the hand can change some parameters of eye movements e.g. latency.

The task of guiding a hand-moved object through a path employs slightly different eye movements than those seen in oculomotor-only behavior. The main reason for this is the need for eye-hand coordination. Nevertheless movements of the eye during guiding tasks is also different than those seen in other eye-hand coordination reliant tasks such as reaching arm movements, oculo-manual tracking and even the most similar: drawing.

With a purpose to evaluate how the gaze position is controlled during the hand-moved object guiding in a simple environment, an experiment was designed and executed: 13 subjects of various ages had to guide a hand-moved object (disc of a diameter of 0.15 deg) through a straight visible paths (no restrictions for hand movements) on a computer screen, which were: 0.21 deg (narrow), 0.33 deg (medium) or 0.85 deg (wide) in width. Subjects were asked to repeat the experimental trial of guiding an object 5 times through each of the paths. They were also asked to choose different object guiding velocity all five times (from precise as possible but slow up

to fast as possible but non-precise). The amplitudes of saccades ( $A$ ), the distance cursor-to-gaze on saccade onset ( $d$ ) and the gain of smooth eye movement periods were calculated and analyzed.

**Table 3.2** Eye movement parameters and their relationship to average hand movement velocity and the width of the path.

Mean velocity of the hand movement	less than 5 deg/s			5-10 deg/s			10-15 deg/s		
	Narrow	Medium	Wide	Narrow	Medium	Wide	Narrow	Medium	Wide
$A$ , deg	1.54	1.93	2.06	2.37	2.29	2.93	2.54	4.61	4.67
$d$ , deg	0.45	0.52	0.95	0.83	0.73	0.89	1.11	1.17	1.40
$\delta_A$ , deg	0.57	0.69	0.78	1.22	1.25	1.48	2.54	2.62	2.67
$\delta_d$ , deg	0.68	0.92	0.65	0.87	0.78	0.96	0.88	0.91	1.49

Data provided in the table 3.2 allows concluding: the largest saccades are elicited and the SD of the saccade amplitude is higher when the hand moves fast and/or the path is wide. Distance cursor-to-gaze on saccade onset has the same dependency, but the dependency is of lower level.

The gain of smooth eye movement periods is above one for hand average velocities up to 8 deg/s. When the hand is being moved faster, the gain of smooth pursuit drops (down to 0.5). Since the guiding eye movements are different in comparison to all other known well-investigated eye-movements, next chapter will be dedicated to them.

### 3.3. Eye movements when guiding a hand-moved object in visual environment and their comparison to smooth pursuit eye movements

#### 3.3.1. The oculo-motor strategies for an object guiding

The aim of this series of experiments was to investigate the eye-hand coordination of a human during an oculo-manual guiding of an object along a path. Experimental trial with different complexity paths was used (Fig. 3.17).



**Fig. 3.17** Paths used in experiments

Six subjects were instructed to guide a hand-moved object (cursor) along the pre-defined path at their comfortable hand movement speed. In addition to that, one of the subjects was also asked to repeat the task using two different velocities: 1)

slowly, but accurately; 2) to be as fast as possible. Later, eye-hand coordination changes at complex parts of the path such as corners, narrowings/broadenings or locations containing visual obstacles, was investigated too. For this purpose subjects had to guide an object 3 times over full-screen sized different components of the path (Fig. 3.20-3.22), shown in a random order to avoid any possible impact of learning.

Two-dimensional trajectories of hand and gaze were recorded and distance between hand-moved object ( $H$ ) and gaze ( $G$ ) were calculated and analyzed for each subject's dataset. Also, some gaze trajectory-specific guiding parameters were introduced, calculated and analyzed on each experiment's data. All the guiding parameters are further explained and presented.

Partial time domain based trajectories of the hand-moved object, of the gaze and the difference between them in the horizontal and vertical coordinates are shown in Fig. 3.18. Plotted experimental results illustrate the strategy of the eye-hand coordination during the guiding task. At the time  $t_1$ , gaze elicited a jump (amplitude is 1.8 deg.) along the horizontal path with the purpose to assess visually the future path for the hand. During time interval  $t_1$  to  $t_2$  hand-moved object was moved by the hand closer to the gaze position, which remained unchanged. At time  $t_2$ , the distance between the gaze and the hand-moved object became small (in the range of 0-0.5 deg.) and the gaze elicited a second jump. Third gaze jump was elicited at the time  $t_3$  and a coordinated motion in the horizontal direction was accomplished at the time  $t_4$ . At the same moment, due to changed direction of path, gaze elicited jump in the vertical direction. During the time interval from  $t_4$  to  $t_5$ , the hand-moved object was moved closer to the location of the gaze position. The described behavior of the eye-hand coordination is based on gaze jumps (GJ) along the trajectory path and could be called GJ strategy.

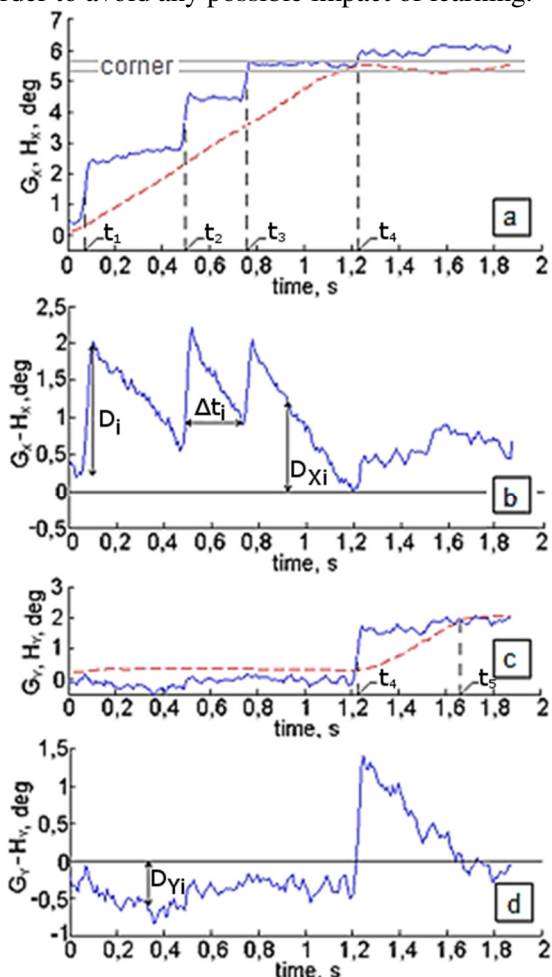


**Fig. 3.18** Partial trajectories in the time domain for the gaze jumps strategy (a, c): hand-moved object (dashed line), gaze (solid line) and the difference between them in the horizontal (b) and vertical (d) axes.  $A_i$  – amplitude of a saccade,  $\Delta t_i$  – time interval between subsequent saccades,  $D_{Xi}$ ,  $D_{Yi}$  – distances gaze to hand moved object in horizontal and vertical axes. Data represent one subject.

Contrary to that, Fig. 3.19 represents the experimental data illustrating scenario without strongly expressed gaze jumps and fixations. Gaze in this situation was moving smoothly and congruently with the hand-moved object. This strategy could be called Gaze Moves Smoothly (GMS) strategy.

The velocity of the hand movement depends only on its position in the path in both of the situations. Main difference between GJ and GMS strategies can be explained by determining the role of a vision. In the GJ strategy, main task of vision is the supplying of information on a future path. During GMS strategy, the gaze is focused not on the path to be passed, but on the hand-moved object. This is clear because eye is not able to execute smooth pursuit or to move smoothly without a target to be tracked [93]. Small variation in gaze to hand moved object distance (-0.5 to 0.5 deg.) can be neglected, knowing that vision is not concentrated only on the point of fixation but is able to change attention in the wider visual field [72].

Therefore, GJ and GMS strategies could not be so clearly distinguished in the guiding process and usually are interchanged. To evaluate how much these eye-hand coordination strategies are common and how much they vary for all six subjects, means and standard deviation of these guiding parameters were calculated and analyzed: amplitudes of saccades ( $A$ ), count of saccades ( $N$ ) during all the guiding time ( $T$ ), time intervals between two saccades ( $\Delta t$ ), velocity of the hand-moved object ( $V$ ), distances between the gaze and the object ( $D_x$  in the horizontal and  $D_y$  in the vertical axis). Majority of these parameters are illustrated in Fig. 4.10.

Guiding parameters of different subjects, each of them using a different eye-hand coordination strategy (GJ and GMS), and means of these parameters for all six subjects are presented in Table 3.3. Brackets contain SD values.

As seen in Table 3.3, GJ strategy was performed with the largest count of gaze jumps (68) with the largest average amplitudes (0.71 deg.) and average frequency of execution – 2.7 saccades/s. Contrary, GMS strategy is implemented with the jump

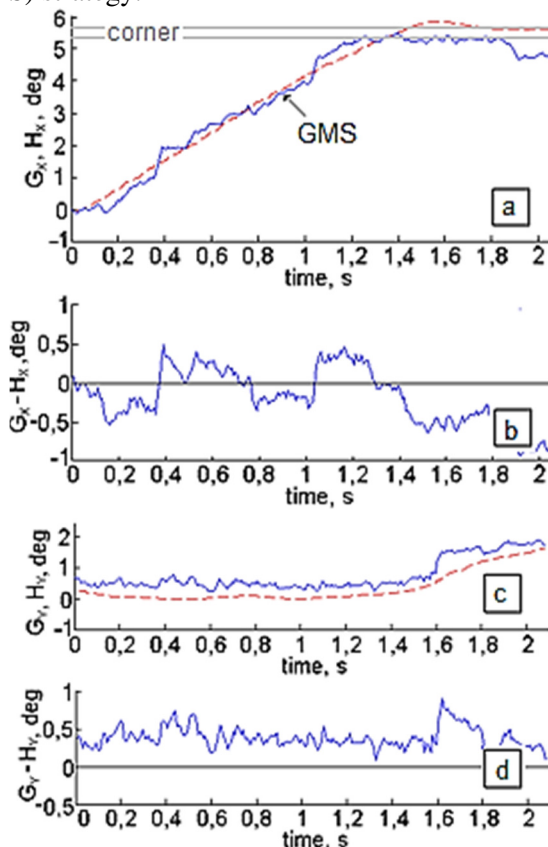


**Fig. 3.19** Partial trajectories in the time domain for the GMS strategy (a, c): hand-moved object (dashed line), gaze (solid line) and difference between them in the horizontal (b) and vertical (d) axes. Data represent one of the subjects.

count of only 51, average jump amplitude 0.6 deg. and frequency – 1.3 saccades/s. However, the most important difference between these two strategies is overall tracking time  $T$ , which is 1.5 longer for GMS strategy. Therefore, it must be summarized that GJ strategy is more efficient by means of time.

**Table 3.3** Parameters obtained during hand-moved object guiding along the path.

Subj.(strat.)	N	A, deg	$\Delta t$ , s	V, deg/s	T, s	D <sub>x</sub> , deg	D <sub>y</sub> , deg
A (GJ)	68	0.71 (SD: 0.4)	0.34 (SD: 0.2)	8.1 (SD: 3.2)	25	0.55 (SD: 1.0)	0.38 (SD: 0.7)
B (GMS)	51	0.56 (SD: 0.2)	0.68 (SD: 0.6)	5.9 (SD: 4.6)	38	0.23 (SD: 0.5)	0.27 (SD: 0.5)
Average (6 subjects)	54	0.6 (SD: 0.3)	0.56 (SD: 0.5)	6.9 (SD: 4.8)	32	0.38 (SD: 0.7)	0.37 (SD: 0.7)

The averages of the parameters of all subjects, indicate, that the subjects equally use both strategies. By analyzing personal data of each subject, it is seen, that there are some regularities in guiding parameters. The more and the larger the saccades, the smaller the time intervals between them and the shorter the overall guiding time.

On a purpose to evaluate how eye movement strategies and parameters depend on the complexity of the path, manual guiding experiments were repeated using different complexity paths. Obtained and averaged results indicated that eye-hand coordination behavior does not depend significantly upon the complexity of the path. Guiding parameters for these trials are shown in Table 3.4. It can be seen, that lower the complexity of the path – higher the guiding velocity. But the relations between the guiding parameters remain very similar.

**Table 3.4** Parameters of during guiding self-moved object along different complexity paths.

Traj.	N	A, deg	$\Delta t$ , s	V, deg/s	T, s	D <sub>x</sub> , deg	D <sub>y</sub> , deg
Fig. 4.9 A	54	0.6 (SD: 0.2)	0.56 (SD: 0.6)	6.9 (SD: 4.8)	32	0.38 (SD: 0.7)	0.37 (SD: 0.7)
Fig. 4.9 B	72	0.62 (SD: 0.3)	0.48 (SD: 0.5)	7.0 (SD: 4.6)	34	0.38 (SD: 0.7)	0.36 (SD: 0.7)
Fig. 4.9 C	86	0.62 (SD: 0.3)	0.38 (SD: 0.3)	7.2 (SD: 5.2)	33	0.39 (SD: 0.7)	0.39 (SD: 0.7)
Fig. 4.9 D	56	0.71 (SD: 0.4)	0.59 (SD: 0.6)	7.8 (SD: 4.5)	21	0.4 (SD: 0.8)	0.34 (SD: 0.8)

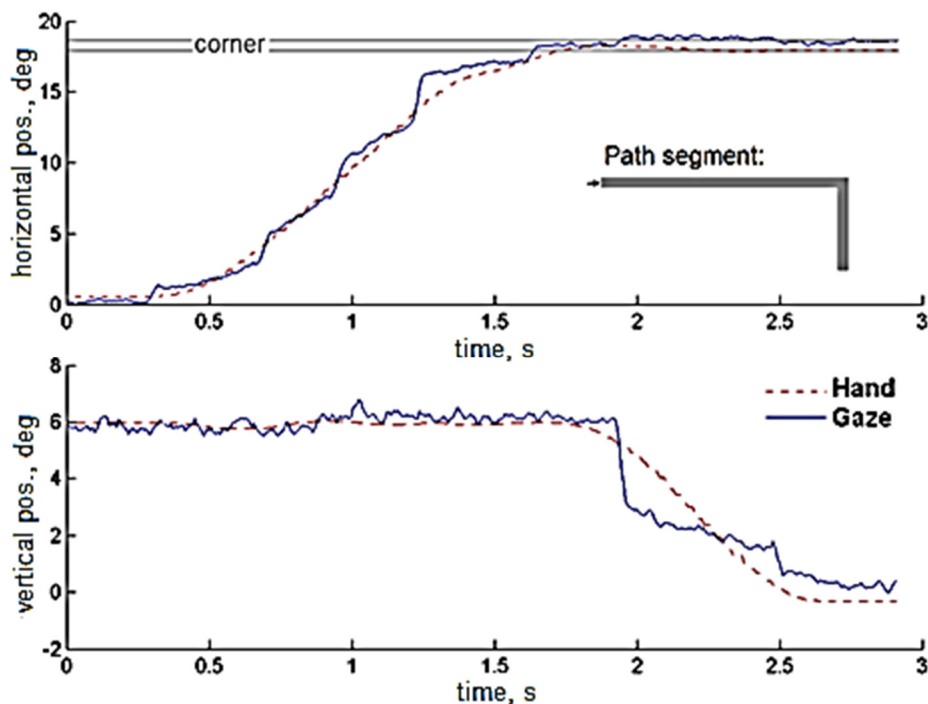
An evaluation of how human hand-gaze coordination depends upon his decision to track the path slowly but more accurately or faster but less accurately, was performed by subject A tracking low complexity path. This subject was instructed to guide the object using two self-chosen, but different as much as possible velocities.

Obtained guiding parameters are presented in the Table 3.5. They illustrate that execution time for slow tracking was 2.5 times larger but required 2.8 times less saccades. All the data confirm that slow tracking increases all the parameters which represent GMS strategy and, contrary to that, choice for fast tracking increases all the parameters which represent GJ strategy (many saccades with large amplitudes and large distance between the gaze and the object).

**Table 3.5** Guiding parameters during fast and slow guiding of hand-moved object along the low complexity path.

Subj.	N	A, deg	$\Delta t$ , s	V, deg/s	T, s	D <sub>x</sub> , deg	D <sub>y</sub> , deg
A (fast)	53	0.92	0.3	8.4	17	0.92	0.67
A (slow)	19	0.47	1.8	6.6	42	0.10	0.11

On a purpose to analyze the transition between strategies, we broke the complex path (Fig. 3.17 B) into basic components and varied their main characteristics. This allowed to investigate and to compare gaze movements (while guiding the hand-moved object) in different situations and when different preclusions (visual-only obstacle in the path, path broadening or narrowing) are encountered. Comparison of gaze movements when the path has sharp direction changes or forces the hand to be moved in multiple axes at a time also was done.



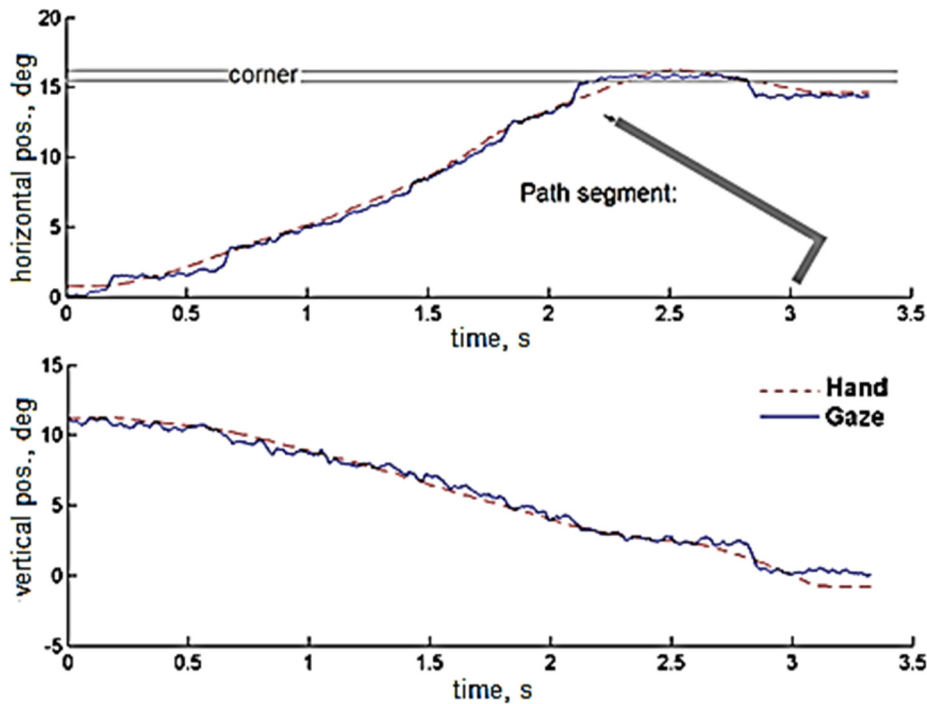
**Fig. 3.20** Trajectories of the hand moved object and the gaze in both axes and the path.

Fig. 4.12 shows that the eyes by some saccades are moved ahead of the hand-moved object to the corner of the path, and changes its movement direction only when object and gaze positions equalizes. In addition, it is seen, that this subject used mixed strategy, because the gaze trajectory has both GJ and GMS attributes. This is the usual case: clear GJ or GMS strategies are used rarely, most of the time subjects use mixed strategies, which can be more close to GJ or more close to GMS.

If a length of the path before the corner is different, subjects behave in the same manner. However, in a case when the path is wider by 40%, the average amplitude of

gaze jumps increased by 32% and the average distance between the gaze and the object in horizontal axis increased too. This could be the effect of the increase in hand movement speed by 25%. Appropriate opposite changes are observed when the path is narrowed.

Decrease of the hand speed and the gaze to object distance is also observed in the case when the path is rotated by 30 deg. (see Fig. 3.21). While guiding the object through such path, subjects usually use the strategy closer to GMS than in cases when the hand moves at the same speed over the path seen in Fig. 3.20. Count of jumps (and the distance between the object and the gaze) is different in cases when the path shown in Fig. 3.20 is rotated by 90 deg. or by 270 deg. When the object is being guided upwards, the average count of jumps is 5.2 and for the case when object is being guided downwards, the average count of jumps is 3.2.



**Fig. 3.21** Trajectories of the hand moved object and the gaze in both axes and the path.

When the path becomes narrower (see Fig. 3.22 A) or contrary - wider, a gaze always makes an extraordinary jump to this peculiar position, the amplitude of the saccade is smaller than amplitudes of all other saccades. After such jump of the gaze, it always waits for a hand-moved object to catch. Sometimes, at this peculiar part of the path, gaze can even temporary use exclusively GMS strategy.

If a visible obstacle (which does not disturb a movement of the object) (see Fig. 3.22 B) is presented instead of the path width change, subjects behave similarly, but a small corrective saccade to an obstacle position is rarer. In such a case, the saccade to the obstacle is usually planned in advance. This could be because of higher attention allocation to such obstacle.

Subject behavior while guiding an object through the path with the rounded corner or with different length paths before or after the 90 deg. corner (see Fig. 3.23) did not revealed any other specific features.

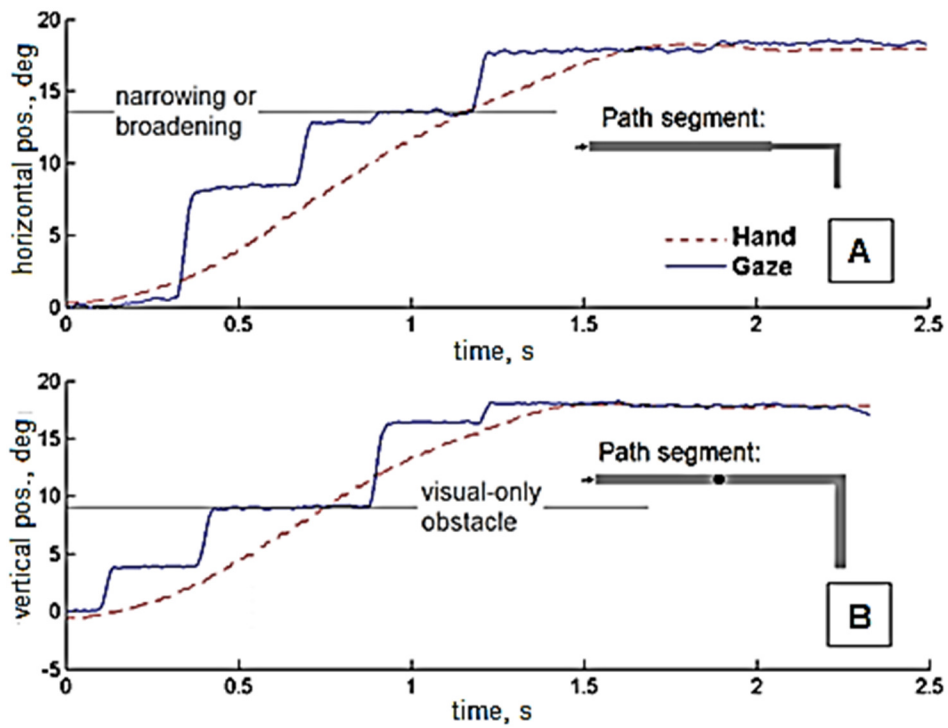


**Fig. 3.22** Trajectories of the hand moved object and the gaze when the width of the path changes (A) and when there is a visual-only obstacle in the path (B).

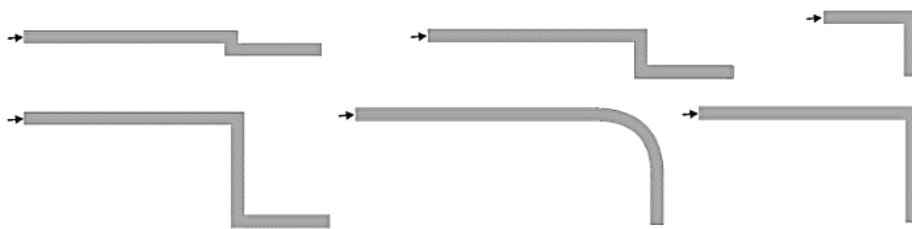


**Fig. 3.23** Other path components used for experiments.

### 3.3.2. Oculo-manual guiding eye movements and their dependence on characteristics of hand movements

In order to extract parameters of eye-hand coordination during oculo-motor guiding along a path tasks, a set of experiments was designed and executed. The characteristics of eye and hand movement were analyzed for two types of paths: straight and circular. Path edges did not restricted movement of the hand or the hand-moved object). Straight path is illustrated in Fig. 3.24. It was of 3 width modifications: narrow (0.21 deg), medium (0.33 deg), wide (0.85 deg). Sixteen subjects were asked to guide an object (a cursor, which was red disc with a diameter of 0.15 deg) through these paths (5 times each). They also were asked to choose the hand velocity themselves, but for it to be variable (including range from very slow and precise to the fastest) all five times. The 4<sup>th</sup> session of 5 trials was similar to a guiding of an object along the medium path, but using larger hand-moved object (0.25 deg in diameter). To compare the characteristics of the guiding in a never-ending path, five subjects participated in second part of the session: hand-moved object guiding in the circular path. Medium width path with a diameter of 20 deg was used. Each subject was asked to move the hand-moved object along this path (also varying the hand movement velocity) for 180 s.

**Fig. 3.24** Path used for an extraction of guiding parameters. Path colors are inverted. Gray areas are used only for illustration: data, when hand-moved object was moving in vertical or near-to vertical parts of the path, was not used for analysis.



Index of difficulty (*ID*) for each setup and trial-assumed indexes of difficulty (*TAID*) for each trial were assessed using the methodology provided in section 2.6. For straight path experimental trials, only the horizontal guiding was analyzed. A set of parameters and their inter-dependencies were analyzed: total horizontal guiding time (*TT*), total eye movement in GMS time (*TT<sub>GMS</sub>*), hand movement velocity (*V<sub>H</sub>*), hand peak velocity (*V<sub>HP</sub>*), eye movement velocity during GMS (*V<sub>GMS</sub>*), retinal slip during GMS (*RS<sub>GMS</sub>*), gain during GMS (*G<sub>GMS</sub>*), amplitude of GMS segment (*A<sub>GMS</sub>*), distance hand-moved cursor to gaze at the time of saccade onset (*D<sub>CGSO</sub>*), time between occurrence of hand catch up and the onset of a saccade ( $\Delta T$ ) (Fig. 3.25), amplitude of a saccade (*A<sub>S</sub>*).

Eye movement related parameter dependency on *ID* or *TAID* graphs has showed no evident trends, but dependencies of most eye movement characteristics on *V<sub>H</sub>* are obvious. On the other hand, clear *V<sub>H</sub>* dependency on *TAID* was observed. This is why some of the analyzed non-significant graphs will be omitted in this report.

As subjects, visually presented with a path, assess its *ID* and, based on this assessment, moves the cursor with some allowed vertical fluctuation, dependency of *TAID* on *ID* for all subjects is presented in Fig. 3.26 A. It was observed, that subjects assess the *ID* independently on the size of the object being moved (*ID* mean values of 46.73 for small cursor and 47.17 for large cursor). This is the reason, why *ID*s were recalculated using the methodology, where the size of a cursor is not

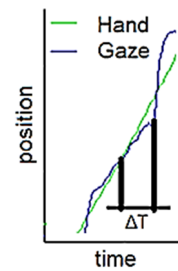


**Fig. 3.25** Time from hand catch-up to the occurrence of a saccade.

important. The results are presented in Fig. 3.26 B. 2<sup>nd</sup> order polynomial line was obtained to identify the *TAID* and *ID* relationship:

$$TAID(ID) = -0.0004 \cdot ID^2 + 0.1061 \cdot ID + 41.3693. \quad (3.1)$$

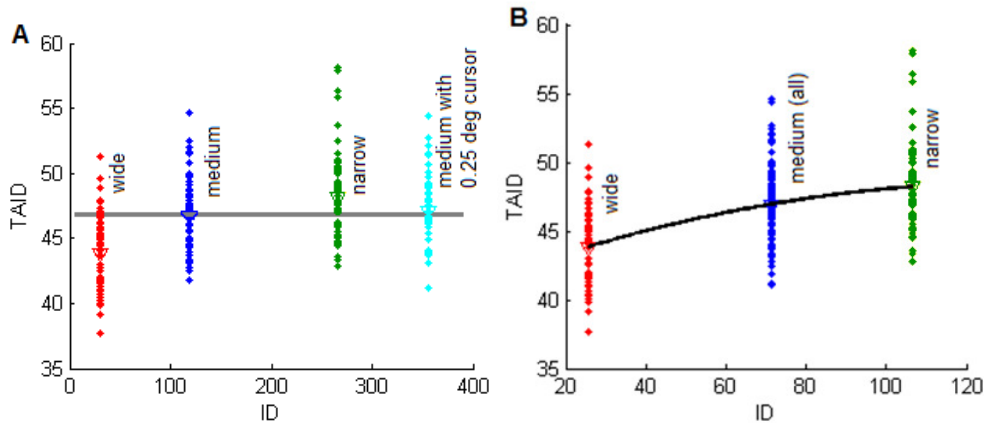
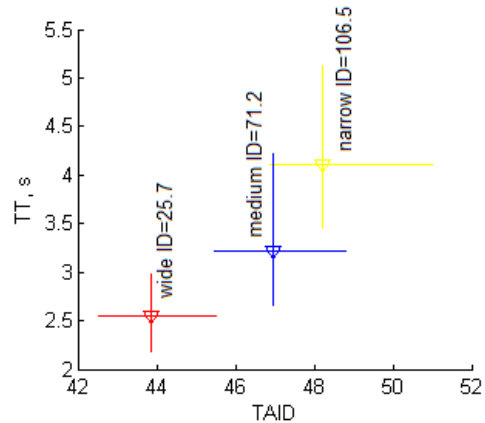


**Fig. 3.26 A:** Subject trial-assumed index of difficulty (*TAID*) as a dependency on calculated index of path's difficulty (*ID*). The gray line indicates similarity of the result for the same path even if the size of the hand-moved object was different. **B:** The same dependency for cursor-size-independent *ID* calculation. Black is a LSF 2<sup>nd</sup> order polynomial line (3.1). Triangles represent the mean values.

Fig. 3.27 is here to present that subjects' choice of *TAID* has a clear impact on total time used (*TT*). It also can be seen that the *TAID*'s in this experiment series are overlapping, what promises guiding parameter graphs without any gaps. Since the *TT* is dependent on *TAID*, it is obvious, that the average velocity of the hand movement ( $V_{HA}$ ) is also dependent on *TAID* (Fig. 3.28 A). As hand's velocity is bell-shaped, ( $V_{HP}$ ) must also depend on *TAID* (Fig. 3.28 B). In fact, these dependencies are easily recognized: as subject decides to increase the guiding precision, the guiding speed must decrease and vice versa. These dependencies were obtained by LSF and identified in equations (3.2) and (3.3):

**Fig. 3.27** Total guiding time (*TT*) and the *TAID* for all experiments. Triangles represent mean values and the lines represent SD.



$$V_{HA}(TAID) = 0.0008 \cdot TAID^3 - 0.1134 \cdot TAID^2 + 4.7498 \cdot TAID - 50.796, \quad (3.2)$$

$$V_{HP}(TAID) = 0.0024 \cdot TAID^3 - 0.3431 \cdot TAID^2 + 14.97 \cdot TAID - 179.1085. \quad (3.3)$$

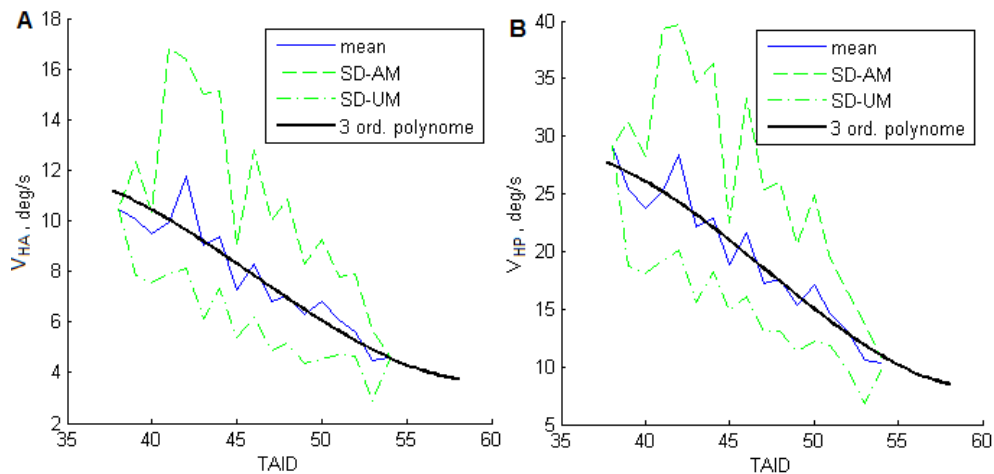


**Fig. 3.28** Hand movement average (A) and peak (B) velocity dependence on *TAID*. Values at the edges of *TAID*'s interval (less than 40 and more than 52) are marginal for this experimental trial. 3<sup>rd</sup> order polynomial lines are in equations (3.2) and (3.3).  $\text{bin}_{\text{TAID}} = 1$ .

As it have been found from earlier experimental sessions, characteristics of eye movements depends on hand-moved object velocity. Since eye movements during oculo-manual guiding can be resolved into GMS segments and saccades, for each such segment, a mean (during the eye movement segment) hand velocity can be calculated ( $V_H$ ). In next few charts, there will be shown that eye movement characteristics has clear dependencies on  $V_H$  (and together on  $V_{HA}$  and  $V_{HP}$ ). It must be noticed, that all following graphs were plotted from all experimental data even if there were very few experimental data for hand movement velocities ( $V_{HA}$  and  $V_H$ ) lower than 3 deg/s and higher than 25 deg/s. These marginal data is presented for a better preview of trends, but are not reliable.

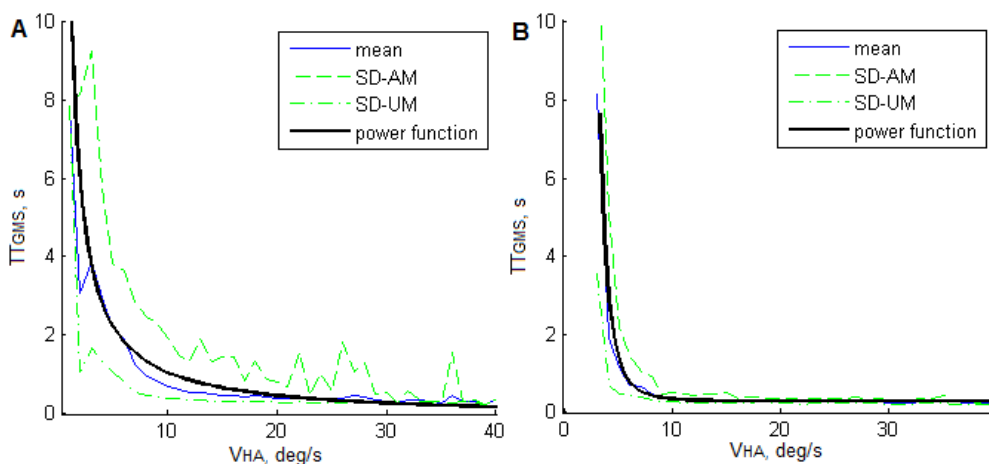


**Fig. 3.29** Total time of GMS segments as a dependency on average hand speed in straight (A) and circular (B) paths.  $\text{bin}_{V_{HA}} = 1$  deg/s. Power functions are LSF and provided in equations:

$$TT_{GMS}(V_{HA}) = 11.7058 \cdot V_{HA}^{-1.003}, \quad (3.4)$$

$$TT_{GMS}(V_{HA}) = 994.44 \cdot V_{HA}^{-4.2512} + 0.2841. \quad (3.5)$$

As  $V_{HA}$  increases, eye movement strategy shifts from GMS to GJ. This can be seen from Fig. 3.29. Total time of GMS segments reduces down to inter-saccadic interval if hand velocity increases.

In order to be sure that the total time of GMS usage reduces when guiding velocity increases because of change in a strategy, and not because of GMS velocity ( $V_{GMS}$ ) increase, this velocity was analyzed and is presented in Fig. 3.30. It can be seen that eye movement velocity indeed is rising (at least in straight paths), but the shape disagreement of 3.29 A and 3.30 A dependencies leads to analysis of the gain of GMS movement (Fig. 3.31).

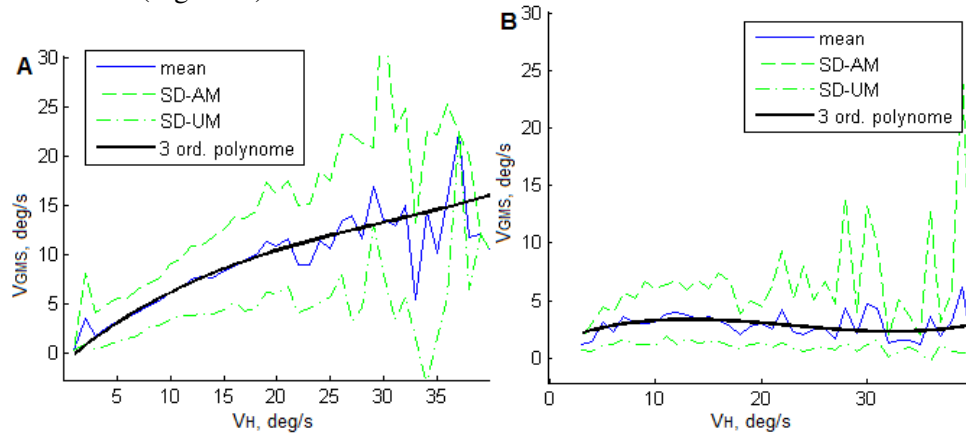


**Fig. 3.30** Eye movement velocity during one GMS segment.  $V_H$  is the mean of hand movement velocity during this segment in straight (A) and circular (B) paths.  $\text{bin}_{V_H}=1$  deg/s. Polynomial equations are (3.6) and (3.7).

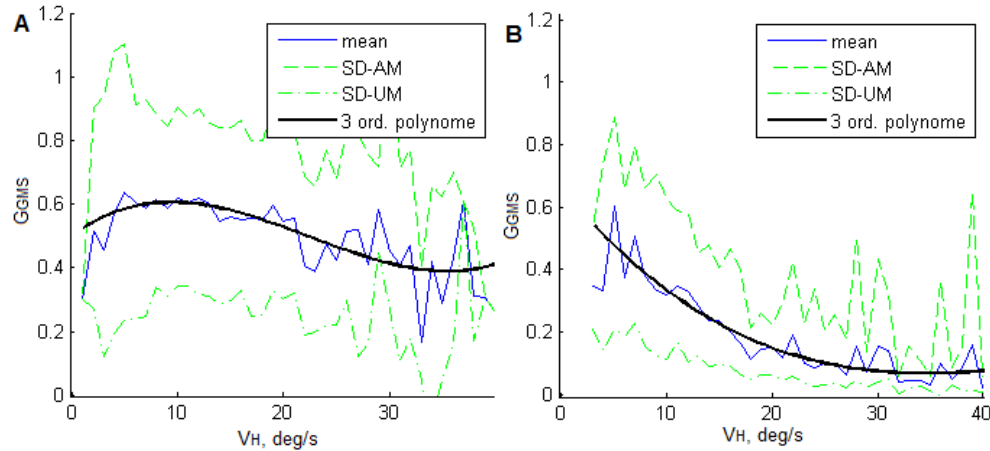


**Fig. 3.31** Eye movement gain during one GMS segment.  $V_H$  is the mean of hand movement velocity during this segment in straight (A) and circular (B) paths.  $\text{bin}_{V_H}=1$  deg/s. Polynomial equations are (3.8) and (3.9):

$$V_{GMS}(V_H) = 0.0002 \cdot V_H^3 - 0.0214 \cdot V_H^2 + 0.9058 \cdot V_H - 1.0098, \quad (3.6)$$

$$V_{GMS}(V_H) = 0.0003 \cdot V_H^3 - 0.02 \cdot V_H^2 + 0.3743 \cdot V_H + 1.2083, \quad (3.7)$$

$$G_{GMS}(V_H) = -0.0016 \cdot V_H^2 + 0.0245 \cdot V_H + 0.5009, \quad (3.8)$$

$$G_{GMS}(V_H) = 0.0009 \cdot V_H^2 - 0.0411 \cdot V_H + 0.6616. \quad (3.9)$$

Since the  $G_{GMS}$  changes while hand movement speed increases, it is evident that not only the increase of the velocity of smooth eye movements compensates for faster oculo-manual guiding. Analysis of retinal slip during GMS segments (Fig. 3.32) leads to an understanding that as guiding velocity increases, hand-moved object's visual representation on retina is allowed to move more (with a decrease in the quality of incoming visual information). As it is now ascertained, strategy changes together with hand movement velocity. If so, the amplitude of eye movement during GMS phase must decrease. This is observed in Fig. 3.33 and equations (3.12) and (3.13).

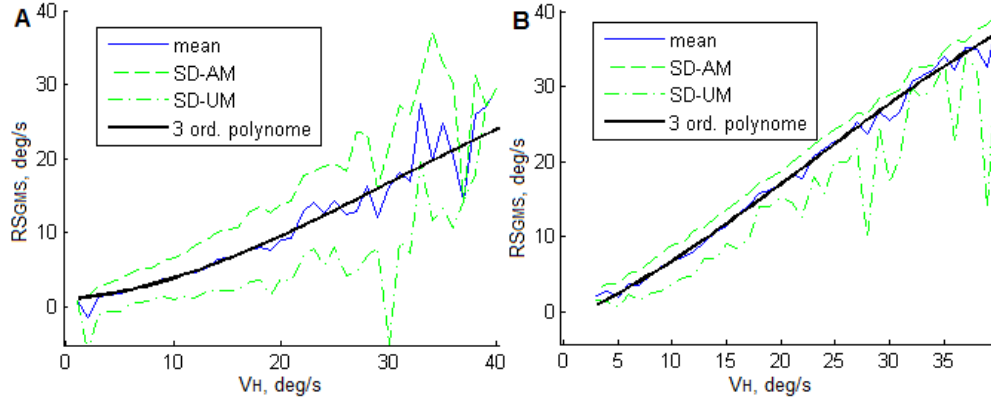


**Fig. 3.32** Retinal slip during one GMS segment.  $V_H$  is the mean of hand movement velocity during this segment in straight (A) and circular (B) paths.  $\text{bin}_{V_H}=1$  deg/s. Polynomial equations are:

$$RS_{GMS}(V_H) = -0.0002 \cdot V_H^3 + 0.0214 \cdot V_H^2 + 0.0942 \cdot V_H + 1.0098, \quad (3.10)$$

$$RS_{GMS}(V_H) = -0.0003 \cdot V_H^3 - 0.02 \cdot V_H^2 + 0.6257 \cdot V_H - 1.2083. \quad (3.11)$$

If, in such conditions, the distance of the smooth eye movements decreases, then eyes must be moved more in another way. It is clearly seen from Fig. 3.34, that the amplitude of saccadic eye movements increase if hand movement velocity increase. One more point of interest is the triggering of such saccades. Two possible sources are probable. During the retinal slip of the object being guided, distance from this object's representation on retina to fovea can become too large (decreasing the sharpness of vision) and a saccade can be triggered. Or, similarly as in smooth pursuit eye movements, a saccades can be triggered like the catch-up saccade: depending on estimated crossing time of gaze movement trajectory and cursor trajectory. To differentiate which method is more reasonable, both parameters:  $\Delta T$  (time interval between the crossing of trajectories and the onset of the saccade) and  $DCGSO$

(distance from cursor to gaze position at the time of saccade onset) as a dependencies on hand velocity were investigated (Fig. 3.35 and 3.36).

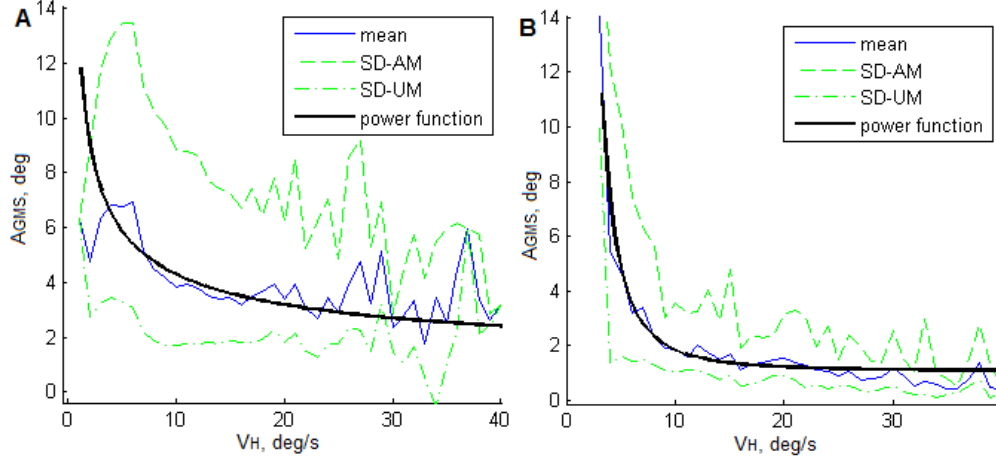


**Fig. 3.33** Eye movement total distance during one GMS segment.  $V_H$  is the mean of hand movement velocity during this segment in straight (A) and circular (B) paths.  $\text{bin}_{V_H}=1$  deg/s. Power function equations:

$$A_{GMS}(V_H) = 11.9977 \cdot V_H^{-0.5105} + 0.5793, \quad (3.12)$$

$$A_{GMS}(V_H) = 134.4135 \cdot V_H^{-2.2394} + 1.0523. \quad (3.13)$$

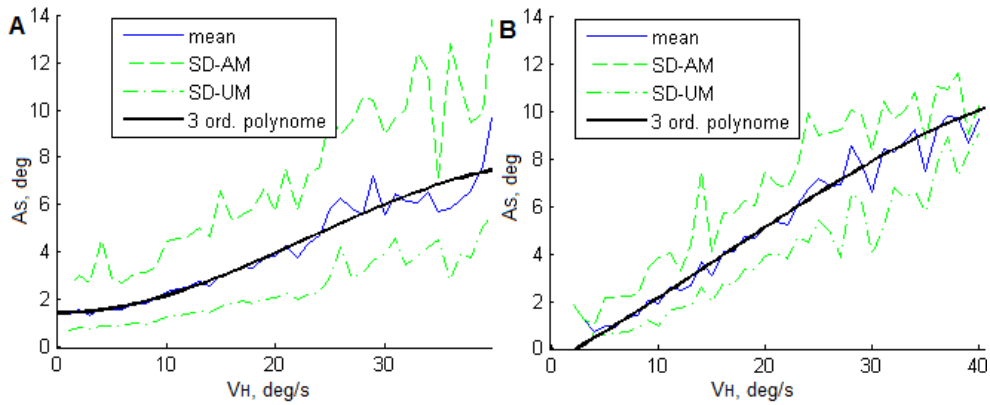


**Fig. 3.34** Saccade amplitude.  $V_H$  is the mean of hand movement velocity during the saccade in straight (A) and circular (B) paths.  $\text{bin}_{V_H}=1$  deg/s. Polynomial function equations are:

$$A_S(V_H) = -0.0001 \cdot V_H^3 + 0.0095 \cdot V_H^2 - 0.009 \cdot V_H + 1.4461, \quad (3.14)$$

$$A_S(V_H) = -0.0001 \cdot V_H^3 + 0.0034 \cdot V_H^2 + 0.2465 \cdot V_H - 0.5841. \quad (3.15)$$

As  $D_{CGSO}$  is constantly variable (all the time growing with no observed limit) and  $\Delta T$  appears to have its minimum value of approximately 150 ms (what looks reasonable as it is close to minimum inter-saccadic interval), it is reasonable to think that crossing time is the saccade triggering condition. Especially knowing that catch-

up saccades during smooth pursuit are triggered in the same manner. As it is known that catch-up saccade is triggered if the estimated crossing time is more than 180 ms or less than -40 ms (i. e. more than 40 ms after crossing), it looks reasonable that 40 ms after the crossing of cursor's and gaze's trajectories, decision for a saccade is made. Later, after an average saccade refractory period of 125 ms, saccade is delivered.

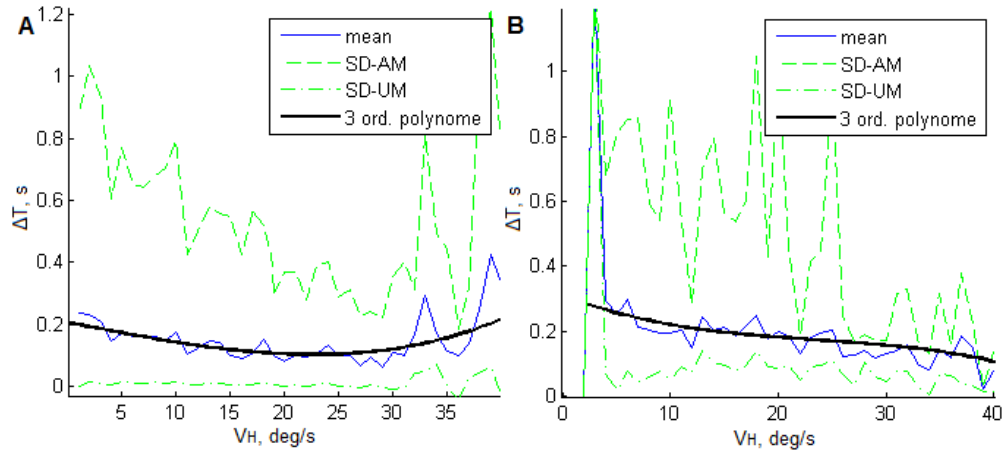


**Fig. 3.35** Time interval between the crossing of gaze and cursor trajectories and the saccade onset.  $V_H$  is the mean of hand movement velocity during this interval in straight (A) and circular (B) paths.  $\text{bin}_{V_H}=1$  deg/s. Polynomial function equations:

$$\Delta T(V_H) = 0.0001 \cdot V_H^2 - 0.0067 \cdot V_H + 0.206, \quad (3.16)$$

$$\Delta T(V_H) = 0.0004 \cdot V_H^2 - 0.0128 \cdot V_H + 0.3092. \quad (3.17)$$

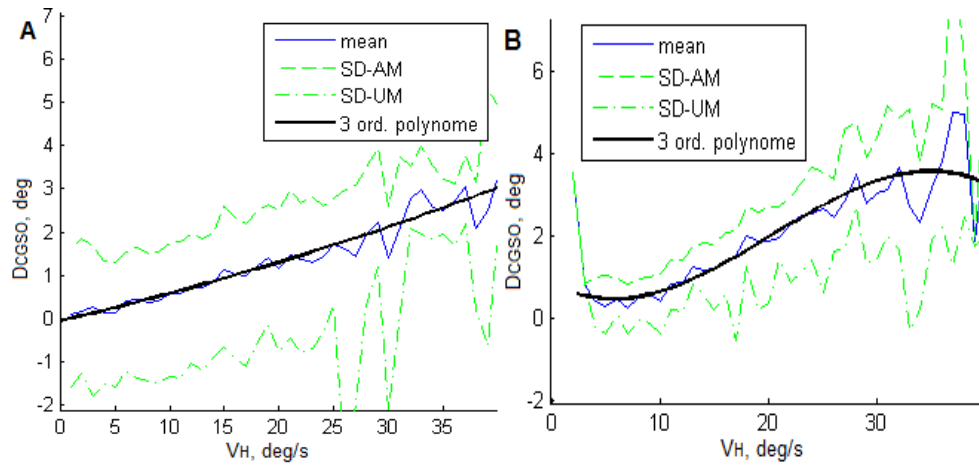


**Fig. 3.36** Distance cursor-to-gaze at the time of saccade onset.  $V_H$  is the hand movement velocity at the time of saccade onset in straight (A) and circular (B) paths.  $\text{bin}_{V_H}=1$  deg/s. Polynomial function equations:

$$D_{CGSO}(V_H) = 0.0004 \cdot V_H^2 + 0.0591 \cdot V_H - 0.0542, \quad (3.18)$$

$$D_{CGSO}(V_H) = -0.0002 \cdot V_H^3 + 0.0152 \cdot V_H^2 - 0.1486 \cdot V_H + 0.867. \quad (3.19)$$

One must have noticed, that the relations of hand movement velocity and eye movement characteristics are slightly different when guiding a self-moved object along straight and along circular paths. A short-term oculo-motor learning influences these differences. Figures 3.30-32 illustrates that GMS segments in guiding along circular paths are more like fixations. Eye movement velocity during these segments is only 3 deg/s. More to that, eye velocity is not  $V_H$  dependent. This looks reasonable, because higher retinal slip in circular path following is allowed as the need for sharp vision is compensated by learned motor pattern. In such a scenario, distance of smooth eye movements is lower than for straight paths (Fig. 3.33), therefore amplitude of saccades must be larger and it is (Fig. 3.34). Conditions for saccade triggering remains the same with similar characteristics (Fig. 3.35 and 3.36).

### 3.3.3. Differences of guiding and smooth pursuit eye movements

When the task is to move manually the object through a visible path, eye movement nature is similar to the smooth pursuit with catch-up saccades (Fig. 3.43). But experimentally obtained parameters of such movements indicate else: comparing to the task of target following, the gain of smooth eye movements is different and usually 1.6-4 times lower; the synchronization of the gaze and the object is also different by means of timing. Saccade landing position is always preceding the hand-moved object what makes these eye movements different from catch-up saccades. Also the gaze is regularly moving smoothly at the same time preceding the object. Such smooth movements, even if similar to smooth pursuit, could not be called smooth pursuit, because they are obviously not pursuing any target. At the same time, they are not similar to any other type of eye movements. One of the hypotheses could explain such eye movements as a position-shifted smooth pursuit (attention precede the foveal region of the retina) [172, 81]. This hypothesis was addressed and denied in a work of J. Tramper and M. Flanders [166, 167]. More to that, attention shifts during smooth pursuit still has much of controversy in eye movement research society as it is not observed in some trials where it is expected to be observed [106].

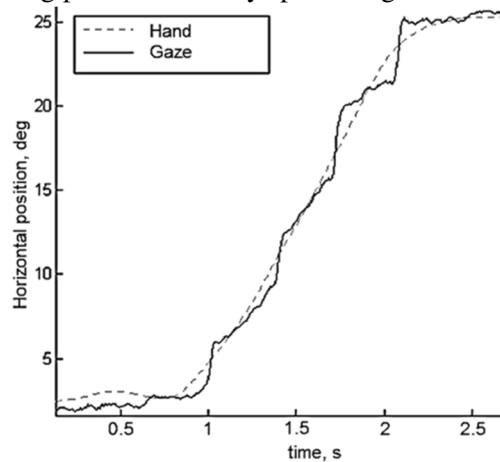


**Fig. 3.37** Eye-hand coordination while guiding a hand-moved object.

### 3.4. Summary and conclusions

1. Oculo-motor tracking parameters are dependent on the instantaneous target's velocity rather than on the average target's velocity. If target is being moved by hand, model must calculate eye movement velocity depending on instantaneous hand movement velocity.
2. Direction of catch-up saccades is oriented towards the target position at the onset of catch-up saccade with the scatter of misalignment inside the 15 deg range. Saccade direction must be calculated while taking into account planned future hand movements. Due to suppression of vision during saccades, the time interval between two catch-up saccades is at least 100 ms.
3. Providing oculo-motor system with additional information about past target motion, does not improve tracking. This means that there is no low-level neural circuitry, which could introduce differences because of all-time vision of a path.
4. If target being tracked becomes invisible, oculo-motor system continues smooth pursuit eye movements using prediction for 200 ms. After this period, gaze is directed towards center of the screen. Model should not use information on planned hand movements for longer term.
5. Smooth pursuit eye movements are not affected by visual illusion, as they do not use peripheral vision, which is prone to it. In the oculo-manual guiding, illusion-based visual error can only influence long-range hand movements, and they are on-line corrected while approaching the illusionary object by central vision. Lower latency of eye repositioning allows the visual signal to be used as a feedback and a guide (by shifting attention forwards) for hand motion control.
6. Tracking prediction system of the hand is more sophisticated than the one of the eye. During oculo-manual tracking, hand movement control system is using a significantly longer-term prediction than the eye movement control system and this makes a long term smooth hand movement planning possible (distinctly from smooth eye movement planning which is only for 200 ms).
7. The precision of the oculo-motor tracking is better than the one of the oculo-manual tracking, what means that eye movements are affected by the presence of manual tracking task. The latency of eye movements while tracking a self-moved object is reduced because of use of the arm's efferent copy signal.
8. Guiding eye movements are similar to the smooth pursuit eye movements but their parameters are different (gain and timing). Also the purpose of their nature is different, so such eye movements cannot be called smooth pursuit. As there are no other suitable group of eye movements, smooth pursuit eye movement group should be called smooth eye movements and incorporate both the smooth pursuit and guiding eye movements.
9. Two different eye-hand coordination strategies during oculo-manual guiding were observed: GMS strategy – gaze is maintained near hand-moved object; GJ strategy – eyes elicit saccades in the direction of the future path and waits for hand-moved object to catch only at the complex locations of the path. Subjects tend to shift their strategy from GMS to GJ, as the speed of hand motion increases (and vice versa). They choose the allowed guiding error (and together the hand

movement velocity) based on trajectory's index of difficulty. The size of a cursor affects this choice in an almost negligible way (at least in tasks when the guiding error is non-critical).

10. Most of eye movement characteristics during oculo-manual guiding strictly depend on instantaneous target (in case of pursuit) or hand (in case of guiding) movement velocity. These dependencies were experimentally obtained in a form of trend-lines. Such model should be tested if it is adequate to eye movement neurophysiology-based knowledge.
11. Different properties of a path segment (not only a width or length, but also angular direction, obstacles, changes in a width or direction of the path, repeatability, etc.) introduces different regulatory mechanisms. Obstacles and path width changes as all other manoeuvres (such as corners) attracts gaze. A gaze fixation to such obstacles lasts while the hand-moved object is guided over this obstacle. Modeling the oculo-manual guiding behavior in other than simple horizontal directions should be tackled only after analysis that is more detailed.

## 4. MODELING OF OCULO-MANUAL COORDINATION SYSTEM

### 4.1. Modeling the human behavior

The task of guiding a hand moved object through a path employs slightly different eye movements than those seen in oculomotor-only behavior. The main reason for this is the need for eye-hand coordination. In oculo-manual object guiding through a visible environment, hand is being moved towards next visible corner so it is natural, that gaze position must lead the hand pointer most of the time. Otherwise, if no corners are nearby, gaze cannot be positioned to far from the hand-moved object, as this would introduce enormous path-following inaccuracy. It is known, that amplitudes of saccades and the minimum distances between the gaze point and the hand pointer are lower when the complexity of the path in sight is lower and when the psychologically stated speed to precision ratio is lower. While the complexity of the visible path or the demanded precision is growing, smooth gaze movements are gradually replacing saccadic eye movements. It is important to mention, that such gaze movements differs from smooth pursuit as the gaze still leads the object. Figure 4.1 presents an example of typical eye-hand coordination.

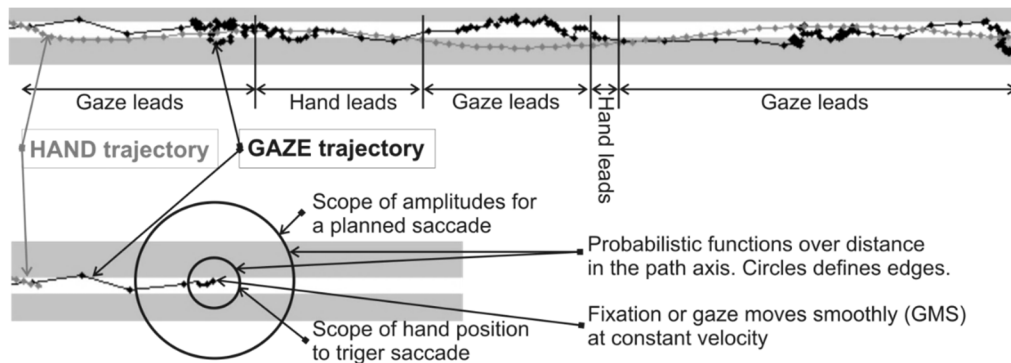


**Fig. 4.1** Eye-hand coordination in straight path and the model.

It is clear, that the next eye movement will be elicited after the time interval, which depends on the distance cursor-to-gaze. Because the object will approach to gaze point from any direction, this distance can be defined as a circle around the gaze point. Just before the eye movement will be triggered, its planned amplitude can also be defined as a circle around the gaze point as shown in Fig. 4.1. As both of these distances are not constant (because of timing estimation errors, section 4.2), they can be defined by a probabilistic distribution functions. It is also obvious, that the parameters of these functions depend on visible path complexity and psychologically demanded precision. In the model, the path complexity and the hand movement velocity, chosen by the subject, can be evaluated Fitt's law derivative steering law (as shown in section 3.3.2). The second parameter is a choice of priority on the hand movement speed or precision (TAID deviation for the same ID in section 3.3.2), so it should be implemented as a variable of the model.

Suggested functional diagram for such model is illustrated in Fig. 4.2. The most important input is a visible path. Because of the eye physiology, it is seen in parts – the diameter of the sharply seen image is only few degrees (depends on particular subject as the retina differs in terms of distribution of rods and cones and in terms of the size of fovea.). It is known from experimental investigation, that the gaze is positioned in a sequence to all complicated locations of the path, or, if none of such preclusions is nearby (i.e. path is straight), to the location towards the peripheral vision (exact position depends on crossing-time estimations as demonstrated in section 4.2). This means, that a detection of preclusions in a visible part of the path is happening (neurophysiological models explain this as signal buildup in SC). A next detected corner (or a preclusion) is assumed as the temporal target for the gaze and the gaze position sets the direction for the hand movement. Elicited eye movements determine the visual information, which is projected on the retina, thus a new visible part of the path.

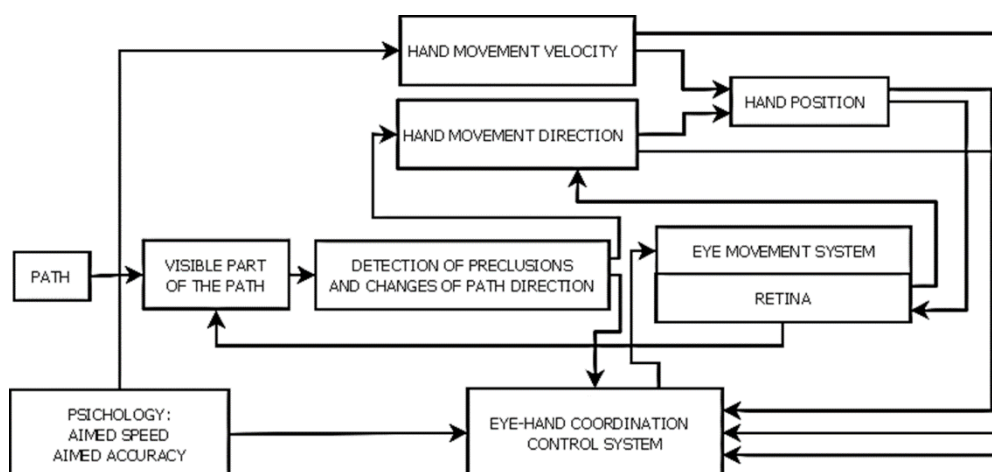


**Fig. 4.2** Functional diagram of the model.

Eye-hand coordination control system, depending on the aimed accuracy (TAID deviation for the path with the same ID in section 3.3.2), controls the hand movement velocity and together all the parameters of the eye movement. These parameters are inter-dependent, so some sets or strategies are being selected (section 3.3.1). It is important to mention that this strategy selection is gradient.

The increase of saccade amplitude and the decrease of GMS amplitude when hand movement velocity increases, can be understood as the expansion of the working image (the area of the retina, used for the detection of the next preclusion). So if the aimed accuracy is high – this area will be small (and all working image seen sharply), otherwise – more peripheral vision is used, thus decreasing the accuracy because of poor vision.

The model presented by S. Lazzari et. al. must be augmented and partially altered to achieve the described functionality. Since we want a model, which simulates only the object-guiding task, the “Setup” block can be removed. In addition, the “Target motion generator” should be replaced by the visual path information. The

hand/object position information from the retina is supplied to the Visual space Reconstructor (VR) as in original model, but the target movement trajectory is replaced with a block, supplying the VR with the information about the detected preclusions in the visible partial area of the path image. As the target is no longer a cursor or a dot presented on a screen, the exit signals of the VR are no longer the position of the visible target. On the other hand, the name "target" is still acceptable for mentioned signals, because they contain the information about the coordinates in a space, where the gaze (or hand) must be positioned soon.

The most important system in a model, the CCS, is augmented with a subsystem, responsible for eye-hand coordination during the manual object-guiding task. The operation of this subsystem is controlled by the subjective human factors: the mood, concentration to the task, expected results, etc. Depending on mentioned factors, two of psychology-determined features can be abstracted. They are opposite to each other – the aimed object guiding speed and the aimed object guiding accuracy. The CCS must control not only the parameters of the smooth pursuit, but also the target position for the gaze and the hand-moved object. Since the model determines the target position for the gaze in the VR, it is obvious that the Object Guiding Subsystem (OGS) must be not only a part of the CCS, but also a part of the VR. OGS exit signals are: the intended hand motion trajectory and the target position for the gaze (usually the subsequent preclusion, but if no preclusion is in a working image – then towards the peripheral vision). The target position for the gaze is formed from two signals: the position (for smooth pursuit) and the retinal error (for saccadic eye movements). The model with modifications was presented in Fig. 2.1.

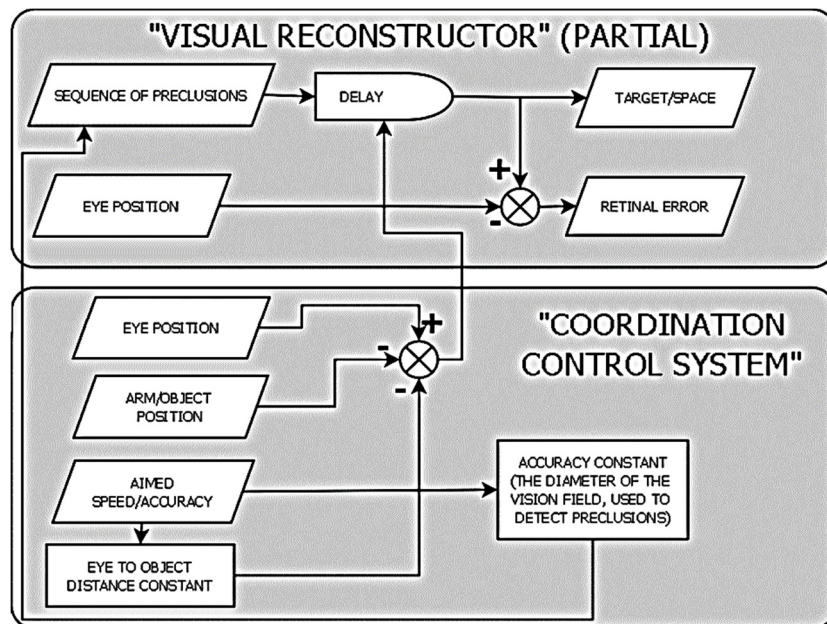


**Fig. 4.3** Functional diagram of the OGS.

The functional diagram of the OGS is illustrated in Fig. 4.3. Preclusions (and points towards vision periphery) become targets for the gaze in a sequence with a variable holding delay. This hold time is determined by a distance between the gaze and the hand-moved object and the TAID-determined parameter – maximum eye to object distance (which depends on estimations of crossing-time). Another subjective parameter – accuracy constant is used for variation of the diameter of the visible part of the path. If this measure is high – preclusions in a sequence are detected not so accurately because of the use of the peripheral vision. Both subjective parameters depend on aimed task fulfillment speed and aimed accuracy (i. e. chosen hand velocity).

Such model is suitable for modeling oculo-manual behavior during an object guiding through a visible complex path with many corners and preclusions. On a way towards quantitative model, the critical part, relating the eye movements to the visual path and the hand-moved object is the coordination of oculo-manual guiding in a straight path segments and it is the starting part. In order for the model to stay physiology-adequate, neurophysiological its implementation must first be prepared.

#### **4.2. Neurophysiological modeling**

In order to understand which neural circuits are responsible for eye movements in oculo-manual guiding, neural eye movement model must be explored. Then it can be augmented. As the best model created on the base of most of key research in this area is presented in section 1.2.3, it is the most suitable for this reason.

Neural pathways involving FEF and SC brain areas are responsible for the decision on voluntary saccade targets [57]. Saliency maps are used to determine the target of the planned saccade. In the object guiding over the visible path task, the corners, visual obstacles and other complex parts of the path [137] has the highest saliency and attracts the attention so a saccadic eye movement is elicited. The time of the decision to trigger a saccade depends on the distance from the hand-moved pointer to the obstacle.

The smooth eye acceleration needed for the tracking of moving target is determined in NRTP, which uses the signal of the actual eye movement velocity from MVN/rLVN and the target movement velocity from the FPA. The gain of smooth pursuit is set and maintained by the MT-DLPN-CBM pathway [57].

The lower layers involving the motor neurons, TN, MVN/rLVN and the PPRF (which has a formation with OPNs for suppression of smooth eye movements during saccades and saccade suppression during near-accurate pursuit, also the negative feedback involved in saccade landing situations) are mainly controlled by the CBM and at the same time by the SC. Also the rostral part of SC can engage OPNs to suppress a catch-up saccade if the target is about to come to the fovea within specific time interval [57, 38].

CBM is the region of the brain, where signals on intended motor actions are translated into signals for motor-related neurons. This translation is done using weights learned depending on the shape of the muscular system.

What is different between the smooth pursuit with catch-up saccades and the visual guiding is the timing and the gain of smooth eye movements. Changes in the gain can be explained by the presence of the information (in CBM) on prosecuted hand movement velocity and direction. As it is known that the signal processing in the CBM is almost entirely feed-forward, but some recurrence that exists consists of mutual inhibition [121], this signal of hand movements induces an inhibition on DLPN-CBM pathway. Also, it is known that arm movements influence eye movements via feedback of arm kinesthetics within the dentate nucleus of the CBM thus significantly decreasing the eye movement latency in eye-hand coordination tasks [175].

Triggering of catch-up saccades is based on the estimation of the gaze-target crossing time: a saccade is triggered if the crossing-time is estimated to be less than 180ms while decreasing (pre-crossing) or more than 40ms while increasing (post-crossing) [38]. The same mechanism realized in the model of the eye movement control for target tracking, is still suitable to explain the triggering of saccades in visual guiding. The only difference between the two eye movement types is the landing position of saccades. While having information on current hand movement, the saccade landing position is calculated to precede the position of the hand-moved object as much as possible, but without challenging a backwards saccade (the new crossing-time after the saccade cannot exceed 180 ms) (Fig. 4.4.). The target for catch-up saccades is always the object being tracked, but in tasks of the visual guiding, the saccade landing position is a spatial area based on attention [Klauda! Nerastas nuorodos šaltinis.]. Attention is the factor driving the build-up activity of neurons in the SC. And the build-up process of the SC is used for eye movement planning [86].

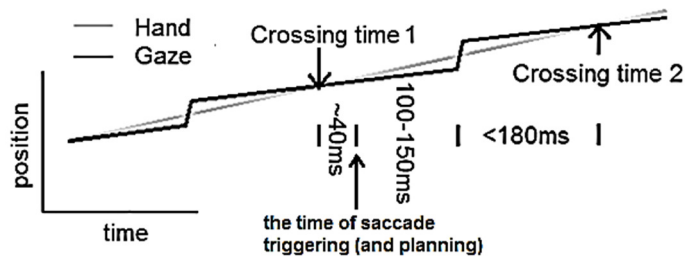


**Fig. 4.4** Saccade timing in the tasks of visual guiding. Amplitude of the saccade is calculated for the estimated crossing-time after it to be less than 180ms (otherwise, a backward catch-up saccade could be triggered).

Fig. 4.4 can be explained this way: 40ms after the Crossing time 1 the decision for a catch-up saccade is made. As all saccades take-place with some latency, this planned saccade will occur after a period of 100-150 ms. Planned saccade amplitude must be estimated from the data on eye and hand movement at the moment of triggering. If this amplitude will be too large, the newly estimated crossing-time (to Crossing time 2) after the occurrence of the saccade will be more than 180 ms and a new backwards-oriented saccade will be triggered. This is not a lowest-possible-effort way. On the other hand, if the saccade will be too small, the newly estimated crossing-time (to Crossing time 2) will be very low or even negative, then the new condition

of 40 ms post-crossing time will be very soon and once again – the lowest-possible-effort will not be employed.

Based on the knowledge above, it can be stated, that eye-hand coordination in visual guiding task reveals that the nature of eye movements involved is the same as of a smooth pursuit with catch-up saccades. The main reason for different gain and timing is the presence of current hand-movement signal in the cerebellum. This signal inhibits the Dorso-Lateral Pontine Nuclei – Cerebellum pathway, thus decreasing the gain of smooth eye movements. The difference of the timing is only an aftermath of different attentional priorities while planning a catch-up saccade. Decreased gain and precedence-allowed saccade amplitudes assure the convenient movement of the scene in the retina (section 2.1) while maintaining a stable and catch-up free crossing-time to saccade time interval.

### 4.3. Model for simulating oculo-manual guiding

Based on the knowledge, experimental data and the models above, a model for the simulation of oculo-manual guiding in one axis in a straight path with points matching the role of corners, where the direction of the path changes or a new same-direction segment of the path starts. These corner-like points can be also thought as the locations of visual preclusions. The basic structure of this model is shown in Fig. 4.5.

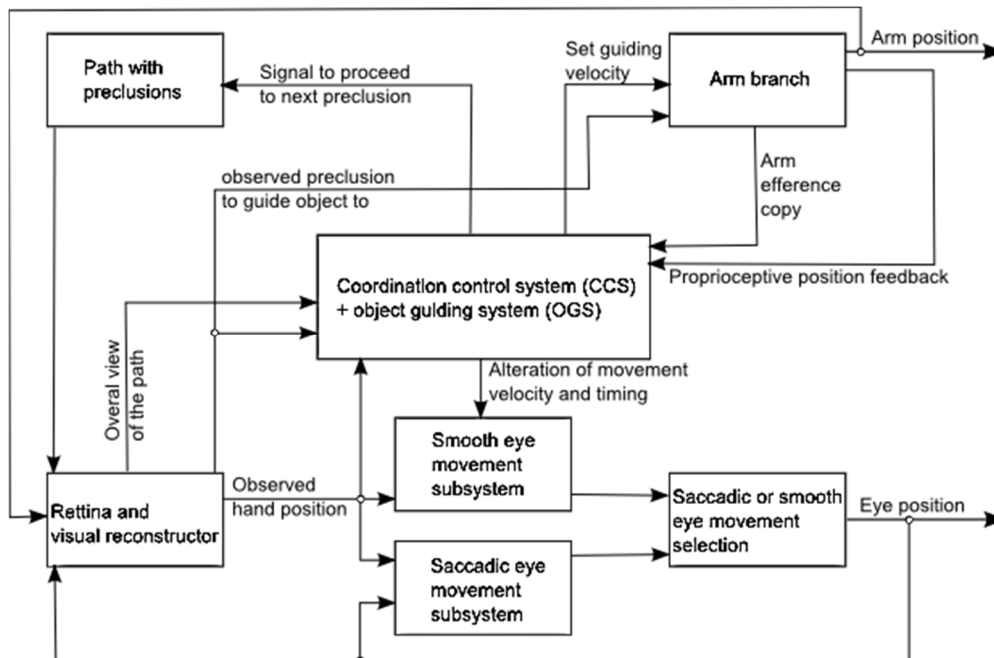


Fig. 4.5 The basic structure of the model.

The retina first provides the overall view of the path to OGS, which selects the TAID and together the peak guiding velocity value (as the hand velocity is bell-shaped, together the average). The retina then is provided with a preclusion in

periphery. The location of this preclusion is assumed to be the target for the arm branch. Arm starts move the cursor to this location and the changing location of the cursor is being seen through the retina. Smooth eye movement subsystem tries to match the velocity of eye movement to the velocity of the hand movement. As the gain of smooth eye movement is inhibited in the CBM, OGS reduces it. Also the maximum eye movement velocity for smooth eye movements is increased and the tracking timing is altered because the self-moved object is being tracked (it is the CCS activity as in previous models). CCS determines that the self-moved object is being pursued by comparing the input of the smooth eye movement subsystem and the signals from arm movement branch.

Observed hand position and the position of the eye is used to estimate the crossing-time and to trigger the catch-up-like saccades. When a saccade is about to occur, the smooth pursuit is inhibited. When OGS detects, that hand position correspond to the location of the targeted preclusion, a new peripheral vision based location (through the retina) is provided to the arm branch for pursuing.

The path with preclusions part is modeled as a list of subsequent preclusion coordinates. Also it provides the width of the path for TAID estimation.

The simplistic model for arm branch in the model by Lazzari et. al. is delaying an intended arm movement by 100 ms because the central processing delay, then differentiates it and sent to the arm motor plant. Input signals are provided from the VR and through a visual corrector. The arm control system has velocity and position feedback loops, which represent proprioceptive information and include the overall somatosensory information related to joint posture and kinematics. Both these loops have a delay of 15 ms. The output signal is the arm position (i. e. the angle of the elbow). The model for oculo-manual guiding is modified (Fig. 4.6). First of all, there is no visual corrector as there is no external target to track. Arm plant's transfer function was updated by the one presented in equation (1.33) and using the parameters from table 1.8 (for horizontal axis). As the hand movement velocity in object guiding along visible paths is not the maximum possible, a velocity profile transformation block was included, which changes the desirable velocity shape from a step to bell-shaped. The peak velocity of the hand movement is controlled by OGS.

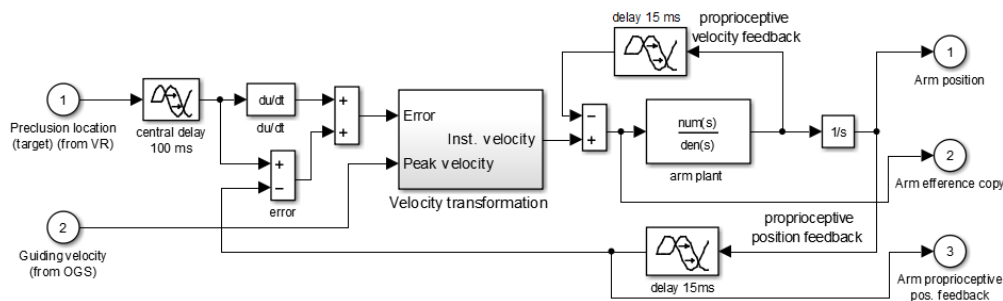


**Fig. 4.6** Simplistic arm branch model.

As retina encodes all the incoming visual information in eye-centered coordinate system, its outputs does not contain global position for seen objects (Fig. 4.7) Information about path width is sent to OGS and all other, cursor and preclusion

related information propagates to VR which, based on eye position feedback signal, restores the positions of hand-moved object and observed nearest preclusion (Fig. 4.7). All this visual information tract is known to have an average delay of 50 ms.

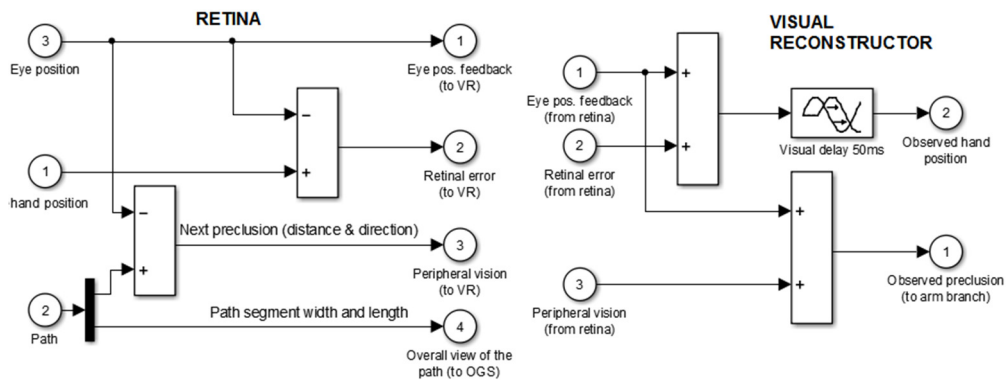


**Fig. 4.7** Models of retina and visual reconstructor.

Smooth pursuit subsystem (Fig. 4.8) is the same used in the model by Lazzari et. al. It uses reconstructed hand position signal, which is differentiated to velocity. Then a 40-100 deg/s variable velocity saturation (depending on mutual coupling signal from CCS) is used to limit it. Smooth pursuit controller has a delay of 50 ms. The overall delay of visual and smooth pursuit systems is compensated by a predictor, which on-line forecasts target (observed cursor) velocity for the next 400 ms, on the basis of a cubic spline interpolation of the actual target velocity during the last 150 ms. The estimated velocity is limited to 110% of the maximal target velocity in order for unrealistic estimations of target accelerations to be avoided. The relative contribution of the predictor to the overall smooth eye movement branch has been set to 0.36, while the SP controller has been assigned a gain of 0.93. The signals coming from CCS (Mutual coupling and timing) were explicitly explained in section 1.5.2.

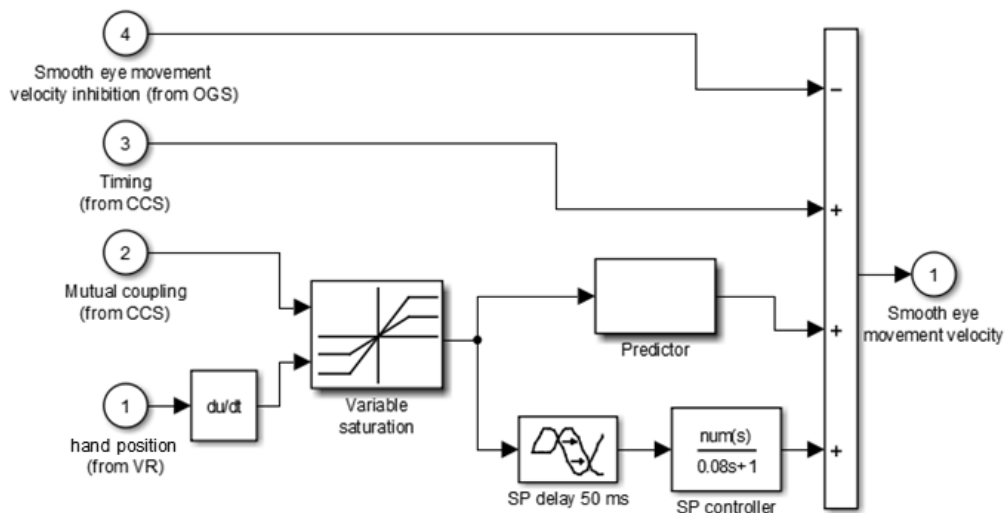


**Fig. 4.8** Model of the smooth eye movement subsystem.

This Smooth pursuit subsystem model was extended to reduce the velocity of smooth eye movements by an inhibitory signal from OGS.

The saccadic subsystem in original model was very simple, reacting to target retinal error, and if it was higher than 0.8 deg, a simplified saccade of 50 ms duration and a 200 ms regeneration time (to ensure the minimum inter-saccadic time interval) was generated. Its velocity was calculated by:

$$SV = 25Err + 4 \frac{d(Err)}{dt}; \quad (4.1)$$

where *Err* is the target retinal error; *SV* is the saccade velocity.

Then the generated saccade was delayed by 150 ms and limited to 800 deg/s. Such a saccade generation method would meet the requirements for object guiding simulation, but the triggering only by a retinal error is not suitable. Now it is known, that saccades are being triggered by crossing-time estimations first, and the retinal error is only an aftermath. Also, amplitudes of saccades in oculo-manual guiding are not dependent on retinal error, but on crossing-time estimations after a saccade. Therefore, the saccadic subsystem had to be remodeled (Fig. 4.9). Main simplification used is the absence of corrective saccades. I. e. single-step saccades are modeled.

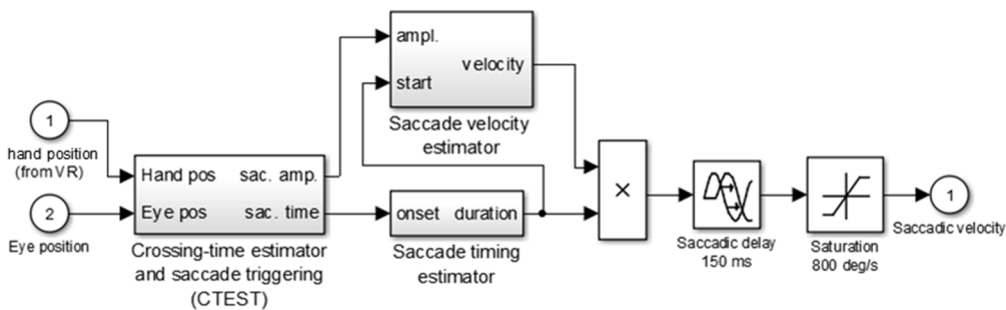


**Fig. 4.9** Model of saccadic eye movement subsystem.

The sub-model called *CTEST* estimates the crossing-time, and checks if the conditions for a saccade triggering are met (see section 4.2). Its internal structure is illustrated in Fig. 5.11. Based on 2<sup>nd</sup> order polynomial line fitting for current and -5 ms prior hand and eye positions, estimated crossing-time is calculated. If it is more than 180 ms or less than -40 ms, a saccade triggering output is set (this does not mean that a saccade will occur instantly – it is explained in next paragraph). Also a saccade amplitude is calculated and outputted from this sub-model too. Saccade amplitude is estimated using the same two 2<sup>nd</sup> order polynomial equations to ensure that after its occurrence, the estimated crossing-time would be as close as possible, but less than 180 ms (see section 4.2 for explanation why).

To ensure that no saccade is triggered earlier than 200ms after previous saccade, a sub-model called saccade timing estimator To ensure that no saccade is triggered earlier than 200ms after previous saccade, a sub-model called saccade timing estimator was implemented (Fig. 5.12). It also sets the duration of a saccade. When a saccade is about to occur, its velocity profile is controlled by a PID controller inside

the Saccade velocity estimator block. Saccade velocity is calculated from estimated saccade amplitude in a way similar to model by Lazzari et. al.

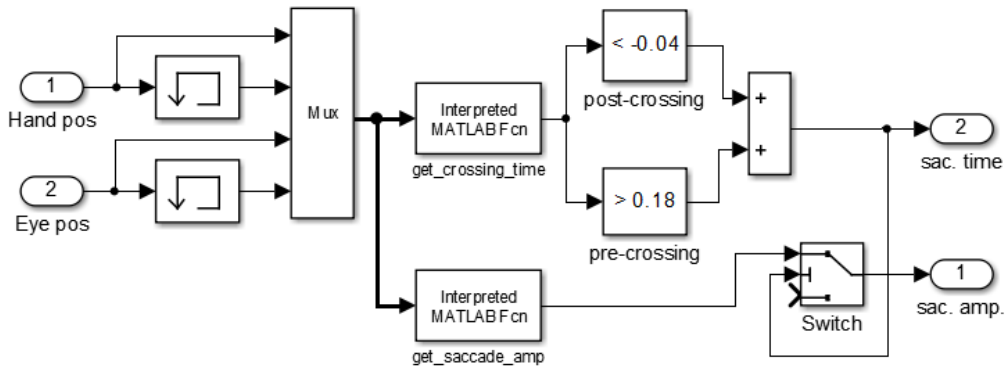


**Fig. 4.10** Sub-model of saccadic subsystem: crossing-time estimator and saccade trigger.

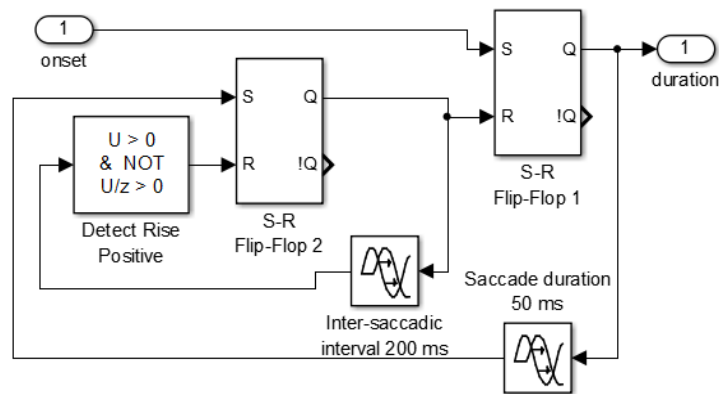


**Fig. 4.11** Sub-model of saccadic subsystem: Saccade timing estimator.

The purpose of coordination control system (CCS) and its influence in smooth eye movement subsystem is already explained in section 1.5.2. This new model extends it by adding object guiding subsystem (OGS), which further alters the behavior of smooth eye movement subsystem. It also selects the guiding speed and the preclusion to become a waypoint. Its structure is shown in Fig. 4.12.

Reducer of smooth eye movement velocity (Fig 4.13) is a sub-model, which according to the direction of eye and hand movement reduces the smooth eye movement velocity by a value obtained experimentally. The polynomial provided in equation (3.10) is used.

OGS also evaluates the segment complexity by calculating the ID (according to Steering law). The ID is then recalculated to TAID using the equation (3.1). Then – to peak hand movement velocity using the equation (3.3). This peak velocity of hand movement is then set as the parameter of the arm branch.

One more purpose of the OGS is the supervision for guiding along the segment completion (sub-model called Guiding aim selection). The hand position is compared to the aimed preclusion. If the difference is less than a width of the path, it is decided,

that it is time to move the hand towards next preclusion. Signal to preclusion generator is sent, what provides the simplified retina (in a form of attention) with a new preclusion location to guide to.

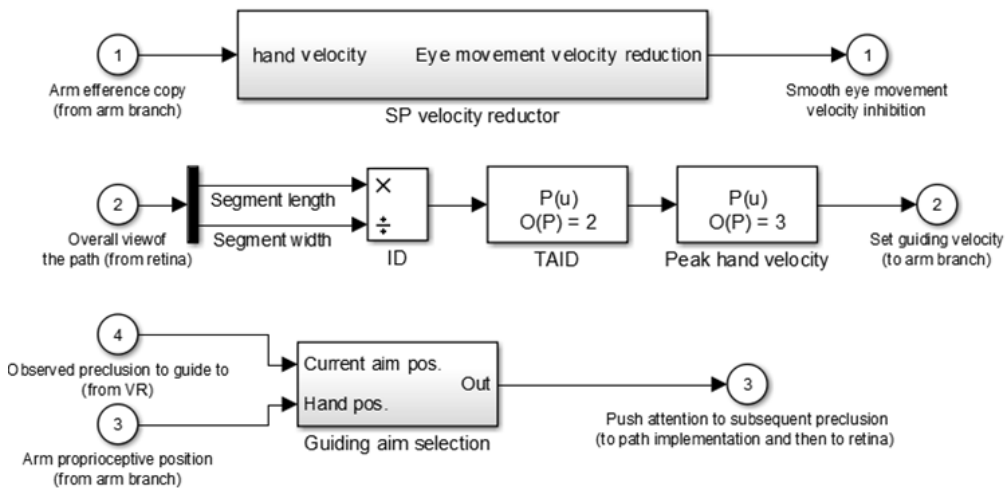


**Fig. 4.12** Model of object guiding subsystem (OGS).

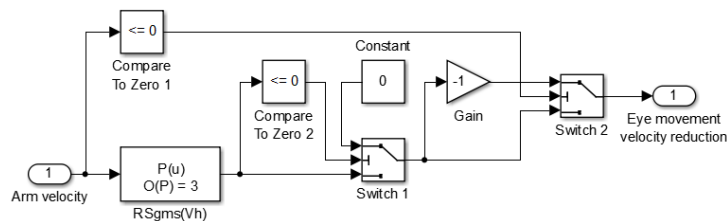


**Fig. 4.13** OGS sub-model: reducer of smooth eye movement velocity.

#### 4.4. Model adequacy

In order to test if the resulting model is adequate to real conditions, a comparison of models' output and experimental data had to be done. The model was realized and tested in MATLAB Simulink modeling environment. As seen from experimental data presented in chapter 3, extra-subject and inter-subject variability of all the parameters involved in oculo-manual coordination is high. As even the same subject is unable to repeat the same trial with the same performance, it is not possible to verify the model by directly calculating cross-correlations on experimentally obtained and synthetic data. Therefore, main dependencies of modeled eye movement parameters were extracted using the same algorithms as for experimental data. This way the averages and the SDs of human and model characteristics can be compared. Average cross-correlation for these simulated and experimental-data dependencies is 0.92.

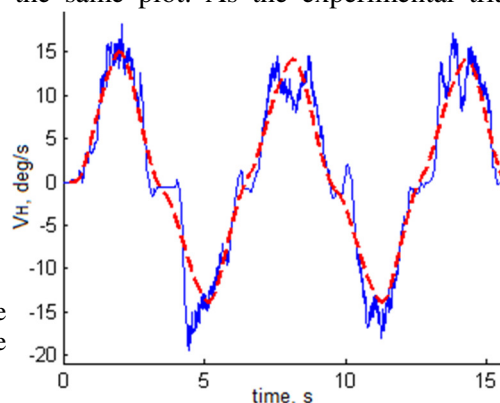
At this point, the model is not introduced with an additional noise. This should be done to achieve the results more similar to experimental data by means of

parameter inter-subject and extra-subject variability. As there is no such variability yet, the TAID values of the model strictly depend (without variability) on ID of the provided path and on experimentally obtained average ID-to-TAID dependency. In such way, the paths used for experimental trials provide only fixed TAID values and the main guiding parameter dependencies obtained must be calculated based on data clustered to three groups. In order to have variable data for model testing purposes, many different (by means of length and ID) path segments were used. Model testing trial consisted of 12 simulations, 10-15 s each. Simulations included both single (long) - segment and multiple (small) - segment oculo-manual guiding.

In order to test the adequacy of the characteristics of modeled hand movements, data of one experimental trial was plotted and its TAID was evaluated. Then a compatible simulation was performed (adequate TAID, adequate amplitudes of path segments and directions, i. e. preclusions at 0-24-0-24-0-24 deg). Then the synthetic hand movement velocity was added to the same plot. As the experimental trial consisted some vertical hand movement (see Fig. 3.24), pauses in-between the horizontal hand movement segments were slightly modified (100 to 500 ms). This plot is presented in Fig. 4.14. It can be seen that modeled hand movements are adequate to experimental data.

All the most important parameters

**Fig. 4.14** Hand movement velocity in a single experimental trial (solid line) and in adequate simulation (dashed line). TAID=48.



of oculo-manual guiding along visual paths as eye movement characteristic dependencies on hand movement velocity were analyzed and are presented in Fig. 4.15. It is obvious that they correspond with the dependencies obtained from experimental data. Total GMS time ( $TT_{GMS}$ ) graph can only be compared by the shape of the trend, but not by values. This is to, because of different configuration of path segments and overall duration of oculo-manual guiding for experimental and simulation trials. All the SDs are lower for modeled data. The adequacy of model is confirmed as the curvature and the values of the fitted polynomial and power equations are obviously similar.

The profiles of hand movement and eye movement velocities are compared in Fig. 4.16. Experimental data has some amount of noise, which is because of precision of eye tracker and fixational eye movements (i. e. micro saccades, tremor, etc.). Position of eye and hand movements of experimental and modeled data in similar conditions is present in Fig. 4.17. From this figure, it can be seen, that just before the preclusion (i. e. corner), during experimental trial, there is an exclusive saccade followed by a zero-velocity fixation to the location of preclusion. In simulation output, there is continued guiding instead. This is so, because the preclusions attract the gaze if it is nearby (introduced in section 3.3.1) and this model is yet designed only for guiding in a long straight paths.

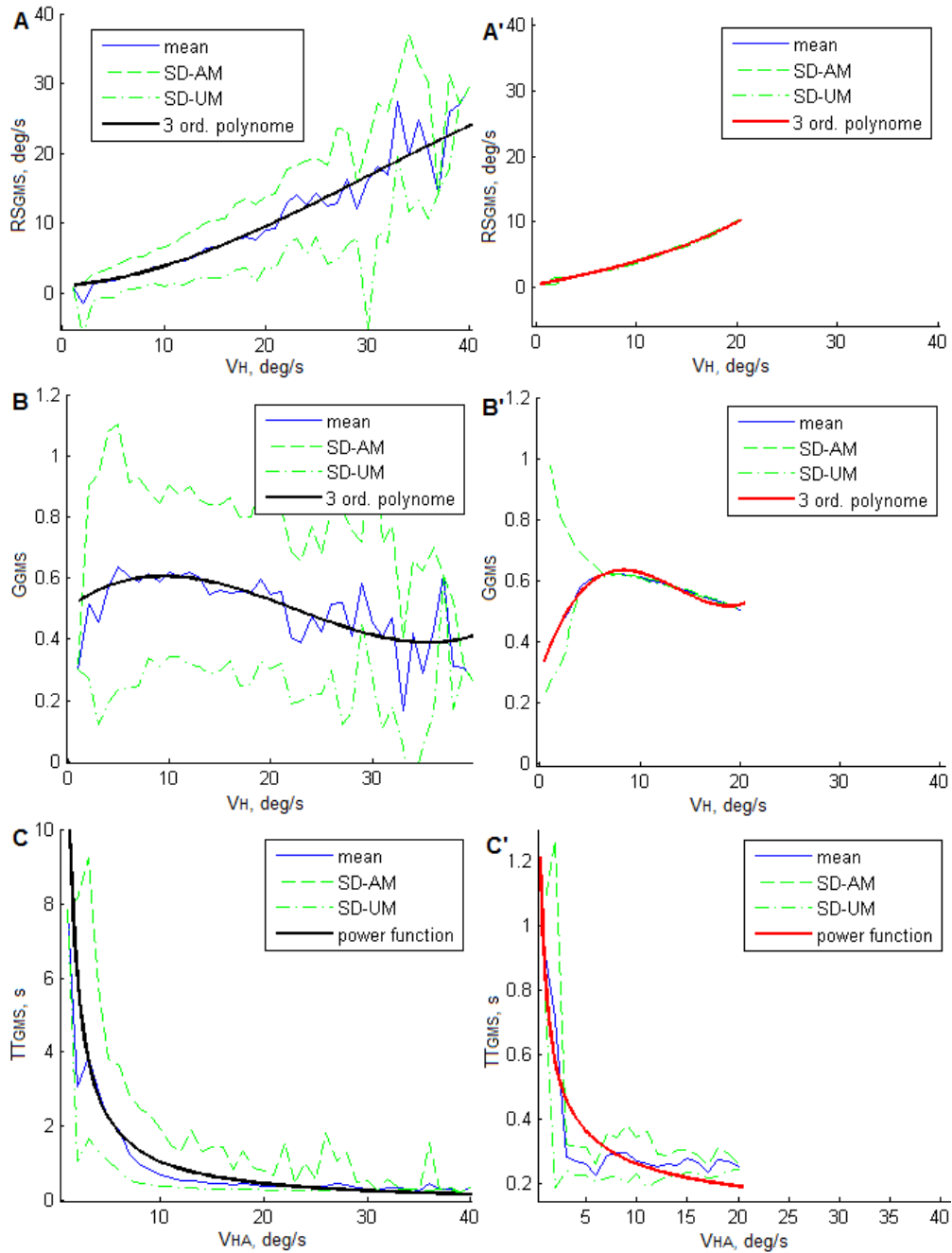


**Fig. 4.15** Comparison of experimentally obtained and simulated eye movement characteristic dependencies on hand movement velocity for: retinal slip (**A**); GMS gain (**B**); total task time (**C**); GMS velocity (**D**); time catch-up to saccade onset (**E**); distance cursor-gaze on saccade onset (**F**); saccade amplitude (**G**). The graphs with a prime (**right**) are the output of the model. The same algorithm as for experimental data (**left**) was used for automated eye movement feature extraction and statistics. Figure is continued on next page.

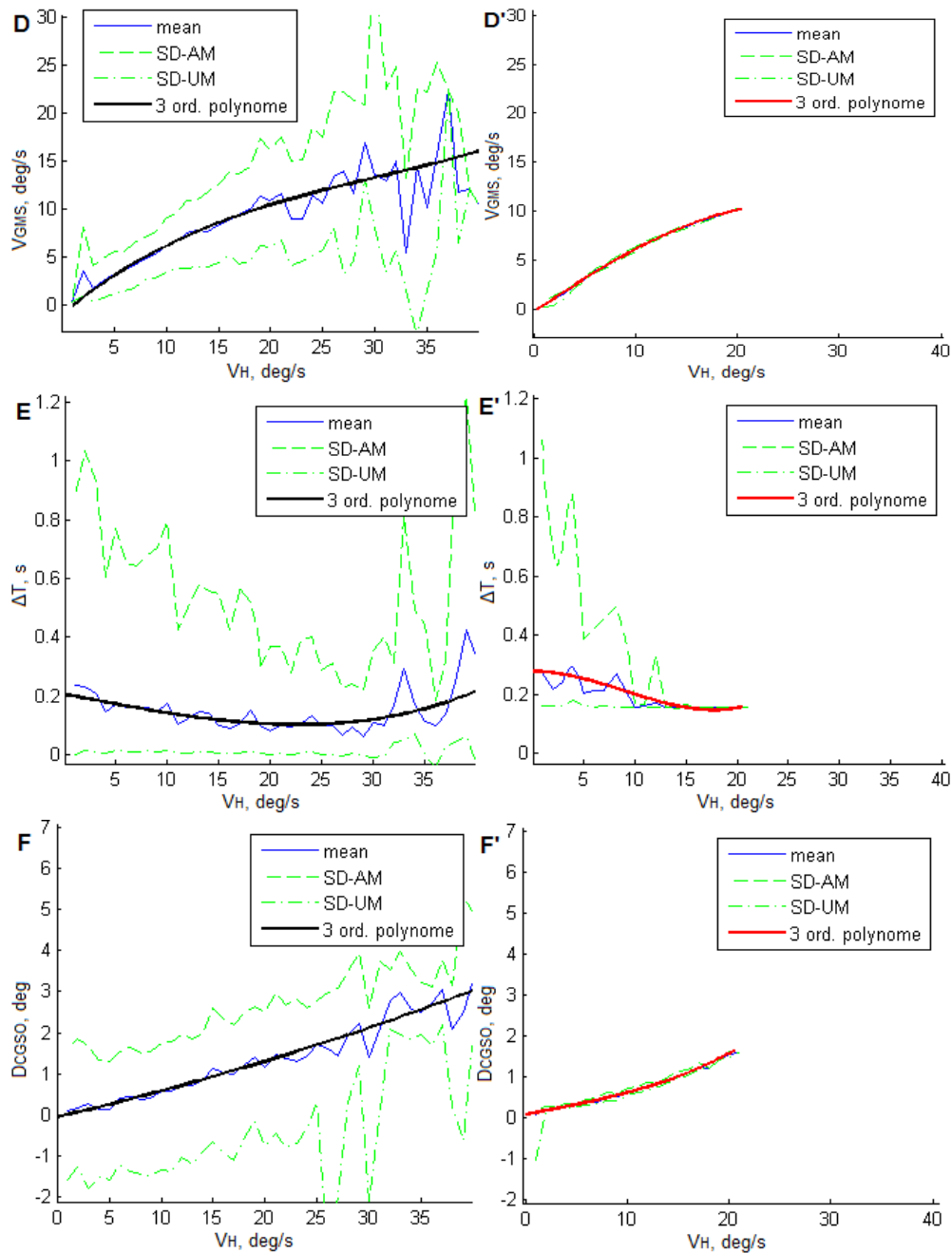


**Fig. 4.15 (continued)** Comparison of experimentally obtained and simulated eye movement characteristic dependencies on hand movement velocity. Figure is continued on next page.

Simulation output is different for different ID (and TAID) of the path. Changes in peak hand movement velocity, saccade amplitudes can be seen from Fig. 4.18. Changes of eye movement profile is illustrated in Fig. 4.19.

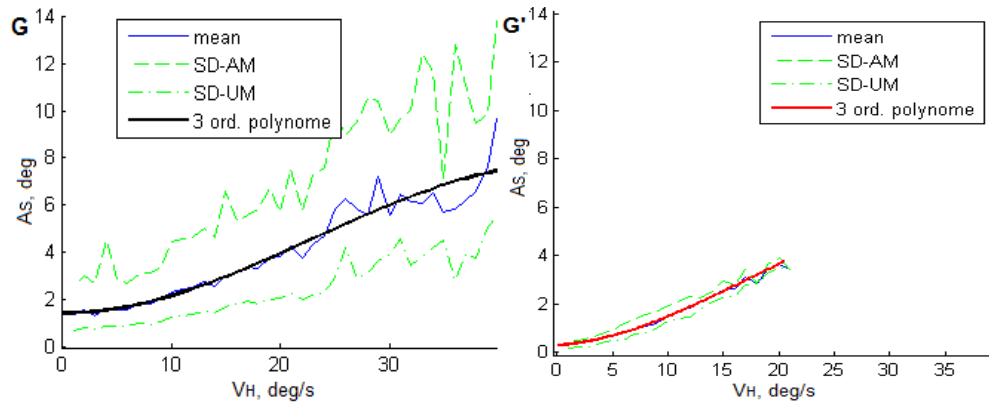


**Fig. 4.15 (continued)** Comparison of experimentally obtained and simulated eye movement characteristic dependencies on hand movement velocity.

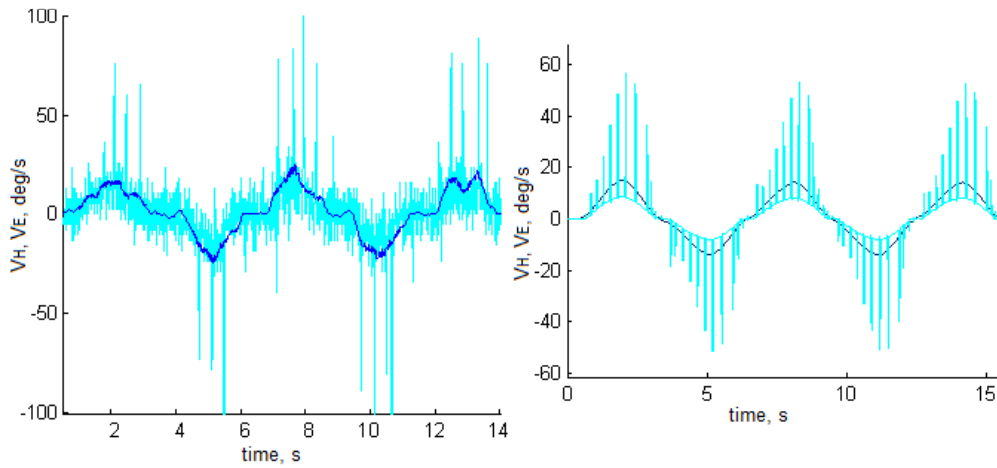


**Fig. 4.16** Eye (black) and hand (gray) movement velocities ( $V_E$  and  $V_H$ ) in similar trials for experimental (left) and simulated (right) data. TAID=48.

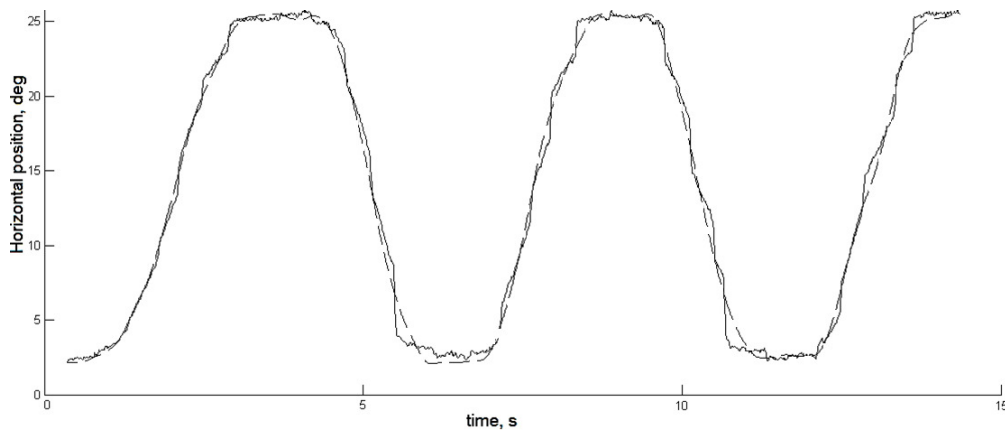


**Fig. 4.17** Comparison of experimental (above) and modeled (in a next page) eye (black line) and hand (dashed line) movements. Figure is continued on a next page.

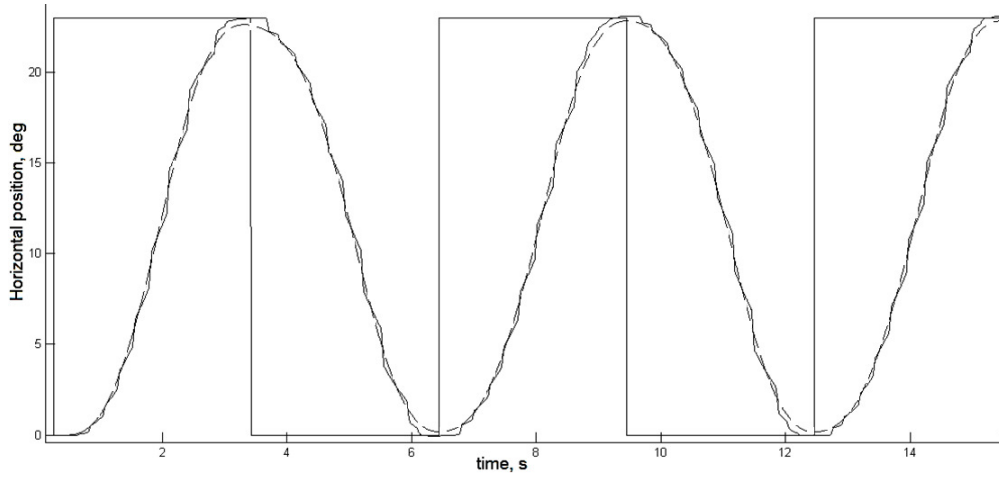


**Fig. 4.17 (continued)** Comparison of experimental (in the page before) and modeled (above this text) eye (black line) and hand (dashed) movements. Rectangles represent the location of the preclusion being aimed. Trials were similar, but not 100% adequate by their conditions.

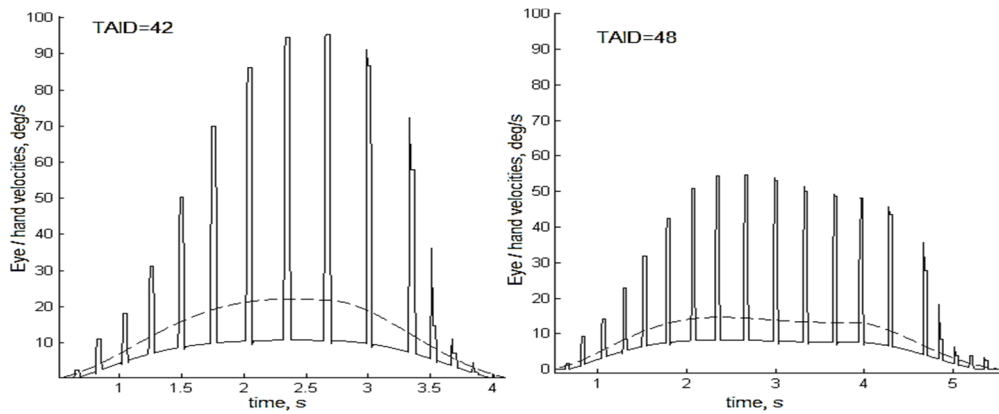


**Fig. 4.18** Simulation output comparison for different TAID values. Dotted line represents velocity of hand movement and solid line represent eye movement velocity.

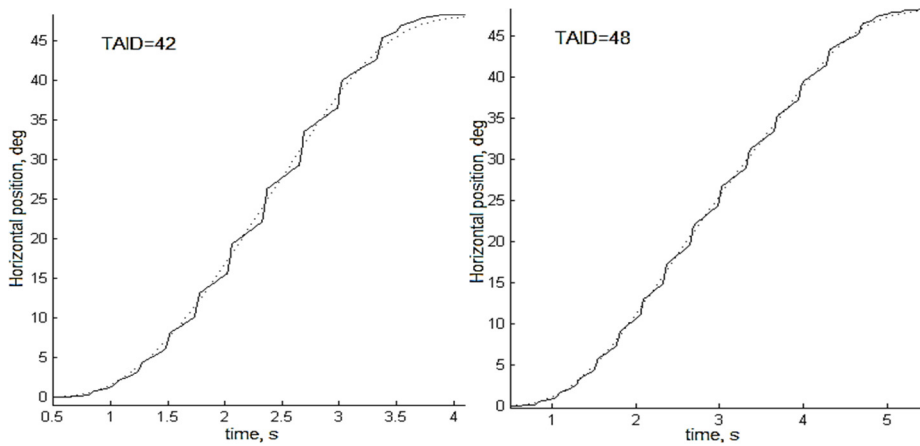


**Fig. 4.19** Simulation output comparison for different trial assumed index of difficulty values.

#### 4.5. Summary and conclusions

1. The behavior of human during oculo-manual guiding along a path could be simply modeled by using probabilistic distance cursor-to-gaze (for saccade triggering) and saccade amplitude functions, but it would not be similar to neurophysiology.
2. Coordination control system, modeled in previous eye-hand coordination models can be extended by adding an object guiding subsystem. This subsystem is responsible for guiding velocity estimation, target location in visual space selection and alteration of smooth eye movements' velocity characteristics.
3. Smooth eye movements, used in oculo-manual guiding, despite some differences in comparison to smooth pursuit eye movements are derived from the same control system. Also, the parametric features, which differ oculo-manual guiding saccades from catch-up saccades, are influenced by different context of use, but realized by the same neural circuits.
4. The model for simulating eye-hand coordination during self-moved object guiding along a visual path was designed and explained. Existing similar model for oculo-motor and oculo-manual tracking of external and self-moved targets had to be redesigned as it was using some simplifications, which were not adequate in order to simulate the oculo-manual guiding along a visible path.
5. Designed model output data was compared to experimental data. As inter-subject variability of performance is high (i. e. subjects never repeat the same trial with the same or even similar results), it is impossible to check the adequacy of the model by calculating correlation-related measures on output signals. The most significant oculo-manual guiding parameter dependencies were obtained by statistical means and compared (average cross-correlation is 0.92). Model was verified, as its output parameters are adequate to parameters obtained in experimental way. As model is designed for oculo-manual guiding simulation in straight long paths, verification procedures has shown, that it must be extended by adding the features for preclusion (e. g. corner) tackling. Also, it can be extended by adding experimental data-evaluated levels of noise to be more variable as human subjects has large guiding parameter variability.

## 5. APPLICATIONS OF EYE AND COORDINATED EYE-HAND MOVEMENTS FOR DESIGNING ELECTRONIC SYSTEMS

### 5.1. Eye movement application in human-computer interaction

Today among the tools in the human and computer interaction (HCI), a mouse, a touchscreen, a touchpad and a keyboard are the primary input devices. Some years ago, gaze-aware interfaces, based on eye tracker as an input device, have been gaining popularity in the HCI community and now there exist many sophisticated HCI methods [186, 90, 41, 155, 154, 68, 158].

Oculomotor system, being important part of the vision, has exclusively important features. There are no other parts of the body than eye, which has so well developed both sensor and motor subsystems in one. Sensory subsystem of the eye, scans the visible interface area, finds an object of interest and motor subsystem of the eye directs the gaze.

The accuracy and the large velocity of eye movements brings the idea to use the visual system not only for acquiring visual information but, measuring the position of the gaze, to perform control commands such as pointing. The pointing by gaze itself has only one major problem: fixational eye movements prevent the precision to be adequate or even close to the precision of a hand. However, most of the problems arise when there is a need for activation. The majority of the early HCI systems used eye-blinks or a fixation duration (called dwell time) to trigger the interface actions. Blinks are uncomfortable because of possible false-activation (or they have to be longer) and losing of accurate gaze direction after blink. Fixation-based selection also introduces a delay in the performance of the action and also can trigger false-activations (i. e. phenomena called Midas Touch) [69]. Due to a high velocity of saccades, they seem to be the most appropriate eye movements, which could be used to trigger the activation. Gaze gestures (e. g. looking to some specific position or direction outside the computer screen) are one more recent alternative for HCI using the gaze [42]. Also eye movements are intended to assist the vision subsystem in acquiring the most important information about the surroundings and it is an unnatural task for the CNS to elicit action-based commands. This overloads the perceptual function.

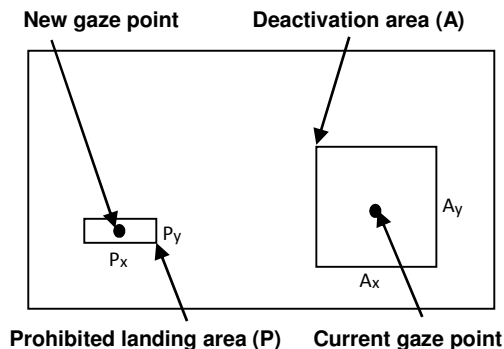
Since the computer cursor is invincible throughout the years, an alternative approach – to use the gaze information only for large cursor shifts is present. In such an approach, gaze pointing only replaces large amplitude manual movements, while precise movements and activation is left for manual control (i. e. the best feature of the gaze – speed, and the best features of the hand – precision and multi-function for activation are mixed). There are a few compelling reasons to motivate such an application. First of all, “what you look at is what you get” [69] is captivating natural feature of our vision and no other input method can act as quickly. Second, using an alternative computer cursor shift for a large amplitude gaze jumps method reduces a fatigue of arms, hands and wrists. This cursor control method is even more attractive having in mind portable computers with a touch-pad, when possibility to use a mouse or touchscreen is limited. And third, eye tracking technology has achieved a great

promotion in gaze tracking by using simple web cameras and other cheap-ware [156, 3, 133, 135].

The key idea is to use the gaze position for redefining the position of the computer cursor to be at the vicinity of the user's area of interest. For this purpose, two possible behavioral conditions can be defined: first, passive condition, when user is moving his gaze only with the purpose to acquire new information (e. g. to read the text) and the second, active condition, when user wants to execute a command. In the passive condition, it is no need to reposition the cursor as it could disturb the vision. For the active condition, cursor must be used for action, so it is necessary to bring it to nearby a place of interest. Selection of an active option can be done by having a hand on the touch-pad or computer mouse and slightly moving it. This way, when user does not want any cursor repositioning – hand can be moved away form a manual control input device. Of course all-time active mode can be used too. When the position of the computer cursor has been redefined, manual control returns back to the user. Now user is able to continue working as usual and small amplitude gaze shifts do not activate an alternative repositioning of the cursor.

It is obvious that the most important parameter is the size of the deactivation area  $A$  (Fig. 6.1). This area is defined by a geometric shape (e. g. rectangle  $A_x \times A_y$ ) moving together with small movements of the eye. If the eye movement amplitude is large enough for the gaze to jump outside this area, alternative cursor repositioning occurs. For better selection, not only the amplitude of the eye movement but also the transient velocity of the saccade can be used to define the threshold of the activation of the alternating cursor control. The thresholds of saccade amplitudes ( $A_T$ ) for cursor repositioning can be defined by equation (6.1). The threshold area can also be defined as a circle with the specific radius [186].

**Fig. 5.1** Boundary for the activation of the alternative cursor repositioning ( $A$ ) and prohibited area for cursor landing ( $P$ ) on a computer screen.



Second important parameter of the alternating cursor control method is the size of the area  $P$ , in which, landing of the cursor is prohibited. At first, it seems that a high accuracy of the positioning after the redirection of the cursor to the point of the gaze is desirable. But, with the purpose not to cover the text or picture with a cursor, better decision is to place the cursor in the vicinity of the target position and let the user to continue further operation using manual input. This is the case anyway, because fixational eye movements disallow the cursor to be repositioned in a needed accuracy.

For experimental testing of such HCI method, the algorithm was designed (Fig. 6.2) and implemented. Computer application runs an infinite loop in background. First, the data at the sampling frequency of 120 Hz is obtained from gaze-tracker. Alterable number  $N$  of data samples (horizontal and vertical gaze coordinates  $G_H$  and

$G_V$ ) are averaged and stored in the circular history buffer, in which values are stored for 0.5 s time interval. Gaze velocity ( $V_G$ ) is calculated:

$$V_H = \frac{|G_H[N] - G_H[N - \Delta t \cdot 120]|}{\Delta t}, \quad V_V = \frac{|G_V[N] - G_V[N - \Delta t \cdot 120]|}{\Delta t}, \quad (6.2)$$

$$V_G = \sqrt{V_H^2 + V_V^2}; \quad (6.3)$$

where  $\Delta t$  is the parameter of the algorithm.

Later, transient gaze velocity  $V_G$  is compared with the threshold value for the gaze velocity  $V_T$ . Instead of the threshold value of the eye movement velocity  $V_T$ , the threshold value of the eye movement acceleration  $a_T$  could be calculated and compared with the current eye movement acceleration  $a_G$ . If the calculated values of the eye movement velocity or acceleration are exceeded by the current values, cursor is repositioned near the current gaze position, ensuring, that it does not land in the prohibited zone  $P$ . If active/passive mode is being used, the repositioning of the cursor occurs only after the hand has moved the cursor. Program allows the correction routine, which enables the repositioning of the cursor for a second time after alterable time interval  $T_K$ . This can be used to adjust position of the cursor after corrective saccades. Inactivity time  $T_I$ , during which repositioning of the cursor is disabled also could be implemented. This option allows inactivating another repositioning of the cursor, for a time interval of up to 500 ms.

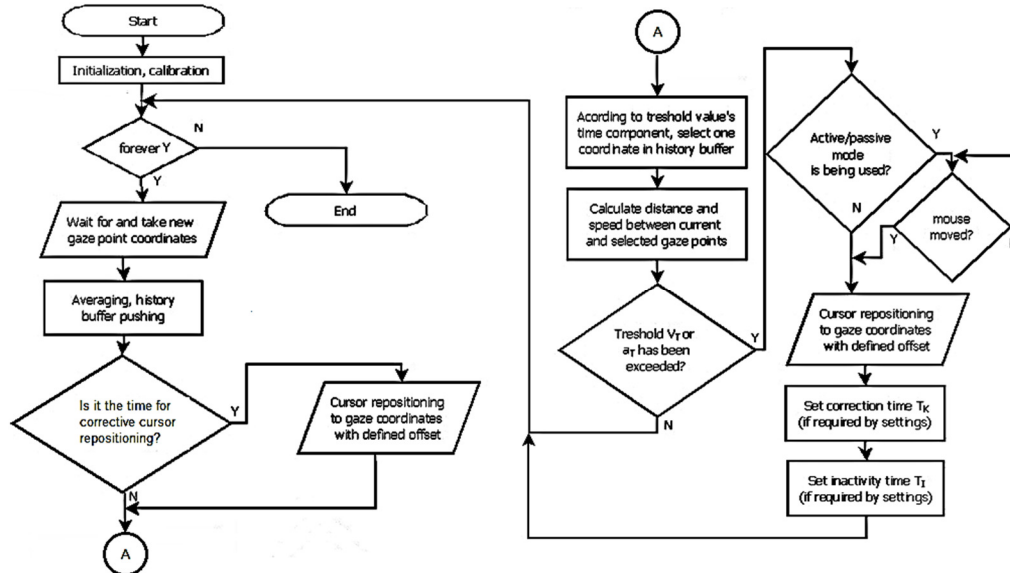


**Fig. 5.2** Algorithm of the alternating control of the computer cursor.

With a purpose to find optimal parameters for the algorithm, experimental investigation of the alternating computer cursor control system performance was designed and executed. Five subjects were asked to perform four different typed computer tasks using a regular PC mouse together with the alternative method. The experiments were: to open and to close nine programs by activating icons on a

computer desktop (E1), to draw the picture by joining the in advance prepared points (E2), to click on the targets appearing each 1 s in non-predictable positions (E3), to correct the mistakes in the text (E4). During these experiments, different sets of the parameters were used and task fulfillment time was measured. The values of optimal parameters were defined and placed in Table 6.1. These parameters were selected and fixed for the further investigation of the effectiveness of the alternating cursor control system.

**Table 5.1** Values of the optimal parameters for the algorithm.

Parameter	N	$\Delta t$ , ms	$V_T$ , deg/s	$a_T$ , deg/s <sup>2</sup>	$T_K$ , ms	$T_I$ , ms
Value	1	8.3	200	10,000	40	500

The effectiveness of the alternating cursor control system was investigated by repeating the earlier described four experiments. Effectiveness was calculated as a ratio of time used for the task using only the mouse and of time using new method. Obtained results illustrated in Fig. 6.3 show that alternating control of the computer cursor is the most effective for activating the targets appearing in the non-predictable positions (E3). In this case effectiveness increase exceeds 40 %. Second experiment, which was performed with an increase of the effectiveness of 20 %, is opening and closing desktop programs (E1). Picture drawing (E2) by joining the prepared points did not reveal the advantage of the method of the alternating cursor control. The task of the correction of the mistakes in the text (E4) revealed that results obtained with mouse-only are better.

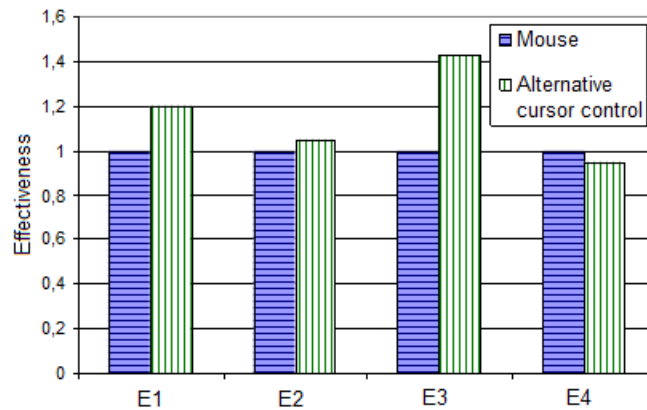


**Fig. 5.3** Results of the effectiveness of alternating control of the computer cursor for four different computer tasks (E1, E2, E3, E4).

Obtained experimental results illustrate that alternative method of the computer cursor control let us get advantage during execution of the computer tasks, when large cursor shifts are dominating (experiments 1, 3). During computer tasks, when the largest part of the job must be done by small amplitude cursor shifts (text correction) and keyboard, used to pick up the right letters, alternating control of the computer cursor is not effective.

It is necessary to point out that the deactivation area was not defined as a parameter of the algorithm. The size of the deactivation area  $A_x$ ,  $A_y$  is defined indirectly by setting the threshold of peak velocity of the saccade  $V_T$ . Main sequence (strict relationship between the peak eye velocity and amplitude of the saccade) indicate that, when  $V_T=200$  deg/s, amplitude of the saccade is more than 3 deg.

Implementation of the modes of the correction time  $T_K$  and the inactivation time  $T_I$  did not revealed any substantial positive features of the new method and it was decided not to use them.

Investigation of the active/passive and active-only modes of the alternating control of the computer cursor method revealed that they have no substantial difference on the effectiveness of the new method. In some computer tasks when not many input commands are executed, more convenient is the active/passive mode (e. g. reading and drawing). However using always-active mode, due to prohibited area, computer cursor is landing below the gaze point and does not disturb vision.

Alternating control of the computer cursor during the first experiments is not comfortable for test-users. Better results of the effectiveness in the range of 20 – 50 % of this alternative method could be obtained for trained subjects. During the experimental investigation, interesting psychological phenomena was observed. First, during experiments with alternative control, when computer cursor appears in the new position, towards which gaze is directed, for subjects seems natural. Second, after the experimental session, when alternating control of the computer cursor was switched off, most subjects had reported a feeling that computer cursor moves too slowly. This supports the observation-based hypothesis about the possible effectiveness increase after some training.

## 5.2. Eye movement application in diagnostics

Each new method for diagnostics or treatment is more and more complicated. It is obvious, that such methods will not be available for each person. Cheap and simple diagnostic tools and knowledge, accessible to all, would be preferential. As the eye movement capturing devices are becoming cheaper, more precise and comfortable, many of them can be used not only in a lab, but also at home. Even low-cost, open source eye-tracking systems are becoming widely available. This step forward in eye-tracking arsenal encourages scientists to reassess the possibility of using the relations between normal and especially abnormal eye movements and mental disorders for diagnosis purpose. As an extra, the eye-movement analysis can reveal the state of the most important sensorimotor patient's system – ocular system. Complete diagnostic test can be in a free, non-irritating form, such, that subjects are familiar with it (e. g. TV clip watching was used in a recent investigation [169]).

**Neurological disorders.** Eye movement analysis can provide valuable data related to brain disorders. Some of disorders can be diagnosed with a quite good reliability in such way. Anyway, the results of eye movement analysis can be used only as a part of diagnosis process for most of the diseases. Undoubtedly, the reliability of diagnosis obtained this way, mainly depends on the data acquisition and processing methods being used.

Even if there is no known medication to stop the Parkinson's disease (PD), an early diagnosis is highly desirable, because an early treatment may help to slow the progression. Today's practice is different: it is very difficult to diagnose Parkinson's in early stages. At this time, it can be diagnosed only by symptoms. Physicians make an incorrect initial diagnosis of PD in 8% to 35% of cases. Even general neurologists have difficulties to identify it correctly. To improve the accuracy of early diagnosis, it is possible to use eye movement data. Recent findings shows, that using data of patient's eye movement while he or she watches TV clips for 15 minutes, after a mathematic feature extraction (four oculomotor-based core features, such as distributions of saccade duration, inter-saccade interval, saccadic peak velocity, and saccade amplitude), it is possible to discriminate patients with PD from age-matched controls with a 86.4% accuracy (14 diseased and 24 controls participated in the trial). If additional features, related to attention, are being used, the overall discrimination accuracy of 89.6% was reached [169]. The saccades of patients with PD were shorter, slower and had lower amplitude. Peak velocity and inter-saccade interval were also affected. It is obvious, that features mentioned, can be a sign of other disorder, but not only PD. Otherwise, such diagnostic method is valuable for assessing disease-suspected patients, or the data obtained, can be a good starting point for further diagnosis process. Another recent research, where higher accuracy eye-tracker was used, obtained outstanding results and excluded one feature, which is specific to patients with PD. One hundred twelve patients (including untreated ones in an early stage of disease) and two (out of 60) controls were discriminated by an evaluation of gaze movement tremors while fixating on a steady target. The specific feature is a tremor, that oscillates at a specific (maximum variation for individual patient is 1Hz) frequency, ranging from 4.3 to 10.9Hz. Mean frequency is 5.7Hz. Amplitude of these oscillating eye movements fluctuates in a regular pattern and has a mean value of 0.27° horizontally and 0.33° vertically. The root mean square velocity during fixation was 5.72°/s with PD versus 3.07°/s among controls [54]. Fixation tremor based diagnosis of PD is promising, but requires an accurate eye-tracker.

Attention Deficit Hyperactivity Disorder (ADHD) can be diagnosed from eye movements while watching TV clips too. Experimental study has shown, that the main feature, which can be used to distinguish ADHD patients (21 subject) from controls (18 subjects), is saliency-based feature set (differential distributions of salience values at human gaze vs. other locations, using saliency maps). Such method can discriminate ADHD from healthy controls with 78.2% accuracy. The best feature for this case is texture processing. Children with ADHD showed a higher correlation with texture contrast and had a propensity to look toward color contrast and oriented edges. For such diagnosis, the oculo-motor and group (correlation between a patient's gaze and aggregate eye traces of controls) features were not discriminating [54]. Another study has shown that ADHD children can track moving stimuli for a maximum period, which is 6 to 10 times shorter than the one of a normal child. This method allows discriminating ADHD children with accuracy of 97%.

Children, having Fetal Alcohol Spectrum Disorder (FASD) can be discriminated using the same saliency-based feature set (with 77.6% accuracy) and group-based feature set (with 69.8% accuracy). For children with FASD, line

junctions, overall salience, and texture contrast were discriminative. Overall accuracy of 79.2% was achieved during this study [54].

It is also known, that children with autism, even in the period of infancy, looks at presented pictures (e. g. human face) in a different way than normal children. Besides that, it is proven, that they exhibit up to three times more saccades while looking to presented stimuli and in between these stimuli [80].

One more, possible to diagnose using eye tracking, disorder is Dislexia. During reading, dyslexic readers exhibit more and longer fixations and a higher percentage of regressions than normal readers [136]. Early warning signs of potential development of ADHD, autism and dislexia are very useful, because the treatment procedures can be started earlier, thus decreasing the struggle of the child.

Some mental illnesses can be diagnosed after analyzing eye movements too. Patients with schizophrenia can be discriminated analyzing their smooth pursuit eye movements. The gain of smooth pursuit of such patients is significantly lower than the gain of the smooth pursuit of healthy control subjects. Previous study evaluated, that the mean difference of smooth pursuit gain between healthy subjects and patients is 0.73 to 0.99. It has also identified, that biological relatives of patients also has reduced smooth pursuit gain characteristic (mean difference at a level of 0.5) [76]. Another recent study has proven, that using neural network and data of subject's visual scan-path, fixation stability and eye movements while performing horizontal and Lissajous pursuit, 98.3% discrimination accuracy of schizophrenia can be achieved [16].

One more mental disorder can be quite successfully diagnosed using eye movement analysis – a pedophilia. Recent study of subjects watching photos has identified, that pedophiles fixated for a significantly longer time and with significantly shorter fixation latencies to a child stimuli than either of the control groups. Discrimination method based on fixation latency performed with a sensitivity of 86.4% and a specificity of 90.0% [50].

**Disorders of vision.** As eye movements are vision-related by their purpose, it is clear, that they can provide some information about subject's ability or inability to see. There are two ways to diagnose the vision disorders by analyzing the eye movements. The first is to detect the abnormal eye movements in specific conditions as an outcome influenced by a learning of eye-movement control system. This learning can be the adaptation to changed characteristics of a vision. E. g. the glaucoma in all the stages (starting from early) introduces delayed by approximately 15 % saccades. The second way is to detect that a subject does not see some specific object. This could be the error in a gradient-color bar, or a moving object. If the subject being tested is asked to look, but does not look to a specific position, where the particular object is presented – it can be automatically (i. e. without an expert-evaluation) stated, that this stimuli is too difficult for a patient to see. Such methods are not more informative to those, which are now used, but they can spare much of patient's and clinician's time.

Such a case was experimentally tested as a part of this thesis by adapting a functional contrast sensitivity test. This test is used for detection of visual acuity deterioration influenced by various disorders (cataracts, corneal damage, etc.) which

often cannot be detected using traditional visual acuity testing. Contrast sensitivity is examined by using an array of sine-wave gratings of five spatial frequencies and nine contrast levels. Each eye is examined separately in two lighting conditions: night (3 cd/m<sup>2</sup>) and day (85 cd/m<sup>2</sup>). During the examination, clinician fills a report when a subject reports the direction of the last visible for her/him grating's waves. Typically, such examination takes 1.5 h.

An intention to prepare an automated testing system arose. In order to compare the results of a new system, five subjects were examined in a traditional way (using a methodic by Dr. Arthur P. Ginsburg and OPTEC 6500 device) first. Later, a computer application-controlled methodic based on a traditional methodic was prepared. Appropriate gratings were presented on a computer monitor. These gratings changed their position by a smooth vertical or horizontal movement or in jumps (to one of eight possible locations). Gaze position was compared to the position of the grating. If an error of the smooth tracking became larger than 3 deg or a cross-correlation between the trajectories of the stimulus and the gaze became less than 0.5, it was considered, that a subject is unable to see the stimulus. For saccadic eye movements, the main parameter was the presence of a last and longest fixation to a correct location where the stimulus is presented. Software can provide the graphs, which are a result of the traditional Ginsburg-test. Overall examination time reduced to approximately 30 min. To obtain required spatial frequency, monitor must have high resolution and the distance eye-to-screen must be recalculated or a lens system is to be used. Also the suitability of optokinetic nystagmus analysis for this purpose was tested. Very high frequencies of the grating prevented the nystagmus even if the stimulus was still visible by the subject.

### **5.3. Possible applications of the eye-hand coordination model**

Models for eye-hand coordination are required in order to understand the functional structure of the brain. Even if the knowledge on human brain in recent years has increased greatly, there are still long way to go. Many researchers and scientist are working and will be working in the future in this area. Any new information about neurophysiological circuits is important for further brain investigation.

Physiologic eye-hand coordination models can be easily used in diagnosis of various disorders in various and even early stages. This is proven by diagnostic capabilities of eye movement analysis. Psychiatrists are also using neurophysiologic knowledge in relating the symptoms to the malfunctioning areas or pathways in the brain. Accurate knowing which part of the brain is affected leads to apt prescription of medicine and better treatment. As eye movements alone provide some interesting and promising diagnostic capabilities, it is expected, that eye-hand coordination parameters can be a source of information on the condition of other, not less significant subsystems of the CNS.

In order to evaluate if some coordination-related areas of the brain are malfunctioning and to determine which ones, knowledge on regular eye-hand coordination is essential. This information is the best provided in a form of behavioral models, which are able to simulate normal (or in a more specialized way – specific

condition related) eye-hand coordination. Then the results of a specific patient can be compared to the simulation results. In fact, at the moment of this dissertation's text preparation, an experimental pilot study is being executed in a local psychiatry hospital. Patients affected by various disorders of various stages and having various history of treatment are examined for their eye-hand coordination during oculo-manual guiding along a visible path. It is expected for the results to show some patterns, which later could be investigated further and then used for diagnosis and understanding of disorders.

Hand movement analysis is being used for a long time. That is because the hand movement recording equipment is available for significantly longer time than the eye movement tracking systems. Also, it is possible to analyze hand movements by using only simple methods such as a sheet of paper and a pencil. It is now clear, that hand movements are used for various purposes where an evaluation of subject's skills or personal (even not hand movement related) characteristics is needed. Especially this is important for selection of specialists for responsible posts, professions or activities. Racing drivers, plane pilots, astronauts, military force are the perfect examples [1, 56], but the demands for good personal coordination characteristics even in a civil area are important and large enterprises can allow themselves to choose suitable candidates not only by the facts about applicants, but also testing their peculiarities. Even if hand-related tasks are being used, in fact an eye-hand coordination is being tested. Therefore, a possibility to evaluate it by analyzing not only hand, but also eye movements looks promising. Such analysis can even explain why the performance of one or another subject is poor in eye-hand coordination particular tasks and propose a suitable training course. It is impossible achieve mentioned benefits without having more or less sophisticated models for simulation and explanation of eye-hand coordination.

Even if while superficially investigating the differences between basketball players and non-players (appendix D), there was no clear evidence of differences in eye-hand coordination, it was observed that different subjects (and even groups of them) has different characteristics. Subjectively a hypothesis based on observations was developed, that humans, who live a healthy (physically and socially) life, demonstrate a better performance in eye-hand coordination tests. More research is needed to support this hypothesis, but research of Carreta T. R. has shown that subjects with better eye-hand coordination characteristics have a higher probability of graduating the course of pilots [31]. This result conforms to my hypothesis that there is a correlation between human social (including education) and physical activity and eye-hand coordination. By the way, this could be the reason of poor performance of advanced basketball player group in experimental trials of chapter 0. Members of this group were living active physical, but inactive social life (only subjective evaluation as no questionnaires were involved in methodology of the investigation). Also, there are some psychological assessment systems (e. g. "Vienna test system"), which incorporate sensorimotor coordination, labyrinth, visual pursuit, multitasking tests. Even if mentioned tests are only the small part of huge numbers of tests involved in all assessment system, it is clear that there is a correlation between eye-hand coordination and overall psychological health and/or personal skills.

One-more relevant application for eye-hand coordination model of human performance simulation during oculo-manual guiding along a visual environment task is HCI development. A perfect example is cascaded menus (e. g. Windows Start menu or application menus). If the designed menus are too narrow or too long, possibility of error increases. Eye-hand coordination model is a perfect tool for testing the possibility of errors and adapting the interface to suit required comfort level. As social integration of disabled people is important, such design of interfaces principle can be used while designing menus for specific groups of users (first the model must be adapted to simulate this group). Of course, there are more computer applications where the models of human eye-hand coordination can be used, e. g. entertainment: computer games can be created and tested using the knowledge of human eye-hand coordination characteristics in a specific visual environment. In such way, developers can predict where the user will be looking (and what is about to be unsighted) in a specific situation.

#### **5.4. Summary and conclusions**

1. Knowledge on eye-hand coordination can be used to create or to develop eye-hand combined HCI methods, which, according to the experimental investigation of one of them, increase the efficiency and the subjective perception of HCI.
2. Eye movement analysis, possible using eye tracking devices, provide 80-95% accurate discrimination of patients, having specific neurological disorder. Besides that, some of these disorders or at least increased their risk level, can be identified earlier than using any other diagnostic methods.
3. Eye movement analysis are about to be used by autonomous systems or applications to evaluate the health of human visual system. Parametric and positional modes of diagnostics can be defined. The first employ the changes in oculo-motor parameters and the second employs the fact, that a subject cannot look directly to or to track a stimulus if it is not visible for him/her. Experimental investigation proves that such autonomous systems can save the examination time (and together to reduce the fatigue).
4. Models of eye-hand coordination during manual object guiding is a promising tool for evaluating human's neurophysiological health and personal-skill related peculiarities. Also, such models can be used in developing and testing various HCI interfaces in entertainment or work-related computer applications.

## CONCLUSIONS

1. Neurophysiology-based models of eye-hand coordination for oculo-manual and self-moved target tracking and reaching arm movements do exist, but there are no models for explaining or simulating eye-hand coordination during oculo-manual guiding in visible environments. This is the problem addressed in this work. For such aim, mathematical and neurophysiological models of eye movements and their control system, also existing models of arm movements and their control system were reviewed, combined and compared to experimentally obtained data of oculo-manual guiding.
2. Eye-hand coordination during object guiding through a visible path was investigated: main principles of such coordination were detected and expressed in experimentally obtained mathematical expressions, which were later used in the proposed quantitative model in which the coordination control system, modeled in previous neurology-based eye-hand coordination models, was extended by adding an object guiding subsystem.
3. Smooth pursuit with catch-up saccades oculo-motor tracking mode was compared to coordinated oculo-manual guiding. As experimentally observed differences can be explained using the same neurophysiological model of oculo-motor system, it is clear, that smooth pursuit eye movement system is used not only for pursuit, but also for guiding.
4. Extended model was verified by comparing the most significant parameter dependencies of oculo-manual guiding – average cross-correlation is 0.92. This model is presented as quantitatively verified qualitative rather than quantitative, because extent of experimental trials was more wide than statistically sound.
5. Suggested model is designed for oculo-manual guiding simulation in long straight horizontal paths of different width. However, experimental data allowed making insights on what is needed to extend it to tackle preclusions. This model also can be extended by adding experimental-data-based levels of noise to be more variable as human subjects has large guiding parameter variability. These extensions were discussed, but not implemented in the quantitative model, as it is complex by itself (because of multiple involved systems and their subsystems). More to that, demand of such extensions and the peculiarities of experimental data to be used to refit this model are application-specific.
6. Knowledge on eye-hand coordination is required for creating or developing eye-hand combined HCI methods, which, according to the experimental investigation of one of them, increases the efficiency by up to 40% and/or the subjective perception of HCI. Eye movement analysis also provide an accurate tool for neurological disorder diagnosis in their early stages and enables human's visual system's health diagnostics in autonomous ways to reduce the fatigue of patient and the duration of the examination. Models of eye-hand coordination during manual object guiding is a promising tool for evaluating human's neurophysiological health and personal-skill related peculiarities. Also, they provide beneficial information while developing and testing various HCI interfaces in entertainment or other computer applications.

## LIST OF REFERENCES

1. Accot, J.; Zhai, S. Beyond Fitts' Law: Models for Trajectory-Based HCI Tasks / Proceedings of ACM CHI. In Conference on Human Factors in Computing Systems, 1997, p. 295–302.
2. Alexik, M. Modelling and identification of eye-hand dynamics. *Simulation Practice and Theory*, 2000, vol. 8, no.1, p. 25-38.
3. Alstrup-Johansen, S.; San Agustin, J.; Skovsgaard, H.; Hansen, J. P.; Tall, M. Low cost vs. high-end eye tracking for usability testing. In *Proceedings of the 2011 annual conference extended abstracts on Human factors in computing systems (CHI EA '11)*. ACM, New York, NY, USA, 2011, p. 1177-1182.
4. Bahill, A.T. Bioengineering: biomedical, medical, and clinical engineering. Englewood Cliffs, NJ, 1981, Prentice-Hall.
5. Bahill, A.T.; Brockenbrough, A.; Troost, T. Variability and development of a normative data base for saccadic eye movements, *Investigative Ophthalmology & Visual Science*, 1981, vol. 21, no.1, p. 116-125.
6. Bahill, A.T.; Clark, M.R.; Stark, L. The main sequence, a tool for studying human eye movements, *Mathematical Biosciences*, 1975, vol. 24, p. 194-204.
7. Bahill, A.T.; Iandolo, M. J.; Troost, B.T. Smooth pursuit eye movements in response to unpredictable target waveforms, *Vision Research*, 1980, vol. 20, p. 923-931.
8. Bahill, A.T.; McDonald, J.D. Model emulates human smooth pursuit system producing zero-latency target tracking, *Biological Cybernetics*, 1983, vol. 48, p. 213-222.
9. Bahill, A.T.; Troost, B.T. Types of saccadic eye movements, *Neurology*, 1979, vol. 29, no.8, p. 1150-1152.
10. Baloh, R.W.; Honrubia, V. Reaction time and accuracy of the saccadic eye movements of normal subjects in a moving-target task, *Aviation, Space, and Environmental Medicine*, 1976, vol. 47, p. 1165.
11. Barnes, G.R.; Collins, C.J.S. The Influence of Briefly Presented Randomized Target Motion on the Extraretinal Component of Ocular Pursuit. *Journal of Neurophysiology*, 2008, p. 831-842.
12. Becker, W. Saccades, in eye movements. In *Carpenter RHS, editor: Vision and visual dysfunction*, Boca Raton, Fla, CRC, 1991, vol. 8.
13. Becker, W.; Jurgens, R. An analysis of the saccadic system by means of double-step stimuli, *Vision Research*, 1979, vol. 19, p. 967-983.
14. Becker, W.; Jurgens, R. Human oblique saccades: Quantitative analysis of the relation between horizontal and vertical components. *Vision Research*, 1990, vol. 30, no. 6, p. 893–920.
15. Bennett, S.J.; Barnes, G.R. Combined smooth and saccadic ocular pursuit during transient occlusion of a moving visual object. *Experimental Brain Research*, 2006, vol. 168, no.3, p. 313-321.
16. Benson, P.J.; Beedie, S.A.; Shephard, E.; Giegling, I.; Rujescu, D.; Clair, D. Simple viewing tests can detect eye movement abnormalities that distinguish schizophrenia cases from controls with exceptional accuracy. *Biological Psychiatry*, 2012, vol. 72, no.9, p. 716-724.

17. Bieg, H.J.; Reiterer, H.; Biilthoff, H.H. Eye and Pointer Coordination in Search and Selection Tasks. *Proceedings of the 2010 Symposium on Eye-Tracking Research & Applications*, 2010, p. 89-92.
18. Blohm, G.; Khan, A.Z.; Crawford, J.D. Spatial Transformations for Eye-Hand Coordination. *Journal of Neurophysiology*, 2004, vol. 92, no.10-19.
19. Boisseau, E.; Scherzer, P.; Cohen, H. Eye-Hand Coordination in Aging and in Parkinson's Disease. *Aging, Neuropsychology, and Cognition*, 2002, vol. 9, no.4, p. 266-275.
20. Boman, D.K.; Hotson, J.R. Stimulus conditions that enhance anticipatory slow eye movements, *Vision Research*, 1988, vol. 28, no.10, p. 1157-1165.
21. Boman, D.K.; Hotson, J.R. Smooth pursuit training and disruption. *Journal of Neuro-Ophthalmology*, 1987, vol. 7, no.4, p. 185-194.
22. Bongers, R.M.; Zaal, F.T.J.M. The horizontal curvature of point-to-point movements does not depend on simply the planning space. *Neuroscience letters*, 2010, vol. 469, no.2, p. 189-193.
23. Botzel, K.; Rottach, K.; Buttner, U. Saccadic dynamic overshoot in normal and patents. *Neuro-Ophthalmology*, 1993, vol. 13, no. 3, p. 125-133.
24. Bowman, D.K.; Hotson, J.R. Predictive smooth pursuit eye movements near abrupt changes in motion direction, *Vision Research*, 1992, vol. 32, no.4, p. 675-689.
25. Bronstein, A.M.; Kennard, C. Saccades Exhibit Abrupt Transition Between Reactive and Predictive, Predictive Saccade Sequences Have Long-Term Correlations, *Journal of Neurophysiology*, 2003, vol. 90, no.4, p. 2763-2769.
26. Brouwer, S.; Yuksel, D.; Blohm, G.; Missal, M.; Lefèvre, P. What triggers catch-up saccades during visual tracking? *Journal of Neurophysiology*, 2002, vol. 87, no.3, p. 1646-1650.
27. Bulatov, A.; Bertulis, A.; Bulatova, N.; Loginovich, Y. Centroid extraction and illusions of extent with different contextual flanks. *Acta Neurobiologiae Experimentalis*, 2009, vol. 69, p. 504-525.
28. Bullock, D.; Grossberg, S. Neural dynamics of planned arm movements: Emergent invariants and speed-accuracy properties during trajectory formation. *Psychological Review*, 1988, vol. 95, no.1, p. 49-90.
29. Bullock, D.; Grossberg, S.; Guenther, F.H. A self-organizing neural model of motor equivalent reaching and tool use by a multijoint arm. *Journal of Cognitive Neuroscience*, 1993, vol. 5, p. 408-435.
30. Carl, J.R.; Gellman, R.S. Human smooth pursuit: stimulus-dependent responses. *Journal of Neurophysiology* 1987, vol. 57, no.5, p. 1446-1463.
31. Carretta, T.R. Cross Validation of Experimental USAF Pilot Training Performance Models. *Military Psychology*, 1990, vol. 2, no.4.
32. Chan, T.; Codd, M.; Kenny, P.; Eustace, P. The effect of aging on catch-up saccades during horizontal smooth pursuit eye movement. *Journal of Neuro-Ophthalmology*, 1990, vol. 10, no.6, p. 327-330.
33. Churchland, M.M.; Chou, I.H.; Lisberger, S.G. Evidence for Object Permanence in the Smooth-Pursuit Eye Movements of Monkeys. *Journal of Neurophysiology*, 2003, vol. 90, no. 4, p. 2205-2218.

34. Collewyn, H.; Tamminga, E.P. Human fixation and pursuit in normal and open-loop conditions: effects of central and peripheral targets. *The Journal of Physiology*, 1986, vol. 379, p. 109-129.
35. Dallos, P.J.; Jones, R.W. Learning behavior of the eye fixation control system. *Automatic, Control, IEEE Transactions On*, 1963, vol. 8, no.3, p. 218-227.
36. de Brouwer, S.; Missal, M.; Barnes, G.; Lefevre, P. Quantitative analysis of catch-up saccades during sustained pursuit. *Journal of Neurophysiology*, 2002, vol. 87, no.4, p. 1772-1780.
37. de Brouwer, S.; Missal, M.; Lefevre, P. Role of retinal slip in the prediction of target motion during smooth and saccadic pursuit. *Journal of Neurophysiology*, 2001, vol. 86, no.2, p. 550-558.
38. de Brouwer, S.; Yuksel, D.; Blohm, G.; Missal, M.; Lefevre, P. What triggers catch-up saccades during visual tracking? *Journal of Neurophysiology*, 2002, vol. 87, no.3, p. 1646-1650.
39. Dean, H.L.; Martí, D.; Tsui, E.; Rinzel, J.; Pesaran, B. Reaction Time Correlations during Eye-Hand Coordination: Behavior and Modeling. *The Journal of Neuroscience*, 2011, vol. 31, no.7, p. 2399 –2412.
40. Deubel, H. Is Saccadic Adaptation Context-Specific? *Studies in Visual Information Processing*, 1995, vol. 6, p. 177–187.
41. Drewes, H. Eye Gaze Tracking for Human Computer Interaction. Dissertation an der LFE Medien-Informatik der Ludwig-Maximilians-Universität München. München, 2010.
42. Drewes, H.; Schmidt, A. Interacting with the Computer using Gaze Gestures. In *Proceedings of Human-Computer Interaction - INTERACT 2007*, 2007, p. 475 – 488.
43. Engel, K.C.; Anderson, J.H.; Soechting, J.F. Similarity in the Response of Smooth Pursuit and Manual Tracking to a Change in the Direction of Target Motion. *Journal of Neurophysiology*, 2000, vol. 84, no.3, p. 1149-1156.
44. Fischer, B.; Boch, R. Cerebral cortex. In *Carpenter RHS, editor: Vision and visual dysfunction*, 1991, vol. 8, (eye movements), Boca Raton, Fla, CRC.
45. Fitts, P.M. The information capacity of the human motor system in controlling the amplitude of movement. *Journal of Experimental Psychology*, 1954, vol. 47, p. 381-391.
46. Flacha, R.; Knoblich, G.; Prinza, W. The two-thirds power law in motion perception. *Visual cognition*, 2004, vol. 4, p. 461-481.
47. Flanagan, J.R.; Wing, A.M. The role of internal models in motion planning and control: evidence from grip force adjustments during movements of hand-held loads. *The Journal of Neuroscience*, 1997, vol. 17, p. 1519-1528.
48. Flash, T.; Sejnowski, T. Computational approaches to motor control. *Current Opinion in Neurobiology*, 2001, vol. 11, p. 655-662.
49. Friedman, L.; Jesberger, J.A.; Abel, A.; Meltzer, H.Y. Catch-up saccade amplitude is related to square jerk rate. *Investigative ophthalmology & Vision Science*, 1992, vol. 33, no. 1, p. 228-233.
50. Fromberger, P.; Jordan, K.; Steinkrauss, H.; Herder, J.; Witzel, J.; Stolpmann, G.; Kröner-Herwig, B.; Müller, J.L. Diagnostic accuracy of eye movements in assessing pedophilia. *The Journal of Sexual Medicine*, 2012, vol. 9, no.7, p. 1868-82.

51. Fu, M.J.; Cavusoglu, M.C. Human Arm-and-Hand Dynamics Model with Variability Analyses for a Stylus-based Haptic Interface. In *IEEE Transactions on Systems, Man, Cybernetics, Part B: Cybernetics*, 2012, vol. 42, no.6, p.1633-1644.
52. Fuchs, A.F. Periodic eye tracking in the monkey. *The Journal of Physiology*, 1967, vol. 193, no.1, p. 161-171.
53. Gauthier, G.M.; Vercher, J.L.; Mussa-Ivaldi, F.; Marchetti, E. Oculo -manual tracking of visual targets: control learning, coordination control and coordination model. *Experimental Brain Research*, 1988, vol. 73, p. 127 -137.
54. Gitchel, G.T.; Wetzel, P.A.; Baron, M.S. Pervasive ocular tremor in patients with Parkinson disease. *Archives of Neurology*, 2012, vol. 69, no.8, p. 1011-1017.
55. Grea, H.; Desmurget, M.; Prablanc, C. Postural invariance in three-dimensional reaching and grasping movements. *Experimental Brain Research*, 2000, vol. 134, p. 155-62.
56. Griffin, G.R.; Koonce, J.M. Review of psychomotor skills in pilot selection research of the U.S. military services. *International Journal of Aviation Psychology*, 1996, vol. 6, no. 2, p. 125-47.
57. Grossberg, S.; Srihasam, K.; Bullock, D. Neural dynamics of saccadic and smooth pursuit eye movement coordination during visual tracking of unpredictably moving targets. *Journal Neural Networks archive*, 2012, vol. 27, p. 1-20.
58. Guitton, D. Control of saccadic eye and gaze movements by the superior colliculus and basal ganglia. In *Carpenter RHS, editor: Vision and visual dysfunction*, Eye movements, Boca Raton, Fla, CRC, 1991, vol. 8.
59. Harris, C.M.; Wolpert, D.M. Signal-dependent noise determines motor planning. *Letters to nature*, 1998, vol. 394, p. 780-784.
60. Haruno, M.; Wolpert, D.; Kawato, M. Multiple paired forward-inverse models for human motor learning and control. In *Advances in Neural Information Processing Systems*. Edited by Kearns MS, Solla SA, Cohn DA. Cambridge: MIT Press, 1999, p. 31-37.
61. Harvey, D.R.; Bahill, A.T. Development and sensitivity analysis of adaptive predictor for human eye movement model. *Transactions of the Society for Computer Simulation*, 1986, vol. 2, no.4, p. 275-292.
62. Havermann, K.; Volcic, R.; Lappe, M. Saccadic Adaptation to Moving Targets. *PLoS ONE*, 2012, vol. 7, no. 6, article e39708, p. 1-9.
63. Heath, M.; Rival, C.; Binsted, G. Can the motor system resolve a premovement bias in grip aperture? Online analysis of grasping the Müller-Lyer illusion. *Experimental Brain Research*, 2004, vol. 158, no.3, p. 378-384.
64. Hemeren, P.E.; Thill, S. Deriving Motor Primitives through Action Segmentation. *Frontiers in Psychology*, 2011, p. 243.
65. Hogan, N.; Sternad, D. Dynamic primitives of motor behavior. *Biological Cybernetics*, 2012, vol. 106, no.11-12, p. 727-39.
66. Horstmann, A.; Hoffmann, K.P. Target selection in eye–hand coordination: Do we reach to where we look or do we look to where we reach? *Experimental Brain Research*, 2005, vol. 167, no.2, p. 187-95.
67. Howard, I.P.; Marton, C. Visual pursuit over textured backgrounds in different depth planes. *Experimental Brain Research*, 1992, vol. 90, no.3, p. 625-629.

68. Isokoski, P.; Joos, M.; Špakov, O.; Martin, B. Gaze Controlled Games. In Stephanidis, C., Majaranta, P., & Bates, R. (eds.) *Universal Access in the Information Society: Communication by Gaze Interaction*, 2009, vol. 8, no.4, p. 323-337.
69. Jacob, R.J.K. The use of eye movements in Human computer interaction: What You Look At is What You Get. *ACM Transactions on Information Systems*, 1991. vol. 9, no.3, p. 152-169.
70. Jarrett, C.; Barnes, G. The use of non-motion-based cues to pre-programme the timing of predictive velocity reversal in human smooth pursuit. *Experimental Brain Research*, 2005, vol. 164, no. 4, p. 423-430.
71. Johansson, R.S.; Westling, G.; Backstrom, A.; Flanagan, J.R. Eye-Hand Coordination in Object Manipulation. *The Journal of Neuroscience*, 2001, vol. 21, no.17, p. 6917-6932.
72. Jonikaitis, D.; Schubert, T.; Deubel, H. Preparing coordinated eye and hand movements: Dual-task costs are not attentional. *Journal of Vision*, 2010, vol. 10, p. 1-7.
73. Kanayama, R.; Nakamura, T.; Sano, R.; Ohki, M.; Okuyama, T.; Kimura, Y.; Koike, Y. Effect of aging on smooth pursuit eye movement. *Acta Oto-Laryngologica*, 1994, vol. 114, no. 511, p. 131-134.
74. Kanjee, R.; Yücel, Y.H.; Steinbach, M.J.; González, E.G.; Gupta, N. Delayed saccadic eye movements in glaucoma. *Eye and Brain*, 2012, vol. 4, p. 63-68.
75. Kao, G.W.; Morrow, M.J. The relationship of anticipatory smooth eye movement to smooth pursuit initiation. *Vision Research*, 1994, vol. 34, no.22, p. 3027-3036.
76. Kathmann, N.; Hochrein, A.; Uwer, R.; Bondy, B. Deficits in gain of smooth pursuit eye movements in schizophrenia and affective disorder patients and Their Unaffected Relatives. *American Journal of Psychiatry*, 2003, p. 696-702.
77. Kaufman, S.R.; Abel, L.A. The effects of distraction on smooth pursuit in normal subjects. *Acta Oto-Laryngologica*, 1986, vol. 102, no.1-2, p. 57-64.
78. Kawato, M. Internal models for motor control and trajectory planning. *Current Opinion in Neurobiology*, 1999, vol. 9, p. 718-727.
79. Keller, E. The brainstem. In *Carpenter RHS, editor: Vision and visual dysfunction*, Boca Raton, Fla, CRC, 1991, vol. 8.
80. Kemner, C.; Verbaten, M.N.; Cuperus, J.M.; Camfferman, G.; Engeland, H. Abnormal Saccadic Eye Movements in Autistic Children. *Journal of Autism and Developmental Disorders*, 1998, vol. 28, no.1, p. 61-67.
81. Khan, A.Z.; Lefèvre, P.; Heinen, S.J.; Blohm, G. The default allocation of attention is broadly ahead of smooth pursuit. *Journal of Vision*, 2010, vol. 10, p. 7.
82. Khan, M.A.; Lawrence, G.P.; Franks, I.M.; Buckolz, E. The utilization of visual feedback from peripheral and central vision in the control of direction. *Experimental Brain Research*, 2004, vol. 158, p. 241-251.
83. Knox, P.C.; Bruno, N. When does action resist visual illusion? The effect of Müller-Layer stimuli on reflexive and voluntary saccades. *Experimental Brain Research*, 2007, vol. 181, no.2, p. 277-287.
84. Komogortsev, O.V.; Ryu, Y.S.; Koh, D.H. Quick models for saccade amplitude prediction. *Journal of eye movement research*, 2008, no.1, p. 1-13.
85. Kowler, E.; Anderson, E.; Doshier, B.; Blaser, E. The role of attention in the programming of saccades. *Vision Research*, 1995, vol. 35, no.13, p. 1897-1916.

86. Krauzlis, R.J. Neuronal activity in the rostral superior colliculus related to the initiation of pursuit and saccadic eye movement. *The Journal of Neuroscience*, 2003, vol. 23, no.10, p. 4333-4344.
87. Krauzlis, R.J.; Miles, F.A. Initiation of saccades during fixation or pursuit: evidence in humans for a single mechanism. *Journal of Neurophysiology*, 1996, vol. 76, no.6, p. 4175-4179.
88. Krauzlis, R.J.; Miles, F.A. Transitions between pursuit eye movements and fixation in the monkey: dependence on context. *Journal of Neurophysiology*, 1996, vol. 76, no.3, p. 1622-1638.
89. Kuchenbecker, K.J.; Park, J.G.; Niemeyer, G. Characterizing the human wrist for improved haptic interaction. *Proc. of the 2003 International Mechanical Engineering Congress and Exposition*, November 2003, p. 1–8.
90. Kumar, M.; Winograd, T. Gaze-enhanced Scrolling Techniques, UIST: Symposium on User Interface Software and Technology. New Port, RI. 2007.
91. Lappe, M. What is adapted in saccadic adaptation? *Journal of Neurophysiology*, 2009, vol. 587, no. 1, p. 5.
92. Latash, M.L. Motor synergies and the equilibrium-point hypothesis. *Motor Control*, 2010, vol. 14, no.3, p. 294–322.
93. Laurutis, V.; Daunys, G.; Zemblys, R. Quantitative Analysis of Catch-up Saccades Executed during Two-dimensional Smooth Pursuit. *Electronics and Electrical Engineering*, 2010, no.2 (98), p. 83-86.
94. Laurutis, V.; Zemblys, R. Bayesian Decision Theory Application for Double-step Saccades. *Electronics and Electrical Engineering*. 2009, 4 (92), p. 99-102.
95. Laurutis, V.; Zemblys, R. Dynamics of Catch-up Saccades during Tracking of Two-dimensional Time-continuous Target Trajectory. *XII Mediterranean Conference on Medical and Biological Engineering and Computing 2010. IFMBE Proceedings*, 2010, vol. 29, p. 1-4.
96. Laurutis, V.; Zemblys, R. Informational characteristics of the double-step saccadic eye movements. *Information technology and control*, 2010, vol. 39, no.1, p. 55–60.
97. Laurutis, V.; Zemblys, R. Quantitative Analysis of Two-Dimensional Catch-Up Saccades Executed to the Target Jumps in the Time-Continuous Trajectory. *MEDICON*, 2010, p. 1-4.
98. Laurutis, V.; Zemblys, R.; Buivis, L. Fixational Eye Movements: Influence on the Accuracy in the Target Pointing Tasks. *Electronics and Electrical Engineering*, 2009, no.5 (93), p. 91-94.
99. Lazzari, S.; Vercher, J.L.; Buizza, A. Manuo-ocular coordination in target tracking. I. A model simulating human performance. *Biological Cybernetics*, 1997, vol. 77, p. 257–266.
100. Lee, W.J.; Galiana, H.L. An internally switched model of ocular tracking with prediction. *IEEE Transactions on Neural Systems and Rehabilitation Engineering*, 2005, vol. 13, no.2, p. 186-193.
101. Leigh, A. Mrotek, John F. Soechting. Predicting curvilinear target motion through an occlusion. *Experimental Brain Research*, 2007, vol. 178, p. 99-114.
102. Leigh, R.J.; Zee, D.S. *The neurology of eye movements*. ed. 2. Philadelphia, 1991.

103. Lisberger, S.G. Postsaccadic enhancement of initiation of smooth pursuit eye movements in monkeys. *Journal of Neurophysiology*, 1998, vol. 79, no.4, p. 1918-1930.
104. Lisberger, S.G.; Morris, E.J.; Tychsen, L. Visual motion processing and sensory-motor integration for smooth pursuit eye movements. *Annual Review of Neuroscience*, 1987, vol. 10, p. 97-129.
105. Lisberger, S.G.; Westbrook, L.E. Properties of visual inputs that initiate horizontal smooth pursuit eye movements in monkeys. *The Journal of Neuroscience*, 1985, vol. 5, no.6, p. 1662-1673.
106. Lovejoy, L.P.; Fowler, G.A.; Krauzlis, R.J. Spatial allocation of attention during smooth pursuit eye movements. *Vision Research*, 2009, vol. 49, p. 1275–1285.
107. MacKenzie, I.S. Fitts' law as a research and design tool in human-computer interaction. *Human-Computer Interaction*, 1992, vol. 7, p. 91-139.
108. MacKenzie, I.S.; Buxton, W. Extending Fitts' law to two-dimensional tasks. *Proceedings of ACM CHI'92 Conference on Human Factors in Computing Systems*, 1992, p. 219-226.
109. Madelain, L.; Krauzlis, R.J. Effects of Learning on Smooth Pursuit During Transient Disappearance of a Visual Target. *Journal of Neurophysiology*, 2003, vol. 90, no. 2, p. 972-982.
110. Martinez-Conde, S. Fixational Eye Movements in normal and pathological vision, *Progress in Brain Research*, 2006, vol. 154, p. 151-176.
111. Martinez-Conde, S.; Macknik, S.L.; Hubel, D.H. The role of fixational eye movements in visual perception. *Nature Reviews Neuroscience*, 2004, vol. 5, p. 229-240.
112. Mays, L.E.; Sparks, D.L. Dissociation of visual and saccade-related responses in superior colliculus neurons. *Journal of Neurophysiology*, 1980, vol. 43, p. 207-232.
113. McCarley, J.S.; Grant, C. State-trace analysis of the effects of a visual illusion on saccade amplitudes and perceptual judgments. *Psychonomic Bulletin & Review*, 2008, vol. 15, no.5, p. 1008-1014.
114. Mennie, N.; Hayhoe, M.; Sullivan, B. Look-ahead fixations: anticipatory eye movements in natural tasks. *Experimental Brain Research*, 2007, vol. 179, no.3, p. 427-42.
115. Meyer, C.H.; Lasker, A.G.; Robinson, D.A. The upper limit of human smooth pursuit velocity. *Vision Research*, 1985, vol. 25, p. 561-563.
116. Miall, R.C.; Reckess, G.Z. The Cerebellum and the Timing of Coordinated Eye and Hand Tracking. *Brain and Cognition*, 2002, vol. 48, p. 212–226.
117. Miall, R.C.; Reckess, G.Z.; Imamizu, H. The cerebellum coordinates eye and hand tracking movements. *Nature Neuroscience*, 2001, vol. 4, p. 638-644.
118. Miles, F.A. The cerebellum. In *Carpenter RHS, editor: Vision and visual dysfunction*. Boca Raton, Fla, CRC, 1991, vol. 8.
119. Missal, M.; Coimbra, A.; Lefevre, P.; Olivier, E. Further evidence that a shared efferent collicular pathway drives separate circuits for smooth eye movements and saccades. *Experimental Brain Research*, 2002, vol. 147, no.3, p. 344-352.
120. Missal, M.; Keller, E.L. Common inhibitory mechanism for saccades and smoothpursuit eye movements. *Journal of Neurophysiology*, 2002, vol. 88, no.4, p. 1880-1892.
121. Mittmann, W.; Koch, U.; Hausser, M. Feed-forward inhibition shapes the spike output of cerebellar Purkinje cells. *Journal of Physiology*, 2005, vol. 563, no. 2, p. 369-378.

122. Moller, F.; Laursen, M.; Tygesen, J.; Sjolie, A. Binocular quantification and characterization of microsaccades. *Graefe's Archive for Clinical and Experimental Ophthalmology*, 2002, vol. 240, no. 9, p. 765-770.
123. Morrow, M.J.; Sharpe, J.A. Smooth pursuit initiation in young and elderly subjects. *Vision Research*, 1993, vol. 33, no.2, p. 203-210.
124. Moschner, C.; Baloh, R.W. Age-Related Changes in Visual Tracking. *Journal of Gerontology*, 1993, vol. 49, no. 5, p. 235-238.
125. Mottet, D.; Bootsma, R.J. The dynamics of rhythmical aiming in 2D task space: relation between geometry and kinematics under examination. *Human Movement Science*, 2001, vol. 20, p. 213-241.
126. Munoz, D.P.; Broughton, J.R.; Goldring, J.E.; Armstrong, I.T. Age-related performance of human subjects on saccadic eye movement tasks. *Journal of Neuro-Ophthalmology*, 1998, vol. 121, no. 4, p. 391-400.
127. Niemann, T.; Hoffmann K.P. The influence of stationary and moving textured backgrounds on smooth-pursuit initiation and steady state pursuit in humans. *Experimental Brain Research*, 1997, vol. 115, no. 3, p. 531-540.
128. Orban de Xivry, J. J.; Missal, M.; Lefevre, P. A dynamic representation of target motion drives predictive smooth pursuit during target blanking. *Journal of Vision*, 2008, vol. 8, no.15, p.1-13.
129. Otero-Millan, J.; Troncoso, X.G.; Macknik, S.L.; Serrano-Pedraza, I.; Martinez-Conde, S. Saccades and microsaccades during visual fixation, exploration, and search: Foundations for a common saccadic generator. *Journal of Vision*, 2008, vol. 8, no. 14, article 21, p. 1-18.
130. Paige, G.D. Senescence of human visual-vestibular interactions: smooth pursuit, optokinetic, and vestibular control of eye movements with aging. *Experimental Brain Research*, 1994, vol. 98, no. 2, p. 355-372.
131. Pernaete, N.; Edwards, S.; Gottipati, R.; Tipple, J.; Kolipakam, V. Eye-hand coordination Assessment. *Therapy using a robotic haptic device. Proceedings of the 9th International conference on Rehabilitation robotics*, 2005, p. 25-28.
132. Pola, J.; Wyatt, H.J. Smooth pursuit: response characteristics, stimuli, and mechanisms. In *Carpenter RHS, editor: Vision and visual dysfunction*, Boca Raton, Fla, CRC, 1991, vol. 8.
133. Ramanauskas, N. Calibration of Video-Oculographical Eye-Tracking System. *Electronics and Electrical Engineering*, 2006, no. 8 (72), p. 65-68.
134. Rashbass, C. The relationship between saccadic and smooth tracking eye movements. *The Journal of Physiology*, 1961, vol. 159, p. 326-338.
135. Raudonis, V.; Simutis, R.; Pukevičius, A.; Narvydas, G.; Friman, O. Discrete eye tracking system using cross correlations in the RGB color space. *Electrical and Control Technologies*, May 3-4, 2007, Kaunas, Lithuania, Kaunas University of Technology, IFAC Committee of National Lithuanian Organisation, Lithuanian Electricity Association. Kaunas: Technologija. 2007, p. 74-77.
136. Rayner, K. Eye movements in reading and information processing: 20 years of research. *Psychological Bulletin*. 1998, vol. 124, no.3, p. 372-422.
137. Reina, G.A.; Schwartz, A.B. Eye-hand coupling during closed-loop drawing: Evidence of shared motor planning? *Human Movement Science*, 2003, vol. 22, p. 137-152.

138. Ren, L.; Khan, A.Z.; Blohm, G.; Henriques, D.Y.P.; Sergio, L.E.; Crawford, J.D. Proprioceptive Guidance of Saccades in Eye-Hand Coordination. *Journal of Neurophysiology*, 2006, p. 1464–1477.
139. Roberts, A.J.; Wallis, G.; Breakspear, M. Fixational eye movements during viewing of dynamic natural scenes. *Frontiers in Psychology*, 2013, vol. 4, article 797, p. 1-12.
140. Robinson, D.A. Models of oculomotor neural organization. In *Bach-y-rita P, Collins CC, editors: The control of eye movements*, New York, 1971, Academic.
141. Robinson, D.A. The mechanics of human smooth pursuit eye movement. *The Journal of Physiology*, 1965, vol. 180, p. 569-591.
142. Robinson, D.A.; Gordon, J.L.; Gordon, S.E. A model of the smooth pursuit eye movement system. *Biological Cybernetics*, 1986, vol. 55, p. 43-57.
143. Robinson, D.A.; Keller, E.L. The behavior of eye movement motoneurons in the alert monkey. *Bibl. Ophthalmology*, 1972, vol. 82, p. 7-16.
144. Rottach, K.G.; Zivotofsky, A.Z.; Das, V.E.; Averbuch-Heller, L.; Discenna, A.O.; Poonyathalang, A.; Leigh R.J. Comparison of horizontal, vertical and diagonal smooth pursuit eye movements in normal human subjects. *Vision Research*, 1995, vol. 36, no. 14, p. 2189-2195.
145. Salman, M.S.; Sharpe, J.A.; Eizenman, M.; Lillakas, L.; Westall, C.; To, T.; Dennis, M.; Steinbach M.J.; Saccades in children. *Vision Research*, 2006, vol. 46, no. 8-9, p. 1432–1439.
146. Sansbury, R.V.; Skavenski, A.A.; Haddad, G.M.; Steinman, R.M. Normal fixation of eccentric targets. *Journal of the Optical Society of America*, 1973, vol. 63, p. 612-614.
147. Scarchilli, K.; Vercher, J.L.; Gauthier, G.M.; Cole, J. Does the oculo-manual coordination control system use an internal model of the arm dynamics? *Neuroscience Letters*, 1999, vol. 265, p. 139-142.
148. Schaal, S.; Sternad, D. Origins and violations of the 2/3 power law in rhythmic 3D movements. *Experimental Brain Research*, 2001, vol. 136, p. 60-72.
149. Schweighofer, N.; Arbib, M.A.; Kawato, M. Role of the cerebellum in reaching movements in humans. I. Distributed inverse dynamics control. *European journal of neuroscience*, 1998, vol 10, p. 86-94.
150. Sekimoto, M.; Arimoto, S. A natural redundancy-resolution for 3-D multi-joint reaching under the gravity effect. *Journal of Robotic Systems*, 2005, vol. 22, no.11, p. 607-623.
151. Selhorst, J.B.; Stark, L.; Ochs, A.L.; Hoyt, W.F. Disorders in cerebellar oculomotor control. I. Saccadic overshoot dysmetria: an oculographic control system and clinico-anatomic analysis. *Brain*, 1976, vol. 99, p. 497.
152. Semmlow, J.L.; Gauthier, G.M.; Vercher, J.L. Mechanisms of short-term saccadic adaptation. *The Journal of Experimental Psychology: Human Perception and Performance*, 1989 vol. 15, p. 249-258.
153. Shakhnovich, A.R. *The brain and regulation of eye movement*, New York, 1977, Plenum.
154. Sharmin, S.; Špakov, O.; Rähä, K.J. Reading On-Screen Text with Gaze-Based Auto Scrolling. In *Proceedings of the Eye Tracking South Africa, ETSA'13*, Cape Town, South Africa, 2013, p. 24-31.
155. Skovsgaard, H.; Raiha, K.J.; Tall, M. Computer control by gaze. In *Gaze Interaction and Applications of Eye Tracking: Advances in Assistive Technologies*, P. Majaranta et al. (eds.), IGI Global, 2012, p. 78-102.

156. Skovsgaard, H.; San Agustin, J.; Alstrup Johansen, S.; Hansen, J.P.; Tall, M. Evaluation of a remote webcam-based eye tracker. In *Proceedings of the 1st Conference on Novel Gaze-Controlled Applications (NGCA '11)*. ACM, New York, NY, USA, 2011.
157. Smith, B.A.; Ho, J.; Ark, W.; Zhai, S. Hand Eye Coordination Patterns in Target Selection. In *Proceedings of the 2000 symposium on eye tracking research & applications*. ACM, 2000, p. 117-122,
158. Špakov, O. Previewable scrolling by gaze. In K. Holmqvist, F. Mulvey & R. Johansson (Eds.), *Book of Abstracts of the 17th European Conference on Eye Movements, ECEM'2013*, 6(3), *Journal of Eye Movement Research*, Lund, Sweden, 2013, p. 469.
159. Squeri, V.; Masia, L.; Vergaro, E.; Casadio, M.; Sanguineti, V.; Morasso, P. Visuo-manual tracking in a robot-generated dynamic environment. *Rehabilitation Robotics, 2009. ICORR 2009. IEEE International Conference*, 23-26 June, 2009, p. 155 – 160.
160. Stark, L. *Neurological control systems: studies in bio-engineering*, 1968, New York, Plenum.
161. Stark, L.; Vossius, G.; Young, L.R. Predictive control of eye tracking movements. *Human Factors in Electronics, IRE Transactions on*, 1962, vol. 3, p. 52-57.
162. Steinman, R.M.; Collewijn, H. Binocular retinal- image motion during active head rotation. *Vision Research*, 1980, vol. 20, p. 415-429.
163. Sternad, D.; Schaal, D. Segmentation of endpoint trajectories does not imply segmented control. *Experimental Brain Research*, 1995, vol. 124, p. 118-136.
164. Tanaka, M.; Yoshida, T.; Fukushima, K. Latency of saccades during smooth-pursuit eye movement in man. Directional asymmetries. *Experimental Brain Research*, 1998, vol. 121, no.1, p. 92-98.
165. Timberlake, G.T.; Omoscharka, E.; Grose, S.A.; Bothwell, R. Preferred Retinal Locus—Hand Coordination in a MazeTracing Task. *Investigative Ophthalmology & Visual Science*, 2012, vol. 53, no.4, p. 1810-20.
166. Tramper, J.J.; Flanders, M. Can subjects use voluntary smooth pursuit to guide hand movement? *Poster in ECEM2013 conference*, 2013.
167. Tramper, J.J.; Gielen, C.C.A.M. Visuomotor Coordination Is Different for Different Directions in Three-Dimensional Space. *The Journal of Neuroscience*, 2011, vol. 31, no. 21, p. 7857–7866.
168. Tramper, J.J.; Lamont, A.; Flanders, M.; Gielen, S. Gaze is driven by an internal goal trajectory in a visuomotor task. *European Journal of Neuroscience*, 2013, vol. 37, p. 1112–1119.
169. Tseng, P.H.; Cameron, I.G.M.; Pari, G.; Reynolds, J.N.; Munoz, D.P.; Itti, L. High-throughput classification of clinical populations from natural viewing eye movements. *Journal of Neurology*, 2012.
170. Tychsen, L.; Lisberger, S.G. Visual motion processing for the initiation of smooth pursuit eye movements in humans. *Journal of Neurophysiology*, 1986, vol. 56, p. 953-968.
171. Uno, Y.; Kawato, M.; Suzuki, R. Formation and Control of Optimal Trajectory in Human Multijoint Arm Movement: Minimum torque change model. *Biological Cybernetics*, 1989, vol. 61, p. 89-101.
172. Van Donkelaar, P.; Drew, A.S. The allocation of attention during smooth pursuit eye movements. *Progress in Brain Research*, 2002, vol. 140, p. 267 – 277.

173. Van Gisbergen, J.A.M.; Robinson, D.A.; Gielen, S. A quantitative analysis of the generation of saccadic eye movements by burst neurons. *Journal of Neurophysiology*, 1981, vol. 45, no.3, p. 417-442.
174. Vercher, J.; Gauthier, G.M.; Guedon, O.; Blouin, J.; Cole, J.; Lamarre, Y. Self -moved target eye tracking in control and deafferented subjects: roles of arm motor command and proprioception in arm-eye coordination. *Journal of Neurophysiology*, 1996, vol. 76, no.2, p. 1133-1144.
175. Vercher, J.L.; Gauthier, G.M. Cerebellar involvement in the coordination control of the oculomanual tracking system: Effects of cerebellar dentate nucleus lesion. *Experimental Brain Research*, 1988, no.73 (1), p. 155–166.
176. Vercher, J.L.; Lazzari, S.; Gauthier, G. Manuo-ocular coordination in target tracking. II. Comparing the model with human behavior. *Biological Cybernetics*, 1997, vol. 77, p. 267–275.
177. Warabi, T.; Kase, M.; Kato, T. Effect of aging on the accuracy of visually-guided saccadic eye movement. *Annals of Neurology*, 1984, vol. 16, p. 449-454.
178. Wells, S.G.; Barnes G.R. Fast, anticipatory smooth-pursuit eye movements appear to depend on a short-term store. *Experimental Brain Research*, 1998, vol. 120, no. 1, p. 129-133.
179. Westheimer, G.; McKee, S.P. Stereoscopic acuity for moving retinal images. *Journal of the Optical Society of America*, 1978, vol. 68, p. 450-455.
180. Wolpert, D.M.; Kawato, M. Multiple paired forward and inverse models for motor control. *Neural Networks*, 1998, vol. 11, p. 1317–1329.
181. Yarbus, A.L. *Eye movements and vision*, New York, 1967, Plenum.
182. Young, L.R.; Stark, L. Variable feedback experiments testing a sampled-data model for eye tracking movements. *Human Factors in Electronics, IEEE Transactions on*, 1963, vol. 4, p. 38-51.
183. Zee, D.S.; Optican, L.M.; Cook, J.; Robinson, D.A.; Engel, W.K. 1976. Slow saccades in spinocerebellar degeneration. *Archives of neurology*, 1976, vol. 33, p. 243-251.
184. Zee, D.S.; Robinson, D.A. An hypothetical explanation of saccadic oscillations. *Annals of Neurology*, 1979, vol. 5, p. 405-414.
185. Zemblys, R.; Laurutis, V. Prediction of target motion drives oculomotor response during target occlusions. *Electronics and Electrical Engineering*, 2012, vol. 18, no.9, p. 55-58.
186. Zhai, S.; Morimoto, C.; Ihde, S. Manual and gaze input cascaded (MAGIC) pointing. *Proceedings of the SIGCHI conference on Human factors in computing systems: the CHI is the limit*, 1999 (May), p. 246-53.
187. Zimmermann, E.; Lappe, M. Mislocalization of Flashed and Stationary Visual Stimuli after Adaptation of Reactive and Scanning Saccades. *Journal of Neuroscience*, 2009, vol. 29, no.35, p. 11055-11064.

## LIST OF PUBLICATIONS ON THE THEME OF DISSERTATION

### Publications referred in the Journals from the master list of Thomson Reuters

#### Web of Knowledge (with impact factor)

1. Laurutis, V.; Niauronis, S.; Zemblys, R. Alternative Computer Cursor Shifts for Large Amplitude Eyesight Jumps. *Elektronika ir elektrotechnika = Electronics and Electrical Engineering*, 2010, no. 9(105), p. 61-64.
2. Niauronis, S.; Laurutis, V.; Zemblys, R. Eye-Hand Coordination during Self-Moved Target Guiding Along Labyrinth Path. *Electronics and Electrical Engineering*, 2011, no. 10(116), p. 71-74.
3. Laurutis, V.; Indrijauskienė, I.; Zemblys, R.; Niauronis, S. Effects of Muller-Lyer Illusion on the Accuracy of Primary Saccades and Smooth Pursuit Eye Movements. *Information Technology and Control*, 2012, no. 41(1), p. 40-45.

### Abstracts in the Journals from the master list of Thomson Reuters Web of Knowledge

1. Laurutis, V.; Niauronis, S.; Zemblys, R. Investigating the effectiveness of manual and gaze cascaded input pointing while performing different tasks. *Journal of Eye Movement Research: Abstracts of the 16th European Conference on Eye Movements – Marseille*, 2011, no. 4(3), p. 39.
2. Zemblys, R.; Laurutis, V.; Niauronis, S. Catch-up saccades: Influence on the quality of smooth pursuit. *Journal of Eye Movement Research: Abstracts of the 16th European Conference on Eye Movements – Marseille*, 2011, no. 4(3), p. 304.
3. Niauronis, S.; Laurutis, V.; Zemblys, R. Investigation of eye-hand coordination during oculo-manual pursuit and self-moved target guiding along labyrinth path. *Journal of Eye Movement Research: Abstracts of the 16th European Conference on Eye Movements – Marseille*, 2011, no. 4(3), p. 305.

### Publications in the Journals from other international databases

1. Niauronis, S.; Zemblys, R.; Laurutis, V. Okulomotorinių tyrimų įrangos vėlinimo eliminavimas. *Mokslas – Lietuvos ateitis*, 2012, no. 4(1), p. 1-4.

### Publications in Reviewed Proceedings of International Scientific Conferences

1. Laurutis, V.; Zemblys, R.; Niauronis, S. Relationship between pursuit gain and parameters of catch-up saccades. *Biomedical Engineering - 2010: Proceedings of International Conference*, 2010, no. 1, p. 74-77.
2. Laurutis, V.; Niauronis, S.; Zemblys, R. Coordination of hand and gaze movements in humans during oculo-manual tracking. *Biomedical Engineering - 2010: Proceedings of International Conference*, 2010, no. 1, p. 78-81.
3. Laurutis, V.; Indrijauskienė, I.; Zemblys, R.; Niauronis, S. Dinaminis regos iliuzijos vertinimas panaudojant sekamuosius akies judesius. *Virtualūs instrumentai biomedicinoje*, 2010, no. 1, p. 7-12.
4. Zemblys, R.; Laurutis, V.; Niauronis, S. Oculomotor response to occlusions in target trajectory. *Biomedical Engineering – 2011 Proceedings of International Conference*, 2011, no. 1, p. 238 - 241.

5. Niauronis, S.; Laurutis, V.; Zemblys, R. Eye-hand coordination during self-moved target guiding along different configuration path. *Biomedical Engineering – 2011 Proceedings of International Conference*, 2011, no. 1, p. 242 - 245.
6. Niauronis, S.; Laurutis, V.; Zemblys, R. Neurological disorders that can be diagnosed using eye movement analysis. *Biomedical Engineering – 2012 Proceedings of International Conference*, 2012, no. 1, p. 200 - 203.
7. Zemblys, R.; Laurutis, V.; Niauronis, S. Intersaccadic intervals of catch-up saccades performed during occlusion of target trajectory. *Biomedical Engineering – 2012 Proceedings of International Conference*, 2012, no. 1, p. 204 - 207.
8. Niauronis, S.; Zemblys, R.; Laurutis, V. Modeling of the manuo-ocular coordination during object guiding through a path. *Proceedings of the 2012 IEEE 12th International Conference on Bioinformatics & Bioengineering (BIBE)*, Larnaca, Cyprus, 2012, no. 1, p. 657-661.
9. Varkalys, A.; Niauronis, S.; Laurutis, V. Akies ir rankos judesių tarpusavio koordinacija ranka vedant objektą taku. *Virtual Instruments in Biomedicine 2013 Proceedings of International Scientific – Practical Conference*, 2013, no. 1, p. 127 - 130.
10. Niauronis, S.; Laurutis, V. Neural pathways for eye movements during self moved object guiding. *Biomedical Engineering – 2013 Proceedings of International Conference*, 2013, no. 1, p. 112 - 116.

#### **Abstracts in Reviewed Proceedings of International Scientific Conferences**

1. Zemblys, R.; Niauronis, S.; Laurutis, V. Shannon's channel capacity versus throughput based on Fitt's index of difficulty: application to oculomotor system. *17th European Conference on Eye Movements*, 11-16 August 2013, Lund, Sweden: Book of abstracts, 2013, no. 1, p. 483.
2. Niauronis, S.; Zemblys, R.; Laurutis, V. Modeling of oculo-manual guiding eye movements. *17th European Conference on Eye Movements*, 11-16 August 2013, Lund, Sweden: Book of abstracts, 2013, no. 1, p. 35.
3. Zemblys, R.; Laurutis, V.; Niauronis, S. Parameters of catch-up saccades while tracking time-continuous transiently disappearing target. *17th European Conference on Eye Movements*, 11-16 August 2013, Lund, Sweden: Book of abstracts, 2013, no. 1, p. 189.

#### **Publications in Reviewed Proceedings of Lithuanian Scientific Conferences**

1. Niauronis, S.; Laurutis, V.; Zemblys, R. Alternatyvus žymeklio valdymas panaudojantis šuolinius akių judesius. *Technologijos mokslo darbai Vakarų Lietuvoje*, 2010, no. 7, p. 214-219.
2. Zemblys, R.; Niauronis, S.; Laurutis, V. Funkcinio kontrastinio jautrumo tyrimas naudojant žvilgsnio krypties nustatymo įrangą. *IV nacionalinė doktorantų konferencija "Mokslas - sveikatai"*, 2010, no. 1, p. 112-113.

## APPENDICES

## APPENDIX A: Evaluation of ageing related changes in catch-up saccade properties using non-traditional mathematical definition of pursuit gain

Previous studies had demonstrated a significant effect of ageing on catch-up saccades during horizontal smooth pursuit eye movement. The number of initiation saccades was found not to change significantly, but frequency of catch-up saccades increased significantly with age [32]. Catch-up saccades correct the position error that accumulates during smooth pursuit tracking when the gain of the pursuit is less than 1.0 [93, 95]. Pursuit gain is one of the most important parameter, which can be used to evaluate the conditions of the tracking performance. Purpose of this experimental trial was to test new mathematical expression of the relationship between pursuit gain and parameters of catch-up saccades, developed in chapter 2.4 and to experimentally investigate values of pursuit gain for different groups of subjects.

Subjects were asked to visually track non-predictable and predictable two-dimensional target trajectories (the same described in chapter 3.1) on the computer screen. Twelve subjects were divided in two groups: younger (age average 23 years) and elder (age average 55 years). Two-dimensional non-predictable identical target trajectories were performed in low (4.9 deg/s), medium (9.8 deg/s) and high (19.6 deg/s) integral velocities. Two-dimensional predictable target trajectories (square-shape and circular) with angular target movement velocities in the range of 10 - 50 deg/s moving in clock-wise direction were performed. Using equation (2.11), average pursuit gain  $G_A$  was calculated. Results for all subject and target velocities are presented in Fig. A.1.

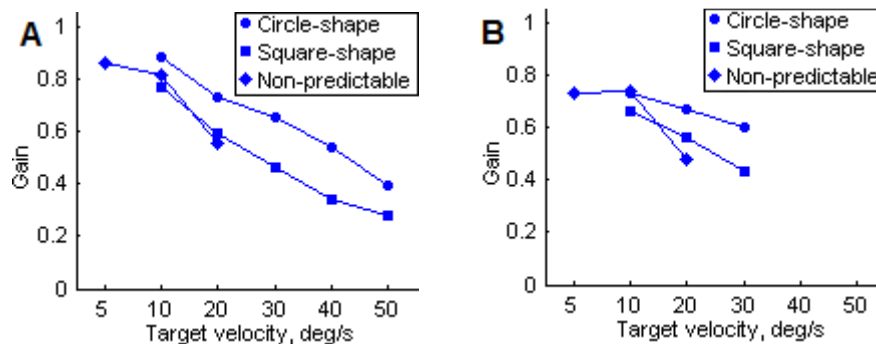


Fig. A.1 Gain values for younger (A) and elder (B) subjects.

As seen in the experimental results, the faster is the target movement, the smaller the pursuit gain is. For the target velocity 20 deg/s, pursuit gain for predictable trajectories is higher (0.64) than for non-predictable (0.5). In all trials, the pursuit gain for elder subjects (Fig. A.1 B) is lower than for younger subjects (Fig. A.1 A).

These long-term tracking experiments of targets moving in different velocity and in both predictable and non-predictable trajectories, revealed adequate relationship between pursuit and saccades.

The developed mathematical definition for pursuit gain evaluation using number and amplitudes of catch-up saccades provides sufficient result. Now pursuit gain could be calculated from a sum of amplitudes of catch-up saccades and overall target trajectory. This definition is a fast and an easy way to calculate pursuit gain and can be used to evaluate the conditions of the tracking performance influenced by the training, disorder or an age of the individuals.

Experimental results were computed using new definition of the pursuit gain. Experimental results have showed that older subjects are executing catch-up saccades more frequently and with larger amplitudes and therefore pursuit gain tends to be lower than for younger subjects.

## APPENDIX B: Smooth pursuit system's reaction to visual occlusions

Prediction of object motion allows overcoming of object occlusions in its trajectory. It is known that oculo-motor system is able to predict both position and velocity of occluded target for several hundred milliseconds [128]. After this period of time velocity of the eye starts exponentially decay to zero when the target is not expected to appear or it reaches a plateau value, when it is expected to reappear.

A lot of research has been done studying predictive mechanisms driving smooth pursuit and saccadic response during target occlusions. Providing post-occlusion information showed that eye velocity at target reappearance was only influenced by expected target velocity. To minimize the influence of pre- and post-occlusion target velocity information, uniformly accelerated motion, or randomized duration of the blanking periods were used in further studies [101], though predictable target trajectories were used.

Five human subjects participated in experiment. They were asked to track a visual target, moving in a non-predictable trajectory (Fig. B.1 A).

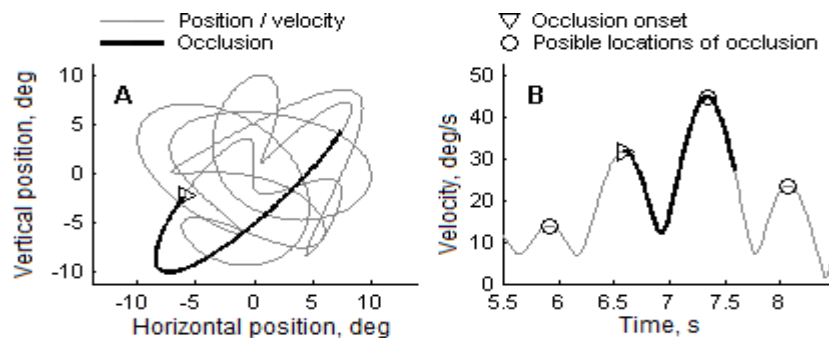


**Fig. B.1** Target movement trajectory (A). Partial graph of the target velocity (B). Thin grey lines represent visible trajectory (in A) and velocity (in B), black thick lines - occlusion.

Occlusions of 1 s were introduced in the trajectory, and started at the peaks of target velocity (Fig. B.1 B). After each of nine occlusions, target reappeared for a period ranging from 0.8 to 1.6 s. With the purpose not to overlay the occlusions, the same trajectory was tracked 3 times with occlusions in different locations. Subject repeated experiment 3 times, to get consistent data.

Target trajectory was produced adding ten sine waves with increasing frequency and random phase shift. Vertical movement trajectory is the same as horizontal, but shifted by  $\frac{3}{4}$  period. Target velocity was in the range from 1.4 to 44.1 deg/s (mean of 20 deg/s with SD of 8 deg/s).

Position errors between target and eye movement trajectories (Fig. B.2 A) user for analysis were calculated at the onset of the occlusions ( $T1$ ), 100 ms ( $T2$ ), 150 ms ( $T3$ ), 200 ms ( $T4$ ) and 500 ms ( $T5$ ) after onset and at the end of the occlusions ( $T6$ ).

As it can be seen from Fig. B.2 A, oculo-motor control system is predicting trajectory of the occluded target for up to 200 ms ( $T1$  to  $T4$ ); therefore, a position error does not increase much. Oculo-motor system is even able to execute a catch-up saccade (Fig. B.2 A)  $S1$  to the predicted target's location [93]. After 200 ms eye

movement velocity starts to decay, and position error increases (Fig. B.2 A),  $T5$  – oculo-motor system is no longer able to predict the location of the occluded target. As the target is still not visible, oculo-motor system executes some saccades (Fig. B.2 A)  $S2$  and  $S3$ , and one can see general tendency of the directions of the saccades is towards the center of the screen. After the occlusion (at  $T6$ ), position error (Fig. B.2 A) is reduced by executing two saccades (Fig. B.2 A)  $S4$  and  $S5$  towards a new position of the target.

In Fig. B.2 B, all trials for all five subjects and for the same target's occlusion are plotted. Gaze position at the occlusion onset (Fig. B.2 B, *circle*), 500 ms after onset (Fig. B.2 B, *star*) and at the end (Fig. B.2 B, *filled circle*) of the occlusion are marked. Analyzing eye movement paths (Fig. B.2 B, *thick gray lines*) one can see general tendency of all subjects to direct their gaze towards the center of the screen, when oculo-motor system is unable to predict occluded target's trajectory.

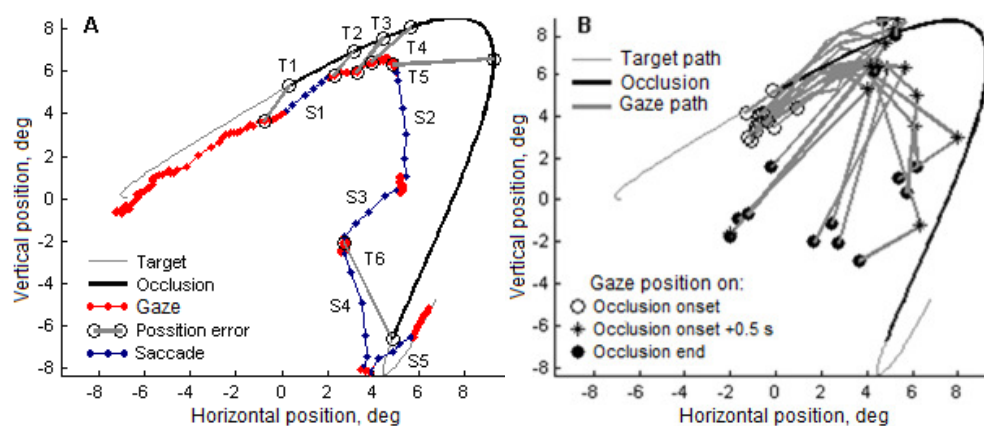


**Fig. B.2 A:** The trajectories of the target (thin gray line) and the position of the gaze 0.5 s before onset and 0.5 s after end of the occlusion (thick black line). Position errors at the time-stamps  $T1 - T6$  connecting a corresponding target and gaze locations (circles). **B:** Gaze locations at the time-stamps  $T1$  (circle),  $T5$  (star) and  $T6$  (filled circle).

With the purpose to understand better the behavior of the oculo-motor system during occlusion of the target, distributions of position error obtained in all experiments are plotted in Fig. B.3.

Distribution of position error at the onset of occlusion is plotted in Fig. B.3 A. Average position error for all subjects is  $1.54 \pm 0.99$  deg. The largest scatter of the position error ( $8.1 \pm 4.05$  deg) were obtained at the end of the occlusion and are shown in Fig. B.3 B. As it was predicted, the scatter became smaller after the recalculation of position error in respect to the center of the screen (Fig. B.3 C). The scatter reduces from 8.1 deg to  $4.86 \pm 2.46$  deg and confirms that oculo-motor system was able to predict probability of the distribution of the overall target trajectory on the screen. This distribution did not significantly differ from the distribution on position errors 500 ms after the end of the occlusion ( $4.62 \pm 2.53$  deg). It was also found that the distributions of position errors 100 ms after the onset of the occlusion ( $1.46 \pm 0.92$  deg), 150 ms ( $1.72 \pm 1$  deg) and 200 ms ( $1.73 \pm 1.17$ ) after the onset of the occlusion did not differ significantly (t-test,  $p < 0.05$ ) from distribution plotted in Fig. B.3 A.

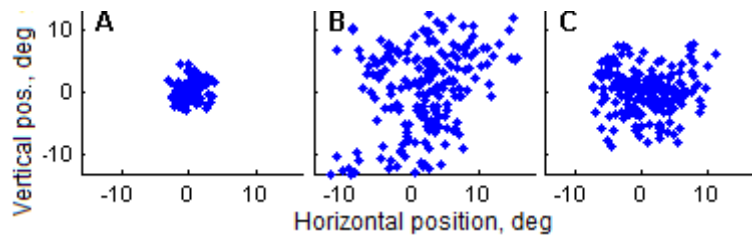


**Fig. B.3** Distributions of position error. **A**: at the onset of the occlusion; **B**: at the end of the occlusion in respect of target position; **C**: at the end of the occlusion in respect of the center of the screen.

After an analysis of experimental data, it can be concluded, that when oculo-motor system is no longer able to predict location of the occluded target, gaze is directed towards center of the screen, expecting that since the target reappearance position becomes less predictable as occlusion duration increases, the most convenient strategy is to position the gaze at the center of the screen (as the shortest catch-up saccade will be needed) or not to reposition the gaze at all. This statement supports basic principles of the Bayesian decision theory which defines how new information should be combined with prior beliefs and how information from different modalities should be integrated [94].

#### **Inter-saccadic intervals of catch-up saccades performed during visual occlusion of the target**

Ocular pursuit relies not only on retinal inputs from direct feedback of visual motion signals, but also use extra-retinal (internal) signals to maintain a stable response with a high gain of the pursuit, despite the visuo-motor delays of 80-100 ms [128]. Internal drive becomes more evident when a moving target disappears or is occluded by other objects in the scene. In this case, pursuit is maintained solely by extra-retinal signals - efference copy, remembered target motion, volition, attention and expectation. Initial part of the ocular response during occlusion (about 150 ms) depends on the visual stimulus' parameters, obtained before the occlusion and development of the secondary component depends on the expectation that target motion will continue in the future [11]. Smooth pursuit continues only if subject has expectation that the target will reappear; otherwise, eye velocity exponentially decays to zero [101]. However, total eye displacement remains similar irrespective of expectation, suggesting that ability to use sampled target motion information to predict future target displacement operates independently of the control of smooth pursuit eye movements. Overall eye position can be maintained along a path that approximates occluded target trajectory using saccadic eye movements.

Previous experimental research [185] revealed that, when tracking a target, moving in a pseudo-random trajectory, oculo-motor system is able to predict target motion only up to 200 ms duration. After this prediction phase, prediction of target position is influenced by the probability of the position of target reappearance accumulated in long-term memory. In most of the cases, oculo-motor system is able

to reduce position error by executing voluntary saccades towards expected target reappearance location.

In this experimental investigation, inter-saccadic intervals of successive saccades, performed before and after or during the target occlusion onset were analyzed. Visual occlusion of the target may occur in two circumstances in respect on ongoing oculo-motor action: during smooth pursuit phase or during ongoing catch-up saccade, therefore may be this affects inter-saccadic intervals.

Eight subjects were asked to track a visual target moving in pseudo-random trajectory with average velocity of 20 deg/s. Thirteen occlusions (duration – 500 ms) each after 1.5 s of normal target tracking were implemented in the trajectory of the target.

When human pursue a moving target that suddenly is occluded for a brief amount of time, target is tracked as if it was visible up to 200 ms after occlusion. Previous research [185] has showed that position error between target's position and gaze's position starts to increase only 200 ms after the onset of the occlusion. Distribution of the catch-up saccade count depending on the relative to the target's occlusion time is plotted in Fig. B.4. Average saccade duration was 41 ms with SD of 9 ms. Time mark 0 denotes the onset of the visual occlusion of the target and all the shaded area is a time slot where the target is not visible. Uniform distribution of catch-up saccade count is observed before and after the target occlusion.

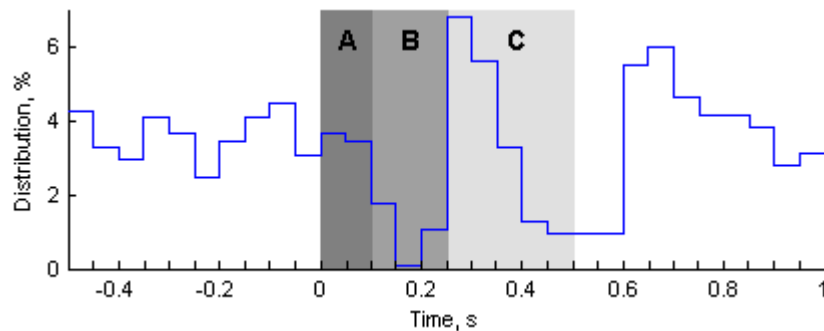


**Fig. B.4** Distribution of the catch-up saccade count before, during and after the visual target occlusion. First 100 ms (A), 100 to 250 ms (B), 250 to 500 ms after the onset of visual occlusion are marked gray.  $n = 1721$ .

In most of the trials, catch-up saccades are executed up to 100 ms after the target occlusion (B.4 A). These catch-up saccades are planned for execution before the occlusion, but because of the motor delays, executed only after the start of occlusion. Even if the oculo-motor system is able to predict target motion for more than 100 ms, there is only 2.9% of catch-up saccades executed during 100 to 250 ms after the target is occluded time slot (Fig. B.4 B).

Number of saccades increase when subjects start to execute voluntary saccades (not catch-up) to the expected target locations (Fig. B.4 C). Subjects have enough time to execute one or two voluntary saccades before the reappearance of the target, but most of them are executed in the first part (250 – 350 ms after target occlusion onset) of saccadic search for a target (SSFT).

When the target reappears after 500 ms of occlusion period, visuo-motor system needs some time (about 100 ms) to calculate a new target position and execute a saccade towards the target. This way number of saccades increase and when the gaze catches-up with the target, pursuit continues in a regular manner.

As the occlusions in the target trajectory are implemented every 1.5 ms, it may start in two circumstances with the respect of ongoing oculo-motor action: during smooth pursuit (e. g. possibly after the regular catch-up saccade – Fig. B.5 A) or during a catch-up saccade (Fig. B.5 B). If the target disappears during a smooth pursuit phase, there will be a saccade before ( $S_1$  in Fig. B.5 A) and a saccade after ( $S_2$  in Fig. B.5 A) the occlusion onset.

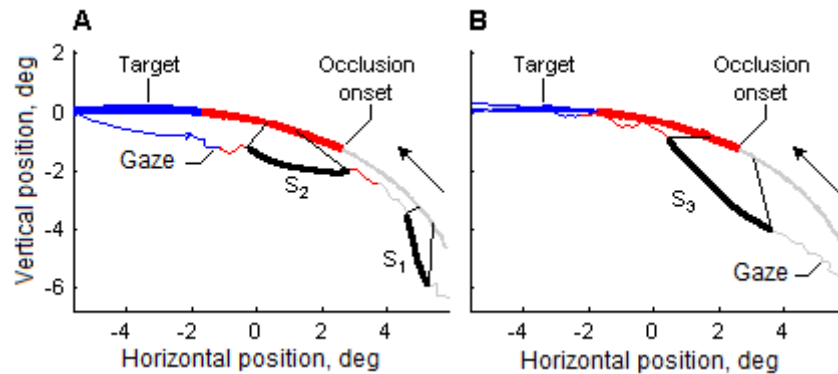


**Fig. B.5** Different behavior during visual occlusion onset: smooth pursuit (A), catch-up saccade (B).  $S_1$ ,  $S_2$  and  $S_3$  are saccades, thin black lines mark corresponding gaze and target locations during saccades and arrow denotes direction of the target motion.

All trials were sorted according to ongoing action during target occlusion onset and inter-saccadic intervals were calculated for both conditions (Fig. B.6). In 0.15 A, a distribution of inter-saccadic intervals between the saccades that were executed before and after target occlusion onset (similar to  $S_1$  and  $S_2$  in B.5 A) is plotted. There is high number (34%) of saccades, which were executed with inter-saccadic interval of 100-200ms – nominal inter-saccadic interval of regular catch-up saccades that are performed while tracking a visible target. Rest of the saccades were executed with longer inter-saccadic intervals. These are voluntary saccades, performed during SSFT.

If the target disappeared during ongoing catch-up saccade, in most of the trials, successive saccade is performed with a longer inter-saccadic interval – 78% of successive saccades have inter-saccadic interval of 250-400 ms, and this means, that majority of them are performed during SSFT.

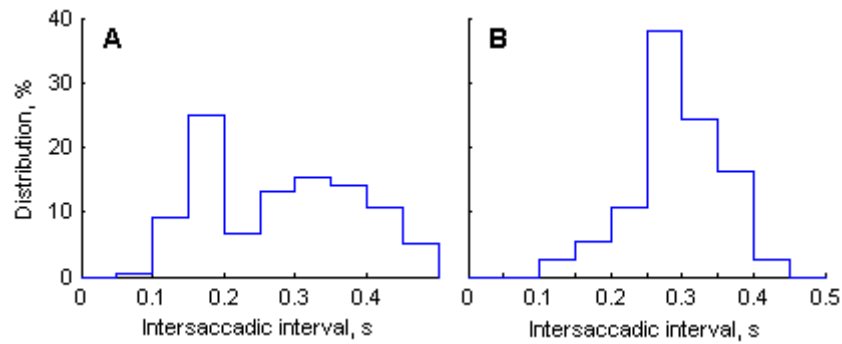


**Fig. B.6** Distributions of inter-saccadic intervals of successive saccades, performed before and after (A),  $n=176$ , or during and after (B),  $n=37$  the target occlusion onset.

Therefore, the oculo-motor system is able to predict target motion up to 200 ms and after this period, position error between target position and eyesight starts to increase. It was found that catch-up saccades are performed only up to 100 ms after target occlusion onset and there are only 2.9% of saccades executed in time interval 100 to 250 ms after the target is occluded. This means that extra-retinal components build from visible target motion, can longer be a source for driving a smooth pursuit than for saccades. Information about target motion, required to prepare a catch-up saccade, is gathered during ongoing smooth pursuit. In case of target disappearance during ongoing saccade, successive saccade is performed with longer inter-saccadic interval (250 – 400 ms) and therefore it probably belongs to SSFT saccades, not the regular catch-up saccades, which have inter-saccadic interval of 100 – 200 ms.

## **APPENDIX C: Smooth pursuit system's reaction to visual illusions**

### **Effects of Muller-Lyer Illusion on the accuracy of primary saccades and smooth pursuit eye movements**

In real world, visual situations known as visual illusions, naturally or unnaturally exists. In such cases, visual information is misinterpreted. The simple way to investigate visual illusions is the method of perceptual judgments. In such way, the effect of misperception of size, length or angle of the objects, enriched with geometrical illusion, is evaluated. The nature of pictorial illusions was investigated by Bulatov et. al. They developed a model based on centroid (distribution of masses) of illusory patterns of various spatial structures, which was integrated in the visual pathways [27] for explaining the nature of visual illusions.

Further investigation of pictorial illusions was performed together with motor actions [63]. It was noticed that the effect of a visual illusion, evaluated during perceptual judgment, differed from the effect of the adequate illusion, which was made with illusory pattern during visuo-motor or/and visuo-manual action. Many experiments proved that illusions evident in subjective reports of stimulus size, length or angle often had little influence on visually guided actions [83]. Currently there is a plausible hypothesis that visual information from frontal eye field is divided in two visual streams: vision-for-perception and vision-for-action. The dorsal subsystem specializes in the visual guidance of action, whereas the ventral subsystem specializes in object perception and recognition. Evidence for the two-visual-systems hypothesis has come from studies comparing the effects of illusions on perceptual judgments and visuo-motor behavior. These two kinds of behavior are mediated by the modality of response: subjective or perceptual-motor. Difference between the stimuli for perceptual and motor tasks could be explained by comparing the influence of Muller-Lyer (M-L) illusion on perceptual judgment and oculo-motor action directing the gaze towards the wings of the shaft in dynamic conditions.

In the papers by Knox and Bruno [83] as well McCarley and Grant [113], the estimation how the perceptive length of M-L stimulus is biased by the illusion during saccadic eye movements was performed. The amplitudes of the reflexive and voluntary saccades to the corners of the arrows of M-L illusion were examined. Presentation of the stimulus was short-term (0.2 s, i. e. stimulus is no longer visible at the end of saccade). It has been found that both types of the saccades could be strongly affected by the illusion. The effect of the M-L illusion on reflexive saccades was comparable to that usually observed with perceptual judgments (an effect size of 22%), whereas the effect on voluntary saccades was smaller (11%). An important difference between reflexive and voluntary saccades is because voluntary saccades were elicited in memory-guided performance. Nevertheless, there is no known investigation on the influence of M-L illusion on the primary saccades, elicited in double-step mode, and on the smooth pursuit eye movements.

Since illusions might be the subject of misinterpretation and the loss of presented information about visible scene, it was decided to examine how M-L illusion affects accuracy of double-step saccades and smooth pursuit eye movements.

An experiment 1 was used to examine the influence of the illusion on the amplitudes of voluntary and reflexive saccades elicited to the arrows of M-L illusion (A, B, and C, D in Fig. C.1). An experiment 2 was used to measure the accuracy of the smooth pursuit eye movements when subjects track the arrow stimulus (E in Fig. C.1) moving left to right and back in three constant speeds: 5, 10 and 20 deg/s. To compare the effect of visual illusion on the accuracy of saccadic and smooth pursuit eye movements to the results, obtained during perceptual judgment, experiment 3 was done. In this experiment, subjects perceptually evaluated the length of the shaft of the M-L illusion. Nine subjects participated in all three experiments.

During the first part of exp. 1, when voluntary saccades were examined, subjects were asked to direct their gaze voluntarily from the left arrow to the right and back. In the second part, when reflexive saccades were investigated, arrows of M-L illusion were alternatively switched on and off and subjects were asked to direct their gaze towards the visible stimulus. The reference stimulus without illusion for voluntary and reflexive saccades was used too. It had the same size properties of M-L illusion stimulus, but the wings of the arrows were in vertical line.

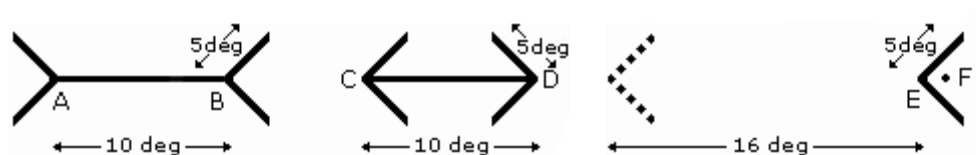


**Fig. C.1** The shape and dimensions of M-L illusion stimulus used in exp. 1 for investigating the accuracy of voluntary and reflexive saccades (**left and center**). Stimulus used in exp. 2 for investigating the accuracy of smooth pursuit eye movement (**right**).

Distributions of position errors of voluntary and reflexive saccades elicited to the stimulus of M-L illusion are presented in Fig. C.2 (A, B and C – voluntary saccades), (D, E and F – reflexive saccades). B and E distributions in Fig. C.2 represent the position errors for “wings-out” stimulus and C, F represent data for “wings-in” stimulus of M-L illusion.

Distributions in Fig. C.2 A and D represent reference data of position errors obtained without illusion. Experimental data for voluntary and reflexive saccades show that saccadic eye movements were quite precise and not affected by the illusion. Moreover, as it was expected, the voluntary saccades were more precise than reflexive. In the experiment with voluntary saccades, the shaft and the wings were seen all the time during saccades, therefore the subjects using visual memory were able to match their gaze position to the ends of the shaft. In the experiment with reflexive saccades, arrows at the ends of the shaft, were flashing (alternating), therefore the subjects could see the stimulus of M-L illusion only for a short time. The mean of position errors of reflexive saccades were 0.02 deg (0.2%) for wings-in stimulus and 0.14 deg (1.4%) for wings-out stimulus. On the contrary, the mean of position errors of the voluntary saccades were negligibly small. Comparing experimental data with the results obtained during perceptual judgment (around 10%

error), it can be concluded that the effect of the visual illusion to amplitude of saccadic eye movements is small.

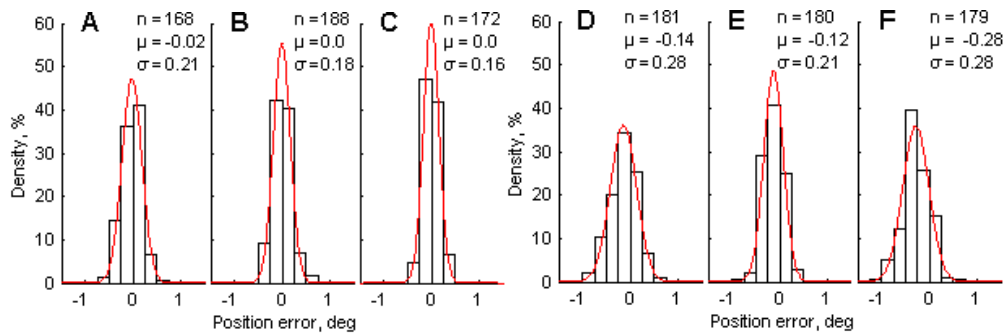


**Fig. C.2** Distributions of position errors of voluntary (A, B, C) and reflexive (D, E, F) saccades for “wings-out” (B, E), “wings-in” (C, F) stimulus of M-L illusion and without illusion (A, D).

Saccadic gaze repositioning is fulfilled in two saccades: primary and corrective [96]. Normally primary saccades take the eye 90 % of the way to the target, followed by 10% corrective saccade.

The distributions of the position errors of primary saccades differ if they are elicited by stationary targets (voluntary saccades) or by jumping targets (reflexive saccades) [40, 187]. The distributions of position errors of primary saccades made to stationary targets were almost symmetrical, whereas the distributions of primary saccades to jumping targets were skewed in the direction of undershoot.

The investigation of the results of voluntary and reflexive saccades, obtained in exp. 1, supported the understanding that complete saccades are not strongly affected by the illusion. Subjects were able to direct their gaze quite precisely to the ends of the shaft of M-L illusion. The question about the influence of M-L illusion on the primary saccades is still open and never analyzed and reported.

Distributions of position errors of primary saccades elicited to the stimulus of M-L illusion in the voluntary and reflexive modes are presented in Fig. C.3 A, B and C illustrate position error distributions of the primary saccades elicited in the voluntary mode and D, E and F – in the reflexive mode. B and F distributions in Fig. C.3 represent the position error distributions for wings-out stimulus and C, F – for wings-in stimulus of M-L illusion. Distributions A and D represent reference data obtained without illusion.

The distributions of position error of primary saccades shows that primary saccades are less scattered than complete saccades. SD values ( $\sigma$ ) for complete saccades are in the range of 0.16 – 0.28 deg comparing with range 0.35 – 0.72 deg for primary saccades. Distributions of position error of primary saccades elicited in the reflexive mode ( $\sigma = 0.61\text{-}0.72$  deg), like distributions of position errors of complete saccades, also executed in reflexive mode ( $\sigma = 0.21\text{-}0.28$  deg, see Fig. C.2), are more scattered than primary and complete saccades, executed in the voluntary mode ( $\sigma = 0.35\text{-}0.45$  deg and  $0.16\text{-}0.21$  deg respectively). It can be stated that M-L illusion mostly affects those primary saccades, which were elicited in the reflexive mode.

Comparing the experimental data of primary saccades elicited in the reflexive mode with the results obtained during perceptual judgment, we can conclude that during the perceptual judgment the effect of the visual illusion was substantially strong: 3.6% comparing to 10% for wings-in stimulus and 4% comparing to 14% for wings-out” stimulus of M-L illusion.

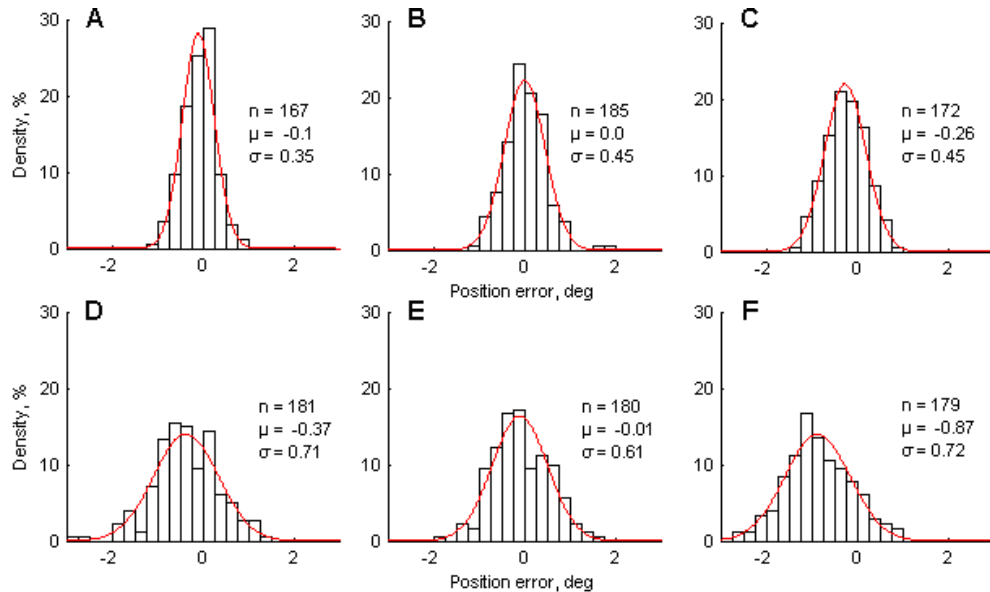


**Fig. C.3** Distributions of position error of primary saccades elicited in the voluntary (A, B, C) and reflexive (D, E, F) modes to the wings-out (B, E), wings-in (C, F) stimulus of M-L illusion and without any illusion (A, D).

It is known that smooth pursuit eye movements demonstrate tracking error and delay even if the stimulus is not affected by an illusion [93]. Therefore, in order to evaluate the effect of M-L illusion we calculated the difference of the position errors obtained during tracking the stimulus with wings-in and wings-out illusion and reference target in the way illustrated in Fig. C.4.

The mean ( $\mu$ ) and SD ( $\sigma$ ) of the tracking error between the averaged recordings of the smooth pursuit eye movements obtained during tracking the stimulus with illusion and reference target were calculated and are provided in Table C.1. Tracking errors were slightly affected by the illusion only in higher target movement velocities. The comparison of the tracking

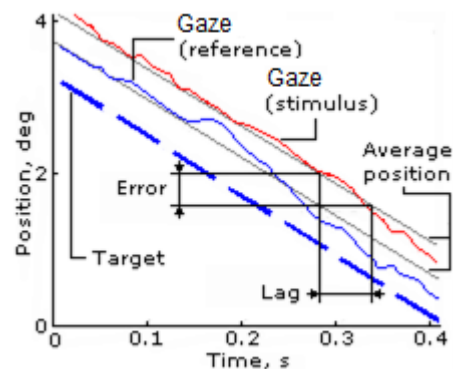


**Fig. C.4** Presentation of the tracking error calculated between the averaged recordings of the smooth pursuit eye movements obtained during tracking the stimulus and the reference target.

errors of pursuit of illusory stimulus and the subjective length estimates of the shaft of M-L illusion, have proved that smooth pursuit eye movements are poorly affected by the effect of illusion.

The purpose of this experimental trial was to investigate whether there were systematic differences between the effects of M-L illusion on saccadic and smooth pursuit eye movements and on the perceptual judgments. The obtained results have revealed that the primary saccades elicited in the reflexive mode were mostly affected by the M-L illusion. The position errors of primary saccades elicited in the reflexive mode were 4% for wings-in illusion and 3.6% for wings-out illusion comparing with the 0.25% and 0.1% for the saccades elicited in the voluntary mode. The position error of complete saccades (0.14% and 0.02%) and the tracking error obtained during smooth pursuit (0.11% and 0.05%) were negligibly small. Nevertheless, experimental results obtained during the perceptual judgment of M-L illusion were substantially larger - 14% and 10% respectively.

**Table C.1** Means and SDs of tracking errors during the pursuit of the moving stimulus with illusion and reference target.

velocity, deg/s	n	no illusion		wings-out illusion		wings-in illusion	
		$\mu$ , deg	$\sigma$ , deg	$\mu$ , deg	$\sigma$ , deg	$\mu$ , deg	$\sigma$ , deg
5	30	0	0,1	-0,05	0,07	-0,02	0,09
10	60	-0,13	0,13	-0,08	0,15	-0,24	0,12
20	120	-0,44	0,32	-0,31	0,3	-0,62	0,23

These findings disagree with the results presented by Knox and Bruno [83] as well McCarley and Grant [113]. The authors noted that reflexive saccades were affected by M-L illusion by 22%. Adequately, the results obtained in this research are 0.14% and 0.02%. The discrepancy of the results was obtained due to the different visibility duration of the target. Mentioned researchers have used short time (0.2 s) of exposure of M-L stimulus. Under such conditions, the saccade is not precise because it cannot be corrected by a secondary saccade due to the absence of visible stimulus. Therefore, saccades examined in those experiments were executed in the memory-guided conditions while now experiments were executed during the active vision. It can be concluded that the time of exposure of the stimulus was the dominant parameter affecting visuo-motor action.

The next factor, important when analyzing the influence of M-L illusion on visuo-motor action, is the site of the retina where the illusory stimulus is projected. Due to density of the distribution of receptors on the retina, the most accurate perception of the stimulus is at the center (fovea) and decreases towards the periphery of the retina. In the conditions of uncertainty, the visual system accepts illusory stimulus as centroid, which is the center of the mass of the figure [27]. The center of the mass of M-L illusion is marked as F in Fig. C.1.

Amplitudes of primary saccades comparing with control (without illusion) were 4 % smaller for wings-in illusion and 3.6 % larger for wings-out illusion.

## APPENDIX D: Oculo-motor guiding parameter dependency on a living-style

Different human subjects develop slightly different abilities. With a purpose to investigate if this is also the case for oculo-manual coordination, one-more experimental trial was designed and executed. Main its purpose was to confirm or reject the hypothesis, that people, whose everyday usual tasks require for their eye-hand coordination to be the best, would develop better (and maybe different) eye-hand coordination than others. Participants of this experimental trial were 19 male subjects in the age range of 23-25 years. This group of similar subjects was chosen to reduce the possibility of parameter variation on age or sex. Subjects were divided into three groups: beginners, intermediate and advanced players in basketball. Advanced players were those, who have 5 and more sessions of basketball play in a week, intermediate – 2-3 sessions, and beginners – those who does not play regularly. It was expected for the eye-hand coordination of the advanced players to be the best in terms of result, which was an error of the hand movement during self-moved object guiding along a path (appearance outside the boundaries of the path).

Experimental trial consisted of 2 different complexity paths (Fig. 3.17 B and 3.17 C). For the conditions to be equal and the results to be comparable, a target of common (for all experiments in this thesis, section 2.3) size and shape, but of very pale gray color (close to a background of the path) was used as an indicator for task fulfilment velocity. At the beginning of each trial, it has changed its color (red-blue-green) for the subjects to prepare to move their hand and after that started to move along the path in a human movement pattern (i. e. reducing the velocity for corners and increasing it for straights). Subjects repeated each of the two paths for three times with different indicator's movement velocity (2.5 deg/s, 5 deg/s, 10 deg/s).

In addition to eye-hand coordination parameters introduced in section 3.3.1, eye movement velocity between the saccades, eye-hand distance when the gaze leads, hand lag time, average hand speed, average distance indicator-cursor ( $D_{IC}$ ), ratio between full guiding time and time when the hand-moved object was outside the boundary of the path (guiding error –  $GE$ ), and their SDs were calculated and compared.

Even if the dependency of  $GE$  on the average distance from the indicator to the hand-moved object is observed:  $GE$  increases together with  $D_{IC}$ , no difference for different groups can be clearly seen (Fig. D.1). It can be thought, that if subject is lagging in comparison to indicator, he tend to guide with higher guiding error. But both these parameters depend on the third parameter: hand movement velocity  $V_H$ . If the indicator is moving fast,  $V_H$  and then both  $GE$  and  $D_{IC}$  increases (Fig. D.2).

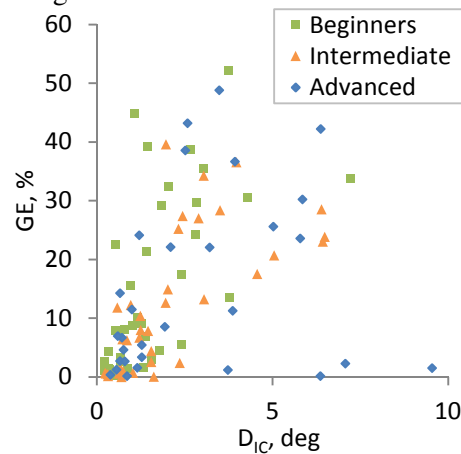


**Fig. D.1** The guiding error as a dependency of the average distance indicator-cursor.

To know if all the subjects and especially the groups were able to maintain comparable hand movement speed, average  $V_H$  of all subjects was plotted in Fig. D.3 and compared to indicator velocity  $V_I$ . As fluctuations of  $V_H$  during one trial of an average subject (Fig. D.3 B) are significantly higher than a discrepancy of mean hand movement velocity in different groups (Fig. D.3 A), it can be stated, that the guiding conditions in term of the average hand movement speed were very similar for different groups and the characteristics of such guiding can be compared. This means that the usage of the velocity indicator was beneficial. It also should be mentioned, that all the gaze trajectories were checked for saccades to indicator or smooth pursuit of the indicator – no such episodes have been found.

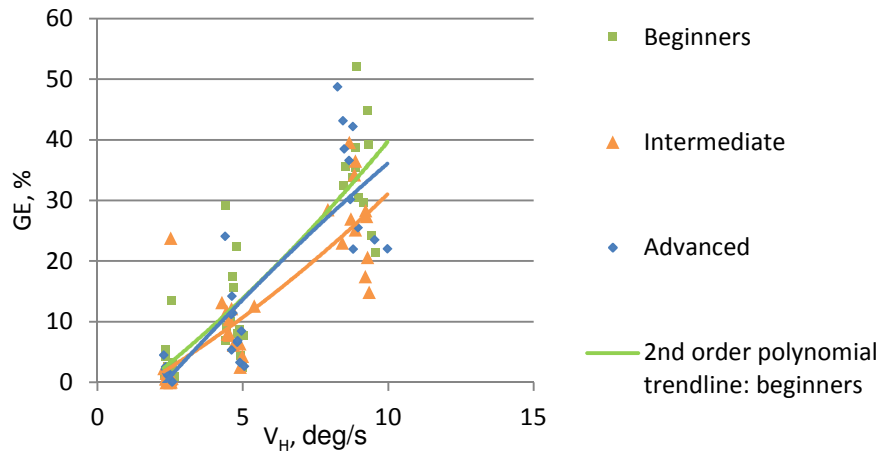


**Fig. D.2** Guiding errors ( $GE$ ) as a dependency on the average hand movement speed ( $V_H$ ).

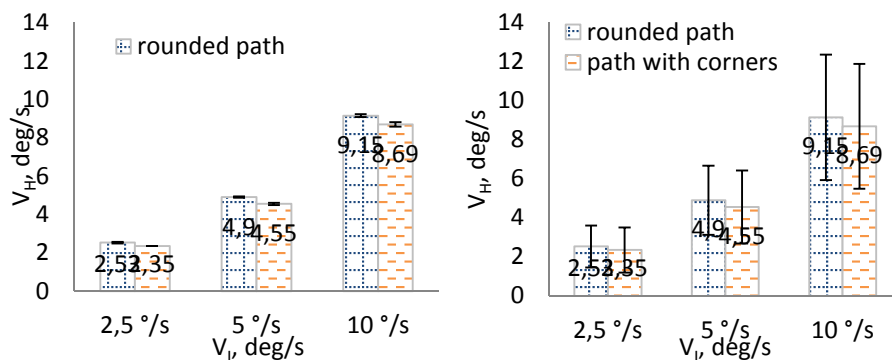


**Fig. D.3** Average hand movement speed ( $V_H$ ) in all 6 trials. **Left** graph shows SD of the mean values of the groups; **right** – average SD of subjects (average  $V_H$  fluctuation during one trial).

The average guiding error ( $GE$ ) of different groups is provided in Fig. D.4. It is seen, that the most precise eye-hand coordination was demonstrated by the subjects in the intermediate group. The hypothesis on better eye-hand coordination development as a skill is falsified.

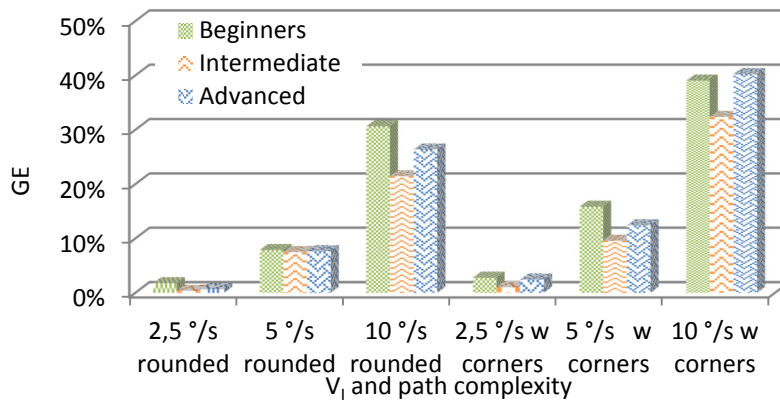


**Fig. D.4** The guiding error (*GE*) for all groups in all conditions.

ANOVA analysis was done with a purpose to evaluate if subject distribution to different groups would provide statistically more valid results. Four possible group combinations were defined: 3 groups as already presented, beginners and others, intermediate players and others, advanced players and others. Fig. D.5 shows the p-values for such ways of grouping. If the cutoff p-value is set at 0.05, the best way of grouping is intermediate players vs. others. In such way, only the results of guiding in 5 deg/s curved path are non-valid. If subjects are grouped to ANOVA-suggested groups, the graph of guiding errors (Fig. D.4) can be re-charted as it is shown in Fig. D.6.

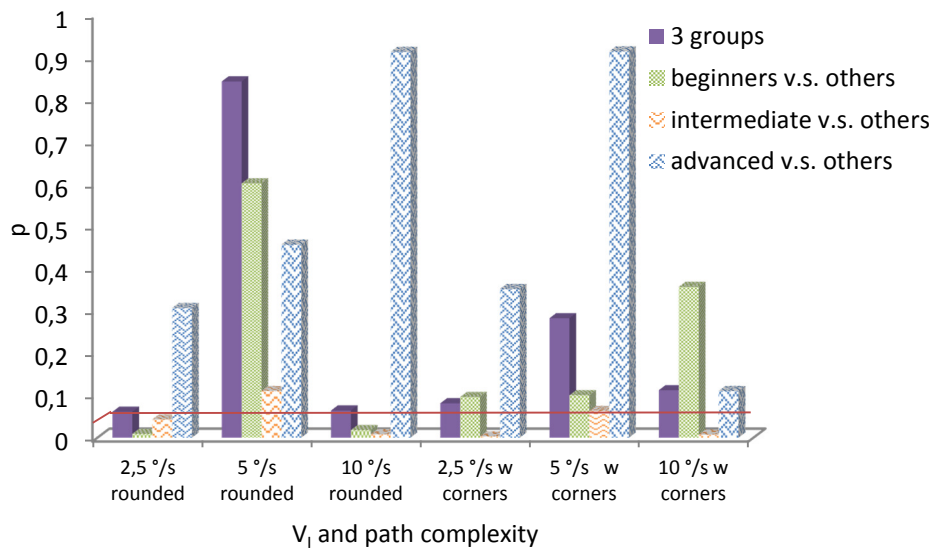


**Fig. D.5** ANOVA evaluation of possible other grouping of subjects. Cutoff p-value is 0.05.

It is observed that intermediate basketball players showed the best eye-hand coordination. While trying to understand the causes of unexpected results, cross-

correlations between  $GE$  and  $V_H$ , also between  $GE$  and  $D_{IC}$ , were calculated and are presented in Table D.1. It is seen that guiding error significantly correlates to both average hand speed and average distance between the velocity indicator and the cursor. Both correlation coefficients of beginners and advanced players are contrary (if intermediate players are taken as a reference), so it is evident, that neither hand velocity, neither concerns on far-leading velocity indicator are the factors for poor performance. One of possible reasons for low  $GE$  of advanced player group might be that such players were less used to do computer-based tasks in sitting position.

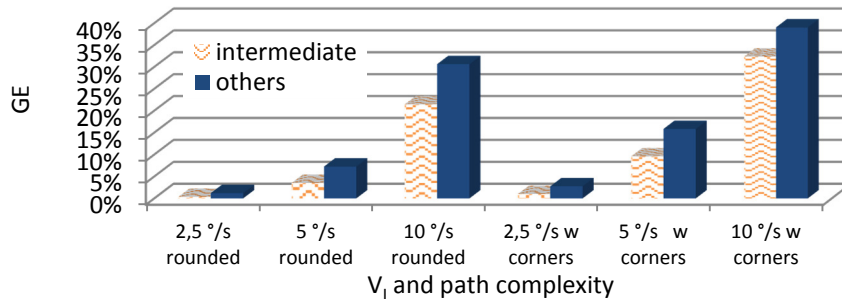


**Fig. D.6** The guiding error ( $GE$ ) for all groups in all conditions using ANOVA-suggested grouping of subjects

**Table D.1** Guiding error cross-correlations to average hand movement speed and average distance between the velocity indicator and the hand-moved object (cursor).

Group	Beginners		Intermediate		Advanced	
	GE vs. $V_H$	GE vs. $D_{IC}$	GE vs. $V_H$	GE vs. $D_{IC}$	GE vs. $V_H$	GE vs. $D_{IC}$
<b>Cross-correlation</b>	0.95	0.97	0.94	0.94	0.92	0.88

All the parameters of eye-hand coordination were also plotted in charts together with SDs of values in groups and with average SDs during one trial. No significant trends between groups was observed. All the differences of all the parameters between groups were chaotic and less than SDs between group members and even less than fluctuations during one trial. It is concluded, that eye-hand coordination can be enhanced by an active living style, but does not depend on specific skills developed during everyday activities.